

This item was submitted to [Loughborough's Research Repository](#) by the author.
Items in Figshare are protected by copyright, with all rights reserved, unless otherwise indicated.

Measurement of grip force and evaluation of its role in a golf shot

PLEASE CITE THE PUBLISHED VERSION

PUBLISHER

© Erin R. Schmidt

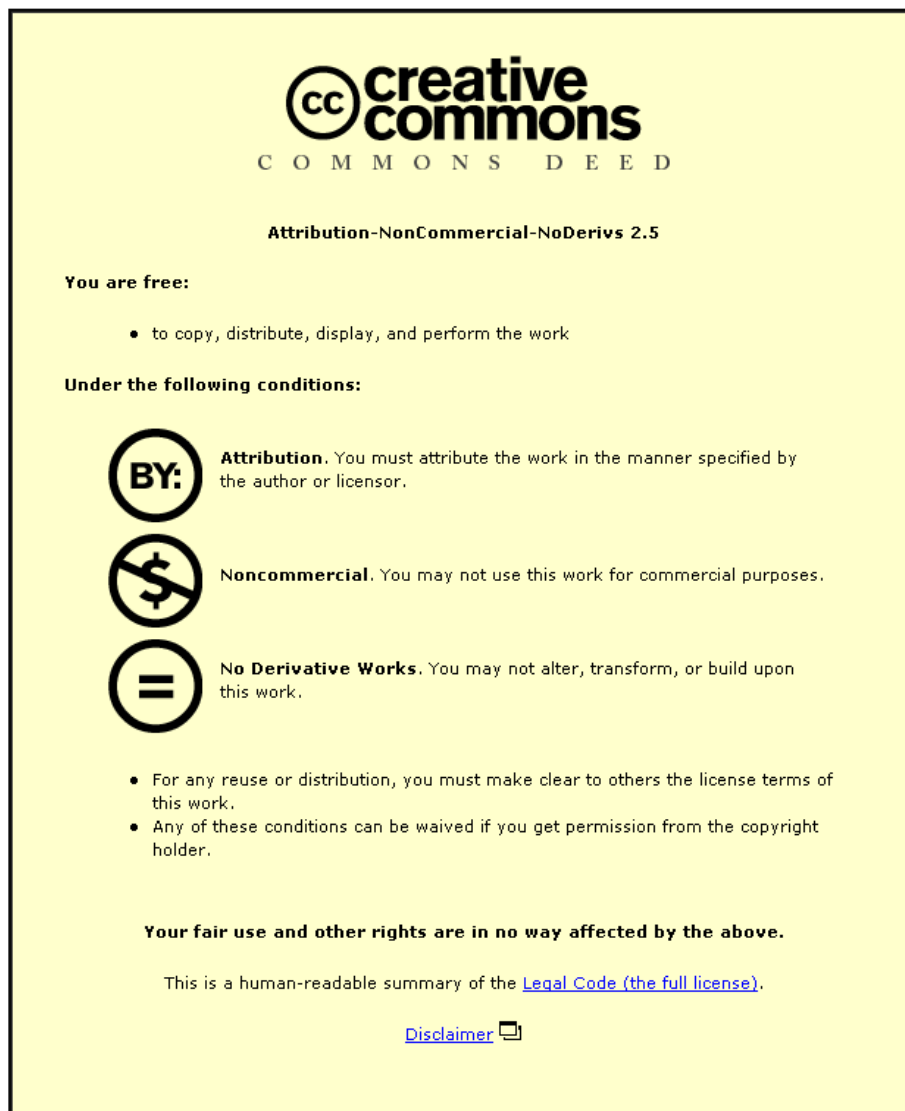
LICENCE

CC BY-NC-ND 4.0

REPOSITORY RECORD

Schmidt, Erin R.. 2019. "Measurement of Grip Force and Evaluation of Its Role in a Golf Shot". figshare.
<https://hdl.handle.net/2134/13125>.

This item was submitted to Loughborough University as a PhD thesis by the author and is made available in the Institutional Repository (<https://dspace.lboro.ac.uk/>) under the following Creative Commons Licence conditions.



For the full text of this licence, please go to:
<http://creativecommons.org/licenses/by-nc-nd/2.5/>



University Library

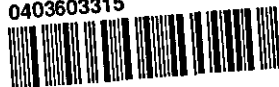
Author/Filing Title SCHMIDT, E.R.

Class Mark T

Please note that fines are charged on ALL
overdue items.

FOR REFERENCE ONLY

0403603315





MEASUREMENT OF GRIP FORCE AND
EVALUATION OF ITS ROLE IN A GOLF SHOT

by

Erin R. Schmidt

A thesis submitted in partial fulfilment of the requirements for the award of

Doctor of Philosophy

Loughborough University

2007

© by Erin R. Schmidt 2007


 Loughborough University Pilkington Library
Date 8/2008
Class T
Acc No. 0403603315

TABLE OF CONTENTS

ABSTRACT	1
ACKNOWLEDGEMENTS	3
1.0 INTRODUCTION	5
2.0 GRIP FORCE RESEARCH.....	11
2.1 HAND AND WRIST PROPERTIES.....	11
2.1.1 Joint Range of Motion	11
2.1.2 Gripping Patterns	14
2.1.3 Grip Force Versus Hand and Wrist Position.....	15
2.2 GRIP STRENGTH.....	17
2.2.1 Grip Strength Measurements.....	17
2.2.2 Factors that Influence Grip Strength	19
2.2.2.1 <i>Gender Differences</i>	19
2.2.2.2 <i>Anthropometric Trends Related to Grip Strength</i>	19
2.2.2.3 <i>Age</i>	20
2.2.2.4 <i>Dominant versus Non-Dominant Hand</i>	20
2.2.2.5 <i>Handle or Object Size</i>	21
2.2.2.6 <i>Glove Use</i>	21
2.3 GRIP FORCE IN SPORT.....	22
2.3.1 Golf.....	22
2.3.2 Tennis	25
2.3.3 Cricket.....	26
2.3.4 Baseball.....	27
2.4 SUMMARY.....	27
3.0 THIN, FLEXIBLE SENSORS FOR GRIP FORCE MEASUREMENT	29
3.1 SENSOR CRITERIA FOR GRIP FORCE STUDIES	29
3.2 THIN, FLEXIBLE FORCE SENSORS.....	30
3.2.1 Tekscan.....	30
3.2.2 Peratech.....	31
3.2.3 Novel	32
3.2.4 Pressurex.....	32
3.3 SENSOR EVALUATIONS.....	33

3.3.1	Sensors.....	33
3.3.2	Calibration.....	34
3.3.3	Static & Quasi-Static Tests	35
3.3.3.1	<i>Quasi-Static Accuracy and Hysteresis Test</i>	36
3.3.3.2	<i>Static Repeatability and Drift Tests</i>	37
3.3.3.3	<i>Curved Surface Test</i>	39
3.3.3.4	<i>Comparison with Data from Literature</i>	40
3.3.3.5	<i>Shear Test</i>	41
3.3.4	Dynamic Tests.....	42
3.4	DISCUSSION	46
4.0	GRIP FORCE PLAYER TESTING – PRELIMINARY STUDIES	49
4.1	SYNCHRONIZATION AND IMPACT TIMING.....	49
4.1.1	Tekscan Video Synchronization System	49
4.1.2	High Speed Video and Light Gates	50
4.1.3	Sound Level Meter and Light Gates.....	51
4.2	PILOT TESTS.....	52
4.2.1	Pressurex Film – Relative Pressure Distribution	52
4.2.1.1	<i>Film on Golf Grip*</i>	52
4.2.1.2	<i>Film on the Hands</i>	54
4.2.1.3	<i>Discussion</i>	54
4.2.2	Six-Sided Grip* Test	55
4.2.2.1	<i>Sensor Application</i>	55
4.2.2.2	<i>Test Design</i>	55
4.2.2.3	<i>Analysis & Results</i>	56
4.2.3	Lessons Learned.....	57
5.0	GRIP FORCE MEASUREMENT IN GOLF	59
5.1	SENSOR CHOICE AND APPLICATION PROCEDURE.....	59
5.1.1	Tekscan 9811 Sensor on Golf Grip*.....	59
5.1.2	Flexiforce Sensors on Gloves	60
5.1.3	QTC Sensors on Gloves.....	60
5.2	GOLF GRIP FORCE TEST DESIGN	61
5.2.1	Tekscan 9811	61
5.2.2	Flexiforce.....	62

5.2.3	QTC.....	62
5.3	RESULTS.....	62
5.3.1	Sensor Degradation.....	63
5.3.2	Thin-Film Sensor Usability.....	63
5.3.3	Analysis Methods.....	64
5.3.4	Tekscan 9811.....	65
5.3.5	Flexiforce.....	68
5.3.6	QTC.....	75
5.3.7	Comparison of Results.....	77
5.3.8	High Speed Video.....	78
6.0	VIBRATION TRANSMISSION AND MEASUREMENT.....	81
6.1	VIBRATION IN THE HAND-ARM SYSTEM.....	81
6.1.1	Vibration Perception.....	84
6.2	VIBRATION AND GRIP FORCE.....	87
6.3	VIBRATION TRANSMISSION THROUGH SPORTS EQUIPMENT.....	88
6.3.1	Measuring Vibration Perception in Golf.....	90
6.4	VIBRATION MEASUREMENT.....	90
6.4.1	Linear Vibration Measurement at the Grip*.....	91
6.4.2	Torsional Vibration.....	93
7.0	GRIP FORCE, VIBRATION TRANSMISSION, AND PLAYER PERCEPTION.....	97
7.1	TEST METHODS.....	97
7.1.1	Force Sensors.....	97
7.1.2	Vibration.....	98
7.1.3	Clubhead Speed.....	99
7.1.4	Impact Location.....	99
7.1.5	Player Perceptions.....	100
7.2	TEST SET-UP AND PROCEDURE.....	100
7.3	DATA ANALYSIS AND RESULTS.....	101
7.3.1	Grip Force.....	101
7.3.2	Vibration.....	106
7.3.3	Force and Vibration.....	109
7.3.4	Player Perception.....	111

7.3.5	Vibration and Perception	112
7.3.6	Summary.....	113
8.0	COMPARING GRIP FORCE WITH A PROFESSIONAL GOLFER.....	115
9.0	RECOMMENDATIONS & CONCLUSIONS.....	119
9.1	RECOMMENDATIONS FOR FURTHER WORK	119
9.1.1	Relating Grip Force to Motion.....	119
9.1.2	Grip Force Measurement	119
9.2	CONCLUSIONS.....	120
	REFERENCES	123
	FIGURES.....	129
	APPENDIX 1 – MAXIMUM GRIP AND PINCH FORCE SUMMARY	223
	APPENDIX 2 – GRIP FORCE IN SPORT SUMMARY.....	225

LIST OF FIGURES

CHAPTER 1

Figure - 1.1 Three primary golf grips

CHAPTER 2

Figure - 2.1 Anatomical features of the right hand (anterior view)

Figure - 2.2 Joints of the hand

Figure - 2.3 Directions of finger motion

Figure - 2.4 Total or global motions of the wrist

Figure - 2.5 Typical grip and pinch patterns

Figure - 2.6 Modified thumb crotch length as defined by Eksioglu (2004)

Figure - 2.7 Grip pressure for three professional and three amateur golfers (Budney 1979)

Figure - 2.8 Grip pressure for a professional golfer (Budney and Bellow 1990)

Figure - 2.9 Golf grip force (Macht 2000)

Figure - 2.10 Forces exerted on hands during golf swing (Nikonovas et al. 2004)

CHAPTER 3

Figure - 3.1 Tekscan 9811 sensor and details from manufacturer

Figure - 3.2 Tekscan Flexiforce single load cell type sensor and details from manufacturer

Figure - 3.3 Simple circuit used with Flexiforce sensors

Figure - 3.4 QTC sensor and electrode

Figure - 3.5 Novel Pedar wireless pressure measurement system

Figure - 3.6 Calibration curves for (a.) Tekscan 9811, (b.) Flexiforce and (c.) QTC sensors

Figure - 3.7 Pressurex calibration curve, with colour intensity values

Figure - 3.8 Results from one set of Pressurex film calibration

Figure - 3.9 Results from quasi-static accuracy test of Tekscan 9811, Flexiforce, and QTC sensors

Figure - 3.10 Novel results from quasi-static accuracy test

Figure - 3.11 Example Tekscan 9811 test applied versus measured force for hysteresis calculation

Figure - 3.12 Static drift test example results

Figure - 3.13 Flexiforce output of one sensor during a single curved surface test

Figure - 3.14 Shear force test set-up

Figure - 3.15 Shear force test example results

Figure - 3.16 Dynamic test set-up

Figure - 3.17 Tekscan 9811 sensor output in response to an applied dynamic load of 15 N at 60 Hz

Figure - 3.18 Flexiforce dynamic test results

CHAPTER 4

Figure - 4.1 Sound level meter and golf club with 6-sided grip* and 9811 sensor near tee on astroturf matt

Figure - 4.2 Typical sound level meter output at impact

Figure - 4.3 Pressurex film on grip* prior to player test

Figure - 4.4 Pressurex on grip* test

Figure - 4.5 32 pieces of Pressurex film on hands

Figure - 4.6 Pressurex film after player test

Figure - 4.7 Tekscan 9811 sensor cut along columns, 6-sided grips* on standard drivers

Figure - 4.8 Total grip force from one player test with 30 shots taken with 9811 sensors on 6-sided grips*

Figure - 4.9 Sensor damage caused during player tests

Figure - 4.10a-c Total grip force results using 6-sided grip*

CHAPTER 5

- Figure - 5.1 Tekscan 9811 sensor on standard golf grip* as used during player tests
- Figure - 5.2 31 Flexiforce sensors on two golf gloves
- Figure - 5.3 31 QTC sensors on two golf gloves
- Figure - 5.4 Schematic of QTC electrode for measuring at three locations per finger
- Figure - 5.5 Example of the seven photographs taken after the completion of each 9811 grip force test
- Figure - 5.6 Player test set-up for Flexiforce and QTC tests
- Figure - 5.7a-b Total force from 10 shots taken by golfers and with 9811 sensor on grip*
- Figure - 5.8 Mean total grip force from 9811 test for four golfers with high cross correlation values
- Figure - 5.9 Peak and RMS total mean grip force versus handicap for Tekscan 9811 sensor on grip* tests
- Figure - 5.10 Total grip force traces produced in study by Budney and Bellow (1990)
- Figure - 5.11 Twelve total force traces for three golfers as measured by Flexiforce sensors
- Figure - 5.12 Twelve left thumb force traces for three golfers as measured by Flexiforce sensors
- Figure - 5.13 Mean total, left hand and right hand grip forces for 20 golfers measured with Flexiforce sensors
- Figure - 5.14 Mean total grip force for three golfers with high cross correlation values
- Figure - 5.15 Mean left hand grip force for three golfers with high cross correlation values
- Figure - 5.16 Mean right hand grip force for three golfers with high cross correlation values
- Figure - 5.17 Left hand forces from Flexiforce tests
- Figure - 5.18 Right hand forces from Flexiforce tests
- Figure - 5.19 Grip force at specific locations indicated as key by golf instructors
- Figure - 5.20 Peak and RMS total mean grip force versus handicap for Flexiforce sensor on grip* tests
- Figure - 5.21 Grip force from Flexiforce on gloves test in regions considered by Budney and Bellow
- Figure - 5.22a-b QTC grip force results for several golfers
- Figure - 5.23 Mean total grip force curves for three golfers with highest cross correlation values from QTC grip force test
- Figure - 5.24 Total grip force traces from eleven consecutive shots taken by player f measured by QTC sensors on gloves
- Figure - 5.25 Normalised mean total force traces from 9811, Flexiforce and QTC player tests
- Figure - 5.26a-c Flexiforce sensor player test results with high speed video data
- Figure - 5.27 Six key points on the total grip force curve for golfer a with corresponding still images

CHAPTER 6

- Figure - 6.1 Power spectra of shaft and grip vibration for central impacts with a Callaway Great Big Bertha (Roberts 2002)
- Figure - 6.2 Directions of vibration (Reynolds and Keith 1977)
- Figure - 6.3 Grip types; (a.) finger grip and (b.) palm grip (Reynolds and Keith 1977)
- Figure - 6.4 Cross-section of the skin (Griffin 1990)
- Figure - 6.5 Equal sensation and vibration perception threshold contours (Miwa 1967)
- Figure - 6.6 Vibration threshold and annoyance curves; finger grip (Reynolds et al. 1977)
- Figure - 6.7 Vibration threshold and annoyance curves, palm grip (Reynolds et al. 1977)
- Figure - 6.8 Grip* adapter used by Roberts et al. (2002; 2005; 2006) to measure acceleration in two directions
- Figure - 6.9 Transfer functions for 12 subjects; 10 mm diameter contactor under centre of fingernail, 2 N force, 0.5 g accelerometer, finger straight (Mann 1994)
- Figure - 6.10 Effect on transfer functions of mass added to the fingernail (Mann 1994)

- Figure - 6.11 Effect of variation of feed force on transfer functions; (Mann 1994)
- Figure - 6.12 Transmissibilities between the handle and the fingernail for subjects pulling at the handle with a force of 30 N (Paddan 1997)
- Figure - 6.13 Transmissibilities between the handle and the fingernail for the subjects pulling at the handle with five different pull forces (Paddan 1997)
- Figure - 6.14 Shaft vibration adapter and adapter on club just below grip*
- Figure - 6.15 Power spectra of angular displacement as measured on the shaft below the grip*

CHAPTER 7

- Figure - 7.1 Location for 18 Flexiforce sensors used in final set of player tests
- Figure - 7.2 Thumbnail block adapter
- Figure - 7.3 Diagram of thumbnail block adapter
- Figure - 7.4 Laser light gates positioned just behind tee to capture clubhead speed at impact
- Figure - 7.5 Mean total, left hand and right hand grip forces for 16 golfers measured with 18 Flexiforce sensors
- Figure - 7.6 Left hand forces from final Flexiforce tests
- Figure - 7.7 Right hand forces from final Flexiforce tests
- Figure - 7.8 Normalised mean total grip force for golfers participating in both Flexiforce test
- Figure - 7.9 Ten total force traces for three golfers as measured by Flexiforce sensors in final test
- Figure - 7.10 Ten left thumb force traces for three golfers as measured by Flexiforce sensors in final test
- Figure - 7.11 Peak and RMS total mean grip force versus handicap for final Flexiforce sensor on glove tests
- Figure - 7.12 Example vibration measurements at both left thumb and shaft
- Figure - 7.13 Typical torsional vibration measurements for (a.) toe, (b.) central and (c.) heel impacts
- Figure - 7.14 Total RMS linear vibration at the thumb as a function of impact location
- Figure - 7.15 Total RMS linear vibration at the shaft as a function of impact location
- Figure - 7.16 RMS torsional vibration as a function of impact location
- Figure - 7.17 Magnitude of first peak in angular acceleration trace as a function of impact location
- Figure - 7.18 Mean combined RMS linear vibration measured on the left thumb
- Figure - 7.19 Power spectra for clubs A and B, accelerometers on the shaft and left thumb
- Figure - 7.20 Power spectra of three golfers for clubs A and B, accelerometers on the shaft and left thumb
- Figure - 7.21 Total force trace from 18 Flexiforce sensors for 3 golfers
- Figure - 7.22a-c Transmissibility and coherence for several shots taken by three golfers
- Figure - 7.23 Mean vibration ratio for several shots by each golfer and mean force from distal thumb sensor during -0.3 to 0 s
- Figure - 7.24 Mean vibration ratio versus mean grip force for time interval -0.3 s to impact
- Figure - 7.25 Mean values for five 'feel' characteristics from golf impacts
- Figure - 7.26 Mean combined RMS vibration measured on the left thumb
- Figure - 7.27 Mean torsional vibration level

CHAPTER 8

- Figure - 8.1 Twelve total force traces produced with 18 Flexiforce sensors on gloves by a professional golfer
- Figure - 8.2 Mean force traces produced by a professional golfer with 18 Flexiforce sensors on gloves
- Figure - 8.3 Mean total grip force curves for two golfers with highest cross correlation values when compared to a professional

- Figure - 8.4 Mean left and right hand grip force curves for two golfers with highest cross correlation values when compared to a professional
- Figure - 8.5 Individual finger forces for a professional golfer measured by 18 Flexiforce sensors
- Figure - 8.6 Grip force of professional golfer measured by Flexiforce sensors on gloves in regions considered by Budney and Bellow
- Figure - 8.7 Images of professional golfer at five points during the swing as noted in the total grip force traces

CHAPTER 9

- Figure - 9.1 Comparison of total grip force and shaft deflection for a single golfer

MEASUREMENT OF GRIP FORCE AND EVALUATION OF ITS ROLE IN A GOLF SHOT

ABSTRACT

This study was conducted with the aim of establishing a method to measure time-varying forces at multiple locations at the hand-grip interface, using this method to record how golfers of varying abilities grip the club during a standard tee shot and investigating a potential link between the variations in vibration seen at the grip and the grip force applied near impact. It is hoped that additional knowledge about grip force during a golf shot will lead to improved training techniques and grip design in the future.

An assortment of technologies were available for the measurement of grip force, but thin-film sensors were chosen as they could be applied to the grip or gloves without altering the characteristics of the club. Reliability and performance for these sensors were not well established and, therefore, a novel set of tests were developed to evaluate their capabilities. Thin-film force sensor performance was examined under controlled laboratory conditions to give an indication of each sensor's quasi-static accuracy, hysteresis, repeatability and drift errors, dynamic accuracy and drift errors, and the effects of shear loads and surface curvature. With this newly developed set of tests, five varieties of thin-film force sensor utilizing four different technologies were assessed.

The sensors had varying levels of success under the controlled conditions of the evaluation tests. Three of the sensors performed well under static and quasi-static loading conditions, with accuracy errors of 10% or less, hysteresis errors near 6%, repeatability near 6% or below, and drift at 60 s after load application under 15%. Two of these sensors were further tested and demonstrated little change in sensor output to loads applied over curved surfaces, although shear sensitivity and dynamic accuracy errors were more substantial. It was also found that some of the sensors lost sensitivity with repeated loading. Even with these drawbacks, the potential of these sensors to provide useful grip force information was clear.

With an understanding of sensor performance in controlled laboratory settings, one sensor type was used to determine regions of peak pressure at the hand-grip interface and three others were used in player tests to obtain time-varying measurements of grip force during a swing. During the player tests, grip force was measured for 10-12 tee shots and impact time was determined. Total force was computed for each shot taken by summing the force output of all the sensing elements positioned on either the grip or gloves. When these total force traces were aligned by impact and plotted for each of the golfers tested, an interesting and previously

unreported phenomenon became apparent. Each player appeared to have their own grip force 'signature', i.e. total grip force for a particular golfer was very repeatable, but varied considerably between golfers. A grip force signature existed for all players tested regardless of ability, and the level of consistency for an individual golfer and the similarities between golfers was analysed using a cross correlation. It was found that nearly all of the golfers tested had swings that were dominated by the left hand, and that the most notable contributions of the right hand occurred after impact. Variations in grip force were also related to key phases of the swing using high speed video footage.

Previously it has been noted that for the same ball, club, and impact location that the vibration on the shaft is remarkably consistent for many different golfers but there is a much greater variation in the vibration at the grip. It was hypothesized that the way a golfer grips the club affects the way vibration is transmitted into their hands and arms. A final set of player tests was therefore conducted with the aim of identifying how grip force affects vibration transmission from the shaft to the hands and the players' perceptions of this vibration. Vibration was measured on the shaft just below the grip and on the golfer's left thumbnail, force was monitored at 18 locations on the hands, and impact location and clubhead speed were recorded. Each golfer's perceptions of the vibration caused by impact were also noted for two standard drivers. It was found that changes in the amount of vibration travelling from the shaft into the hands is affected by the grip force applied by the golfer. This is the first study to analyse the effects of grip force on vibration transmission into the hands and arms due to a golf impact.

ACKNOWLEDGEMENTS

I would like to start by thanking Professor Steve Rothberg and Dr. Jonathan Roberts who have shown me that it is possible to have supervisors who are both knowledgeable and personable. I could not have chosen a better pair to work for, and I feel indebted to you for the constant support and guidance you have provided throughout this project.

Thanks need to be directed to Nev Carpenter, Gareth Charles, Steve Carr and Rue Hallam for their assistance in developing various aspects of the testing systems used for this project. Alex Cork deserves credit for his help in collecting grip force data in early stages of the project, as does Tom Harper who contributed some of the high speed video presented. I am grateful also to a large number of golfers who have been incredibly willing to donate their time and talents to take part in these tests.

I have always known that when it comes to family and friends that I have been very blessed, and such knowledge is only strengthened during a project such as this. Having such a level of support and unconditional love has lessened my burden. A special thanks has to go to my parents who repeatedly told me as a young child that I could do “anything my heart desires” as long as I work hard. Their love and encouragement has instilled in me the confidence and drive necessary to complete this work.

And to Pauli, I will simply say this – thank you for the being my carer and comforter in moments of stress and distress, for helping me to celebrate my moments of success, and for promising to be a part of all those little moments in the future. Kiitos ja minä rakastan sinua.

1.0 INTRODUCTION

At the beginning of this century there were reported to be 30,000 golf courses and 55 million people playing golf around the world (Farrally et al. 2003). The Sporting Goods Manufacturers Association reported that, in 2003 in the United States alone, 27,314,000 people played golf at least once in the year and that the wholesale value of manufacturers' shipments of golf equipment was valued at over \$2.4 billion (Sporting Goods Manufacturers Association 2004a; Sporting Goods Manufacturers Association 2004b).

The scientific community has been showing interest in the game of golf for nearly half a century. The first landmark publication that officially discussed the sport in technical terms was Cochran and Stobb's *Search for the Perfect Swing* (1968). Since then, papers have been published on everything from the biomechanics of the golf swing to the aerodynamics of a golf ball. Research in these fields has led to improved performance by both high level and elite golfers. The changes in the equipment are evidenced by the shift away from wooden 'woods' and the decline in the use of wound golf balls (Farrally et al. 2003).

One area of the club that has not seen such drastic changes, however, is the grip. A golfer is provided with a few choices in grip material, with rubber, cord, Kraton, blended and leather grips created in either moulded or wrap-on styles. Based on what is written in some clubfitting guides, it appears that the effect of the grip is not wholly understood even by those professionally trained to match golf clubs to the players. Most clubfitters have simply come to the conclusion that the best grip for the player is the one that feels the best (Aldridge 1994; Jackson 1993; Lancaster 1994; Wishon 1996). It is surprising that so little is known about the grip, it remains the most inexpensive part of the club and has been researched the least considering it is the only point of contact that the golfer has with the club. To avoid confusion later in this text, the word used to describe the sleeve at the end of a golf shaft where the player holds onto the club will be written 'grip*' and when referring to the way a player grasps the club, it will be written simply 'grip'.

In addition to varying views on what type of grip* material and size to apply to the club, there is also a range of opinions on the type of grip (i.e. the position of the hands) and grip force that should be applied during the shot. Professional golfers, coaches and instructors have produced numerous books and articles addressing all factors in the game. There are disagreements over which technique is most advantageous for a particular shot, while much of the information provided that advocates a particular technique over others is based solely on personal opinion and experience (Hay 1993). Overall on the topic of grip, there is disagreement on who should use which grip style and when.

There are three main categories of grip that deserve mention. The overlapping (also called Vardon), interlocking and 10-finger (also called baseball) grips are mentioned in nearly all of the literature. Examples of these three grips can be seen in Figure 1.1, with the overlapping, interlocking and 10-finger grips in frames a, b and c, respectively. The overlapping grip is by far the most popular grip, and its use is recommended most often (Alliss and Trevillion 1969; Couples 1994; Hay 1980; Irwin 1980; Jacobs 1963; Leadbetter 1993; Leadbetter 2000; Lewis 1990; Locke 1954; Miller 1976; Nelson 1947; Palmer 1965; Snead 1961; Trevino 1976). However, many of those instructors and professionals who use or prefer the overlapping grip for themselves have mentioned that the other two grip types might be beneficial, especially for those with small or weak hands (Alliss and Trevillion 1969; Couples 1994; Irwin 1980; Jacobs 1963; Leadbetter 1993; Lewis 1990; Palmer 1965). There are also those golfers who favour the interlocking grip for a variety of reasons but they usually acknowledge that the other grip types might be preferable for others (Lopez and Wade 1987; Luxton 1985; Nicklaus and Bowden 1974). Many of the golf professionals and instructors believe that there is no one grip better than the others, but that each golfer has a grip that is best suited to him or her. Factors such as hand size, hand strength, and flexibility need to be considered before an optimum grip type can be determined (Alliss 1926; Cochran and Stobbs 1968; Cotton 1948; Torrance 1989).

Noble (1963a) approached the issue more scientifically, comparing what he termed the overlapping, natural and baseball grips. Eighteen male students took nine swings with each grip, and a measure of the power of the stroke was taken with a ballistic pendulum. The study revealed no apparent advantage of one grip over the others. It is hard to draw any firm conclusions from this experiment, however, as power is not the only important aspect of a golf shot and most of the subjects were only familiar with one of the grip styles.

Grip pressure during the swing has also been an area of debate amongst golf's instructors and professionals. The majority of the literature supports the idea of gripping the club firmly but gently – just tight enough to keep a grip on the club (Alliss and Trevillion 1969; Cochran and Stobbs 1968; Irwin 1980; Jacobs 1963; Leadbetter 1993; Leadbetter 2000; Lewis 1990; Locke 1954; Lopez and Wade 1987; Miller 1976; Palmer 1965; Wiren 1990). There are others, however, who believe that the best grip involves holding the club as lightly as possible (Couples 1994; Faldo and Saunders 1989; Luxton 1985), while still others favour gripping firmly above all else (Cotton 1948; Hay 1980; Nelson 1947; Nicklaus and Bowden 1974; Torrance 1989).

Additionally, there are varying views on where this grip pressure should be applied and how the roles of the left and right hands vary. In terms of distribution of grip pressure, many professionals and instructors feel that it is the last two fingers of the left hand and the middle two fingers of the right hand that push against the club the most (Faldo and Saunders 1989; Hay 1980; Lewis 1990; Luxton 1985; Nicklaus and Bowden 1974; Palmer 1965; Torrance 1989).

However, there are individuals who feel that the most pressure should be applied by the left thumb (since the right palm rests atop it) and the right index finger (Leadbetter 1993). In addition, some believe that the left hand should provide a firmer grip than the right (Couples 1994; Nelson 1947), whereas others feel it is the right hand that should be more firm (Faldo and Saunders 1989).

When reading gripping advice from golf's foremost performers and instructors, there is even more ambiguity when it comes to the roles of the two hands. Some say the left hand is more important or the guiding authority (Alliss 1926; Hay 1980; Lewis 1990; Trevino 1976), others say the two hands are equal (Alliss and Trevillion 1969; Leadbetter 2000; Wiren 1990), and still others believe that the left hand is meant for control and the right hand for power (Lopez and Wade 1987; Torrance 1989). There is also some inconsistency on which part of the hands should be gripping and, thus, controlling the club. One school of thought suggests that a golfer should grip primarily with the fingers of the right hand and the palm of the left hand (Hay 1980; Leadbetter 2000; Lewis 1990; Miller 1976; Snead 1961), while another group believes that since a better sense of feel can be produced in the fingertips than the palm, the club should be held in the fingertips of both hands (Alliss and Trevillion 1969; Faldo and Saunders 1989; Lopez and Wade 1987). With all of these varying viewpoints on correct grip position and pressure, it is apparent there is a need for better understanding of the golf grip.

Besides looking at grip force as a means to identify how and where the hands apply pressure to the club, it might also be a means of helping to understand vibration transmission from the grip* into the hands and arms. Vibration of equipment in sports that require the player to hold an implement to strike some object (e.g. golf, tennis, cricket, baseball, etc.) is often of interest for two main reasons. First, certain upper extremity injuries have been linked with hand-arm vibration from sports impacts, with one of the most common being lateral epicondylitis (tennis elbow) (Engel 1995; Hatze 1992; Henning et al. 1992). Second, the design of sporting equipment affects the way vibration travels through it, and, in turn, affects the vibration that the player will eventually feel. How the equipment feels in the hands of the player, especially during and after impact, can greatly affect how the equipment is viewed, whether it is desirable and of high quality or not (Hedrick and Twigg 1994; Hocknell et al. 1996; Roberts et al. 2006). With a huge consumer market for sporting goods, it is indeed very important that designers and manufacturers produce the right 'feel' in their equipment. This requires understanding of vibration transmission through the equipment, and how it will be perceived by those using it.

In golf, it has been found that vibration in the shaft of a club is relatively consistent between golfers but that there is a great deal of variability in the vibration at the grip* (Roberts 2002). This finding adds to the notion that grip force may affect the way that vibration travels through the shaft into the hands, but also leads to the question of how grip force can affect shot

performance. Besides quantifying grip force in a golf shot, questions of vibration transmission and players' perceptions will be considered in this research project.

There is currently a need for a measurement system that can accurately quantify grip force throughout the golf swing in order to answer these questions about vibration transmission, to aid in advancements of grip* design, and to potentially serve as an instructional tool. The objectives of this PhD are to conduct a comprehensive evaluation of potential force sensors suited for this task, to apply these sensors to the hand-grip* interface (on the grip*, gloves, or directly on the hands), and to measure grip force at multiple locations throughout the swing. These grip forces will then be appraised along with linear and torsional vibration measurements taken at the grip* and player perceptions of vibration. Comparisons will be made between golf shots and golfers.

Chapter 2.0 focuses on grip force research. Hand and wrist properties including joint range of motion and gripping patterns are discussed, as well as the relationship between hand and wrist position and grip force. Methods of measuring grip and pinch forces are considered, as well as how gender, age, handle size, and other factors influence maximal grip strength. The chapter concludes with an introduction into grip force measurement in sport, highlighting measurement methods and values obtained.

Chapter 3.0 examines the requirements of a sensor to measure grip force during golf, and introduces thin, flexible sensors as a viable option. A set of novel laboratory tests are introduced that evaluate sensor output under known static and dynamic loading conditions. The tests are used to compare several thin, flexible sensors prior to use in player tests.

A discussion of preliminary golf grip force player tests is included in Chapter 4.0. Methods of synchronising shots based on impact and results from some pilot studies are presented along with lessons learned.

Chapter 5.0 reviews three sets of player tests, each utilizing different grip force measurement technologies. Sensor performance and usability is considered, and grip force measurements are compared to those from previously reported studies.

Vibration transmission and measurement techniques are examined in Chapter 6.0. Hand-arm vibration is discussed, as well as vibration due to impacts in sports equipment. Methods of measuring both linear and torsional vibration are also considered.

Chapter 7.0 looks at a final set of player tests that incorporate grip force and vibration measurements along with golfer perceptions of vibration. The effect of grip force on vibration transmission into the hands and arms is evaluated and is compared between golfers.

Chapter 8.0 compares the grip force produced by a high level professional with that of the amateurs who participated in previous tests, and Chapter 9.0 gives recommendations for how

this work might move forward in the future and a summary of the conclusions that have been reached during the course of this project.

2.0 GRIP FORCE RESEARCH

Before one attempts to answer questions about grip force, an understanding of what the human upper extremity is capable of is required. This chapter provides information on the properties of the hand and wrist, including joint range of motion, basic gripping patterns, and the links between grip force and wrist position. Maximum grip force is discussed for various populations, with several external factors considered, and, finally, grip force in sports such as golf, tennis, cricket and baseball is examined.

2.1 HAND AND WRIST PROPERTIES

In order to better understand the grips used for a golf shot, it is important to first consider how the hand and wrist work during prehensile actions. Active control of the hand and wrist is produced via the coordinated movement of both intrinsic musculature (with origins in segments of the wrist and hand) and extrinsic musculature (with origins in the forearm and humerus). Such muscular control provides both stability and mobility during hand and wrist activities (Nordin and Frankel 2001). The human hand and wrist are truly remarkable in their versatility and utility, with a vast number of movements possible, both powerful and subtle. The thumb's opposition to the fingers, the 27 primary bones in each hand and wrist, the approximately 35 muscles that work across roughly twenty joints, and the particularly acute skin sensitivity on the palm and fingertips are some key factors leading to these exceptional abilities (Carlsöö 1972; Oatis 2004). A diagram of some of the key anatomical features of the hand is shown in Figure 2.1.

2.1.1 JOINT RANGE OF MOTION

To get a better idea of the movements available at the hand and wrist, numerous researchers have studied joint range of motion (ROM). Table 2.1 displays some typical values measured for the various joints in the wrist and hand. The numbers represent a large population spectrum, including variations in age, gender, and hand dominance. Based on the results from three such studies, Oatis (2004) indicates that age and gender appear to have only slight effects on ROM.

Table 2.1 Wrist and hand range of motion (Hamill and Knutzen 2003; Nordin and Frankel 2001; Oatis 2004)

Joint	Motion	Range of Motion	
Wrist (overall)	Flexion	60-100°	
	Extension	50-80°	
	Radial Deviation	15-35°	
	Ulnar Deviation	25-50°	
	Forearm Pronation	60-80°	
	Forearm Supination	60-85°	
Carpometacarpal 1 st (thumb)	Flexion-Extension	50-80°	
	Flexion	15°	
	Extension	20-80°	
	Abduction-Adduction	25-80°	
	Rotation	10-15°	
	2 nd -3 rd (index, middle)	-	Nearly immobile
4 th (ring)	Flexion-Extension	10-30°	
5 th (little)	Flexion-Extension	10-30°	
Metacarpophalangeal	1 st (thumb)	Flexion	30-90°
		Extension	15°
	2 nd (index)	Flexion	70-100°
		Extension	25-60°
	3 rd (middle)	Abduction-Adduction	20°
		Flexion	70-100°
	4 th (ring)	Extension	25-55°
		Abduction-Adduction	20°
	5 th (little)	Flexion	70-105°
		Extension	25-60°
	2 nd -5 th (little)	Abduction-Adduction	20°
		Flexion	70-110°
		Extension	25-60°
	Abduction-Adduction		20°
		Interphalangeal 1 st (thumb)	Flexion
Extension			0-35°
2 nd -5 th PIP (fingers)	Flexion		105-110°
2 nd -5 th DIP (fingers)	Extension	10-20°	
	Flexion	70-90°	
Extension	0-25°		

Not included in Table 2.1 is any mention of wrist angle when finger joint angles were measured and vice versa. Many of the muscles that control the motion of the most distal segments of the fingers originate in the forearm. A muscle influences every joint it traverses; consequently the finger flexor muscles flex the wrist, metacarpophalangeal (MCP) joint, and the proximal and distal interphalangeal joints (PIP and DIP). Figure 2.2 depicts these joints of the

hand. Conversely, the extensor muscles extend all of these joints as well. If the flexor muscles are permitted to flex across each joint they cross in the fingers and wrist, they will reach their maximally shortened length (each muscle has a maximum shortening capacity determined by the length of its fibres) prior to rotating the joints through their complete excursions. An easy way to see this in action is to try to make a fist (i.e. flex the hand/finger joints) while the wrist is flexed maximally. The motion is difficult and causes discomfort on the volar (palmar side) and/or dorsal (back) surface of the forearm. Alternatively, it is not easy to extend the fingers when the wrist is maximally extended (see Figure 2.3 for directions of finger joint motion and Figure 2.4 for directions of all wrist motions). The difficulty of these tasks is in part caused by two factors. The first of these is active insufficiency, which means that a biarticular muscle (i.e. one that crosses more than one joint) is unable to create enough tension to sufficiently shorten to allow full ROM in both joints simultaneously. The second problem is termed passive insufficiency, and means that a biarticular muscle cannot stretch enough to complete the full ROM in both joints concurrently (Oatis 2004). This type of incident is not just limited to the hand and wrist, but can be seen in most places where a muscle crosses several joints. A further example in the upper limb could include the wrist extensors which act over and create movement at the elbow. Again, the position of the elbow joint is influential on wrist extensor function (Hamill and Knutzen 2003). Consequently, the range and ease of motion for a given joint in the hand and wrist can be affected by the position of the other joints.

The body does, however, have strategies to eliminate or reduce active and passive insufficiency. There are dedicated wrist muscles that are active when the extrinsic muscles of the fingers are contracted. The well-developed pattern of finger and wrist synergy was noted by Oatis (2004) in observations of an individual opening and closing their fist. While the fingers flex and close in a tight fist, the wrist automatically extends. Wrist extension takes place during finger flexion to preserve sufficient length of the finger flexors, permitting closure of the fingers. Additionally, the wrist extension gives the extensor tendons enough slack to allow required finger flexion excursion. Likewise, the opposite occurs when the wrist flexes - the fingers extend.

This hand and wrist synergy is interesting when considering the grip taken during a golf swing. There is a great deal of wrist action during the swing, making finger position an important consideration in allowing ease of motion in the wrist. Additionally, hand and wrist position can have a significant effect on potential grip strength, as will be discussed in later sections.

2.1.2 GRIPPING PATTERNS

Due to the versatility previously mentioned, humans have the ability to utilize a diverse assortment of grasping patterns, which are usually classified based on finger and thumb position, the contact area, and the force required. Two categories of grip are traditionally recognized, usually under the titles of precision and power grip, or something comparable (Carlsöö 1972; Hamill and Knutzen 2003; Nordin and Frankel 2001; Oatis 2004). Examples of the most common types of grip can be seen in Figure 2.5.

The precision grip, usually divided into sub-categories of pinch type, is typically performed with an object held between the thumb and the distal, palmar sections of the fingers. As the name indicates, this type of grip is typically used for manipulating objects in a finely controlled manner. A whole variety of precision grips or pinch types are available as the need arises. Four categories tend to be fairly representative of those available, and include the tip-to-tip (or just tip), pulp-to-pulp (sometimes called pulp 2 and pulp 3), lateral (or key) pinch, and the chuck (or three-point chuck) pinch. The tip pinch is a grip between the most distal portions of the thumb and index finger. A pulp pinch indicates a pinch grip where force is generated between the pad of the thumb and pad of the finger. Pulp 2 and pulp 3 describe the finger used in the pinch, either the second (index) or third (middle) digit. The chuck pinch is a grip between the pads of the thumb and the pads of both the index and middle fingers. The lateral pinch occurs between the pad of the thumb and the radial side of the index finger's middle phalanx (Dempsey and Ayoub 1996). In most of these pinch activities, the wrist maintains a position of extension, and the thumb is moved into a position of opposition with the index and sometimes middle finger (Oatis 2004).

The power grip is characterized by the involvement of a larger portion of the hand than in the precision grip. Typically, all of the fingers and portions of the palm are utilized, with the object being grasped between the fingers and palm. In this case, larger available force outputs are substituted for precise motion control. When a powerful grip is required, the fingers tend to flex more, with a fist arrangement with the MCP, PIP and DIP joints flexed being the most powerful (see Figure 2.2 for a description of the finger joints). A further way to identify a powerful grip is by noting thumb location. If the thumb stays in an adducted position in the plane of the hand, a power position is produced (Hamill and Knutzen 2003). If precision needs to be added to the power grip, the thumb will shift its contact location to the side of the index finger, and will come into contact with the object being grasped rather than the dorsum (back) of the clenched fingers (Rosse and Gaddum-Rosse 1997). The exact position of the thumb and fingers relative to one another will be determined by the size and shape of the object as well as the overall objective for the grip. Even characteristics of the object such as weight, temperature, moisture level, and consistency affect the grip chosen (Carlsöö 1972).

As one might expect, there is no clear demarcation for where the precision grip ends and a power grip begins. Certain prehensile actions require aspects of both power and precision grips, and golf is certainly no exception. The ultimate goal of the golf swing is to have the clubface arrive to the ball perpendicular to the line of the shot at impact with the maximum clubhead speed (for long distance shots). Such goals demand both power and precision, and as such, the grip should reflect this. A golf grip bears some resemblance to portions of the power grip and key pinch. In golf, fingers 2-5 on both hands are all flexed at the MCP, PIP, and DIP joints, which is typical of a power grip. Additionally, there is some contact made between the club and the palms of the hands, though this is more evident in the left hand. However, the golf grip deviates from the power grip in a number of areas. First, during a power grip on a cylindrical object, all of the phalanges of the thumb and fingers align themselves more or less perpendicularly to the long axis of the cylinder, with the thumb opposing the fingers. In golf, the club is placed diagonally across the palms, changing the angle that the fingers wrap themselves around the club. Second, the thumb takes on a completely different role in golf than in a power grip. It is the position of the thumbs that gives the golf grip its precision grip feel. These are only general observations that represent most grip types, but as the ideal grip style for a golf shot is currently unknown, it is not surprising that with the gripping abilities of the hands that there are so many viewpoints on how best to grip the club. The following sections begin to discuss the relationship between grip and grip force, and measurements of grip force that have been taken in the past.

2.1.3 GRIP FORCE VERSUS HAND AND WRIST POSITION

Many of the muscles in the hand are extrinsic muscles that originate in the forearm. This causes the muscle to cross several joints and means that the ROM of a particular joint is dependent on other joint angles. The same dependency on joint angles exists for the maximum force that the various muscles of the hand and wrist can produce.

A firm grip involving maximal output uses the extrinsic muscles, while fine, precise movements, such as pinch, will use additional intrinsic muscles to refine the movements. Position of the wrist can augment or diminish the strength of grip. It has been found that situating the wrist in ulnar deviation increases the strength produced by the PIP and DIP flexor muscles to the greatest extent, followed by wrist hyperextension. Therefore, a grip that is taken with the wrist positioned in slight ulnar deviation and hyperextension can be strengthened, whereas the grip will be weakened if the wrist is put in a flexion position. Hamill and Knutzen (2003) mentioned that with 40° of wrist extension, grip strength is more than three times greater than when the wrist is at 40° of flexion. Others have reached similar conclusions, finding that both maximum grip and pinch force exertions are greater when the wrist is in a neutral or

extended position than when in flexion (Dempsey and Ayoub 1996; Hallbeck and McMullin 1993; Jung and Hallbeck 2002; Mogk and Keir 2003; Shih and Ou 2005). In general, it was found that a neutral wrist position was most suitable for producing peak maximum grip forces. Notably, neither wrist is typically flexed in a full golf shot before impact, giving the golfer more control over grip forces achieved.

Deviation from the neutral position in radial or ulnar directions at the wrist or pronation (rotation of the hand and forearm so that the palm faces downward when elbow is bent at 90°) or supination (rotation of the hand and forearm so that the palm faces upward when elbow is bent at 90°) of the forearm can also affect maximum grip and pinch forces. Mogk and Keir (2003) found that forearm posture did affect maximum power grasp, where less force was produced in pronation than in both supination and neutral positions, but this was only the case when the wrist was simultaneously flexed. Li (2002) found that peak forces from individual fingers and total grip force were reached at 20° of wrist extension and 5° of ulnar deviation when measuring force through nearly the full ROM in both directions. As wrist angles deviated from this position, grip force decreased but the effect of wrist position in the radial/ulnar deviation was less remarkable than in the flexion/extension direction.

As one might expect, the opposite of the above is true as well – larger grip forces inhibit wrist mobility. It is easy to move a relaxed hand either side-to-side in radial and ulnar deviation, or up and down in extension and flexion, and the complete ROM can be achieved. When the fist is tightly clenched, however, it becomes a lot more difficult to make these movements and ROM is decreased. This occurrence was noted by Noble (1963b) who looked at the effect of grip force on flexion, extension, and radial and ulnar deviation. Ten subjects performed maximum grip strength tests with a neutral wrist position, and maximum ROM was noted in each of the four directions mentioned. Afterward, the subjects were asked to maintain a grip force of 75, 50 or 25% of their maximum while maximum range of motion was again measured. Range of motion decreased quite substantially with increasing grip force in all four directions, as shown in Table 2.2.

Table 2.2 Percent reduction in range of motion when gripping at selected pressures; modified from Noble (1963b)

		Flexion			Extension			Radial Deviation			Ulnar Deviation		
% of Maximum Grip Force		75	50	25	75	50	25	75	50	25	75	50	25
% Reduction in ROM	Mean	64	44	25	64	40	18	58	21	5	71	34	14
	SD	16.8	18.5	15.4	18.4	13.2	9	25	16.8	10.7	24	19.7	15.6

This finding, that grip force and wrist motion are inherently linked, is clearly important when looking at the golf shot. During a full shot, both wrists will move in flexion-extension, radial-ulnar deviation, and both arms will move in pronation-supination. The golfer needs to apply a certain amount of grip force during the shot to accelerate and direct the club to impact, but smooth-flowing wrist motion is essential for creating a good shot. Again, it is apparent that understanding grip force during a golf shot will lead to a better understanding of what makes a desirable golf grip. The following section looks at how grip force has been measured previously.

2.2 GRIP STRENGTH

Grip strength, which can be defined as maximum grip force, has been a quantity of interest for scientists in many different fields. It is often used to help diagnose injury or evaluate the effectiveness of rehabilitation efforts. This past research is relevant to this investigation for two main reasons. First, several methods for measuring grip force have been developed and evaluated in these grip strength studies. These measurement methods and the means by which they were evaluated were considered when developing a grip force measurement system for this project. Second, the grip strength studies are useful because they provide maximum grip force data for various grip configurations and populations, which helps to determine the force range required for sensors to be suitable for applications in golf.

2.2.1 GRIP STRENGTH MEASUREMENTS

Researchers usually measure forces for several types of grip when studying hand strength. These grips typically represent the main categories of power and precision grip discussed earlier. Power grip, tip pinch, key pinch, and palmar pinch are among the most commonly measured, and examples of each are presented in Figure 2.5.

Grip and pinch strength have been measured in a number of different ways. In clinical settings, and in cases where maximum forces are desired under static conditions, off-the-shelf dynamometers (devices that measure muscular force or power) and pinch meters are very common (Bao 2000; Blackwell et al. 1999; Eksioglu 2004; Hallbeck and McMullin 1993; Mathiowetz et al. 1985; Mogk and Keir 2003; Nicolay and Walker 2005; Noble 1963b; Schmidt and Toews 1970). Others have made their own version of the dynamometer or pinch gauge by embedding load cells in some type of handle (commonly cylindrical) (Freund et al. 2002; Jung and Hallbeck 2002; Shih and Ou 2005; Turrell et al. 1999). Another method is to embed small cantilever beams equipped with strain gauges into handles of various types to measure either total grip force, force from specific phalanges, or total pinch force depending on the design of the device (Amis 1987; An et al. 1980; Chadwick and Nicol 2001; Dempsey and Ayoub 1996; McGorry 2001; Tsaousidis and Freivalds 1998). A final method of measuring grip force is by

using any one of a number of thin, flexible sensors placed on either a cylinder or glove. Examples of sensors used for such studies are the capacitive Novel sensors (Welcome et al. 2004), the force sensing resistors from Tekscan (Kong and Lowe 2005; Loskutovaa et al. 1998) and Interlink Electronics (Yun et al. 1992), or Fuji pressure sensitive film (Lee and Rim 1990).

Using off-the-shelf dynamometers, grip strength has been measured with mean maximum grip values over certain conditions and populations ranging from around 170-550 N (Bao 2000; Blackwell et al. 1999; Eksioglu 2004; Hallbeck and McMullin 1993; Mathiowetz et al. 1985; Mogk and Keir 2003; Nicolay and Walker 2005; Schmidt and Toews 1970). The conditions and populations represented include gender, age, handle size, and dominant or non-dominant hand. Individual maximum grip strength can be much higher than these values, which represent the mean of a particular group studied. Custom made dynamometers or other cylindrical devices for measuring grip force have also produced mean maximum grip strengths well within the range measured by standard off-the-shelf dynamometers (Chadwick and Nicol 2001; Tsaousidis and Freivalds 1998).

Thin film force sensors, although capable of measuring total grip force, have been used frequently to measure the contribution of individual fingers, sometimes being able to give information on the phalanges separately. Understanding the contribution of the different parts of the hand to maximum grip strength gives useful information about the capabilities of the fingers and how this might affect potential golf grip configurations and application of force. The middle finger has been shown to have the highest load generating capability, producing an average of 33-35% of total grip force. The index and ring fingers follow, with 23-30% of the total, and the little finger provides the least force with 14-15% of the mean maximum grip force (Kong and Lowe 2005; Lee and Rim 1990). Similar values have been produced using multiple load cells or several cantilever beams and strain gauges within a single handle to measure the contribution of the fingers - the index, middle, ring and little fingers produce 30-35, 30-31, 22, and 12-18%, respectively (Amis 1987; Freund et al. 2002). Additionally, Kong and Lowe (2005) have shown that each finger divides its own force production between the distal, middle, and proximal phalanges and the distal metacarpal head. These four locations produce 42, 24, 19 and 16% of the mean total force from each finger, indicating that the largest grip force capabilities come from the most distal segments of the fingers. Again, this can be important in analysing the golf grip, as certain types of grip rely on the fingertips to apply the grip force, whereas others require the palm, especially near the distal metacarpal heads, to be more involved.

The above values need to be viewed with caution, however. This data gives an insight into maximum force capabilities and relative force production for distinct portions of the hand, but it is important to note that these values were produced during maximum power grip force, something that is very unlikely to be emulated during a golf shot.

Further studies have been conducted that look at maximum force that can be produced during more precise gripping actions, namely pinch. Again the majority of studies use off-the-shelf pinch gauges, but a variety of custom devices have been utilized as well. These studies have shown mean maximum pinch strength varying from 34-90 N, depending again on population, right or left hand, gender, and pinch type used in the study (Dempsey and Ayoub 1996; Hallbeck and McMullin 1993; Shih and Ou 2005). This information can be used in much the same way as that from the maximum grip strength studies, giving clues as to the peak forces that the thumb, index and middle fingers might produce when taking on a posture for more precise gripping. For a summary of measurement methods used and peak forces attained, a table in Appendix 1 summarises the studies mentioned here.

2.2.2 FACTORS THAT INFLUENCE GRIP STRENGTH

As well as being highly dependent on forearm, wrist and hand positions, grip force has been found to vary due to gripping conditions (handle size, glove use, etc.) and individual characteristics (gender, body build, etc.). These variations are important to consider when looking at grip force in a golf swing because golfers come in many different forms, and trends such as these may explain variations in grip force noted in actual player tests. Therefore, this section will give a brief summary of the trends found with varying populations and gripping conditions.

2.2.2.1 *Gender Differences*

There is a clear gender difference in maximum voluntary grip force, either in the form of a power grip or any number of pinch postures. Females have been found to reach anywhere between 52-74% and 60-70% of male maximum voluntary force in power and pinch grips, respectively (Bao 2000; Dempsey and Ayoub 1996; Hallbeck and McMullin 1993; Kong and Lowe 2005; Mathiowetz et al. 1985; Mogk and Keir 2003; Nicolay and Walker 2005; Schmidt and Toews 1970; Shih and Ou 2005). It is noteworthy, however, that in many of these studies only a single grip diameter was used. As women tend to have smaller hands than men, a large grip or pinch span will give those with larger hands an advantage and may affect the numbers presented above.

2.2.2.2 *Anthropometric Trends Related to Grip Strength*

Studies have also been conducted trying to link a whole assortment of anthropometric parameters with grip and pinch strength. Schmidt and Toews (1970) found that grip force was directly proportional to height up to 191 cm (75 in) and to weight up to 98 kg (215 lbf). Nicolay and Walker (2005) have shown that, in general, forearm and hand measurements are better

predictors of grip strength than height and weight, but that height, weight, forearm circumference, palm width, and palm length are all strongly correlated. Of these measures, palm width was the most closely linked with maximum voluntary force. They also found that grip fatigue is not related to any of these anthropometric measures. Amis (1987) determined that for the 17 subjects that were tested, there was no link between grip strength and height, but there were small weak correlations with weight, hand size and forearm circumference. Other researchers have found that various hand measurements can be related to optimal grip span or handle diameter, which is determined in terms of maximum achieved grip force and/or perceived comfort. Kong and Lowe (2005) found that the optimal handle diameter was 19.7% of the user's hand length, and Eksioglu (2004) determined that optimal grip span should be in the range of modified thumb crotch length (TCLm, as defined in Figure 2.6) minus 2 to 2.5 cm.

Anthropometric measurements have also been linked to maximum pinch strength. Dempsey and Ayoub (1996) found that there were no correlations between pinch strength and female anthropometric measurements, but males had strong and statistically significant correlations with weight, hand length, and hand thickness.

2.2.2.3 *Age*

People of all ages play golf, and age is another attribute that has been linked to grip strength. Schmidt and Toews (1970) found that strength increased with age until the range of 30-32 years, and decreased thereafter. Mathiowetz and Kashman (1985) reached similar conclusions, showing that grip strength peaked in the 25-39 year age group for men and women. They also looked at age effects on pinch strength and found that maximum pinch force remained relatively stable until 59 years, and began a gradual decline thereafter. However, it should be noted that Hallbeck and McMullin (1993) performed a study looking at maximum grip and pinch strengths in three age groups (20-25, 40-45 and 60-65 years) and found no age effect on the force produced.

2.2.2.4 *Dominant versus Non-Dominant Hand*

As one might expect, most of the literature has shown that on average the dominant hand is stronger than the non-dominant hand. The non-dominant hand tends to generate both maximum grip and pinch forces that are 90-95% of those from the dominant hand (Hallbeck and McMullin 1993; Nicolay and Walker 2005; Schmidt and Toews 1970). This result, however, varied considerably between individuals. Schmidt and Toews indicated that 28% of those tested actually had a stronger non-dominant hand and Nicolay and Walker (2005) noted that non-dominant hand ranged from 33-135% of the dominant hand grip force.

2.2.2.5 *Handle or Object Size*

Another sub-set of grip strength research has measured forces at multiple parts of the hand while gripping cylinders and handles of various sizes. Most of these investigations have been for industries in which workers use various hand-tools. However, this work relates well to the golf grip scenario, and will give an indication of the maximum grip force individuals can create. Because grip force can change significantly with the size of the object being grasped, cylinder and handle sizes closest to a men's standard golf grip* of 24 mm (0.900 in) diameter at a location of 51 mm (2 in) down from the grip* cap are the focus.

Several studies that have looked at grip strength as a function of handle diameter have found the two to be inversely proportional to one another. This was the case for Amis (1987) who looked at cylinders ranging from 31-116 mm in diameter, Lee and Rim (1990) who considered diameters of 25.4-50.8 mm, and Kong and Lowe (2005) with cylindrical handles of 25-50 mm diameter. For these cases, the smallest handle size provided the greatest maximum voluntary contraction (MVC), and was between 25-30 mm in diameter.

Other studies, however, suggest that the optimal handle diameter should be considerably larger. Eksioglu (2004) studied optimum grip span relative to an individual's hand anthropometry for an isometric grasp. Nine diameters were used, separated at 0.5 cm intervals from the thumb's modified crotch length (defined as the distance from the middle furrow of the middle finger to the base of the thumb, denoted TCL_m and shown in Figure 2.6) to $TCL_m - 4$ cm. Based on perceived comfort, maximum voluntary grip, and muscle efficiency, the optimal handle span was in the range of $TCL_m - 2.5$ cm to $TCL_m - 2$ cm, which corresponded to a handle diameter of 61.33-66.33 mm for the twelve subjects tested. Blackwell, et al. (1999) looked at the effect of grip spans from 31.8-57.3 mm diameter on isometric grip force and the fatigue of one of the flexor muscles. They determined that the highest MVC was produced for handles in the range of 41.4-50.9 mm, and that handle size did not affect fatigue.

Similar studies have also linked pinch strength to grip width. Dempsey and Ayoub (1996) found that from pinch widths of 10, 30, 50 and 70 mm, the 50 mm pinch width produced the highest pinch force. Shih and Ou (2005) found that pinch strength increased as span increased for their entire tested region of 20-80 mm, but the magnitude of the increase lessened as the span got wider for both males and females.

2.2.2.6 *Glove Use*

Glove use also plays a factor in determining maximum grip force. With subjects wearing unlined leather gloves, Tsalousidis and Frievalds (1998) found that maximum grip force was reduced by 15% and the force development rate dropped by 24-38% when wearing the gloves. Hallbeck and McMullin (1993) looked at the difference in grip forces produced by a bare hand

and while wearing gloves classified as thermal, knit, reinforced knit, a layered combination of thermal and knit, and a layered combination of thermal and reinforced knit. The addition of the gloves significantly reduced the amount of force that could be exerted, and the bulkier and less form fitting the glove was, the greater the decline in force produced.

The above studies also looked at maximum pinch force with gloved hands and in both cases there was no significant difference between the gloved and bare hands. It has been suggested that much of the strength reduction in the power grip may be due to the bunching of material at the joints, interfering with the hand-grip* interface. This interference would have its greatest effect on digital flexion. Digital flexion is less pronounced in pinch than the power grip, so it is unsurprising that gloves do not hinder pinch to the same extent (Hallbeck and McMullin 1993). Most gloves used in golf are primarily for providing extra traction and to reduce blisters and calluses on the hands. Because it is not necessary for these gloves to provide protection or warmth, they tend to be more close-fitting and flexible than the average work glove. Although peak grip forces may be decreased by a small extent, it should be at the lower end of the values quoted. Additionally, if the glove used does indeed increase the friction between the hand and grip*, lower normal grip forces are required to keep the club from slipping out of the hand due to centripetal forces. Therefore, any decrease in peak grip force is likely balanced out by added traction.

2.3 GRIP FORCE IN SPORT

In sports that are played with the participant using an implement such as a club, bat, or racket to strike a ball or other object, gripping technique can greatly influence performance. In these sports, the athlete has only one point of contact with the implement – at the grip*. There are many ongoing debates among coaches about where, when, and how much force should be applied for various situations. Researchers have tried to quantify the grip forces in test scenarios that are as realistic as possible, but usually there are a number of assumptions that have to be made to overcome the shortcomings of the measurement technology available. The following sections describe the main developments in grip force measurement within sports research.

2.3.1 GOLF

To date, there have been few studies that have looked specifically at grip force during a golf swing. The major contribution has been by Budney (1979) and Budney and Bellow (1990), while some additional observations have been made by Cochran and Stobbs (1968), Macht (2000) and Nikonovas et al. (2004). These authors put forward similar reasons for why understanding grip force is important. Most notably, they explained how the range of motion and freedom of wrist actions are impeded when any object is gripped tightly in the hands. This

could be predicted based on the known relationship between grip strength and wrist position. Addressing this from a golfer's point of view, Cochran and Stobbs (1968) reported an apparently simplified version of the grip force versus wrist angle test. A summary based on ten people gripping a golf club at various fractions of their 'strongest possible grip' is shown in Table 2.3. Cocking and uncocking movements of the wrist are assumed to be motions of primarily radial and ulnar deviation, respectively, although this is not specified.

Table 2.3 The effect of grip on hand mobility (Cochran and Stobbs 1968)

Strength of Gripping	Range of Cocking-Uncocking Movement at Wrist	
	In Degrees	Percent of Maximum Range
Maximum (320 N)	0°	---
¾ Maximum	26°	32%
½ Maximum	57°	74%
¼ Maximum	70°	91%
Zero	77°	100%

While it has been shown that wrist mobility is lost with a tight grip, the grip must also produce centripetal forces in excess of 400 N (Mather 1994). Given these factors, it can be assumed that the ideal grip force for an individual player would vary during the golf shot. The range of ideal pressures would depend on individual characteristics such as strength, suppleness or agility of the wrists, and swing characteristics such as clubhead speed.

Budney first tried to quantify this ideal pressure region in 1979 with a steel-shafted driver that incorporated three force transducers. These transducers were located under the last three fingers of the left hand, the pincer fingers of the right hand, and under the left thumb. These locations were chosen as Budney felt they were representative of the area that controls the club during swing, where the right-hand thrust is generated late in the swing, and where the degree of wrist cocking was expected to be limited with increasing force, respectively.

In this study, a tubular aluminium handle, with openings for the force transducers (simply supported beams with metal foil electrical strain gauges bonded to the bottom surfaces), was covered with a thin layer of rubber latex and replaced the grip* on a golf club that was of equal weight. Strain gauges were also placed on the shaft near the clubhead to detect the exact moment of impact.

Grip forces for three professional golfers and three amateur golfers are displayed in Figure 2.7. Each of these six golfers played right-handed. For the professionals, during the downswing both the left thumb and right pincer fingers apply a short duration increase in force that peaks

about 50-60 ms before impact. The left hand grip pressure for these golfers appears to reach local maxima just before and after impact.

The results of a further, similar study by Budney and Bellow (1990) are shown in Figure 2.8. The plots show that the start of the downswing occurred approximately 0.25 seconds before impact, and it was indicated that most golfers take about one second from the start of the take away until impact. At the start of take away, a local maximum occurred in the two left-hand sensors, 27 N (6 lbf) in the hand and 13.5 N (3 lbf) in the thumb. At the top of the backswing, the left hand force increased to about 32 N (7 lbf) and a force of 58 N (13 lbf) on the left thumb was used to brake the backward motion of the club and to initiate the downswing. Pressure peaks then occurred during the downswing in both the right hand and left thumb. At 0.10 seconds before impact, a maximum of 80 N (18 lbf) was applied by the left thumb and at 0.05 seconds before impact, 35 N (8 lbf) was applied by the right hand. At impact both left hand transducers measured a force of 44 N (10lbf). Following impact, the transducer under the three fingers and the left thumb peaked again while the right hand force decreased to zero.

As part of a project to develop a mathematical model for the golf swing, Macht (2000) created golf gloves with thirteen Tekscan thin-film conductive ink sensors placed on each hand. Five of the sensors were attached to the distal phalanx of each finger and eight throughout the palm area. Grip force plots showing the summation of left and right hand forces, along with the finger forces, palm forces, and the thumb force of the left hand are shown in Figure 2.9. While it was not apparent if more than one test subject or trial contributed to the data given, the data did seem to display many of the characteristics shown by Budney and Bellow.

Examining total grip forces, the left hand maintained a higher force at all points for the duration of the swing than the right hand. Early peaks at about 0.6 s in the left hand, left palm and left thumb traces show that the motion of the backswing is stopped and the downswing is initiated by the left hand. Two larger peaks follow this, and it is assumed that the first is the same that Budney and Bellow (1990) noted that occurs just before impact. One interesting point to note, however, is that the magnitude of the maximum peak at the left thumb is about 16 N (3.5 lbf), which is much lower than the 80 N (18 lbf) found by Budney and Bellow. This may be due to differences in the active area of the sensors used by Macht.

A final study by Nikonovas et al. (2004), although not concentrating on golf, included golf grip force measurements in the evaluation of thin film force sensors. In this study, twenty Tekscan Flexiforce sensors were placed directly on each of the subject's hands. Figure 2.10 shows the forces that were measured on the left thumb and the proximal phalanges of the left and right hands. These curves seem to follow nearly identical trends to those described by Budney and Bellow, especially for the sensors under the right hand.

Although this research provides some good data for comparison, there have not been nearly enough players tested to draw any firm conclusions about typical grip pressures and how they vary between golfers. Questions in this research field still remain unanswered, such as how grip force affects shot accuracy, vibration transmission and the feel of a golf club, what the roles of the left and right hands are during the shot, which coaching theories about the grip are most accurate, and if there is a connection between grip force and handicap. Additionally, it appears that there are two main ways to approach measuring grip force – either monitor a number of locations to obtain information about force produced by specific parts of the hands, or look at the total grip force for each golfer. Although the latter is useful for noting when the largest forces are applied, it is desirable to note the contribution of different parts of the hand and in particular the fingers and parts of the palm. This was therefore a major consideration when force sensors were chosen for this study.

2.3.2 TENNIS

Grip forces during a tennis stroke have been studied to a greater extent than in golf, due mainly to the interest in common upper extremity injuries such as lateral epicondylitis (tennis elbow). As in golf, it has also been deemed desirable to determine the best grip pressures to apply before and after impact in order to create the best shot.

Several researchers have quantified the grip force applied in various match-like scenarios. Knudson and White (1989) used two force sensing resistors placed on a tennis racket handle to measure force at key locations during the tennis forehand drive. The sensors were positioned under the base of the index finger and the hypothenar eminence (beneath the last three fingers of the hand, as described by the authors). For three varsity and four professional tennis players, peak forces at the hypothenar eminence were found to be somewhat consistent, ranging from 5 to 71 N while the post-impact peak forces under the index finger were quite variable, ranging from 4 to 309 N. Knudson (1991) also studied the grip forces produced during a one-handed backhand. In this case, two miniature load cells were positioned on the handle, one at the base of the thenar eminence (fleshy base of the thumb) and one at the lower portion of the hypothenar eminence (locations of thenar eminence and hypothenar eminence are depicted in Figure 2.1). Average post-impact forces at both sensor locations were determined to be similar, at about 50 N. Peak forces produced at the thenar eminence were quite varied, ranging from 6 to 124 N.

Other researchers have investigated the effect of grip force in tennis but without actually quantifying it. Hatze (1976) fitted a tennis racket with strain gauges to record the impulsive forces caused by impact. It was determined that a reduction in grip force during and just after impact can lead to a reduction in unpleasant vibrational shocks occurring in the hands.

Watanabe et al. (1979) sought to determine the effect of grip force on ball velocity after impact and concluded that for any given velocity at impact, the ball velocity after impact is independent of grip force. Elliot (1982) also looked into the effect of grip force on post-impact ball velocity as well as reaction impulse but, in contrast to Watanabe et al., found that increased grip force leads to increased reaction impulse and rebound velocity, especially for off-centre impacts.

The main methods of measuring force during a tennis stroke have resembled those seen in golf, with thin flexible sensors, miniature load cells, or strain gauges being used for the task. Knudson and White (1989), who used the thin, flexible force sensing resistors, commented that these sensors were advantageous because they were small, non-invasive, resilient, inexpensive and can fit irregular surfaces. They also noted that this particular sensor suffers from nonlinearity and hysteresis, but with careful calibration this can be accounted for. Based on their evaluation, sensors of this nature deserve consideration for measuring grip force in a golf shot as well.

2.3.3 CRICKET

Like tennis, grip force on a cricket bat has been quantified for a number of different shot types. A standard cricket bat was equipped with two pressure sensors to measure the grip force of the top and bottom hands simultaneously. These pressure sensors used a piezoresistive element on an etched silicon diaphragm. The first study looked at the grip force when a player faced a medium-paced bowler on a turf pitch. During a forward defensive stroke the peak forces in the top and bottom hands were (mean \pm standard deviation) 129 ± 42 N and 74 ± 38 N, respectively (Stretch 1994). A second study used the same instrumented cricket bat along with a hand dynamometer to determine the grip strength of the subjects tested. The mean peak grip forces for players facing medium-fast paced bowlers on a turf pitch performing a drive off the front foot was 199 N for the top hand and 92 N from the bottom hand. It was also determined that no significant correlation could be made between maximal grip force and the peak forces exerted just before impact (Stretch et al. 1995).

A third experiment was conducted to analyse the front foot drive and the forward defensive stroke, the two most common strokes in cricket, and again the same instrumented bat was used. Similar values for grip force were found in the top and bottom hands for each stroke as in the previous studies, and it was shown that the top hand plays the dominant role during the execution of the drive, with the bottom hand reinforcing it at impact. From this analysis, it appears that the roles of the two hands in cricket are quite similar to the roles they play during a golf swing (Stretch et al. 1998).

The instrumented cricket bat used in this study adds another potential design that could be used on a golf club. In practice, however, this design might be more difficult to implement, as it

would likely mean replacing the top portion of the shaft and grip* with four solid pieces that have force sensors in each the top and bottom halves. The new grip* would need to maintain the same weight distribution as the original and the sensors would need to be placed carefully so that they would measure the force for each hand separately. Because the most common golf grips involve some overlap of the two hands, this would be a difficult task, compounded by the fact that golfers do not all hold the club in the same place. Therefore, although it is interesting to note the findings of these cricket studies so that their methods and results can be compared with those in golf, this is unlikely to be the best method for measuring grip force in golf.

2.3.4 BASEBALL

Grip research in baseball has been conducted by Eggeman and Noble (1985), who added two force transducers to the handle of an ordinary bat. The transducers were made of simply supported beams with strain gauges and located such that forces could be recorded at two locations on each hand. The data recorded from two swings of the bat revealed that, for a right-handed batter swinging at medium-speed fast balls going through the centre of the strike zone, the top hand peak forces were 340 N in the thenar eminence and 260 N at the fingers. On the bottom hand the peak forces were measured at 270 N and 180 N at the thenar eminence and fingers, respectively. Both regions of the top hand and the thenar eminence of the bottom hand showed peak forces occurring just before impact, similar again to the findings of other sports.

This method of measuring force has been shown to be successful in measuring grip force in golf by Budney and Bellow. There are limitations as to the number of locations where force can be measured, but it is a tried and tested technique that has been shown to produce reliable results.

2.4 SUMMARY

Grip and pinch strength have been discussed within a variety of study conditions. The golf grip is most closely related to a combination of the power grip and the key pinch. In a study that included over 1,200 test subjects, the mean maximum power grip strength was found to be 500 ± 70 N (Schmidt and Toews 1970). Maximum key pinch strength was found to exceed 180 N in some subjects as noted by Mathiowetz, et al. (1985). The aim in golf, however, is not to grasp the club as tightly as possible so, even with stronger individuals, the force should not reach these values. (Note that as two hands are applied during a golf shot total grip force could approach twice that of a single hand grip).

The middle and index fingers are capable of producing the most force, followed by the ring and then little finger. The most distal portions of the fingers generate the majority of this force. It is a grip with the fingers that offers the greatest tactile sensation and precision, but as long as

the most distal segments of the fingers have good contact with a golf club, it can be seen that considerable grip force can be generated.

A number of additional factors have been linked to maximum grip force. Men tend to have considerably higher grip strength than women and the dominant hand is marginally stronger than the non-dominant on average. Grip strength appears to peak when a person is in their thirties. Glove use can decrease maximum grip force, with thicker, bulkier gloves causing the largest decrement. The size of the object being grasped has a significant effect on total grip or pinch force, with peak forces being produced on handles just slightly wider than the top of a standard golf grip*. All of these factors individually or combined have the ability to affect the forces achieved during a golf swing.

Research into the role of the grip in golf has been limited to date, but research from other sports and from industry provides a good basis for future work. The table in Appendix 2 shows a summary of these grip force studies, including key values obtained. From this, a reasonable estimate can be made of the grip forces one might expect to see during a golf shot. Although maximum grip and pinch strengths were noted earlier, a more appropriate range of expected grip forces can be gathered by looking at the works of Budney, Bellow, Macht, Nikonovas and colleagues (Budney 1979; Budney and Bellow 1990; Macht 2000; Nikonovas et al. 2004). Around 165 N can be expected as the total force exerted by the left hand, with a local maximum of up to around 80 N at the left thumb. The right hand might produce a slightly lower total force, in the vicinity of 110 N. These expected grip force values will be considered when evaluating all potential sensors for future work on this project.

Additionally, a variety of sensors have been used to measure force applied during gripping. Most of those mentioned could be useful for looking at golf grip force, depending on the goals of the project. Key considerations in determining the best sensor include number of locations where force will be measured, force range, method of application on grip*, gloves or hands, and how much the sensors interfere with the natural feel of the club.

These studies also raise questions about potential test populations to use in a study. The majority of the players tested were either professional or high level amateurs. Although groups such as these might not represent the 'average' golfer, they tend to have a well-practiced technique that produces repeatable results.

3.0 THIN, FLEXIBLE SENSORS FOR GRIP FORCE MEASUREMENT

A variety of sensors are considered in the following chapter for the task of measuring grip force during a golf shot. A list of priorities is established that includes not altering the feel and shape of the golf grip and taking measurements at numerous locations simultaneously, and as a result thin-film force sensors are identified as the primary sensor category of interest. This section describes a number of thin-film sensors that are available commercially, introduces a set of novel tests to evaluate sensor response to various loading conditions, and gives a description of how several sensor types performed during these tests.

3.1 SENSOR CRITERIA FOR GRIP FORCE STUDIES

Grip force is measured in clinical and research settings for a host of reasons. In such studies, it is typical for real-life gripping scenarios to be recreated to determine entities such as maximum grip force and the effects of a given loading configuration on vibration transmission and wrist range of motion. The requirement to reproduce representative grip conditions means that it is vital that the force sensor used does not significantly alter the performance characteristics of the device that is being grasped or the operator's ability to use the device.

Force sensors are available in numerous formats, many of which are well suited to a typical cylindrical handle shape. Standard load cells are commonly used in hand dynamometers where force is measured in one direction, and miniature load cells or simply supported beams with strain gauges have been used to measure force at several locations simultaneously, but these methods of force measurement have limitations for grip force measurement. Spatial resolution tends to be poor as sensor size and rigidity make it difficult to apply multiple sensors to curved gripping surfaces, with this difficulty increasing with the complexity of surface geometry. Consequently, while load cells tend to be the most accurate and reliable force sensors available, it is not always feasible to use them when monitoring realistic gripping conditions (Amis 1987; An et al. 1980; Bray et al. 1990; Chadwick and Nicol 2001; McGorry 2001; Van der Kamp et al. 2001; Yun et al. 1992).

Thin, flexible force sensors have appeared as an alternative solution for many force measurement applications where load cells are not appropriate. These sensors fit easily over curved surfaces, are extremely light weight and are available in a wide variety of formats. For measurement of grip force, sensing elements can be placed on a glove, directly onto a hand, or onto a handle or grip* surface.

Table 3.1 lists some of the sensor characteristics considered and how the various sensor types fare in each category. Due to the versatility of the thin-film sensors, and the advantages they have over other sensors in terms of spatial resolution and adaptability, a further

investigation of these sensors took place. It is these thin, flexible force sensors that will be the focus for the remainder of this research project.

Although there are clear benefits to using thin-film force sensors for certain applications, sensor performance and reliability have been uncertain. In order to study the capabilities of an assortment of sensor types, researchers have conducted a variety of evaluation tests (Bachus et al. 2006; Buis and Convery 1997; Ferguson-Pell et al. 2000; Hsiao et al. 2002; Pavlovic et al. 1993; Polliack et al. 2000; Werner et al. 1995; Wilson et al. 2006; Wilson et al. 2003; Woodburn and Helliwell 1996). No single study, however, has provided a comprehensive analysis of performance under both static and dynamic loading, combined with information about sensor performance in realistic test environments. The purpose of this chapter is to examine several different thin-film force sensors under controlled laboratory conditions to give an indication of each sensor's quasi-static accuracy, hysteresis, repeatability and drift errors, dynamic accuracy and drift errors, and the effects of shear loads and surface curvature.

Table 3.1 Force Sensor Comparison (Ashruf 2002; Bray et al. 1990; The Institute of Measurement and Control 1998)

Sensor Type	Flexible	Spatial Resolution	Time-Resolved Measurements	Accuracy	Cost	Durability
Load Cell	No	Poor	Yes	High	Moderate	High
Miniature Load Cell	No	Moderate	Yes	High	Moderate	High
Cantilever Beams & Strain Gauges	No	Poor to Moderate	Yes	High to Moderate	Low	Moderate
Thin-Film Force Sensors	Yes	High	Yes, in most cases	Moderate	Varies	Low to Moderate

3.2 THIN, FLEXIBLE FORCE SENSORS

Several companies produce thin, flexible force sensors, using an assortment of technologies and producing sensors of various configurations. Such sensors will now be described in more detail.

3.2.1 TEKSCAN

Tekscan, Inc. has created a number of thin-film, flexible force sensors utilizing a semi-conductive ink that is applied between electrical contacts and thin polyester sheets with a resultant thickness of 0.1 mm. These sensors respond to a change in force with a linear change in resistance, which can be calibrated for. The sensors are available as a single load cell, called the Flexiforce sensor, or in a large variety of matrix configurations (Tekscan 2007). The matrix

sensors come ready-to-use with all necessary hardware and software, whereas the Flexiforce sensors are sold as sensors only and the user is required to create a suitable circuit and interface for gathering the data. Both varieties are relatively easy to use.

The hardware and software required to operate the matrix-based sensors cost in the region of \$10,000 (USD, system purchased 5 years ago), with additional matrix sensors costing less than \$60 (USD, current price). However, new, wireless systems are available and cost in the region of £13,000. The Flexiforce sensors do not require the purchase of any Tekscan hardware or software and sensors cost around \$100 (USD) for a pack of eight sensors.

The two Tekscan sensors tested in this study were a matrix configuration (F-Scan 9811, Figure 3.1) with a pressure rating from 0-517 kPa (75 psi) and a single load cell type (Flexiforce, Figure 3.2) with a force rating of 0-111 N (25 lbf, or 1556 kPa). Each 9811 and Flexiforce sensing element has a sensitive region with an area of approximately 50 mm² and 71 mm², respectively. The 9811 software automatically assumes the pressure in the non-sensitive regions between the sensing elements matches that in the adjacent sensitive regions. The 9811 sensor has a 6 by 16 matrix, or a total of 96 sensing elements. This particular sensor can be cut into 6 separate strips allowing it to be positioned on curved surfaces (such as a golf grip*) more easily. As mentioned previously, the Flexiforce sensor needs user-supplied circuitry, and the circuit used for all testing is a modified version of that recommended by the manufacturer and shown in Figure 3.3.

3.2.2 PERATECH

Peratech Ltd produce a pressure-sensitive material known as a quantum tunnelling composite, or QTC. This material changes from a near perfect insulator to a conductor when deformed. Compression, twisting or stretching of the QTC will all change its conductivity, resulting in a material that can be used for force measurement (Peratech 2007). QTC is available as a 1 mm thick rubbery material, called the Pill Substrate, and as an extremely thin paper-like substance referred to as Next Generation QTC (Next Generation QTC material was used in all sensor tests described in the following sections). QTC is less mature as a commercial technology and Peratech does not typically provide anything but the material for the creation of force sensors, so the circuitry and all other hardware or software needs to be created by the user. This has its advantages in that it allows the user to have complete control over sensor configuration and is partially responsible for the low price for the QTC (an A4-sized sheet of Next Generation QTC costs £40). Because the sensors need to be created by the user, this offers huge advantages in flexibility of creating sensors of almost any shape and size. The disadvantages of QTC include the time and cost for developing force sensors suitable for a given application, and non-linear sensor output. All of the QTC sensors used in the

performance studies had square electrodes (area 100 mm²), an example of which is shown in Figure 3.4.

3.2.3 NOVEL

Thin, flexible pressure sensors in both matrix and single load cell configurations are also available from Novel GmbH. A capacitive technology is used for these sensors, with the sensors being enclosed in various elastomeric materials rather than a thin film (Novel 2007). This material makes these sensors considerably thicker than those listed above (~2 mm), but also more durable. Sensors are available in an assortment of configurations with custom shapes a possibility as well. All Novel systems are completely wireless and cost approximately £13,000. The sensors, although more durable, cost in the region of £700 each.

For the sensor evaluation tests, a matrix configuration insole sensor (Pedar Insole Y, Figure 3.5) was used. This was a capacitive sensor, with 99 sensing elements and a pressure rating of 20-600 kPa.

3.2.4 PRESSUREX

Pressurex, a pressure sensitive film formerly known as Fuji Prescale Film, was the final sensor technology method considered. Unlike the systems previously mentioned, this film does not provide time-varying pressure measurements, but instead only shows the peak forces that occur during an event. Pressurex Ultra Low film was used during testing (quoted pressure range 193-586 kPa) and comes as two separate sheets, each made with very thin (0.102 mm) mylar film. By positioning the two pieces of film together correctly, the colour-forming material on the donor sheet is able to react with the colour-developing material on the receiver sheet. When pressure is applied to the sheets, a pink colour develops with increasing intensity as pressure rises. Sensor Products Inc., a supplier of the film, also sells a special scanner and software package to analyse the pressure distributions on used film but a simple flatbed scanner and image analysis software is all that is really required to analyse the film.

The Pressurex film costs \$59 (USD) per foot (0.3 m), or can be purchased as a whole roll (270 mm x 4 m) for \$565 (USD). Besides being relatively cheap, the film offers similar advantages as QTC because it can be cut to any size or shape and is capable of indicating force magnitudes everywhere the film is located. The main downfall of the system is that time-resolved information cannot be obtained. This makes the film unsuitable for the bulk of this research project, but the ease of use and peak force information can be useful in locating areas where other sensor types should be placed on the grip*.

3.3 SENSOR EVALUATIONS

As all of the above thin, flexible sensors could potentially provide useful information about the grip force used in golf, an investigation was conducted to make a more informed decision about which would best serve the purpose. This section describes a novel set of tests created to evaluate the sensors. Many researchers have approached this issue with varying degrees of complexity. A number of studies have investigated the thin-film sensors only in static conditions (Bachus et al. 2006; Ferguson-Pell et al. 2000; Hsiao et al. 2002; Matsuda et al. 1995; Polliack et al. 2000; Wilson et al. 2006; Wilson et al. 2003; Woodburn and Helliwell 1996), while others have included at least some mention of the dynamic performance of the sensors as well (Buis and Convery 1997; Otto et al. 1998; Pavlovic et al. 1993; Werner et al. 1995). Information such as accuracy, repeatability, hysteresis and drift errors and effects of surface curvature were typically given in the aforementioned papers. In all of these studies, however, none included all of the listed error measurements, considered the sensors in both static and dynamic conditions, evaluated the effects of shear loads, and gave information on sensor performance and degradation in real-life situations.

High sensor accuracy and repeatability and low drift and hysteresis errors are desirable in any situation where absolute values of force are required. In order to measure grip force in golf, a flexible sensor will be deformed to follow the contours of the hands or the golf grip* and it is important therefore that sensor output is not greatly affected by bending. Furthermore, it is desirable that the high shear forces that occur during a golf shot at the hand-grip* interface do not greatly affect sensor durability or the normal force measurements. As the golf swing is a dynamic event, with the downswing lasting approximately 0.25 s (Budney 1979; Budney and Bellow 1990), the grip force will vary considerably during that time. In order to properly evaluate the sensors available, therefore, a test scheme was developed that studied the sensors under both static and dynamic loading conditions and is described in the following sub-sections.

3.3.1 SENSORS

Five types of thin, flexible force sensors were subjected to a series of tests to ascertain their characteristics. The 9811, Flexiforce and QTC sensors utilize materials that change resistance with applied load, the Pedar Insole changes capacitance, the Pressurex sensor indicates regions of peak pressure based on colour intensity of burst miniature ink capsules. Because of the inability of the Pressurex sensor to produce anything but peak force information, it could not be used in the majority of the sensor evaluation tests.

For the actual sensor evaluations, three sensing elements on each of three 9811 sensors were used (for a total of 9 sensing elements tested), three regions on the Pedar sensor were assessed and four of each of the Flexiforce and QTC sensors were examined. A new piece of

Pressurex film was necessary for every test run. Tests were designed to measure quasi-static accuracy, hysteresis, repeatability and drift errors, the effects of shear force and surface curvature, and dynamic accuracy and drift. The Novel system was only available for tests measuring quasi-static accuracy, hysteresis, repeatability and drift errors.

3.3.2 CALIBRATION

Prior to the sensor evaluation tests, all sensors were calibrated. Manufacturer's guidelines were used where appropriate, and alternative calibration methods were developed when necessary.

For the 9811 sensor, calibration occurred in a two-step process referred to as equilibration and calibration (Tekscan 2004). For equilibration, a custom-made bladder device, which is made of a thin, flexible membrane, was pressurized against the sensor to apply an extremely uniform pressure of 310 kPa. The output from the 96 sensing elements was recorded and cell sensitivity variations were compensated for by scale factors in the software. Calibration then converted the raw digital output of the sensor into actual pressure or force units. For this, the bladder device was again used to apply a uniform load (310 kPa), and the Tekscan software matched sensor output to the chosen applied load and created a linear calibration curve running through zero, as shown in Figure 3.6a. The equilibration and calibration loads were chosen as approximately 60% of the maximum expected during the real grip force scenario of interest (a golf shot). During the course of testing the sensor, it was discovered that sensor drift during the calibration procedure introduced a systematic error to the measurements. A correction for this error is introduced later in § 3.3.3.2.

The Flexiforce and QTC sensors differ from the 9811 sensors in that they come with no circuitry or software produced by the manufacturer. Each was used as a single load cell and connected to custom circuitry that was designed based on sensor output in the expected load range. These sensors were calibrated by establishing the relationship between applied load and sensor output. Eleven weights ranging from 0.37 to 11.2 kg were applied to the sensors via a stainless steel cylindrical applicator (diameter 10 mm, sized to fit within the active area of the sensors) with a thin (2 mm) rubber layer on the surface in contact with the sensor. The compliant layer was inserted to ensure that the load was evenly distributed across the active sensing area, avoiding local high pressures at edges, for example. Prior testing had shown that thin film sensors do not react well to large loads applied through sharp edges. In the case of the Flexiforce sensors, the four sensors evaluated were stacked atop one another and calibrated simultaneously. Sensor output was recorded after each change of mass during at least four load-unload cycles. Output voltages from each sensor were plotted versus the known applied load and a linear curve fit passing through zero was applied to the Flexiforce data and a cubic curve

fit passing through zero was applied to the QTC data. These calibration curves were used to convert sensor output to units of force for all subsequent tests, and examples can be viewed in Figure 3.6b-c. The variations seen in sensor output are due mainly to hysteresis effects which will be discussed later. Additionally, like the 9811 sensor, it was found that sensor drift during the calibration procedure introduced systematic errors that needed to be corrected for.

Calibration of the Novel Pedar sensor was conducted by the manufacturer, using a bladder device similar to that employed for the Tekscan 9811 calibration. Calibration points were measured for each of the 99 sensing elements for several loads between 20-600 kPa.

In order to calibrate the Pressurex film, the same eleven loads used in the Flexiforce and QTC calibrations were applied to individual pieces of the film using an applicator with rectangular area (12.7 mm x 12.9 mm). After a force was applied, the two pieces of film (donor and receiver sheets) were carefully separated. The piece with the pink colour markings was then scanned in a flatbed scanner (Hewlett-Packard ScanJet 5300C). The scanned image file was imported into Matlab and, using a program specifically written for the task, it was converted into 8-bit grey scale, which has grey values from 0 (black) to 255 (white). The image was then blocked into regions of user-determined size and the mean colour intensity of each region was plotted. Mean intensity values over the entire region of applied load were then compared to the actual pressure applied to create calibration curves for the film. Each of the eleven loads was applied four times and a linear curve-fit was added to the applied load versus colour intensity plot to create the calibration curve shown in Figure 3.7. Figure 3.8 shows the results of one calibration run, with the film in grey scale and after it has been blocked in two sizes.

3.3.3 STATIC & QUASI-STATIC TESTS

The majority of tests previously conducted on thin-film sensors have applied static or quasi-static loads in order to determine sensor characteristics. Sensor accuracy has typically been evaluated by applying a known load and comparing sensor output to the load applied (Hsiao et al. 2002; Pavlovic et al. 1993; Polliack et al. 2000; Wilson et al. 2003). Hysteresis has been found by steadily increasing applied load to a certain point, and then decreasing the load at a similar rate (Ferguson-Pell et al. 2000; Pavlovic et al. 1993; Polliack et al. 2000; Woodburn and Helliwell 1996). Sensor repeatability characteristics have been determined by applying a specific load to the sensor a number of times and then looking at the variation in sensor output for the repeated tests (Ferguson-Pell et al. 2000; Pavlovic et al. 1993). Sensor drift tests are frequently conducted by applying a load to the sensor and monitoring the change in sensor output over a specific length of time (Buis and Convery 1997; Ferguson-Pell et al. 2000; Otto et al. 1998; Polliack et al. 2000; Werner et al. 1995; Woodburn and Helliwell 1996). The effect of surface curvature has been measured by bending sensors around objects of various shapes, applying known loads or

pressures to the sensor, and then comparing sensor output in the curved condition to sensor output on a flat surface (Ferguson-Pell et al. 2000; Polliack et al. 2000). To date, no information has been given to quantify how sensor output changes when shear loads are applied.

The current study involves a set of tests not too dissimilar to some of those mentioned above, with the closest resemblance to studies by Polliack et al. (2000) and Ferguson-Pell et al. (2000). The sensors in this study were subjected to a series of static and quasi-static loading conditions in order to determine accuracy, hysteresis, repeatability and drift errors, and the effects of shear loads and surface curvature.

3.3.3.1 *Quasi-Static Accuracy and Hysteresis Test*

Accuracy and hysteresis errors were found by using either Lloyd or Instron tensile testing machines to apply compressive loads on those sensors that could measure time-varying forces. During each test, loads were applied (at approximately 2-3 N/s for most cycles) to a specified peak force and reduced back to zero. A load cell on the testing machine (accuracy error < 1% for both machines) measured the applied load at sampling rates of 10 Hz and 100 Hz for the Lloyd and Instron machines, respectively. For the 9811 sensor, loads from 0-21 N were applied via a square applicator (4.8 mm x 4.8 mm), and the Tekscan hardware acquired the data at 120 Hz. During each test of the Flexiforce and QTC sensors, loads from 0-105 N were applied via the same cylindrical applicator used for calibration. The larger load values were chosen because of the higher load ratings and calibration levels for these two sensors as compared to the 9811. The sensor output was recorded by a digital oscilloscope at 25 Hz. The Novel tests used loads from 0-45 N, with sensor output being recorded at approximately 101 Hz. The test was repeated on each sensor ten times.

The force sensor data was resampled to match the load cell sampling rate, and each sensor's output was aligned with the applied load. Accuracy error for each sensor was then calculated as the absolute difference between applied and measured forces as a percentage of applied load as in Equation 3.1.

$$\text{Accuracy Error} = 100\% \cdot \frac{1}{(N+1)} \sum_{n=0}^N \left[\frac{|F_{ref}(n\Delta t) - F_{sens}(n\Delta t)|}{F_{ref}(n\Delta t)} \right] \quad 3.1$$

For this and other equations that follow in this chapter, in each test, $N+1$ samples are taken with a time increment Δt giving a sample length T . Error terms are derived from force measurements, $F(n\Delta t)$. The subscripts *ref* and *sens* are used to indicate the reference measurement and the associated sensor output, respectively. The equations indicate the error associated with measurements from each sensing element. The error values given in Table 3.2

are typically quoted as the mean of the errors from all runs on all test sensing elements of each sensor type \pm the standard deviation (PD 6461-3 1995). The sensor output and applied load for the quasi-static test of each sensor type is shown in Figure 3.9 for the 9811, Flexiforce and QTC sensors and Figure 3.10 for the Novel sensor.

Hysteresis can be defined as the maximum difference in sensor output for a given force level during loading and unloading, and is often recorded as a percentage of the maximum applied load (Bray et al. 1990; The Institute of Measurement and Control 1998). The hysteresis error was determined by using the data from the same quasi-static tests. Polynomial curve-fits were applied to each load-unload curve (applied load versus sensor output), and hysteresis was computed using Equation 3.2, where n_u is the point in the unload half of the cycle when the applied load is the same as at n_l in the load half of the cycle (i.e. $F_{ref}(n_u \Delta t) = F_{ref}(n_l \Delta t)$). The maximum value is found from all possible matching pairs of n_u and n_l . Figure 3.11 shows an example of one cycle of the quasi-static loading and unloading of a 9811 sensor.

$$\text{Hysteresis Error} = 100\% \cdot \left[\frac{\max(|F_{sens}(n_u \Delta t) - F_{sens}(n_l \Delta t)|)}{\max(F_{sens}(0:T))} \right] \quad 3.2$$

During the quasi-static testing of each sensor, it was noted that sensor output during the unload half of the cycle always exceeded that during the load half of the cycle for a given load. For the Tekscan 9811 and QTC sensors, it was observed that the sensors underestimated the magnitude of the applied load for the loading portion of every cycle, and that during the unload cycle sensor output tended to match applied loads more closely, although the sensors still often underestimated the load. These systematic errors indicated a problem with the calibration and this will be addressed in the next section.

3.3.3.2 Static Repeatability and Drift Tests

Static tests were also conducted to determine sensor repeatability and drift error. For these tests, loads equivalent to approximately 300 kPa were applied. During the 9811 and Novel repeatability tests, 5 seconds of data were collected at 264 and 101 Hz (the maximum sampling rates for the two sensors), respectively, and the test was repeated ten times. The Flexiforce and QTC tests were conducted with sensor output being collected by a Data Physics signal analyzer running SignalCalc software at 1280 Hz for 5 seconds. Twenty repeat tests were conducted for each of these sensors.

The 'Starting Point' (the point where the load had been fully applied to the sensor) was determined by analysing the change in slope of the sensor output in Matlab. The repeatability of each sensor output was compared using the output at 0.5 s after this Starting Point (in order to

ensure that there were no effects from the actual load application) according to Equation 3.3, in which the difference between the sensor output for a given run and the mean output for all runs by that particular sensing element is given as a percentage of the mean sensor output. Within the equation n_r is the single, chosen point after the Starting Point at which comparison is to be made. Repeated measurements on each sensing element enabled the calculation of a mean value.

$$\text{Repeatability Error} = 100\% \cdot \left[\frac{F_{sens}(n_r, \Delta t) - \overline{F_{sens}(n_r, \Delta t)}}{\overline{F_{sens}(n_r, \Delta t)}} \right] \quad 3.3$$

The drift tests conducted were similar to the repeatability tests, but with sensor output being measured for 65 s. Ten repeats were carried out for each sensing element, with Flexiforce and QTC being sampled at 640 Hz. Drift errors at $t = 1, 10$ and 60 s after the Starting Point were calculated using Equation 3.4, which indicates the difference between sensor output at a given time, t , and at the Starting Point as a percentage of the output at the Starting Point. Within the equation n_0 and n indicate the points where the load is first applied and when the drift calculation is being made, respectively (i.e. $(n - n_0)\Delta t = 1, 10, 60$ s).

$$\text{Drift Error (Static)} = 100\% \cdot \left[\frac{F_{sens}(n\Delta t) - F_{sens}(n_0\Delta t)}{F_{sens}(n_0\Delta t)} \right] \quad 3.4$$

Figure 3.12 shows the drift tests for each of the sensors, with the force ratio indicating the ratio between the measured force at time, t , and the measured force at the Starting Point. The initial steep portion of each curve is where the load is being applied, and the Starting Point for each curve is indicated by a circle. The repeatability tests for each sensor looked much the same, but for a shorter time duration.

When drift errors were calculated, it was found that the Flexiforce and Novel sensor outputs stabilized almost instantly after a static load was applied, whereas the outputs from both the Tekscan 9811 and, in particular, the QTC sensors were still increasing 60 s after the load had been applied.

The large drift errors associated with the Tekscan 9811 sensor are problematic because during the equilibration and calibration process, a uniform load is applied to the sensor for approximately 45 s before the calibration point is determined. The sensor drift during calibration produces a systematic error in sensor output, causing the supposedly calibrated sensor output to underestimate the value of applied force. In order to account for this problem, a correction factor was found by minimizing the area between the applied and measured load

curves during the quasi-static test. It was determined that a scale factor of 1.13 was optimal for minimizing the area. Additionally, although the exact time needed for calibration varies, the sensor drift error at 45 sec was determined to be nearly 15%, which is very close to the correction factor chosen. A similar correction was done for both the Flexiforce and QTC sensors as well, with scale factors of 0.956 and 1.14 being used, respectively. The correction factor was not used for the Novel data, as problems with noise and load placement (discussed in later §3.4) limited the number of usable quasi-static runs available for this sensor. Figure 3.9 a, c and e show the outputs for these sensors during the quasi-static test prior to the calibration drift correction, and b, d and f display the outputs after the correction. In all of the data presented in this chapter for each of the three sensors (including figures), this correction factor was used to adjust the sensitivity obtained from the manufacturer's recommended method of calibration.

During the repeatability and drift tests, it was noted that both Flexiforce and QTC sensors tended to underestimate the value of the applied load even after the correction using the quasi-static test data. This was most likely due to the fact that the sensors are calibrated by matching sensor output to applied loads during a full load-unload cycle, meaning that loadings that include no hysteresis effects will be underestimated. If the sensors are to be used for measurements of monotonically increasing or decreasing loads, it is recommended that an alternative calibration method be used, with data points collected for increasing or decreasing loads only.

The fifth sensor, Pressurex film, was evaluated for static accuracy and repeatability only as hysteresis and drift error measurements are not possible. The same eleven loads used in the calibration were applied another six times for each test, and the error results were calculated in a similar manner to previous tests.

3.3.3.3 Curved Surface Test

Thin-film force sensors are often required to bend around curved surfaces so it is important to understand the effect of such deformation on sensor output. Four different surfaces were selected for this test -- flat and with diameters of curvature of 30, 25 and 20 mm. Seven loads were applied via the same applicators described previously to three sensors of each type. The rubber layer of each applicator conformed to the curved surfaces. For the Tekscan 9811 sensor tests, loads varied between 0 and 33 N, and for the Flexiforce and QTC tests the loads ranged from 0 to 110 N. Three repeats of each test were performed.

In each test run, sensor output at zero load was recorded in order to measure the preload caused by sensor deformation. In all cases, the apparent preload measured on the curved surfaces was under 1.5 N. Sensitivity for a load cell or force sensor has been defined as a ratio of sensor output variation to change in applied load (Bray et al. 1990). For each test run, the

sensor sensitivity was calculated from a plot of sensor output versus applied load following the subtraction of the preload using a linear curve-fit. The difference in sensitivity between the flat and curved surfaces was computed for each diameter of curvature as a percentage of the sensitivity on the flat surface as in Equation 3.5, and is listed as surface curvature error. For this equation S is the sensor sensitivity (as described above), and subscripts c and f indicate test runs for the sensor on curved and flat surfaces, respectively. An example of the sensor output for one test run of a Flexiforce sensor is shown in Figure 3.13.

$$\text{Surface Curvature Error} = 100\% \cdot \left[\frac{S_c - S_f}{S_f} \right] \quad 3.5$$

Surface curvature did not appear to have a huge effect on Tekscan 9811 or Flexiforce force measurements, but produced a large decrease in sensor output for the QTC sensors. A summary of sensor characteristics under static and quasi-static loading conditions measuring accuracy, hysteresis, repeatability, drift and surface curvature error is given in Table 3.2.

Table 3.2 Mean error results from static and quasi-static tests; all values shown as percentages, standard deviation listed in parentheses

	Tekscan 9811	Flexiforce	QTC	Novel	Pressurex
Accuracy	6.7 (4.8)	10 (3.5)	13 (2.8)	7.6 (0.94)	75 (26)
Hysteresis	6.0 (1.5)	6.3 (2.9)	20 (3.2)	5.8 (0.61)	---
Repeatability	3.3 (0.73)	4.5 (0.57)	7.1 (2.2)	6.1 (3.3)	40 (33)
Drift (1 sec)	+4.1 (2.8)	+1.6 (2.1)	+10 (3.3)	+1.4 (2.0)	---
Drift (10 sec)	+11 (4.7)	+1.5 (2.6)	+34 (6.8)	+5.1 (2.4)	---
Drift (60 sec)	+15 (6.4)	-0.51 (3.2)	+59 (11)	+7.6 (2.6)	---
Surface Curvature (30 mm)	-1.4 (3.8)	+2.1 (2.0)	-11 (8.0)	---	---
Surface Curvature (25 mm)	-5.2 (1.9)	+0.95 (2.7)	-25 (6.5)	---	---
Surface Curvature (20 mm)	-1.0 (3.4)	+2.9 (4.0)	-31 (8.0)	---	---

3.3.3.4 Comparison with Data from Literature

The static test results obtained from this study are broadly in agreement with data previously reported in the literature for various Tekscan sensors under static conditions. Accuracy errors between 1.3-56%, hysteresis errors from 5.4-42%, repeatability error as low as 2.3-6% and drift errors between 12-39% have been recorded (Bachus et al. 2006; Ferguson-Pell et al. 2000; Hsiao et al. 2002; Pavlovic et al. 1993; Polliack et al. 2000; Werner et al. 1995; Wilson et al. 2006; Wilson et al. 2003; Woodburn and Helliwell 1996). There were two cases in which rather high hysteresis values were reported, but for those studies hysteresis was either calculated as the maximum value found in all test runs for a given sensor (Polliack et al. 2000), or only a single

sensor was considered in the study (Woodburn and Helliwell 1996). Other studies have also found that the accuracy of the Pressurex sensor in determining force and contact area is significantly less than that of the various Tekscan sensors (Bachus et al. 2006; Cormier et al. 2002; Harris et al. 1999; Matsuda et al. 1995). The Novel Pedar system has been reported to have accuracies in the range of 0.6-13.4%, repeatability errors of up to 15% and drift of up to 14% (Barnett et al. 2001; Hsiao et al. 2002; Hurkmans et al. 2006; Putti et al. 2006). Because Peratech does not make flexible force sensors, the next generation QTC is a relatively new product and the sensors used in the study were designed by the author, there is no data currently available to compare with the results of these tests.

3.3.3.5 Shear Test

A novel, final, static test was conducted to determine the effects of shear loads on sensor output. No information has been found in literature indicating how thin-film sensors react to this type of loading. Shear forces are often present in dynamic gripping actions, so it is important to ascertain how these sensors behave under this loading condition. The shear loads chosen for this test were based on peak shear forces of around 500 N, which occur between the hands and the grip* during golf shots (Budney 1979; Mather 1996), and then scaled based on the area over which they were applied. A three-legged circular load carrier (cylindrical legs, 6 mm diameter, 120° spacing with 2 mm-thick rubber surface on each leg) was used to apply normal loads of 9.2 and 15.75 N to each sensor, as shown in Figure 3.14. Data was collected from each sensor for 5 s and after the data collection had begun, a shear load of 1.6 or 3.2 N was applied to each sensor via the load carrier. Example tests for each sensor type subjected to 9.2 N normal and 3.2 N shear loads are displayed in Figure 3.15, where the force ratio indicated in the plots is the measured sensor output divided by the applied normal load.

It was revealed that a typical error calculation (change in load divided by applied load) does not adequately describe the shear error, as the magnitude of the change in sensor output due to the addition of the shear force remains relatively constant for most sensor types, regardless of the normal load (i.e. doubling the normal load applied typically results in a shear error reduction of 50%). Therefore, rather than listing shear force errors for each sensor type, a shear force sensitivity was calculated. To determine the change in output due to shear over each 5 s test, the overall change in sensor output was first calculated by subtracting the mean sensor output from the last 0.5 s of data from the mean of the first 0.5 s. The contribution to this change in sensor output due to drift was then calculated and this was subtracted from the overall change in sensor output to give the contribution due to the application of a shear force. The sensitivity due to shear was then determined by dividing this value by the applied shear load, as in Equation 3.6, where $n_1\Delta t$ is a chosen length of time (0.5 sec) over which the sensor output is

averaged at the beginning and end of each test, ΔF_{drift} is the change in sensor output due to drift which is estimated by using the slope of the sensor output at the beginning and end of each test, and F_{shear} is the applied shear force for a given test.

$$\text{Shear Sensitivity} = 100\% \cdot \left[\frac{\frac{1}{n_1} \sum_{n=N-n_1+1}^{n=N} F_{sens}(n\Delta t) - \frac{1}{n_1} \sum_{n=0}^{n=n_1-1} F_{sens}(n\Delta t) - \Delta F_{drift}}{F_{shear}} \right] \quad 3.6$$

Table 3.3 displays the results from the shear force test. Note that values are not given for shear sensitivity of QTC for the higher applied normal loads. This is because the sensor overloaded during the majority of tests with the higher normal force as soon as the shear load was applied. All three sensors show considerable sensitivity to shear (24-51%) causing an increase in sensor output, although the effects of changing shear and normal forces differ for each. The Tekscan 9811 sensor shear sensitivity increases with shear magnitude but is independent of normal force, the Flexiforce sensor shear sensitivity appears independent of shear and normal load, and the QTC sensor shear sensitivity was nearly constant for changes in shear load for the lower normal force. At this point it is unclear what the underlying causes are for the variations in sensor behaviour with shear and normal loading.

Table 3.3 Results of shear force tests; values shown are percentage change in force output due to shear per unit shear load; all values shown as percentages, standard deviation listed in parentheses

Load	Tekscan 9811		Flexiforce		QTC	
	Shear 1.6 N	Shear 3.2 N	Shear 1.6 N	Shear 3.2 N	Shear 1.6 N	Shear 3.2 N
Normal 9.2 N	+28 (19)	+49 (19)	+37 (22)	+33 (20)	+25 (13)	+30 (12)
Normal 15.8 N	+24 (18)	+51 (19)	+41 (26)	+37 (21)	---	---

3.3.4 DYNAMIC TESTS

For the golf grip application, the force sensors will be required to monitor dynamic loads. Very few examples have been found in the literature where thin-film force sensors were tested under dynamic loading conditions. There are several cases in which a quasi-static ramped loading was applied to the sensor (see §3.3.3), but in these cases the load was consistently increased or decreased at a relatively slow rate for the length of the test. This does not give an indication of the sensor's true dynamic capabilities in which loads might be increasing or decreasing rapidly. One such study was conducted by Otto et al. (1998) in which they determined not only static drift of the sensors but also the response of the sensors to loads

applied from 0.1-20 Hz. A special pressure vessel was designed to apply spatially homogenous transient or constant loads. The dynamic loads were sinusoidal, with peaks of either 10 or 20 MPa. The dynamic response of the system was analysed but very little quantitative data was presented.

A novel approach to measuring dynamic accuracy was necessary. Rather than test the response to dynamic loads over a large area, as has been done previously, oscillating forces were applied over a region much closer in size to an individual phalanx and was entirely contained within the active area of a single sensing element. In this study, Tekscan 9811, Flexiforce and QTC sensors were subjected to a dynamic load created by placing the sensors under one of three legs of a load carrier (described in §3.3.3) that rested atop a platform as shown in Figure 3.16. The platform was fixed to an electromagnetic shaker for vertical excitation, with stability provided by restricting the horizontal motion of two of the legs (Figure 3.16b). With this set-up, one-third of the total static and dynamic load applied to the carrier was directed through the test sensor via the 6 mm diameter cylindrical leg. Sinusoidal loads were applied to the sensor at frequencies of 15, 60 and 100 Hz, such that the 6.3 kg load achieved nominal maximum peak accelerations of 2.4, 4.8 and 7.1 m/s², measured by an accelerometer (accuracy error of 1-2% over the frequency range used) placed on the load carrier just above the sensor. The load applied through the sensor follows readily from the product of the mass and the accelerometer measurement. Each dynamic load and frequency combination was repeated five times on each sensing element tested.

The dynamic loads applied to the 9811 sensors were recorded at 264 Hz. These loads were applied for a total of 10 s, but 20 s of data was recorded to investigate sensor output drift during the test, as shown in Figure 3.17. The initial portion of the curve in this figure shows the load resting atop the sensor, then the shaker ramps up the acceleration until it reaches the desired level, which it holds for a given amount of time before ramping back down to zero. The final portion of the curve is the sensor output for the static load. For the Flexiforce and QTC sensors, a signal analyzer was used to collect the output from the sensors and accelerometer at 1.28 kHz. The dynamic load was applied for a total of 5 s, but 10-15 s of data were recorded.

Dynamic drift error was calculated using Equation 3.7 where $n_1 \Delta t$ is a chosen length of time (0.25 sec) over which the sensor output is averaged at the beginning and end of the 10 s interval during which the dynamic drift error is considered. Dynamic drift error was then evaluated as the change in mean force from the beginning to end of the interval as a percentage of the initial force. Mean dynamic drift error was found to be between -2.9 to +13% for the three sensor types and large standard deviations indicate that this was quite variable from test to test.

$$\text{Drift Error (Dynamic)} = 100\% \cdot \left[\frac{\frac{1}{n_1} \sum_{n=N-n_1+1}^{n=N} F_{sens}(n\Delta t) - \frac{1}{n_1} \sum_{n=0}^{n=n_1-1} F_{sens}(n\Delta t)}{\frac{1}{n_1} \sum_{n=0}^{n=n_1-1} F_{sens}(n\Delta t)} \right] \quad 3.7$$

From the dynamic data gathered, 8 s segments of each 9811 load curve and 4 s segments from each Flexiforce and QTC load curve were found for which the peak oscillating load was applied the entire time. The static load and low frequency drift were first filtered out of each segment. The RMS force measured from each sensor was then compared to the applied RMS force calculated from the accelerometer output for each test. The accuracy of the sensors was calculated as the difference between measured and applied loads as a percentage of applied load as in Equation 3.8, where \tilde{F}_{ref} and \tilde{F}_{sens} were high-pass filtered to remove the static load and low frequency drift from F_{ref} and F_{sens} , and n_1 and n_2 are the first and last points in the data segment that was used (data segments were 4-8 sec long, depending on sensor).

Dynamic Accuracy Error =

$$100\% \cdot \left[\frac{\sqrt{\frac{1}{n_2 - n_1 + 1} \sum_{n=n_1}^{n=n_2} (\tilde{F}_{sens}(n\Delta t))^2} - \sqrt{\frac{1}{n_2 - n_1 + 1} \sum_{n=n_1}^{n=n_2} (\tilde{F}_{ref}(n\Delta t))^2}}{\sqrt{\frac{1}{n_2 - n_1} \sum_{n=n_1}^{n=n_2} (\tilde{F}_{ref}(n\Delta t))^2}} \right] \quad 3.8$$

An example of the Flexiforce sensor under a dynamic load of 15 N at 60 Hz can be seen in Figure 3.18, in which (a) shows the applied force calculated from the accelerometer measurement, (b) is the force output from the sensor, (c) shows the segment of the data that is analysed for the accuracy error calculation, (d) is that segment after the preload and low frequency drift has been filtered out, and (e) is a close-up view of a portion of the segment.

A summary of all dynamic test data is shown in Table 3.4. For dynamic loads, all sensors have a decreased accuracy as compared to static loads with a much larger variation in output between runs. Dynamic drift error values were based on the absolute difference between the sensor outputs from the start to the end of a 10 s segment of the test. It was found that sensor output decreased with increasing frequency of applied load for the Flexiforce and QTC sensors, while the 9811 sensor underestimated the applied load to a similar magnitude for all three load frequencies (15, 60 and 100 Hz). Larger standard deviations were computed for the dynamic accuracy errors for all three sensors as compared to the quasi-static tests, with QTC having the largest variation. It was also noted that the run order affected the dynamic accuracy of the

sensors. The calculated dynamic accuracy of QTC sensors decreased as the testing progressed, while for Flexiforce sensors it increased. In the case of the 9811 sensor, different sensors seemed to show different run order effects. Decreasing output with continued testing may indicate sensor degradation, while increasing output with continued testing is harder to explain but may represent some residual drift-like effects.

Table 3.4 Results of dynamic evaluation tests; values shown as percentages with standard deviation listed in parentheses

	Dynamic Drift (10 s)	Accuracy	Dynamic Accuracy		
	Based on All Frequencies	0 Hz	15 Hz	60 Hz	100 Hz
Tekscan 9811	+13 (5.9)	6.7 (4.8)	-57 (9.7)	-64 (10)	-58 (11)
Flexiforce	-10 (5.0)	10 (3.5)	-16 (21)	-25 (14)	-25 (18)
QTC	-2.9 (15)	13 (2.8)	+28 (62)	-15 (40)	-38 (34)

Sensor performance during the accuracy tests may be improved with the addition of a compliant layer between the sensor and the rigid load applicator (leg of the load carrier) and would be recommended for future tests. However, the results from the current set of tests represent the first known attempt to quantify the dynamic accuracy.

One further comment should be made with respect to the 9811 sensor and the dynamic tests. This sensor did not react well to the dynamic loads, often overloading during the tests, which automatically sends the output to zero. It was found that by applying the dynamic load over a longer time-period, the shaker ramped to the peak load in such a way that the sensor did not overload. This is because the shaker ramps up to maximum acceleration at a rate that is dependent on the length of the test. Originally, dynamic loads of 25 N were going to be applied to the sensors, but because the 9811 sensor output drifted so much during the course of the test, the sensors overloaded too regularly and the maximum test load was set at 15 N. Even after these measures were taken, data from a number of tests had to be discarded. Additionally, the Flexiforce and QTC sensors were sampled at much higher rates, and file sizes would have been quite large if the test time had not been reduced. These other two sensors did not exhibit any of the problems found with the 9811 sensor.

Although the QTC sensor did not suffer from identical problems to the Tekscan 9811, it is possible that the results presented for this sensor may be less reliable. The full extent of the sensor's lack of durability was not realised until after the completion of the dynamic test. It was noted during player tests (described later in §5.3.1) that sensor sensitivity to load decreased significantly within 20-30 load cycles. It is believed that the dynamic test actually presented a considerably more harsh loading condition than the player tests and, as each sensor endured five runs at three different load and frequency conditions (for a total of 45 test runs), it is thought

that the sensor calibration curves would have been invalid by the end of the test. In the future, to look more closely at the QTC force sensor dynamic response, each sensor should be calibrated before and after use and no sensor should be used in more than 20 runs.

3.4 DISCUSSION

The sensor evaluation tests were very informative, not only in quantifying measurement errors, but showcasing the abilities and limitations of the different sensors. Several important details emerged about each sensor.

The first discovery concerned the way in which the Tekscan 9811 software evaluates the applied load. As previously discussed in §3.2.1, the sensor software automatically makes assumptions about the area over which a force is applied, assuming that a load applied to the active area of the sensor is also being applied to the passive region that surrounds it, which stretches midway to the next active sensing element in each direction (see Figure 3.1). Because of this assumption and the fact that in all tests the load was applied entirely through the active region of a sensor, the force outputs from sensor software were more than double the true applied load, giving a calculated accuracy error of 128%. To account for this, a correction factor suggested by Tekscan engineers was used to adjust the sensor output. The correction factor was the approximate active sensing area of the sensors divided by the total area as seen in the software calculations for one sensor (active and passive area combined).

During the quasi-static testing of each sensor, it was noted that sensor output during the unload half of the cycle always exceeded that of the load half of the cycle. Additionally, systematic errors were identified that were traced back to sensor drift during calibration. These errors were accounted for using scale factors of 1.13, 0.956 and 1.14 for the 9811, Flexiforce and QTC sensors, respectively.

From the results of the repeatability and drift tests, it was noted that the Flexiforce and QTC sensors tended to underestimate the value of applied load. It was concluded that this was due to the calibration technique of using a full load-unload cycle. It is recommended therefore that if these sensors are to be used for measurements of monotonically increasing or decreasing loads, an alternative method of calibration should be used with a load cycle similar to that of the test scenario.

An additional problem with the QTC sensor was discovered during the evaluation tests. As each QTC sensor calibration or test proceeded, the sensitivity of the sensor decreased, which affected the sensor's accuracy over time. It is believed that the decrease in sensitivity contributed to the high static and dynamic accuracy and curved surface errors that were measured for this sensor.

The Novel system offered the benefit of being wireless, but this resulted in greater accuracy error as it was found that signal interference produced additional noise within the measurement. Additionally, if the load was applied over more than one sensing element, then accuracy again dropped considerably (accuracy error of 40% was seen when the load applicator applied load to several regions simultaneously). A partial explanation for this is that when the load was spread over several sensors, each individual sensor would be forced to measure only a fraction of the total applied load. The increased error in this situation indicates that the Novel sensor has accuracy problems when measuring loads on the lower end of the calibrated region. Another problem that was seen with this sensor was that frequently the force output would momentarily drop to 0, and then resume the measurement as before. It was unclear whether this was due to interference within the wireless system, or if the sensor was overloaded. The latter should not have been an issue as applied loads were always kept below 600 kPa. Finally, this particular sensor was not suitable for the golf grip measurement application due to its thickness. Novel sensors are all approximately 2 mm thick. If they were used on a golf grip*, this would mean an increase in grip* diameter of 4 mm which is the equivalent of increasing the grip* by several sizes.

Although the 9811 sensor had difficulty coping with dynamic loads, was not designed for loads with high spatial frequency (compared to its sensing element spacing), had a fairly low sample rate and large drift errors to contend with, the sensor also had a number of advantages. The system as a whole is very easy to use, and the software is capable of producing useful visual displays of the data collected. There is also the benefit that this is a complete force sensing package, with little for the user to do but turn everything on and start collecting data. Additionally, the sensor collects data from 96 points simultaneously, meaning that the entire contact area between a golfer and the grip* can be monitored at once.

The Flexiforce sensor performed well overall in the sensor evaluation tests, and minimal effort was required to produce the simple circuits for each sensor. If one wants to sample a large number of sensors simultaneously, however, work will be required in the development of the circuitry and data acquisition system.

Peratech's next-generation QTC is the newest of the technologies, and the least developed in terms of force sensing. Either silver-coated or copper electrodes were etched (17.5 micron thickness) onto an insulated polyester material, with the QTC material simply taped in place as shown in Figure 3.4. Any size or shape of sensor can be created in a similar way, and the circuitry required is again quite basic. The non-linear output of the sensor is slightly troublesome, but can be overcome with careful calibration. More advanced circuitry could potentially eliminate this problem all together. As with the Flexiforce sensor, sampling a large

number of sensors could significantly increase the development time and costs involved in using these sensors, but even so, this is a relatively cheap technology.

Like the Tekscan 9811 system, the Pedar Novel wireless system can be purchased as a complete, ready-to-use package. Again the software is straightforward, and it appears that it is capable of making reasonable force measurements. Having a wireless system can be a great benefit, but it appears that the system currently suffers from some noise problems. Further investigation in this area would be informative. The cost and thickness of the Novel sensors are two limiting factors and so investigation of this sensor was not taken to the next stage.

The Pressurex film did not fare well in the accuracy or repeatability tests, but has proven its usefulness in terms of showing relative pressures on a single piece of film. This technology can be best used for determining ideal locations for the other sensors to be placed, either on the golf grip* or hands. Additionally, the film has potential for use by golf instructors as a way to show their students which fingers are producing the largest grip forces. This could be done simply and quickly without the use of a computer.

Overall, any of the first four sensor types could successfully provide useful information about the grip forces produced during a gripping event. Therefore, the three that were deemed usable in the golf grip force scenario (Tekscan 9811, Flexiforce and QTC) were used in player tests to make further comparisons. Additional comments on sensor durability and performance under real testing conditions will be made in Chapter 5.0.

4.0 GRIP FORCE PLAYER TESTING – PRELIMINARY STUDIES

The prior sections of this thesis have provided a number of reasons why studying grip force during a golf shot is an interesting and useful exercise. This section will now describe preliminary studies looking at how these grip force measurements can be carried out. Details will be provided on methods for synchronizing data and determining impact times, and a discussion of some initial tests and the lessons learned from them will be included.

4.1 SYNCHRONIZATION AND IMPACT TIMING

In order to compare data from successive grip force tests, a method needed to be created to align the grip force traces from each shot and to note key points during the swing (e.g. impact). Synchronization of the forces with video or sound is critical to identifying the moment of impact in the force traces. There are simple ways of aligning the traces, such as using light gates to trigger the start of the force measurement when the club passes through a beam of light at a particular point in the swing. This method by itself, however, will not provide information on when impact occurs. A means of detecting impact needed to be added to the system and several methods were considered including video or sound recordings, and applying strain gauges to the club. These methods are described below for use with the Tekscan F-Scan 9811 system and the method chosen for actual player tests was then adapted for use with the Flexiforce and QTC systems.

4.1.1 TEKSCAN VIDEO SYNCHRONIZATION SYSTEM

In a first attempt, video was used to determine the moment of impact. Conveniently, the F-Scan system has a built-in video synchronization feature. A digital camcorder is connected to the Tekscan computer via a Firewire cable, and both the camera and force sensor can be set to begin recording simultaneously using a trigger from the Tekscan software. The digital camcorder in this case recorded at 25 frames per second. Due to the speed of the signals passing through the Firewire system and the Tekscan software, the recorded video frames often lag behind the force trace, even though the two recordings were triggered to start at the same time. According to Tekscan (2004), for a particular computer, the latency of each video should be fixed and, if the lag time could be determined for one set of video and force recordings, the same lag time could be applied to other recordings. This system was tested by recording an impact or series of impacts on a single sensing element in order to record latency time between the video and force trace. This latency was then applied to other similar videos to see if the forces measured on the Tekscan sensor were aligned in time with the video image of the force being applied. Unfortunately, the lag time from the original test did not properly align the force

trace and video for subsequent tests, indicating that the lag between the force traces and video recordings did not remain constant. Without knowing the latency between the video and force outputs, moment of impact could not be accurately determined using this system. Furthermore, the digital camcorder sampling rate was much slower than desired.

4.1.2 HIGH SPEED VIDEO AND LIGHT GATES

When it was clear that using the F-Scan internal video synchronization would not work for locating impact and aligning force data, a second video method was attempted. Light gates were used to trigger both the 9811 sensor and a high speed video camera during a golf shot. Again there was a latency between the force trace and video recording, but since there was no Firewire system involved and the Tekscan video triggering system was not used, it was hoped that the lag time would be constant.

To test the lag time, the light gates, high speed video and force sensors were all connected as they would be during a normal player test. The light beam was then broken, triggering the start of the video and force recordings, and an obvious impact was made on the 9811 sensor. The force sensors were sampled at their highest rate, 264 Hz, and the camera was sampled at both 250 and 500 Hz. Impacts were made using a nylon tipped impact hammer, a dropped golf ball and an index finger. The frame on which the impact occurred was found on both the high speed video footage and the force trace, and the time to impact was calculated. The difference between these two times was considered to be the lag. The lag seemed to be somewhat consistent, but there was potential for error in the technique. It was difficult to determine the exact video frame on which the impact occurred, and it was hard to judge where sufficient force would be applied such that it was recorded by Tekscan. This was most difficult when using the index finger, due to the soft, deformable tissue that was first in contact with the sensor that did not transmit much force at first contact. Another difficulty came in getting the 9811 sensor to actually record the impact. Impacts with the more rigid surfaces of the nylon impact hammer and golf ball often went undetected by the force sensors. This is likely due to the short duration of the impact relative to the sampling rate, and highly localised peak forces.

Eventually twenty impacts were recorded using the nylon impact hammer with the camera recording at 250 and 500 frames per second. It was discovered that Tekscan lagged behind the video recording by 0.049 ± 0.016 s when the video was sampled at 250 Hz, and by 0.037 ± 0.015 s when sampled at 500 Hz. It is not clear why the lag differed when the video was recorded at different frame rates. In each case, the standard deviation is about the same, which gives an indication of the amount of human error that was involved in determining the first impact frame. Besides the potential human error involved with this method, the camera used required that each recording be downloaded before the next was taken. This process took a few

minutes each time and made the time duration of the player test much longer than desired. Although this technique was successfully used to determine impact location for several golf swings, a better method was sought.

4.1.3 SOUND LEVEL METER AND LIGHT GATES

Rather than using digital video to locate the moment of impact visually, a sound level meter can be used to locate the moment of impact based on the sound produced. The means of doing this was essentially the same as the video method with light gates, but with a sound level meter taking the place of the high speed camera. The sound level meter was triggered to record sound on a digital oscilloscope at the same moment that the 9811 sensors began recording force. As before, the force recorded lagged slightly behind other recordings and this latency needed to be quantified. Again a nylon impact hammer was used to strike the sensor, which created a clearly audible sound that the sound level meter would detect.

During both the latency measurement and player tests, the sound level meter was placed as close to the impact location as possible. This was to avoid any time delays in the sound recording due to the finite speed of sound. At the distances used in both tests (only a few centimetres), this was calculated to be negligible. Figure 4.1 shows the sound level meter and the golf tee used in player tests. The distance between tee and sound level meter shown in the picture is the same as used in all player tests.

The lag of the 9811 sensor was determined from twenty impacts with a nylon impact hammer. During this test, all connections between light gates, sound level meter, force sensor and oscilloscope were exactly as they would be for the player test. Prior to each impact, the light beam of the light gate was broken, triggering the sound level meter and force sensor to begin recording. An impact was then made on a single sensor. The Tekscan 9811 sensor was sampled at 264 Hz, and the oscilloscope at 2500 Hz. The voltage output of the sound level meter was analysed using Matlab, and when a specified threshold value and slope criterion were met, the point was denoted as the start of impact. Figure 4.2 shows a typical sound level reading during a player test, with the impact time marked. On this occasion the lag for twenty impacts was found to be 0.63 s, with Tekscan trailing the sound level meter. The latency was tested on several occasions between player tests, and was always found to be in the region of 0.6 s with a standard deviation in the region of 0.01 s.

Using light gates and a sound level meter was deemed to be the best of the three methods to determine the impact location in grip force traces during a golf shot. Human error was eliminated by removing the need to guess when impact actually happens and the time needed to save each sound trace was minimal. This method was used for all further tests conducted with the Tekscan 9811 sensor. Additionally, this method of synchronization was very simple to

employ with the Flexiforce and QTC systems. One of the channels on the data acquisition system was reserved for the sound level meter and, therefore, there was no lag between the force and sound recordings as they were both being recorded through the same system. This in fact made impact time determination simpler and more accurate in the Flexiforce and QTC systems.

4.2 PILOT TESTS

Several pilot studies were conducted, during which sensor location was determined and the effects of factors such as grip* diameter and surface curvature were observed. Pressurex film was utilized to determine relative pressure distributions, and special golf grips* were designed so that the 9811 sensors could lie flat on the grip*. Information about these tests and lessons learned is provided in this section.

4.2.1 PRESSUREX FILM – RELATIVE PRESSURE DISTRIBUTION

There are two main limitations with the use of Pressurex film – it cannot provide time-resolved data and the accuracy of the force measurements is considerably worse than the other sensors tested. However, Pressurex film can provide a simple and effective method of determining localized high pressure regions. For this purpose, the film was utilized in two ways. First, it was applied directly to the golf grip* so that areas of peak grip force could be found with respect to grip* locations. And second, small pieces of the film were attached directly to the golfer's hands so that peak grip forces could be determined in relation to key points on each hand.

4.2.1.1 *Film on Golf Grip**

For player tests using Pressurex film on the grip*, several initial trials were conducted to determine the best size film to use, a method to attach it to the grip*, and a way to apply and remove the film without creating false pressure marks. The best method to use was to first use small pieces of electrical tape along the outside edges of the film to align the donor and receiver sheets. Paper was then placed between the sheets to prevent contact and was only removed after the film was attached to the golf grip*. Double-sided tape was used to attach the two pieces of film to the grip* and small pieces of electrical tape were used at the top and bottom to make sure it was securely fastened. Just prior to the test, the piece of paper was carefully removed from between the two pieces of film. A mark was made on the film to indicate where the manufacturer's logo was on the grip*, thus allowing all pressure readings to be located in relation to grip* position.

For each test, the club was gently placed in the golfer's hands and once a shot had been taken, the tester removed the club from the player's grip immediately after follow-through. The film was then carefully removed from the grip*, the two pieces of the film separated so that no further pressures would be recorded, and the receiver sheet was analysed. Figure 4.3 shows several images of the film on the golf grip* with the subject grasping the club just prior to a test shot. After each test, the film was analysed as described in §3.3.2. Figure 4.4 shows the film after a test, when it has been scanned and turned to 8-bit gray scale and blocked with block lengths of 20, 40, 60 and 80 pixels. Several key regions of the hands contribute to local peak pressures and are labelled as follows: left little (LL), ring (LR), and middle (LM) fingers, the left thumb (LT), and right ring (RR), middle (RM), and index (RI) fingers, and right thumb (RT). This test was conducted with three golfers hitting four shots each. The golfers had handicaps ranging from 0-12 and clubhead speeds from 86-106 mph. The mean colour intensity in the key regions mentioned was computed over the four shots for each golfer and using a prior calibration the pressure was calculated and is displayed in Table 4.1. The values measured for each finger are quite high, and this is most likely due to the effect of the high shear loads produced during a golf shot. This table is most useful for looking at relative loads rather than the actual pressure magnitudes.

Table 4.1 Mean grip pressure in key regions on the hand from tests with Pressurex film on golf grip*

Player	CH Speed (mph)	Handicap	Mean Peak Pressure Over Four Shots (kPa)							
			LL	LR	LM	LT	RR	RM	RI	RT
1	106	0	991	982	976	1247	789	1107	1018	783
2	92	7	1265	854	750	1203	801	774	738	1217
3	86	12	604	545	839	955	759	795	917	997

In general it has been assumed in the past that the highest pressure is applied by the left thumb (Budney 1979; Budney and Bellow 1990). Player 1 appears to demonstrate this manner of grasping the club, however the higher handicap golfers 2 and 3 both apply similar pressures to both left and right thumbs and Player 2 has another high pressure region under the left little finger. Although no hard conclusions can be drawn from this data, the peak grip pressures generated appear to vary considerably between players. Additionally, it appears that overall the regions of peak pressure lie underneath the fingers and thumbs, and this should be taken into consideration when determining sensor position for future tests.

4.2.1.2 *Film on the Hands*

A second type of test conducted with the Pressurex film involved placing 32 pieces of the film, cut to size, on the golfer's hands. The two sides of the film were again held together by electrical tape and separated by paper until just before the test was performed. Double-sided tape held the film in place on the fourteen phalanges of each hand and on two positions on each palm. An image of the film on a test subject's hands can be found in Figure 4.5.

Again the colour intensity of the broken ink capsules was analysed in Matlab, and Figure 4.6 shows the result of blocking the individual pieces of film as well as the region they were positioned during the test. Player 1, who participated in the previous test with the film on the grip*, took several tee shots with the film on both hands. Again it was found that the highest grip forces for this player were under the left thumb. Additionally, high pressures were measured in both regions of the left palm. The pressure in these two regions could not typically be distinguished when the film was over the entire grip* as the pressure was not high enough relative to surrounding regions.

4.2.1.3 *Discussion*

Many interesting results emerged with the use of Pressurex film. It was found that the film could easily be applied to a golf club grip* and, with a flatbed scanner and Matlab code, regions of relative colour intensity and, therefore, relative pressure could be identified. It was also shown that, with slightly more work, the film could be applied directly to a player's hands and could again give relative pressures. Finally, it was noted that each player seems to be fairly consistent in applying similar relative pressures at specific regions of the hands for each swing. The locations and magnitudes of peak pressure regions, however, vary between players.

Some difficulties in using this film for pressure or force measurement were also encountered. The most notable of these was the effect of shear forces applied to the film. This made determining quantitative pressure values in player tests nearly impossible and the use of the calibration curves less accurate than initially expected. Additionally, since the accuracy of this film is low even without shear loading, the film is best used as a device for determining regions of relatively high and low pressures.

Even with the problems that arise due to shear forces affecting the reliability of the Pressurex film readings, it still appears that this may be a valuable research tool for a number of reasons. First, the film can be used to help determine the location of a player's fingers on the club. This may be valuable when designing sensors and tests in the future. Second, this is a very simple way to determine which part of the hands a player uses to apply the highest pressures. This can again be useful for future pressure test designs, but may also be a useful tool for golf instructors. With Pressurex film on the club, instructors can give their clients an idea of

how tightly they are gripping the club and which fingers they are using to provide most of the force.

4.2.2 SIX-SIDED GRIP* TEST

For the preliminary golf grip force player tests, the Tekscan 9811 sensor was used as its characteristics were well understood and, of the sensors evaluated, it was the only one that had all hardware and software readily available.

4.2.2.1 *Sensor Application*

In early tests, the sensor was wrapped around the grip* and held in place by double-sided tape between the sensor and grip*. Masking tape was then applied over the top of the sensors. This setup created problems in that sensor locations could not easily be seen, some sensing elements were positioned atop others, and all of the sensing elements were curved or bent to fit around the grip* which can affect sensor performance. Although it was possible to measure grip force with this configuration, another method of attaching the sensor was sought that eliminated these problems.

To allow all 96 sensing elements to lie flat against the grip*, 6-sided grips* were rapid manufactured with outside diameters that were the same as three typical golf grip* sizes – men's standard, jumbo, and one size smaller than a women's standard. These three sizes were chosen because they represent the majority of the size range available. The 6-sided grip* was attached directly to the shaft using double-sided tape on the inner surface and wrapped with electrical tape on the outside. Although not the exact shape of real golf grips*, a selection of high level golfers agreed that the 6-sided grip* felt surprisingly similar to a real grip* and that it did not distract them during a shot.

The 9811 sensors were carefully cut along the columns to separate the sensor into six strips and each of the strips was attached to one edge of the 6-sided grip* using double-sided tape. Very thin strips of electrical tape were run around the outside of the sensor, between sensing elements, to help secure the sensors in place and to keep the sensor layers from splitting. A picture of a 6-sided grip* on a golf club, a 9811 sensor cut along the six columns, and the sensor attached to a grip*, is shown in Figure 4.7. It was in this sensor configuration that grip force was measured in preliminary golf shot tests.

4.2.2.2 *Test Design*

Player tests using the 6-sided grip*, Tekscan 9811 sensor, light gates and sound level meter were conducted to determine grip force during a golf shot using three different sized grips*. Fifteen golfers with handicaps ranging from 0-7 were recruited to participate in the study. The

three sizes of the 6-sided grip* were attached to three identical drivers. Tekscan 9811 sensors were calibrated and positioned on the 6-sided grips* as described in the previous section. The sensor cuff (which connects the flexible sensor to the circuitry leading to the computer) was strapped to the golfer's left forearm, and the cable was run over their left shoulder and down their back so that a natural swing could be taken without any interference from the equipment. The light gates were aligned relative to the tee so that the light beam would be broken at the start of the back swing, triggering both the digital oscilloscope connected to the sound level meter and the Tekscan system to start recording. The 9811 sensors were sampled at 264 Hz, while the sound level meter was sampled at 2500 Hz. After each shot was completed, both the sound pressure and force traces were saved, giving the subject about one minute to rest. Each player took ten shots with each club, for a total of thirty shots. Prior to the test, each golfer was allowed to take as much time as they wanted to warm up, and several swings were taken after they were fitted with the sensor cuff in order that they would become familiar with the feel of the equipment before the test commenced. The entire test lasted less than one hour, and the golfers exhibited no signs of fatigue. All shots were taken in a controlled laboratory environment, with the golfer hitting off a tee positioned within artificial turf and into a net. Golfers were required to wear two well-fitted golf gloves to minimize slippage between the sensor surface and the hand, and each signed an informed consent form indicating that they understood the nature of the test and were happy to continue. Ethical approval for this study was obtained.

4.2.2.3 Analysis & Results

Data for each shot was collected and analysed in Matlab. Impact time was located in each sound pressure trace and the lag time was subtracted to determine impact time on the force traces. Total force traces were created for each shot taken by summing the force over all of the sensing elements whose entire surface lay flat against the grip* (some sensing elements were positioned beyond the end of the grip*, as seen in Figure 4.7b). All thirty force traces for each golfer were aligned by impact and plotted as shown in Figure 4.8 for one golfer. It was found when aligning the force traces based on the impact time that some of the lag times were incorrect due to changing lag times between tests, most likely caused by small differences in the test set-up (e.g. using different oscilloscopes). This meant that for some of the golfers, shots could not be aligned by impact. To prevent problems in the future, it was determined that lag time measurements must be taken prior to each test session.

During the test for the fifteenth golfer, the 9811 sensors on one of the clubs sustained substantial damage due primarily to the shear forces applied during the golf swing. One of the six columns of sensing elements ripped apart in the middle, as seen in Figure 4.9. This caused

some concern as to the state of the other sensors and a small amount of damage was detected on other strips as well. Once the tests were completed, the force traces for all golfers were checked. After viewing the data for the fifteen golfers, it was noted that the total grip force started to decrease from the first golfers tested to the last. Following a closer investigation of the data, it was discovered that two columns of sensing elements for one of the sensors had ceased to function by the fourth golfer, and nearly all data collected after the third golfer was severely altered because of these sensor problems. Although these problems with sensor durability prevented the collection of a full set of accurate data, there was still information that could be gained by analysing the data for several of the golfers.

The ten force traces for each grip* size and player combination were averaged to create one mean force trace, as displayed in Figure 4.10a-c. It should be noted that all three of these golfers play at a very high level and each had a handicap of 0. Further analysis was performed on the data from the first three golfers tested, although it will not be discussed at length here. It was determined that no difference could be seen in total grip force output for the different size grips*. One additional point to make was that already at this early stage of testing the repeatable nature of a golfer's grip force was apparent as evidenced in the figure.

4.2.3 LESSONS LEARNED

Although only limited quantitative information about grip force in golf was obtained from the preliminary tests described, a valuable foundation of knowledge for future tests was gained. It was found that thin-film force sensors such as the Tekscan 9811 cannot endure the high shear forces created during a golf tee shot without protection. Furthermore, even when protected, the sensors may be prone to failure after a certain number of shots.

Additionally, lag time measurements did not remain accurate over several days of testing. To prevent problems in future tests, it was decided that lag measurements would be taken prior to each test session to eliminate the effects of any potential variations in the test set-up.

An additional lesson learned during the course of pilot testing was the importance of checking all data early and often. During the 6-sided grip* tests, total force curves were monitored during every test session. It was not until the end of testing, however, that data from individual sensing elements were inspected and the faulty data spotted. Had this been observed earlier in the pilot test, new sensors could have been applied to the grips* and data of a higher quality collected.

5.0 GRIP FORCE MEASUREMENT IN GOLF

The following section describes a series of golf grip force tests to evaluate the suitability of thin, flexible force sensors described in Chapter 3.0. Details on method of application and test procedures is given, followed by a summary of results that includes particulars on ease of use and durability of the sensors and information gained about how the typical golfer grips the club during a standard tee shot.

5.1 SENSOR CHOICE AND APPLICATION PROCEDURE

The thin-film force sensors that were assessed in the evaluation tests performed at varying levels. Each of the sensors have potential to offer useful information and, depending on the situation, each might prove to be the most appropriate. Therefore, tests were conducted with Pressurex film (discussed previously in §4.2.1), Tekscan 9811 matrix sensors, and Flexiforce and QTC individual load cell type sensors. Appropriate Novel sensors were not available for player testing, but in any case, their thicker construction made them less suited to this application.

5.1.1 TEKSCAN 9811 SENSOR ON GOLF GRIP*

Although the 6-sided grips* seemed to provide a fairly realistic feel for the golfers while eliminating preloads on the sensors, it was decided that for all remaining tests the actual golf club and grip* would be left unaltered. Evaluation tests described in §3.3.3 indicated that sensor output errors due to surface curvature were small. The Tekscan 9811, with its rectangular matrix of 16 by 6 sensing elements, was therefore attached directly to the grip*. To facilitate this task, the sensor was cut along its columns, leaving 6 strips of sensing elements that were connected on one end, which could then be evenly spaced running down the length of the golf club grip*. Double-sided tape was used to attach the sensor to the grip* and thin strips of electrical tape were positioned over the non-sensitive regions of the sensor to hold it in place. Micropore tape (a permeable, non-woven, surgical, synthetic adhesive manufactured by 3M) was wrapped around the sensor to help protect it from potential damage by shear forces produced during a golf shot. The use of Micropore tape and limiting the number of shots taken with a particular sensor prevented the problems with sensor durability seen in previous tests (§4.2.1.3 and Figure 4.9). When attached to the golf grip*, 84 of the 96 sensing elements rested entirely against the grip* surface, and it is those elements that were considered in all analysis. Additionally, to account for the preload imposed on the sensors due to the curved surface of the grip*, a zero-force measurement was taken prior to every test session. Images of the sensor on the grip* are displayed in Figure 5.1.

5.1.2 FLEXIFORCE SENSORS ON GLOVES

Being a single load cell type sensor, Flexiforce has the benefit that any number of sensors can be used simultaneously and be placed independently of one another. However, as the number of sensors increases, both the complexity of the data acquisition system and the time spent calibrating sensors increase. For measuring grip force, a 32-channel data acquisition (daq) system was employed and code to control it was written in Visual Basic. Similar configurations have been used in the past to measure grip force (Kong and Lowe 2005; Nikonovas et al. 2004). All 32 channels were utilized during the golf tests, with one channel reserved to record sound data (in order to determine the moment of impact, as discussed in §4.1.3), and all other channels connected to force sensors. The 31 force sensors were then attached to strategic locations on two golf gloves as shown in Figure 5.2. These locations were chosen based on areas of peak loading seen during the Pressurex tests (described in §4.2.1.1), key locations noted during preliminary Tekscan 9811 and Flexiforce tests and on the important regions of the grip described by previous researchers (Budney 1979; Budney and Bellow 1990; Nikonovas et al. 2004). Double-sided and Micropore tape were again used to help position, secure and protect the sensitive area of each sensor. The remainder of each sensor was directed along the most convenient route to the back of the hand using hand-sewn loops of elastic thread as a guide.

5.1.3 QTC SENSORS ON GLOVES

Next generation QTC is merely a material that can be used to make force sensors, which gives the user freedom to create sensors of any shape and size, but consequently requires additional time and energy for the actual design and production. Like the Flexiforce sensors, if the user wants independent measurements to be taken at multiple locations, a data acquisition system and associated software are necessary.

The limitless number of layout options available for this sensor meant that sensors could be created in order to be attached to either the grip* or gloves. For the player tests, the 32 channel daq system was used to control 31 sensors attached to two golf gloves as in Figure 5.3. Electrodes were made by etching copper (17.5 micron thickness) onto a thin, flexible, insulated polyester material. The sensitive area of the 27 sensors on the fingers were all square in shape (10 mm x 10 mm), and the sensitive area of the four sensors positioned on the palms were enlarged to cover a greater area (10 mm x 40 mm and 10 mm x 60 mm). The shape of each sensor was designed specifically for this application, attempting to minimize interference of the sensor with the golfer's grip of the club and to enhance ease of attachment to the gloves. An example of this is shown in Figure 5.4 where the electrode layout for a sensor measuring force at three locations on a finger is displayed. As with the Flexiforce sensors, double-sided and Micropore tape held the sensors in place, and all leads were guided by loops of elastic thread.

5.2 GOLF GRIP FORCE TEST DESIGN

Player tests were conducted for each of the three sensor types separately, however the basic test design was the same for each. All tests were conducted in an indoor netted enclosure facility, with golf shots being taken from an artificial turf matt with a rubber tee. Each golfer was required to wear golf gloves on both hands to protect the force sensor from perspiration and to provide adequate friction between the hands and grip* to ensure the club did not slip during the shot. For each test, one or more leads extended from the force sensors. This test, as well as all other player tests described in this thesis complied fully with the Loughborough University Ethical Advisory Committee code of practice for investigations with human participants. Upon arrival, the tests were explained to each golfer, they were asked to fill out an informed consent form, and were then given as much time as necessary to warm up. After the warm-up the golfers were asked to take a number of tee shots for which grip force was measured, with further details described below.

5.2.1 TEKSCAN 9811

A Tekscan 9811 force sensor was attached to the grip* of a standard driver (graphite shaft, titanium head, 9.5° loft) as described in §5.1.1. Twenty golfers of varying ability (handicaps ranging from 0-22, plus two players new to the game and without handicap), with a mean age of 22.3 ± 4.7 years, participated in the grip force tests.

After the warm-up, the sensor box was strapped to the golfer's left forearm, with the associated cord run over their shoulder and positioned out of the way of the swing. The player was then given time to familiarize themselves with the feel of the sensor box strapped to their forearm and the sensors on the golf grip*. The golfers reported that the sensor box, weighing 153 g, did not impede their swing in any way and could be ignored after a few practice shots.

Once ready, the golfers took ten shots with the driver fitted with the force sensors. Light gates were placed such that the beam was broken just after takeaway to trigger the force sensor and sound level meter measurements, using the method described in §4.1.3. The lag time between the start of recording for the force and sound was determined prior to each test session, and combined with the information from the sound recordings, the moment of impact was determined on each force trace. For each test, the force and sound data were sampled at 264 and 500 Hz, respectively. After the completion of each test, seven photographs were taken of the golfer gripping the club so that hand position relative to the sensing elements could be estimated as closely as possible. An example of these images from one player test is shown in Figure 5.5.

5.2.2 FLEXIFORCE

Thirty-one Flexiforce sensors were fitted to two golf gloves as explained in §5.1.2. Twenty male golfers aged 29.2 ± 15 years were recruited to participate in this test, with handicaps ranging from 0-18 and one player without a handicap. A 32 channel daq system was employed to collect data from the 31 force sensors and one channel was devoted to measurements from a sound level meter. In order to connect the force sensors to the Flexiforce circuits and daq system, 25 pin serial cables were used. The 16 sensors on the left hand and the 15 on the right hand each had their own cable. Due to the weight of each cable, all golfers were asked to wear a pair of braces, with the straps crossed in front to prevent the brace from slipping off their shoulder during the shot. The cables were held in place on each forearm with adjustable elastic straps, and the cables were then guided over the players' shoulders and down their back with velcro straps holding the cable to the braces as shown in Figure 5.6a-b. Golfers commented that they were able to adjust easily, and in many cases found this arrangement preferable to having the Tekscan 9811 sensor box strapped to their forearm. As in previous trials, the golfer was allowed to take practice shots while wearing the gloves with force sensors.

Due to the fact that both the force sensors and sound level measurement were being recorded with the same data acquisition system, it was unnecessary to use light gates to trigger the start of a measurement. Instead, both were triggered manually after the golfer indicated that a shot was about to be taken. 5 s of data was collected for each of 12 shots, with all channels being sampled at approximately 1 kHz.

5.2.3 QTC

Thirty-one custom-made QTC force sensors were fitted to two gloves as explained in §5.1.3 and shown in Figure 5.3. Six male golfers aged 24.3 ± 4.9 years with handicaps 0-22 participated in this test. The test was conducted in the same manner as that with the Flexiforce sensors, save for the number of golfers.

5.3 RESULTS

Based on the three sets of golf tests, comments will first be made on sensor degradation and usability. This will be followed by an in-depth look at grip forces that are produced during a standard tee shot, including methods of analysis, comparisons with previous grip force data, and an evaluation of how the suggestions of instructors and golf professionals match up with the data collected.

5.3.1 SENSOR DEGRADATION

Sensor durability was assessed based on wear during the player tests. It was discovered that each of the three sensor types experienced a decreasing sensitivity to applied force with use. This could be partially compensated for by conducting an additional calibration after tests were completed, but such a calibration could not be done for the 9811 sensor due to the state of the sensor once it had been removed from the grip*. A post-test calibration was used for Flexiforce tests conducted in the later stages of the sensor's life.

There was a discernible difference in the amount of sensor degradation for the sensors used. The sensitivity of the QTC sensors decreased considerably faster than either the 9811 or Flexiforce sensors. It was determined that 9811 and Flexiforce sensors could typically last for 5-6 golfers before the decrease in sensitivity became a major factor, while QTC sensors only lasted for 2-3 golfers (each golfer took 10-12 shots with the force sensors in place). For the QTC sensors, it is difficult to be sure if it was the QTC material itself that was deteriorating, or if it was another part of the sensor such as the electrodes.

It was also observed that the 9811 sensors seemed to withstand physical damage from shear forces much better than in previous tests using 6-sided grips* (§4.2.2). It is assumed that the addition of the Micropore tape around the sensor and the decrease in number of shots taken were the reasons for this.

5.3.2 THIN-FILM SENSOR USABILITY

Through extensive use during player testing and sensor evaluation tests, knowledge of the usability of each sensor type has been obtained. Tekscan 9811, Flexiforce and QTC sensors each have their advantages and disadvantages as discussed throughout this thesis. In terms of usability, there is a large variation for each sensor with regards to the set-up time required.

Of the three sensor types, the Tekscan 9811 requires the least amount of time for preparation. As all software and hardware is purchased as a system, all that is required of the user prior to testing is to condition, equilibrate and calibrate each sensor. This process takes no longer than 10 minutes. An additional benefit with this system is that the software includes features that allow the user to view plots of force output immediately after the completion of a shot, or data can be exported if the user prefers to analyse it elsewhere.

Systems utilizing Flexiforce sensors can have a large range in complexity depending on the number of sensors involved. A fairly simple circuit needs to be made, connecting wires need to be soldered at two places, and calibration curves must be created for each sensor in use. Additionally, a method of acquiring the data is required, and when more than eight sensors are required, the data acquisition system needed tends to become more complex and difficult to

operate. Preparing a set of four Flexiforce sensors for a test did not take much longer than the Tekscan 9811, but a system of 31 sensors took 1-2 hours longer to prepare.

The QTC sensors require all of the work necessary for Flexiforce sensors, but with the added time of creating the actual sensors. Electrode layouts needed to be designed, copper had to be etched onto the thin insulated polyester, QTC material was attached, and sensors were cut to shape and had additional material added for strength. These additional processes added another few hours to the time required to produce a set of 31 sensors. However, for this additional time spent, the user has complete control over sensor design.

5.3.3 ANALYSIS METHODS

For each of the player tests, the grip force for 10-12 shots was recorded. A total grip force was computed in each case by summing the force output from all sensing elements positioned either on the grip* or on gloves. The exact moment of impact was determined for each trace and denoted as time = 0 s, and every shot for a particular golfer was aligned at this point. The total force traces for each test will be discussed individually in the following sections, but the methods of analysing these traces will first be considered. When the force traces for each golfer were plotted, an interesting phenomenon became apparent. Each player appeared to have their own grip force 'signature', i.e. total grip force for a particular golfer was very repeatable, but varied considerably between golfers. A means to quantify the level of correlation between total grip force for different golfers and between shots for an individual golfer was developed and is discussed in the following section. Additionally, a method to compare player ability and the forces measured is introduced. This is followed by a summary of the data from the golf tests conducted with each of the three sensor types.

To look at the grip force 'signature' phenomenon more closely, a cross correlation (CC) was developed to compare different force profiles. (Example total force profiles measured by the Tekscan 9811 sensor are shown in Figure 5.7a-b, and will be discussed in detail in the next subsection.) The aim of this cross correlation was to give an indication of the repeatability of an individual golfer's force profile and quantify the similarity between different golfers. An approximately 2 s segment of the recorded force traces, from 0.75 s prior to impact through to 1.25 s after impact, was used in all calculations. To account for variations in peak force seen between golfers, the force trace for subject m and shot p was normalized as in Equation 5.1, where the mean of that trace was subtracted from each point of that trace, and this difference was then divided by the standard deviation. Data was aligned to impact and a mean normalized trace for golfer m was computed as in Equation 5.2, where P is the total number of shots taken by that golfer. Finally, the cross correlation was computed between the normalized mean for player n and the normalized force for the pth shot of player m and this was divided by the

autocorrelation of the force profile for player n , as seen in Equation 5.3. The result of the cross correlation was taken as the peak of the cross correlation function for the two data lengths being compared because the data were synchronized by impact. Values of the cross correlation typically lie between 0 and 1, where numbers closer to 1 indicate a stronger correlation.

$$\tilde{f}_{mp}(j) = \frac{f_{mp}(j) - \bar{f}_{mp}}{\sqrt{\text{var}(f_{mp})}} \quad 5.1$$

$$\tilde{F}_m(j) = \frac{1}{P} \sum_{p=1}^{p=P} \tilde{f}_{mp}(j) \quad 5.2$$

$$\hat{\gamma}_{n,mp} = \frac{\sum_{j=1}^{j=J} \tilde{F}_n(j) \tilde{f}_{mp}(j)}{\sum_{j=1}^{j=J} \tilde{F}_n(j) \tilde{F}_n(j)} \quad 5.3$$

A link between the forces produced during the golf shots and player ability was also sought. Handicap was chosen as the most obvious indicator of player ability, although there are limitations with handicap in that it does not indicate distance or accuracy of tee shots which are being compared here. The values of force that were used in the comparisons were the peak and RMS force from each golfer's mean total force trace. A Spearman's rank order correlation was used to compare the relationship between handicap and peak or RMS force.

These two tools, the cross correlation and Spearman's rank order correlation, will be used to compare force traces for multiple shots by an individual golfer, compare shots between golfers, compare shots taken using different force sensors, and to compare force output with player ability in the following sections. The information produced gives some insight into the level of repeatability of the grip forces produced during a tee shot and how this varies between players.

5.3.4 TEKSCAN 9811

The data from each of the ten shots taken was saved and processed in Matlab. Total grip force was taken to be the sum of the forces recorded at all sensing elements lying entirely on the grip* minus the preload in each of these sensing elements created by the slight bending of the sensor around the curved surface of the grip*. For each golfer, total grip force was computed for every shot, was aligned by impact and was plotted, with impact denoted as time = 0 s, in Figure 5.7a-b. The number in parentheses on each plot indicates the handicap for that particular golfer (NH denotes no handicap). Although only impact time is marked on the traces, other key points in the swing can be estimated based on research from Cochran and Stobbs

(1968). The downswing lasts approximately a quarter of a second, while the duration of the time from takeaway until impact typically ranges from about three-quarters of a second to just over one second. In most cases, the start of takeaway is not shown in the plots as only 0.75 s is shown prior to impact. Further information about the timing of the swing with respect to the force traces is discussed in §5.3.8.

From these tests it was found that each player appeared to have their own virtually unique grip force 'signature'. A grip force signature existed for all players tested, even for the two players who had only started playing golf six months prior to the test (players s and t). A cross correlation was conducted to quantify the similarities between golfers and between the shots of a single golfer. Estimated peak cross correlation values are displayed in Table 5.1.

All 200 individual total force traces were compared to the twenty mean force curves using this method. With $P=10$ shots taken, this results in ten normalized cross-correlations for each combination of players from which an average was computed. In each case, as expected, the cross correlation is highest when the force traces of a particular golfer are compared to the mean trace for that same golfer (all greater than 0.95). There was only one other occasion where such high correlation was reached, and that was for golfers f and g.

It is important to consider the results from the sensor evaluation tests while contemplating the measured grip force values. For the 9811 sensor it was found that shear forces and surface curvature caused the sensor to overestimate the applied load, while dynamic loads were underestimated. Additionally, this particular sensor estimates the load applied to passive regions of the sensor by considering the applied load in neighbouring sensing elements.

Although it is difficult to split the various grip force signatures into categories with only twenty golfers tested, a few trends do appear to emerge. In nearly all cases, impact occurs near a local minimum, with local maxima on either side. A number of golfers seem to have a fairly defined double peak occurring with impact lying somewhere in the middle (including golfers b, d, f, g, h, m, p and q). It is interesting to note that some of the higher handicap golfers have less defined peaks surrounding impact. Additionally, in many cases it is comparisons between golfers with double-peak profiles that produce the higher cross-correlation values. According to the correlation, the two players that have the most similar total grip force profiles are f and g (mean normalized cross correlation value of 0.95). These two players are included in a group of four that all have high cross correlations with one another (above 0.9), which include f, g, n and q. Figure 5.8 shows the mean total force curve for each of these four golfers for ease of comparison. Another group with high cross correlations is p, g and l, suggesting the existence of families of grip force signatures. In the groups of golfers named, each set has a peak before and after impact, but the timings of the peaks produce the variations in cross correlation that are seen.

Table 5.1 Estimated peak cross correlation values from player tests using Tekscan 9811 sensor on the grip*, each is a mean of the correlation of 10 total force traces produced by the golfer listed in the top row when compared to the mean total force trace of the golfer indicated on the left

	a. (0)	b. (4)	c. (5)	d. (5)	e. (5)	f. (6)	g. (7)	h. (8)	i. (8)	j. (8)	k. (9)	l. (9)	m. (11)	n. (12)	o. (13)	p. (15)	q. (18)	r. (22)	s. (NH)	t. (NH)
a. (0)	0.996	0.695	0.585	0.772	0.800	0.731	0.791	0.914	0.653	0.786	0.756	0.752	0.467	0.689	0.633	0.771	0.783	0.758	0.801	0.564
b. (4)	0.703	0.985	0.519	0.540	0.837	0.903	0.880	0.784	0.915	0.740	0.826	0.756	0.537	0.876	0.575	0.744	0.881	0.911	0.633	0.722
c. (5)	0.595	0.519	0.980	0.636	0.456	0.693	0.670	0.686	0.470	0.533	0.388	0.620	0.449	0.628	0.401	0.679	0.566	0.617	0.699	0.443
d. (5)	0.773	0.533	0.625	0.993	0.553	0.696	0.813	0.781	0.467	0.522	0.559	0.846	0.382	0.684	0.471	0.900	0.627	0.624	0.907	0.542
e. (5)	0.810	0.837	0.454	0.560	0.983	0.776	0.776	0.834	0.841	0.779	0.851	0.738	0.637	0.796	0.819	0.705	0.758	0.891	0.663	0.723
f. (6)	0.742	0.905	0.696	0.709	0.777	0.982	0.957	0.846	0.859	0.654	0.809	0.888	0.641	0.927	0.557	0.849	0.915	0.889	0.786	0.743
g. (7)	0.795	0.873	0.661	0.815	0.770	0.947	0.991	0.864	0.838	0.697	0.777	0.907	0.533	0.902	0.547	0.909	0.906	0.873	0.823	0.698
h. (8)	0.920	0.779	0.677	0.784	0.828	0.837	0.865	0.989	0.767	0.771	0.796	0.867	0.656	0.848	0.747	0.859	0.870	0.860	0.845	0.767
i. (8)	0.659	0.913	0.467	0.472	0.839	0.856	0.841	0.769	0.987	0.760	0.798	0.740	0.592	0.832	0.633	0.710	0.873	0.894	0.535	0.732
j. (8)	0.800	0.740	0.528	0.528	0.782	0.650	0.701	0.777	0.763	0.978	0.616	0.546	0.285	0.630	0.628	0.694	0.704	0.769	0.523	0.498
k. (9)	0.788	0.853	0.404	0.585	0.874	0.835	0.810	0.825	0.826	0.635	0.958	0.822	0.730	0.873	0.674	0.696	0.835	0.877	0.738	0.781
l. (9)	0.757	0.751	0.613	0.851	0.734	0.879	0.909	0.868	0.738	0.544	0.792	0.989	0.724	0.898	0.636	0.903	0.801	0.824	0.868	0.811
m. (11)	0.474	0.538	0.448	0.387	0.638	0.641	0.538	0.661	0.595	0.287	0.713	0.729	0.984	0.740	0.709	0.526	0.578	0.659	0.583	0.848
n. (12)	0.696	0.873	0.623	0.691	0.792	0.921	0.907	0.850	0.830	0.627	0.844	0.901	0.734	0.988	0.668	0.838	0.860	0.914	0.812	0.850
o. (13)	0.662	0.593	0.411	0.496	0.842	0.574	0.571	0.776	0.655	0.644	0.678	0.661	0.728	0.696	0.956	0.630	0.570	0.767	0.617	0.791
p. (15)	0.777	0.741	0.671	0.907	0.703	0.842	0.913	0.862	0.710	0.691	0.671	0.905	0.524	0.839	0.606	0.986	0.776	0.782	0.842	0.735
q. (18)	0.787	0.875	0.560	0.631	0.753	0.907	0.906	0.870	0.869	0.700	0.802	0.800	0.573	0.856	0.548	0.773	0.992	0.840	0.711	0.713
r. (22)	0.771	0.914	0.619	0.636	0.894	0.890	0.885	0.868	0.900	0.773	0.853	0.832	0.657	0.923	0.745	0.790	0.849	0.980	0.767	0.786
s. (NH)	0.801	0.626	0.688	0.906	0.656	0.773	0.820	0.841	0.531	0.518	0.708	0.864	0.577	0.806	0.590	0.836	0.708	0.754	0.994	0.658
t. (NH)	0.587	0.735	0.451	0.563	0.737	0.756	0.719	0.790	0.748	0.509	0.775	0.833	0.862	0.872	0.781	0.752	0.734	0.800	0.679	0.968

Note: Boxes indicate cross correlation between force traces and mean trace from the same golfer; correlations in bold indicate value greater than or equal to 0.9

Some additional comments can be made about magnitudes in the total force traces. The peak values ranged from around 300-1100 N, with all category 1 golfers in the range of 600-750 N. The four female golfers (b, n, o and t in Figure 5.7a-b) tended to have peak values in the lower to mid region at about 300-600 N. There was less variation in the total grip force at impact for the 20 golfers, with a mean of approximately 435 ± 125 N. The peak and RMS values from each golfer's mean total force trace were also plotted against handicap in Figure 5.9. From these plots there did not appear to be a connection between peak or RMS grip force and handicap, but a Spearman's rank-order correlation was conducted to verify this. It was found that there was no relationship between either pair of variables, even at a significance level of $\alpha = 0.10$.

A basic comparison can be made between the data collected in this study and that reported by Budney and Bellow (1990). They showed grip force from two professional golfers and one amateur, with force being measured by three transducers consisting of simply supported beams with metal foil electrical resistance strain gauges situated under the last three fingers of the left hand, under the pincer fingers of the right hand, and under the left thumb. Figure 5.10 displays force profiles for each of the three golfers showing the approximate total force produced when summing the force output from the three transducers. Similarities exist between these three curves and the total force curves in Figure 5.7a-b. Impact occurs at a local minimum for all three traces, and there are local maxima on either side of impact. The peak total force for the three Budney and Bellow traces is considerably lower than that found in this study, but that is to be expected as the force contribution from the whole of both hands is being compared to that from three isolated locations on the hands.

5.3.5 FLEXIFORCE

Total mean grip force curves for every golfer were once again calculated but this time the mean force output for every sensor was computed first and the mean total force was taken to be the sum of the mean output from each of the 31 sensors. This was done so that on occasions when a single sensor did not work properly during a test (as evidenced by a sharp spike in the data), the output from that sensor could be removed rather than having to eliminate an entire total force curve.

The existence of grip force 'signatures' was again verified in the Flexiforce tests. The individual total force curves from three golfers were aligned by impact and plotted to demonstrate this in Figure 5.11. In Figure 5.12 the summed force from the two sensors on the left thumb of each golfer are displayed to show the repeatability of the force produced at individual regions of the hands as well. The left thumb traces showed a bit more variability, particularly for golfer i, but this may be partially due to small shifts in the way the sensors make

contact with the hands and grip* between shots. A cross correlation was conducted using the methods described in §5.3.3 to compare the mean total force for these three golfers with the individual total force curves for each particular golfer. It was found that the individual total force curves for each golfer were highly correlated with the mean for that golfer, with mean CC values of 0.976, 0.985 and 0.993 for golfers i, v and b, respectively.

The mean total, left hand and right hand forces were compared between the twenty golfers to identify similarities using the cross correlation method. This time, however, only mean force traces were used in the cross correlation. The total, left hand and right hand traces for each golfer are shown in Figure 5.13, with the handicap for each golfer in parentheses in the upper left portion of the plot along with a one or two letter identification for each test subject. This identification carries through from the previous test (9811 sensor on the grip*) so that golfers who participated in both tests can be identified. In performing a CC between the normalised mean traces of two golfers rather than a mean and individual traces, the resulting CC value for each pair of golfers is the same regardless of which of the two is chosen to be the reference trace, making the tables of CC values symmetric matrices and the CC value for each golfer's mean compared with itself equal to 1.0. Tables 5.2 to 5.4 show the values acquired from the cross correlation for the normalised total mean force, mean left hand force and mean right hand force traces, respectively.

From the total force cross correlation, it was found that the three golfers with the highest correlations with one another were a, y and aa. A plot of the mean total grip force from these three golfers can be seen in Figure 5.14. In this case, it was not just the location of the primary peaks that caused the high correlation between these golfers. Each had a fairly steady increase in force starting about .4 s before impact and a peak after impact. What might be more interesting to note about these three golfers is that although they have the most similar total grip forces from the Flexiforce test, they have considerably different abilities in terms of handicap (0, 6 and 11) and strike the ball at very different speeds (average clubhead speeds varying from 86-107 mph).

Table 5.2 Estimated peak cross correlation values between mean total grip force of 20 golfers as measured by Flexiforce sensors

Mean Trace Used in Cross Correlation	a. (0)	1.000																			
	u. (0)	0.651	1.000																		
	v. (0)	0.816	0.501	1.000																	
	x. (4)	0.860	0.664	0.860	1.000																
	c. (5)	0.654	0.423	0.635	0.692	1.000															
	e. (5)	0.773	0.856	0.589	0.716	0.344	1.000														
	w. (5)	0.847	0.754	0.739	0.762	0.492	0.876	1.000													
	f. (6)	0.816	0.684	0.796	0.752	0.562	0.829	0.845	1.000												
	y. (6)	0.950	0.765	0.832	0.862	0.679	0.794	0.882	0.873	1.000											
	i. (7)	0.746	0.383	0.771	0.705	0.354	0.684	0.820	0.842	0.739	1.000										
	j. (8)	0.788	0.466	0.891	0.832	0.540	0.629	0.816	0.800	0.820	0.896	1.000									
	l. (8)	0.848	0.787	0.753	0.762	0.551	0.881	0.846	0.903	0.869	0.714	0.667	1.000								
	k. (9)	0.643	0.608	0.371	0.380	0.127	0.811	0.667	0.734	0.639	0.592	0.376	0.789	1.000							
	z. (10)	0.853	0.602	0.891	0.855	0.807	0.597	0.695	0.788	0.896	0.616	0.787	0.750	0.414	1.000						
	aa. (11)	0.936	0.578	0.886	0.881	0.774	0.706	0.801	0.838	0.902	0.743	0.801	0.862	0.548	0.905	1.000					
	bb. (11)	0.872	0.780	0.858	0.880	0.642	0.865	0.920	0.896	0.906	0.781	0.806	0.917	0.629	0.845	0.902	1.000				
	cc. (13)	0.803	0.724	0.689	0.842	0.682	0.800	0.795	0.755	0.812	0.639	0.705	0.767	0.516	0.747	0.815	0.874	1.000			
	dd. (17)	0.790	0.895	0.571	0.672	0.583	0.890	0.859	0.793	0.836	0.527	0.530	0.886	0.724	0.665	0.749	0.866	0.816	1.000		
	q. (18)	0.858	0.759	0.844	0.771	0.599	0.783	0.866	0.910	0.937	0.740	0.786	0.867	0.658	0.877	0.832	0.921	0.754	0.829	1.000	
	s. (NH)	0.853	0.605	0.687	0.733	0.706	0.746	0.776	0.766	0.793	0.628	0.588	0.855	0.640	0.715	0.900	0.857	0.851	0.851	0.740	1.000
	a. (0)	u. (0)	v. (0)	x. (4)	c. (5)	e. (5)	w. (5)	f. (6)	y. (6)	i. (7)	j. (8)	l. (8)	k. (9)	z. (10)	aa. (11)	bb. (11)	cc. (13)	dd. (17)	q. (18)	s. (NH)	

Cross Correlation Between Mean Total Force Traces of Golfer Indicated in Bottom Row and Mean Trace Indicated on the Left

Table 5.3 Estimated peak cross correlation values between mean left hand grip force of 20 golfers as measured by Flexiforce sensors

Mean Left Hand Trace Used in Cross Correlation	a. (0)	1.000																		
	u. (0)	0.682	1.000																	
	v. (0)	0.798	0.560	1.000																
	x. (4)	0.873	0.664	0.859	1.000															
	c. (5)	0.775	0.636	0.831	0.763	1.000														
	e. (5)	0.924	0.702	0.657	0.817	0.680	1.000													
	w. (5)	0.913	0.754	0.784	0.846	0.820	0.895	1.000												
	f. (6)	0.907	0.627	0.862	0.865	0.834	0.895	0.884	1.000											
	y. (6)	0.952	0.736	0.823	0.877	0.859	0.897	0.941	0.928	1.000										
	i. (7)	0.875	0.480	0.801	0.913	0.731	0.824	0.852	0.840	0.857	1.000									
	j. (8)	0.852	0.461	0.923	0.882	0.837	0.719	0.814	0.855	0.869	0.910	1.000								
	l. (8)	0.888	0.774	0.794	0.828	0.815	0.902	0.902	0.937	0.890	0.759	0.740	1.000							
	k. (9)	0.761	0.592	0.407	0.617	0.485	0.891	0.714	0.690	0.704	0.675	0.469	0.742	1.000						
	z. (10)	0.803	0.552	0.900	0.805	0.921	0.697	0.753	0.898	0.865	0.733	0.884	0.805	0.465	1.000					
	aa. (11)	0.810	0.489	0.773	0.768	0.826	0.822	0.823	0.941	0.841	0.754	0.804	0.878	0.594	0.872	1.000				
	bb. (11)	0.836	0.815	0.852	0.894	0.870	0.817	0.895	0.886	0.870	0.808	0.801	0.922	0.633	0.828	0.805	1.000			
	cc. (13)	0.770	0.747	0.623	0.827	0.729	0.823	0.839	0.787	0.826	0.764	0.697	0.808	0.658	0.682	0.754	0.862	1.000		
	dd. (17)	0.718	0.879	0.497	0.580	0.689	0.796	0.840	0.706	0.763	0.527	0.457	0.842	0.705	0.548	0.650	0.806	0.781	1.000	
	q. (18)	0.867	0.744	0.894	0.839	0.875	0.751	0.873	0.866	0.918	0.794	0.839	0.843	0.573	0.864	0.720	0.894	0.733	0.720	1.000
	s. (NH)	0.722	0.657	0.592	0.608	0.726	0.818	0.794	0.837	0.744	0.582	0.540	0.923	0.712	0.667	0.856	0.794	0.734	0.863	0.670
	a. (0)	u. (0)	v. (0)	x. (4)	c. (5)	e. (5)	w. (5)	f. (6)	y. (6)	i. (7)	j. (8)	l. (8)	k. (9)	z. (10)	aa. (11)	bb. (11)	cc. (13)	dd. (17)	q. (18)	s. (NH)
	Cross Correlation Between Mean Left Hand Force Traces of Golfer Indicated in Bottom Row and Mean Trace Indicated on the Left																			

Table 5.4 Estimated peak cross correlation values between mean right hand grip force of 20 golfers as measured by Flexiforce sensors

Mean Right Hand Trace Used in Cross Correlation	a. (0)	1.000																				
	u. (0)	0.642	1.000																			
	v. (0)	0.876	0.443	1.000																		
	x. (4)	0.767	0.724	0.635	1.000																	
	c. (5)	0.706	0.479	0.584	0.853	1.000																
	e. (5)	-0.075	0.524	-0.129	0.179	-0.066	1.000															
	w. (5)	0.250	0.453	0.179	0.217	0.043	0.720	1.000														
	f. (6)	-0.104	0.227	-0.097	-0.044	-0.133	0.668	0.644	1.000													
	y. (6)	0.816	0.812	0.685	0.825	0.675	0.295	0.453	0.239	1.000												
	i. (7)	0.191	-0.007	0.276	0.007	-0.070	0.221	0.526	0.686	0.263	1.000											
	j. (8)	0.439	0.736	0.369	0.567	0.364	0.584	0.608	0.259	0.588	0.091	1.000										
	l. (8)	0.265	0.478	0.242	0.199	0.018	0.644	0.634	0.763	0.556	0.646	0.309	1.000									
	k. (9)	-0.011	0.334	-0.051	-0.118	-0.259	0.491	0.349	0.739	0.268	0.534	0.080	0.843	1.000								
	z. (10)	0.783	0.806	0.685	0.742	0.639	0.232	0.336	0.090	0.912	0.040	0.547	0.429	0.176	1.000							
	aa. (11)	0.678	0.466	0.721	0.481	0.309	0.294	0.592	0.450	0.746	0.729	0.370	0.751	0.441	0.620	1.000						
	bb. (11)	0.849	0.647	0.812	0.547	0.384	0.221	0.578	0.253	0.816	0.452	0.466	0.602	0.310	0.772	0.888	1.000					
	cc. (13)	0.802	0.608	0.806	0.729	0.638	0.327	0.581	0.200	0.781	0.352	0.678	0.463	0.060	0.725	0.752	0.802	1.000				
	dd. (17)	0.708	0.752	0.645	0.569	0.386	0.541	0.751	0.536	0.821	0.539	0.619	0.788	0.505	0.729	0.868	0.906	0.831	1.000			
	q. (18)	0.724	0.652	0.731	0.462	0.298	0.317	0.631	0.411	0.797	0.524	0.489	0.658	0.441	0.757	0.860	0.943	0.753	0.916	1.000		
	s. (NH)	0.768	0.325	0.745	0.392	0.423	0.070	0.518	0.158	0.502	0.462	0.372	0.369	0.050	0.453	0.697	0.793	0.814	0.725	0.683	1.000	
	a. (0)	u. (0)	v. (0)	x. (4)	c. (5)	e. (5)	w. (5)	f. (6)	y. (6)	i. (7)	j. (8)	l. (8)	k. (9)	z. (10)	aa. (11)	bb. (11)	cc. (13)	dd. (17)	q. (18)	s. (NH)		

Cross Correlation Between Mean Right Hand Force Traces of Golfer Indicated in Bottom Row and Mean Trace Indicated on the Left

The cross correlation of the left hand forces indicated that there are several groups of golfers that use their left hand in a similar fashion. One such group involved golfers a, e and y, which includes two of the golfers with the highest total force CC value. The total left hand forces for these three golfers can be seen in Figure 5.15. The three golfers all have an early increase in their left hand force that is approximately maintained until impact, with an additional peak just after impact followed by a decrease in force until around the end of follow-through. It is interesting to note that golfers a and y have high CC values for both total and left hand forces, while golfer aa correlates well with these two for total force only and golfer e has a high correlation with a and y for left hand force alone. This indicates that although golfers may have high cross correlation values for total force, they may not be using their hands to grip the club in the same manner.

The cross correlation values for the right hand revealed that there was a much greater variation in the way that the golfers tested gripped with this hand. Very few players had a $CC > 0.9$ with another golfer. One group of golfers did exhibit a higher level of correlation, and they are q, bb and dd. The right hand forces for these three golfers are displayed in Figure 5.16 for ease of comparison. During the downswing, each of these golfers maintained a rather steady right hand force, which began to increase prior to impact and peaked after impact before dropping down again. An additional smaller peak occurs at approximately the end of follow-through.

Due to the number and location of the force sensors used in this test, the forces produced can be localised to smaller regions of the hands. Figures 5.17 and 5.18 display the individual finger and palm forces of each golfer for the left and right hands, respectively. Although there is great variation between golfers, again there were a few trends. For the left hand, there was often a dominant peak before impact produced either by the thumb (golfers i, j and aa) or a combination of the ring and little fingers (golfers c, q, v, w and y). Additionally, a large number of golfers appeared to have a more even distribution of force over their left hand, with peaks before and after impact containing contribution from all parts of the hand (golfers a, e, f, k, l, s, x, z, bb, cc and dd). For the right hand, it appeared that many golfers used their middle and ring fingers to control the club during part of the take-away and backswing evidenced by peaks early in the trace (golfers a, c, i, j, u, v, x, y, z, cc and dd). Additionally, a large number of golfers had peaks just after impact using one or more of the index, middle and ring fingers (golfers a, i, j, q, s, u, v, w, x, y, z, cc and dd). Otherwise, the force outputs from the various regions of the right hand tend to be similar.

Force data such as that provided here can be used to finally answer some of the questions raised by the differing theories on how best to grip the club. Two basic questions that were considered in the introduction were which hand should provide the firmer grip throughout the

swing (Couples (1994) and Nelson (1947) indicated left hand should grip firmer, and Faldo and Saunders (1989) thought the right hand should have the tighter grip) and which smaller regions provide the highest forces that control the swing (is it the left thumb and index finger (Leadbetter 1993) or is it the last two fingers of the left hand and middle two fingers of the right (Faldo and Saunders 1989; Hay 1980; Lewis 1990; Luxton 1985; Nicklaus and Bowden 1974; Palmer 1965; Torrance 1989)).

For the first question, the total, left hand and right hand forces for each golfer from Figure 5.13 can be referred to. For all twenty golfers that were tested, the left hand grip force exceeded the right hand force for the majority of the shot, and for most of the golfers, the left hand force was considerably larger than the right hand force around and during impact. Whether right or wrong, it appears that most golfers apply a larger left hand grip force throughout the shot.

To address the second question, there are two ways that the data can be used to provide evidence for or against the specific regions of the hand listed as being dominant. The summation of the force for the fingers indicated by each group of instructors could be used to see which provides the highest total force, or, since two fingers (left thumb and right index) are being compared to four (left ring, left little, right middle and right ring), the individual finger forces can be compared. When the summation of force for the two cases are used, in every case (for all 20 golfers), the force output of the four fingers exceeds the two fingers. This is unsurprising due to the fact that the summation is comparing the output from 5 sensors to 12, and it was shown earlier that many golfers have a fairly even distribution of force across each hand. However, when looking at each of these regions by finger, it is less obvious which region produces the most force. Figure 5.19 shows both the summation of forces and the forces for each finger for three golfers. The red traces represent output from the left thumb and right index finger, while traces in blue are for the left ring, left little, right middle and right ring fingers. Based on the golfers taking part in this test, it seems that the fingers listed by both sets of instructors provide a large portion of the grip force, but it is difficult to say which part of the hand is more important during the shot. Like many of the instructors indicated, much of the way a golfer grips the club should be based on their own personal build and abilities and therefore will naturally vary between golfers. This seems to be the case with this second question about grip force.

A comparison was also made, as with the Tekscan 9811 tests, between the handicaps of the golfers in the Flexiforce grip tests and the peak and RMS forces from the mean total force traces. The peak and RMS forces were plotted against handicap in Figure 5.20. A Spearman's rank-order correlation was conducted again, and it was found that there was no relationship between RMS force and handicap, but there was a correlation between peak force and handicap at the 0.05 level, however this relationship appears to be highly dependent on a few 0 handicap

golfers with high grip forces. The relationship found was that the better golfers (lower handicaps) tended to have higher peak total forces occurring during their shot. This finding may be a product of several things. First, it could be that the better golfers do indeed grip the club differently due to their experience, and this contributes to their lower handicaps. Or second, it is very possible that because many of the lower handicap golfers have higher clubhead speeds, the peak forces around impact are required to accelerate the club. This second explanation would explain why there is not always a strong correlation between the grip force and handicap, as not all low handicap players are longer drivers, and not all high handicap players have low clubhead speeds.

As predicted by Budney and Bellow (1979; 1990), relatively high loads were often recorded at the left thumb, but it is important to note that there were only two force sensors on this digit compared to three on the other fingers, and the portion of the thumb in contact with the grip varied between players such that for some golfers the sensor may not have been able to collect the entire force applied by the thumb. In order to better compare the forces produced in this study with those found by Budney and Bellow (shown in Figures 2.7 and 2.8), the total forces in the three regions noted in the Budney and Bellow studies were calculated and plotted in Figure 5.21 for six of the category 1 golfers that participated in this study. The right hand region was considered to be the palm sensors on the right hand, as well as the sensors under the proximal phalanges of the right index, middle and ring fingers. The left thumb force was the summation of forces from the two thumb sensors, and the left hand region was considered to be all sensors under the middle, ring and little finger of the left hand. The grip forces found in this study exhibited many of the same trends as the previous studies. The left thumb and hand forces were shown to have peak forces just before and after impact for most of the golfers, but, in this study, it did not appear that the right hand played such a large role prior to impact as seen in the Budney and Bellow studies. It is hard to know the exact location of the three sensors in relation to the golfers' hands from the Budney and Bellow study, but, based on the descriptions from both papers, it is assumed that a reasonable approximation has been made. Differences in sensor area covered by the fingers will affect the magnitude of the forces measured, but trends in the grip force for the golfers in both studies have been found.

5.3.6 QTC

The output from each player test in which 31 QTC sensors were attached to golf gloves was analysed using the same methods as the Flexiforce sensors. Due to the additional time necessary to create the electrodes and sensors, reduced accuracy as compared to the other sensors studied, and rapid sensor wear, QTC sensors were only used to test 6 golfers. The total

grip force and forces at particular regions of the hands for each golfer are displayed in Figure 5.22a-b. As in all previous studies, grip force ‘signatures’ for each golfer were easily identifiable.

A cross correlation was conducted in the same manner as for the Flexiforce data between the mean total force curves of each golfer to identify any similarities. The results of this correlation are shown in Table 5.5. It was found that there were no correlation values of 0.9 or greater, but a group of three golfers were close at 0.89. Figure 5.23 displays the mean total force curves for these golfers (f, s, and v), and again handicap varies considerably (0-22) for the golfers with similar grip force signatures.

Until these player tests, the full extent of sensor degradation during testing had not been recognised. Post-test calibrations were not made immediately after testing was complete, and so the sensitivity of the sensors after the third (and final) test for each pair of gloves is unknown. It has been observed that peak forces decreased consistently with consecutive golfers. In the player tests, the first set of gloves were used by golfers j, c and v, respectively, and the second set of gloves by golfers s, f and i. The peak total force dropped from 106 N with the first golfer to 64 N with the third golfer for set 1, and from 178 N to 74 N with set 2. Variations in total grip force of this magnitude had not been seen between these golfers in previous testing. Furthermore, the drop in sensor sensitivity is clearly visible from shot to shot taken by a single golfer. Figure 5.24 shows the total force measured from each of 11 shots taken by player f. The legend indicates the shot number corresponding to each trace, and the decrease in total force as measured by the sensors drops as each consecutive shot was taken. The peak grip force in these traces drops nearly 19% from the first shot to the last, and a Spearman rank-order correlation shows that the peak force decreases with each successive shot with significance at the 0.01 level. The same is true for the traces from the other golfers that participated in this test. Due to the dramatic changes in sensitivity and therefore the peak and RMS forces seen throughout the tests, no further statistical analyses were conducted.

Table 5.5 Estimated peak cross correlation values between mean total grip force of 6 golfers as measured by QTC sensors

Mean Trace Used in Cross Correlation	v. (0)	1.000					
	c. (5)	0.596	1.000				
	i. (5)	0.652	0.517	1.000			
	f. (6)	0.890	0.642	0.871	1.000		
	j. (8)	0.642	0.632	0.867	0.779	1.000	
	s. (22)	0.758	0.632	0.696	0.899	0.615	1.000
		v. (0)	c. (5)	i. (5)	f. (6)	j. (8)	s. (22)

Cross Correlation Between Mean Total Force Traces of Golfer Indicated in Bottom Row and Mean Trace Indicated on the Left

(Correlations in bold indicate value greater than 0.89)

5.3.7 COMPARISON OF RESULTS

It is difficult to compare the results of the grip force tests from the three different sensor types as the area covered by the sensors varies so much. The total area of the 9811 sensor is nearly six times that occupied by the 31 Flexiforce sensors, but the area over which golfers' hands are actually applying a load directly to the sensor varies by golfer. It was found that peak total forces in the 9811 study varied from 350-1100 N, ranged from 80-380 in the Flexiforce tests, and totalled 80-180 N in the QTC study. In order to account for these variations in sensor area, normalised versions of the force traces can be utilized. The normalization is conducted by subtracting the mean from each trace and then dividing by the standard deviation, giving a trace that has a mean of 0 and a standard deviation of 1.

Five golfers participated in all three tests, and, for these golfers, normalised mean total grip forces from each test are aligned at impact and plotted in Figure 5.25. For the individual sensor types, these golfers produced typical peak forces of 500-750 N for the 9811 test, 150-180 N for the Flexiforce test, and 75-160 N in the QTC test. Considering the magnitudes of error identified during the sensor evaluation tests, it is important to note that all three sensor types provided very similar and repeatable data. In an attempt to quantify the similarities between the force traces, a cross correlation was conducted in the same manner as described in §5.3.3. For the cross correlation to be carried out, the data from the three force sensors were resampled to 500 Hz, and ten data points from the start and finish of each trace were removed due to resampling errors at those points. For each of the five players, the normalised mean total force trace produced by a given sensor type was cross-correlated with the mean for the other two sensors for that same golfer. The CC values between two sensors for a given golfer was the same, regardless of which was chosen as the reference trace, so the correlation for each pair of sensors is shown in Table 5.6 for the five golfers. Although the CC values for a given golfer are lower than when comparing force traces produced with a single sensor type, overall they tend to be higher than when comparing two different golfers with forces measured by the same sensor, adding to the idea that grip force 'signatures' exist. Furthermore, it is important to note that several months lapsed between data collection using each of the three sensors.

Additionally, it was noted that sampling rate influenced the total force traces. The slower sampling rate of the 9811 sensor (264 Hz, as compared to 1 kHz for Flexiforce and QTC sensors) meant that a small peak due to vibration travelling through the club after impact was usually not present in the force traces, and it is likely that some other peaks were underestimated.

Table 5.6 Estimated peak cross correlation values between mean normalised total force traces measured with three different sensor types

Player	9811 & Flexiforce	9811 & QTC	Flexiforce & QTC
c	0.875	0.974	0.900
f	0.885	0.951	0.897
i	0.971	0.919	0.928
j	0.870	0.890	0.939
s	0.944	0.961	0.928

5.3.8 HIGH SPEED VIDEO

To further the understanding of what is happening at the grip during each golf shot, 18 of the 20 golfers that participated in the test with Flexiforce sensors on golf gloves had their swing captured on high speed video. Two shots were recorded for each golfer using a Photron Fastcam Ultimate APX high speed video camera sampling at 500 frames per second. For each player, the start of takeaway, start of downswing, impact time and end of follow-through were determined, and the total downswing and follow-through times were calculated as the mean of the two shots. Identification of all of these points in the swing, excluding impact time, is somewhat subjective, and it is estimated that each point is within ± 3 frames (± 6 ms). It was noted that downswing time for each golfer was the most consistent part of the swing, having the lowest standard deviation. Total time for downswing and follow-through were plotted on mean total force curves as shown in Figure 5.26a-c. With this additional information it is possible to see where in the swing various peaks occur. The addition of the start of downswing and end of follow-through information helps compare traces of the different golfers and gives a better idea of the timing. It was interesting to note that the first peak for the double-peak golfers occur at different moments in the swing. For golfers i and j the peak occurred at or just after the start of the downswing, golfers q, w, x, and z had the first peak mid-way through the downswing, and with golfers c, e, f, l, u, bb, and aa the first peak occurred at or near impact. For these double-peak profiles, the timing of the second peak was much more consistent, taking place shortly after impact.

The swing of one golfer was analysed further using highspeed images captured at 1000 frames per second with reflective tape used on the shaft. Six key points in the total grip force profile of the golfer were identified, each being local maxima or minima. These are indicated in Figure 5.27, where the start of the downswing, impact and end of follow-through are also

shown, and the golfer's position in the swing that corresponds to each of the six key points is displayed.

Point 1, a local minimum, is when the golfer has brought the grip* end of the club to nearly its full height in the backswing, and just before the golfer starts the transition from backswing to the start of the downswing. The following peak, Point 2, occurs during the initial part of the downswing. Points 3 and 4 occur just on either side of wrist release during the downswing, and Point 5 is just after impact. Point 6 occurs during the follow-through after the right hand wrist cross-over, just as the left wrist begins bend with radial deviation.

6.0 VIBRATION TRANSMISSION AND MEASUREMENT

In order to assess the vibration characteristics of a golf club as part of an investigation of the properties of its feel, Roberts (2002) measured vibration directly at the hand-grip* interface. This differed from previous studies that had measured vibration at points along the shaft or below the grip*. Accelerometers were used to collect vibration data at this location and also on the shaft 35.6 cm (14 inches) from the butt end of grip*. In this study it was found that, for the same club, ball and impact location, the shaft vibration spectra were remarkably consistent between the golfers tested. At the grip*, however, a great deal more variability was observed in the frequency spectra across the range of 0-800 Hz. Typical plots illustrating this data are displayed in Figure 6.1, which shows x-axis (the direction of strike) vibration of both the shaft and grip*. This finding is significant in that it shows that some variation must exist in the grip of the players tested to make such a difference to the way the vibration is transmitted through the club and grip* material to the hand. Thus far, no conclusive explanation has been provided for this phenomenon, which was one of the motivations for the current research project. This chapter is not just about this very important question, but also about the general issue of vibration transmitted into the hand and arm, vibration transmission through sports equipment, human perceptions of vibration and methods of measuring impact-induced vibration from a golf shot.

6.1 VIBRATION IN THE HAND-ARM SYSTEM

To understand the role that the grip plays in vibration transmission during a golf swing, it is important to first understand the basic concepts of how vibration travels into and through the hand and arm. Many variables determine how vibration is transmitted into the hand-arm system, including characteristics of the vibration itself, characteristics of the person involved, and how the implement is used (Griffin 1990). In golf, examples of these variables include the magnitude, frequency and direction of the vibration, dynamic response of the individual's hand, type of grip used, posture, grip and push forces applied, swing characteristics, and whether the golfer wears a glove.

Much research has been done in the past concerning the measurement and quantification of hand-arm vibration transmission in the field of ergonomics, due to the frequent occurrence of vibration related ailments in workers. Reynolds and colleagues studied the effects of vibration transmitted from a handle to the hand grasping it (Reynolds and Angevine 1977; Reynolds and Keith 1977; Reynolds et al. 1977). In the first of these experiments, the hand was excited by a 1.905 cm diameter handle constructed from thick-walled aluminium tubing. A full bridge strain gauge setup was used on the handle to monitor grip force, and the handle was vibrated in three

mutually perpendicular directions: vertically (up and down in a vertical plane parallel to the subject's torso), horizontally (in a horizontal plane perpendicular to and directed towards the torso) and axially (left and right in the horizontal plane, perpendicular to the torso), as shown in Figure 6.2. The frequency of the vibration directed into the hand varied from 5 to 1000 Hz and the participants used two types of grip (finger grip and palm grip, shown in Figure 6.3) and two grip force magnitudes (9 N and 36 N). Grip forces were monitored during the test and feedback was given to the subject in order to maintain the desired force level. A mathematical model was also created that predicted the displacement mobility (displacement/force) of the hand for the same loading configurations. With this model, the amplitude of total instantaneous energy transferred into the hand could be determined by considering the displacement mobility, the amplitude of vibration, the phase angle between the force and displacement signal and the energy dissipated into the hand. From this model and experimental data gathered, it was determined that the instantaneous values of energy supplied to the hand were a function of grip configuration and grip force. In general, the energy directed into the hand was slightly higher for the palm grip than the finger grip and more energy was transmitted for the 36 N (8 lbf) force than the 9 N (2 lbf) force (Reynolds and Keith 1977).

It was also determined that the nature of the energy directed into the hand was a function of vibration direction. For signals above 100 Hz in the vertical direction almost all of the energy directed into the hand was dissipated. For vibration in both the axial and horizontal directions, nearly all of the vibration energy directed into the hand was dissipated or absorbed by the hand for almost all frequencies. According to data gathered by Roberts (2002), the most important direction of vibration for a golf swing would be in the vertical direction as labelled by Reynolds.

A second experiment was run, similar to the first, but with eight subminiature piezo-resistive accelerometers attached to skin above the bone in eight locations between the subjects' fingertips and shoulder (Reynolds and Angevine 1977). It was found that, as frequencies increased above 100 Hz for horizontal and axial vibration and above 400 Hz for vertical vibration, vibration became more localised in the fingers. At vibration frequencies below these levels, however, vibration was transmitted almost unattenuated from the portion of the hand in contact with the handle to the back surfaces of the fingers. A third study was conducted in this series of experiments, and will be discussed later as it relates to the perception of vibration.

In another set of studies, (Burström and Sörensson 1999; Sörensson and Burström 1996; Sörensson and Burström 1997; Sörensson and Lundström 1992) vibration transmission was recorded from a handle mounted on an electrodynamic shaker to twelve points on the hand (all points on dorsal surface of hand and wrist, with 3 points on middle finger, one on each the thumb and little finger, one on MCP joint of the middle ring and little finger, 2 on the middle metacarpal, and 2 on the wrist), energy exposure to white noise vibration was looked at,

vibration transmission to the knuckle, wrist and elbow was considered, and shock-type vibration was compared to non-impulsive vibration. Although these were ergonomic studies, several of the results are relevant to the golf grip scenario. When investigating how vibration is transmitted throughout the hand it was determined that, in general, vibration below 40 Hz was transmitted to all twelve test points (Sörensson and Lundström 1992). For test points located adjacent to the wrist, the vibration transmission decreased significantly at higher frequencies. It was noted that vibration was fully transmitted to the tips of the thumb and middle finger for frequencies up to 500 Hz, but only up to 200 Hz for the little finger. Additionally, it was noticed that at some test points and in the frequency range around 100 Hz an amplification of transmitted vibration seemed to occur. It was concluded that this is likely due to a resonant frequency for the skin.

Using white noise vibration, absorption at various frequencies seemed to follow the same trends as determined by Reynolds and colleagues. Interestingly, females showed consistently lower absorbed energy levels for all vibration frequencies. This difference between males and females was most notable in the lower frequency range. One possible explanation for this phenomenon is that these dissimilarities are due to physiological factors (e.g. age, weight, height, hand volume, blood pressure, etc.), but it is uncertain whether this explanation is valid at higher frequencies where the vibration is concentrated more locally to the surface between the hand and the vibrating handle (Sörensson and Burström 1996).

While looking at how energy is transmitted from knuckle to wrist to elbow, Sörrenson and Burström (1997) showed that 52% of the average total energy across all one-third octave bands (random vibration) was absorbed before it reached the knuckle, 85% before the wrist, and 92% was absorbed before getting to the elbow. When looking at sinusoidal vibration exposure, the average energy absorbed was 40%, 60% and 60% for the knuckle, wrist and elbow, respectively. Again an amplification of energy transmitted to the knuckle occurred at frequencies around 100 Hz.

Many percussive tools create shock-type vibration, more closely resembling a golf shot. Burström and Sörrenson (1999) attempted to measure the influence of shock-type vibrations by measuring the quantity of energy transmitted to and absorbed by the hand, with the assumption that a higher quantity of absorbed energy per unit time (power) indicates an increased risk of injury and a decrease in comfort. The shock-type impulse created by a chipping hammer was used in the experiment and compared to non-impulsive vibration that had approximately the same one-third octave band frequency spectrum. It was determined that the shock-type vibrations induced increased vibration absorption by about 10% when compared to non-impulsive vibrations.

It has been shown that a large number of variables contribute when considering transmission of vibration through the human fingers, hand and arm. The following section discusses how some of these and other factors influence the perception of vibration as felt by the individual.

6.1.1 VIBRATION PERCEPTION

Humans have a number of receptors that respond to mechanical stimuli. Stimulation of these mechanoreceptors in the skin can result in a large variety of touch-pressure sensations, such as hair bending, vibration, and deep pressure or superficial touch (Vander et al. 2001). A cross section of the skin displaying the receptors is shown in Figure 6.4. On glabrous skin (hair-free, such as on the palms of the hands) Merkel discs and Ruffini endings are considered to be for static or slow-changing pressure sensations. More rapid changes in pressure, such as felt when moving the fingers over an uneven surface, are detected via Meissner's corpuscles and Pacinian corpuscles (Griffin 1990; Reynolds et al. 1977). Of these two receptors that respond to vibration, it appears that Meissner's corpuscles are involved in sensations below 80 Hz, while Pacinian corpuscles are involved with vibration over approximately 40 Hz (Griffin 1990). Brisben et al. (1999) suggested that the transition from Meissner's to Pacinian corpuscles might occur at frequencies around 20-25 Hz.

A large number of variables that affect perception of vibration in the hand and arm have been reported. These factors include vibration frequency, duration, direction, contact geometry, contact area, contact pressure, surround of contact, prior vibration stimulation, skin site, skin temperature, age, and pathology (Brisben et al. 1999; Griffin 1990). It is interesting to note that many of the variables that were important in determining maximum grip force, such as body size and muscle tension (not including that associated with grip force) have not been linked to individual's mechanical or subjective response to vibration (Reynolds and Keith 1977).

In order to study the impact that the mentioned variables have on vibration perception, two primary techniques have been used. Determination of perception thresholds usually includes a subject noting when vibration at a specific frequency can just be detected as the amplitude is varied. The lowest vibration level detected 50% of the time for each frequency is plotted to produce a vibration threshold curve. A second technique used to look at the variables involved with vibration perception is the equal sensation contour. To create these contours, the subject determines vibration magnitudes that produce similar sensations at different frequencies. The results of these studies illustrate how the key variables mentioned above affect vibration perception as it is transmitted through the hand and arm and are discussed in the following section.

Miwa (1967) conducted a study to determine threshold and equal sensation contours for vibration in horizontal and vertical directions on the hands for frequencies between 3 and 300 Hz. The hands of 10 subjects were vibrated by either pressing the palm against a flat plate or by holding a handle, with the horizontal direction indicating vibration along the palm in the direction of the fingers and vertical along the palm but perpendicular to the direction of the fingers. It was found that there was no difference in detection of vibration for movement in the vertical or horizontal direction, or for contact forces of 49 N or 98 N. These equal sensation and vibration perception threshold curves were found to be the same regardless of vibration direction and contact force, and are shown in Figure 6.5.

Using the same equipment and grip configurations as in the two previously mentioned experiments by Reynolds and colleagues, a series of equal sensations, threshold and annoyance tests were conducted. For the threshold and annoyance tests, each subject's hand was excited either by a single discrete frequency (ranging from 25 to 1000 Hz) or a single 1/3 octave band vibration signal (centre frequencies ranging from 25 to 630 Hz). The subjects determined the threshold or annoyance level for each signal. For the equal sensation tests, the reference signals had a frequency of 100 Hz and vibration levels of 2.54×10^{-6} m, 2.54×10^{-5} m, and 1.27×10^{-4} m. After vibrating the hand with one of the reference signals, a test signal at a designated frequency would then be applied. The subject then adjusted the test amplitude until it produced the same perceived sensation as the reference signal. For the discrete frequency test, frequencies between 16 and 1000 Hz were tested, and for the 1/3 octave band test, the 1/3 octave bands were obtained by filtering white noise between 25 to 1000 Hz. As in the previous studies, all four grip configurations and three directions of vibration were included. The results of the equal sensation study showed that an individual's perception of vibration was a function of the direction of vibration, grip configuration, reference signal amplitude and the frequency content of the signal. From the threshold test, it was found that the lowest threshold level occurred around 200 Hz. The vibration threshold and annoyance curves from this study are shown in Figure 6.6 for the finger grip and Figure 6.7 for the palm grip. It was also noted that test subjects indicated that low frequency vibration entering the hand (20-80 Hz) was felt in a region between the wrist and shoulder, while higher frequency vibration (125-1000 Hz) was primarily localised in the hands and fingers (Reynolds et al. 1977).

Brisben et al. (1999) conducted a series of five experiments to systematically test the effects of contact area, direction of vibration, contact force, and the shape of the stimulus probe on vibration thresholds. Using a 32 mm diameter cylinder with vibrations of frequency 10 to 300 Hz, the mean minimum threshold was found between 150 and 200 Hz with an amplitude of $0.03 \mu\text{m}$, but thresholds below $0.01 \mu\text{m}$ were observed in some subjects. In a second experiment, stimuli were applied under passive pressure (0.5 N) to eight different sites (3 on the

phalanges of the middle finger, 3 on the phalanges of the middle and ring fingers combined, and 2 on the palm). The subjects grasped the same cylindrical handle mentioned above, and thresholds were measured at 40 and 300 Hz. There were significant differences in thresholds for some of the locations, with the threshold of the middle phalanx at 40 Hz being significantly greater than the rest, and at 300 Hz the threshold was lowest in the palm and then rose as the cylinder moved toward the fingers. Additionally, when two phalanges were stimulated, the thresholds were, on average, lower than when a single phalanx was vibrated. The third experiment looked at the effect of increasing contact force from 0.05 to 1.0 N. It was found that there was no significant difference in threshold for this range of contact forces. The fourth experiment looked at vibration thresholds at the same eight locations on the hand and two frequencies used in experiment 2, but this time with the stimulus being applied with a small probe having a 1 mm diameter tip. On average it was found that the probe thresholds at the fingers were lower at 40 Hz and higher at 300 Hz than the thresholds of the palm, but this was only significant at 300 Hz. Additionally, the probe thresholds were significantly greater than the thresholds with the cylinder at both the fingers and the palm. The final experiment looked at vibration direction and contact area by applying vibration in two directions (parallel and perpendicular to the skin surface) over two areas (using the cylinder and probe previously mentioned). This test was performed on the distal phalanx of the middle finger at 40 and 300 Hz. It was shown that vibration direction only had a small effect, while contact area was the primary source of threshold variation, with the larger contact area providing lower thresholds.

Verrillo and colleagues have conducted a number of studies on vibrotactile sensation, including two which looked at the effects of stimulus duration and contact area. For the contact area experiment, a series of seven graduated contactors were used having areas from 0.005 to 5.1 cm², and frequencies from 25 to 640 Hz were examined. It was found that the area of stimulation was a significant parameter for vibration perception (increased contact area led to decreased threshold levels), but that at low frequencies (25 and 40 Hz) the threshold was independent of area, and for very small areas (0.005 and 0.02 cm²) the threshold is independent of frequency (Verrillo 1963).

The study on stimulus duration was conducted with vibrations being delivered via a 2.9 cm² circular contactor at 250 Hz on the right thenar eminence of the subjects. Subjects were asked to rate a series of nine intensities ranging from 2.0 to 40 dB above threshold that were randomly applied for 10, 80, 600 and 900 ms. It was determined that vibrotactile sensitivity for all levels of intensity reached a maximum at approximately 600 ms (Verrillo and Smith 1976).

This section has discussed the transmission of vibration through the hand-arm system and a number of variables that influence it. It was shown that at lower frequencies vibration travels well through the hand and arm, but as frequencies rise above 100 Hz in the horizontal and axial

directions and 400 Hz in the vertical direction, vibration becomes more localised in the fingers. It was also seen that human perception of vibration reaches its peak in these lower regions, with threshold levels having minimum magnitude at around 200 Hz. Contact area affects threshold levels, with increased area (above 0.02 cm²) for frequencies above 40 Hz leading to decreased threshold levels. The following section will continue to look at vibration transmitted into the hands, but now with focus on the effects of grip force.

6.2 VIBRATION AND GRIP FORCE

In golf and wherever vibration is transmitted to the hand and arm, the dynamic response of the hand and arm will have an effect on the way the vibration moves through the body and the vibrational characteristics of the implement being used. One method of examining the response of the finger, hand and arm is to measure the dynamic response of the hand or fingers while the subject is holding a handle mounted on a shaker. The dynamic response considers the relationship between the driving force and the resultant movements (apparent mass is the ratio of force over acceleration, mechanical impedance is the ratio of force over velocity, and dynamic stiffness is the ratio of force over displacement) (Griffin 1990; Griffin et al. 1982).

It has been noted that, when coupling between the hand and a handle is increased, impedance, or resistance to motion, also tends to increase (Griffin 1990). Therefore, a larger grip force will be associated with greater impedance than a small grip force. The way impedance changes with frequency is affected by grip force and this effect is also dependent on the orientation of vibration. It has also been shown that apparent mass varies between individuals, but this variation has less effect on impedance than variations in grip force by a single subject (Griffin 1990).

Two studies by Gurram et al (1994; 1995) investigated the effect of factors such as magnitude of vibration excitation and grip force on transmissibility and driving point mechanical impedance. In this case, impedance was calculated from a ratio of the applied force over the velocity measured at the driving point, and transmissibility was the ratio of the vibration measured at a given location of interest (such as fingertip, knuckle or wrist) over the input vibration levels. As with the Griffin study, it was found that an increase in grip force led to an increase in the impedance magnitude, especially for frequencies below 500 Hz. It was also found that an increase in grip force tended to lead to an increase in transmissibility for nearly the entire frequency range (10-500 Hz in this particular study).

Another group, Aldien et al. (Aldien et al. 2006a; Aldien et al. 2006b), produced a pair of studies that monitored total absorbed power and driving point mechanical impedance. In the first of the studies, total absorbed power was computed as the real part of the cross spectrum of the measured force and velocity. It was found that, for applied broadband random vibration

with constant spectral density in the 8-1000 Hz region, an increase in grip force (10, 30 and 50 N considered) led to a significant increase in absorbed power across the frequency range 40-200 Hz. This particular study also indicated that an increase in push force resulted in a similar increase in absorbed power for the same frequency range. The second paper by this group considered driving point mechanical impedance, and like Gurram et al. (1995), found that an increase in grip force produced a corresponding increase in impedance for frequencies above 25 Hz. It was also noted that, along with a higher magnitude peak in the impedance, increased grip force served to increase the frequency of the corresponding peak, suggesting a stiffening of the hand-arm system.

Based on the studies presented above, it is clear that there is a potential for the grip force produced by the golfer during a shot to influence the vibration that reaches their hands and fingers. This could explain the findings of Roberts (2002), where it was found that near-identical shots taken by two golfers produced similar vibration levels on the shaft, but differing vibration levels at the grip*. It could be hypothesized that one reason for the difference was a relative stiffening of the fingers and hands for those golfers that used a firmer grip. This idea will be investigated and later discussed in Chapter 7.0.

6.3 VIBRATION TRANSMISSION THROUGH SPORTS EQUIPMENT

The transmission of vibration through sports equipment has been considered in previous studies for sports such as golf, tennis and baseball. Some of the fundamental research in this field has been to determine the 'sweet spot' of various pieces of sporting equipment. The location on a club, bat or racket that is struck by an object can greatly affect the amplitude and frequencies of vibration that are transmitted through that implement to the hands of the player using it. The 'sweet spot' is a term that is often used to describe a zone on the racket or club that creates the best feel at impact. Many definitions have been created to describe this area, such as the centre of percussion, a vibration node or the point of maximum coefficient of restitution. In the sporting world, this topic has been considered widely as a means to better understand what makes a good piece of sporting equipment and the role that the hands play. Sweet spot location has been regularly discussed in golf (Wicks et al. 1998), tennis (Kotze et al. 2000) and baseball (Brody 1986; Cross 1998; Noble and Walker 1994).

Additionally, it has been found that specific types of vibration have been deemed more desirable by players. Hocknell et al. (1996) determined that a more desirable sensation in the hands can be achieved by exciting modes of vibration in a golf shaft-club head system in the frequency range of 500 Hz to 2.5 kHz. In the region of 100 Hz, the vibration was deemed less pleasant. This unpleasant feeling may be due in part to the amplification of transmitted vibration that was noted by Sörrenson and Lundström (1992), which they attributed to a

resonance for the skin in certain locations. Humans are also most sensitive to frequencies between 100 and 300 Hz and this could be another possible reason for the unpleasant feeling caused by the vibration.

Impact induced vibration of hand-held sports equipment and the way this vibration is transmitted into the hand and arm is not just affected by location of collision but by the type, location and strength of grip used by the player as well. To study the performance of a golf club either experimentally or computationally, for instance, a repeatable but representative gripping condition is required that simulates real play conditions. Kotze, et al. (2000) summarised five categories of experimental gripping conditions, as shown in Table 6.1.

Table 6.1 Experimental gripping conditions (Kotze et al. 2000)

Gripping Condition	Definition
Hand-held	Implement held by human but not necessarily carrying out a shot, therefore not necessarily representative of play
Free	Implement is supported by some method that through impact contributes little or no resistance to implement motion
Grip*-pivoted	Implement is supported by some sort of pivot at the butt end of the handle which allows it to rotate freely about that location at impact
Grip*-clamped	Implement is clamped at the grip* by a restraint that allows no rotation or translation in the fixed area
Head-clamped	Implement is fixed to a solid object, eliminating any contribution from the rest of the frame (e.g. in tennis the head of the racket would be rigidly clamped).

There have been many arguments over the gripping condition that best represents actual playing conditions. Wicks et al. (1999) studied the grip*-clamped, free and hand-held gripping conditions using experimental modal and finite element analyses. They concluded that the dynamics of the club most closely conform to the free boundary condition when held by a golfer. A similar conclusion was reached for a baseball bat by both Brody (1989a) and Cross (1998), but Cross added that the hands have a strong damping effect with the result that all vibrations are damped in one or two cycles.

As mentioned earlier, grip force has been shown to alter vibration transmission through sporting equipment. On tennis rackets (Brody 1989b; Henning et al. 1992) and baseball bats (Cross 1998), it has been shown that increased grip tightness increases the vibration experienced in the hand and arm by the subjects tested as well as increasing the damping of vibration, which is in agreement with the findings of Reynolds and Keith (1977). It was noted, however, by

Brody that grip tightness at impact should not affect the post-impact ball velocity, although grip tightness would have an influence on the bat velocity and control up to impact.

This previous research has shown that vibration transmission through a golf club and into the hands is dependent on type of grip and force applied by the golfer. With all that is known about how vibration is transmitted through sports equipment, there are still currently gaps in the knowledge. One aim of this study is to bridge these gaps by relating vibration at the grip* with grip force.

6.3.1 MEASURING VIBRATION PERCEPTION IN GOLF

Studies of player perception of vibration during a golf shot have been conducted in the past (Roberts 2002; Roberts et al. 2005; Roberts et al. 2006). The first of these studies, by Roberts (2002), included preliminary work in which elite golfers were interviewed in order to identify properties that affect a golfer's perception of the equipment they are using. 'Feel from Impact' was identified as one of the major contributors to perception. Variations in club vibration from impact were therefore compared with player perceptions for an assortment of golf clubs. After each shot for which vibration was recorded, golfers were asked to rate the shot on a scale from 1-9 for five questions describing the feel of the shot and the vibration produced. For later tests by Roberts et al. (2006), improvements were made on these perception test techniques to help improve the quality of the subjective data. The main variation in the test protocol was the use of the paired comparison method in place of the rating scales. Golfers were asked to take shots with a pair of clubs and then rate the clubs against one another. This eliminated problems that were found with golfers finding it difficult to apply a numerical value to the magnitude of a 'feel' sensation, as well as ensuring that the golfer has a clear enough recollection of the characteristics of the clubs rated earlier in the comparison to give reliable relative ratings. Based on the findings of Roberts et al., it was determined that the best way to elicit useful subjective data from the golfers was by following the method of paired comparisons.

6.4 VIBRATION MEASUREMENT

There are essentially three categories of transducers used to measure vibratory motion, characterized by the property that they measure – displacement, vibration or acceleration. Typically, acceleration is most commonly measured, as accelerometers tend to be small in size, accurate, have a large frequency response and dynamic range, and are very rugged (Girdhar 2004; Wowk 1991).

There are several types of accelerometers that are commonly used, including piezoelectric (charge), integrated electronics piezoelectric (IEPE), piezoresistive and capacitance. In

piezoelectric accelerometers, a mass is mounted on a piezoelectric crystal so that applied accelerations create forces on the piezoelectric element, resulting in a charge that is proportional to the acceleration of the vibratory motion. IEPE accelerometers are piezoelectric accelerometers with the addition of integral preamplifiers. Piezoresistive accelerometers typically contain a small beam element with strain gauges, which when accelerated deform and produce an electrical output whose resistance changes with acceleration (Brüel & Kjær 2007).

6.4.1 LINEAR VIBRATION MEASUREMENT AT THE GRIP*

In order to determine the effect of grip force on vibration transmission to the hands and arms, it is necessary to measure the vibration level at the grip*. In previous research by Roberts et al. (2002; 2005; 2006), an adapter was developed to measure linear vibration at the grip* in two directions as shown in Figure 6.8. This adaptor was placed between the grip* and the golfer's left hand, with the accelerometers located 63 mm below the butt end of the club. Although the adapter used did cause the golfers to grip the club in a manner slightly different than usual, none of the golfers reported having any problems with the adapter and it seemed to provide a reasonable method for mounting two accelerometers at the grip*. However, with the addition of force sensors, the adapter was deemed to be too much of an obstruction. Simply attaching accelerometers on the shaft below the grip* would not sufficiently describe what is happening at the hand-grip* interface, and would not aid in answering questions about how grip force affects vibration transmission into the hands and arms. A new way of measuring vibration at the grip* was therefore required.

As positioning the accelerometers directly on the grip* would either require modification of the club or interfere with the placement of force sensors, methods of attaching accelerometers to a knuckle or some other point on the hands were considered. Positioning the accelerometers on the skin can create problems with local tissue-accelerometer vibration. These problems have been previously addressed by preloading a low-mass accelerometer to increase the congruence of motion between the tissue and accelerometer and by using a data correction method (Kitazaki and Griffin 1995; Wakeling and Nigg 2001). For this study, preloading the accelerometer could be complicated due to positioning of gloves and force sensors, and the data correction methods require additional testing for each subject involved, making neither solution perfect.

A preferred approach was to avoid attaching the accelerometers to the skin and to attach them to a fingernail instead. The fingernail provides a convenient base for accelerometer attachment, allowing for many methods of adhesion, including double-sided tape, wax, or fast-drying glue. Vibration transmission to the fingernail has been studied, and is described below.

Griffin et al. (1982) investigated methods of determining vibration transmission to the fingers to monitor the influence of protective gloves. A measure of a glove's transmissibility was calculated as the ratio between acceleration on the handle side of a glove to the acceleration on the hand side of the glove. Two methods for mounting accelerometers on the fingers within a glove were considered: (1) mounting an accelerometer to a ring weighing 3.5 g that was placed over the distal phalanx of the finger, and (2) mounting the 0.5 g accelerometer onto a fingernail using wax. To compare the two methods, experiments were conducted using a swept frequency (sine wave) source of vibration applied to a handle that subjects gripped with forces of 5 and 15 N. In all cases it was found that the ring-mounted vibration data had a lower resonant frequency and greater attenuation at higher frequencies. It was concluded that the mass of the ring was large compared to the active mass of the finger at frequencies above 300 Hz and thus limited this method's usefulness to measure transmissibility above 100 Hz. The small accelerometer mounted on the fingernail, however, showed transmissibility near unity for most conditions studied up to around 400 Hz.

Mann (1994) studied a number of factors that affect vibration transmission from the finger to the fingernail. These factors included variations in the mass added to the fingernail, contact force, location of applied vibration, curvature of the finger and the area over which vibration was applied to the finger. Computer-generated broad-band random vibration was applied to parts of the right index finger via a contactor mounted on an electrodynamic vibrator. The applied vibration had an approximately flat power spectrum from 10-1000 Hz, and had a magnitude of 68 m/s² RMS, giving a frequency-weighted magnitude of 10 m/s² when using BS 6842 (1987). Vibration was monitored by a 0.5 g accelerometer fixed to the fingernail with wax, and from the acceleration output of an impedance head that was attached to the contactor. Transmissibility was computed as the ratio between vibration at the fingernail and at the input.

Intersubject variability was considered and it was found that there were differences in vibration transmission for the 12 subjects tested, as shown in Figure 6.9. Transmissibility was found to be about 1.0 until 100 Hz, with resonance frequencies between approximately 350 and 650 Hz where the transmissibility varied between 1.1 and 1.6 depending on the individual. Adding mass to the fingernail reduced the resonant frequency while increasing the transmissibility magnitude at resonance, as seen in Figure 6.10. However, the transmissibility of the 0.5 g accelerometer alone remained relatively constant until nearly 1000 Hz. No statistical differences were found between the transmissibilities of vibration applied to the finger when in a straight or flexed position. It was found that moving the location of vibration stimulation away from the distal end of the finger had the effect of increasing motion at the fingernail and decreasing the frequency of peak transmissibility. Increasing the contact push force caused

greater vibration at the fingernail (forces were applied between 0.25 and 8 N) as displayed in Figure 6.11, but increasing contact area appeared to produce the opposite effect.

Kihlberg (1995) studied vibration transmission to the fingernail, wrist and elbow for subjects grasping a vibrating handle that replicated vibration produced by an impact hammer and a grinder. Both simulated vibrations were produced with frequency weighted accelerations of about 8 m/s^2 (ISO 5349 (1984) was used). An accelerometer was built into the test handle, and another, attached to a small piece of plastic, was used to measure vibration at the fingernail. Subjects produced grip and push forces of 50 N during the test. It was found that transmissibility to the fingernail remained at about 1.0 until frequencies of 250 Hz.

Paddan (1997) investigated the effects of pull force on vibration transmission to the fingernail, and also considered differences due to inter- and intra-subject variability. In the study, a handle (40 mm diameter) was made such that push and grip force could be measured, and it was attached to an electrodynamic shaker. Accelerometers weighing 0.65 g were attached to the handle and to the fingernail of the middle finger of the right hand using double-sided adhesive tape. Computer-generated vibration having a nominally flat spectrum and a frequency-weighted magnitude of 5 m/s^2 RMS (BS 6842 (1987) used for weighting) was applied to the handle in the range of 5-1800 Hz. Transfer functions were calculated between vibration of the handle and of the fingernail using the cross-spectral density function method. It was found that variation in transmissibility between subjects was greater than the variation for a single subject performing repeat tests, as seen in Figure 6.12. Changes in vibration transmissibility was also considered for situations with no grip force and pull forces varying between 10 and 50 N, displayed in Figure 6.13. It was found that below 400 Hz, pull force had no effect on transmissibility, but for frequencies above 700 Hz the increase of pull force from 10 up to 30 N had the effect of increasing transmissibility. Increasing pull force beyond 30 N did not cause any greater change in transmissibility up to frequencies of 1400 Hz.

Overall it has been shown that vibration transfer from the palm or underside of the finger to the fingernail has a transmissibility of unity up to a few hundred Hz regardless of posture, feed force (as long as it is above 1 N), pull force or contactor size as long as the accelerometer mass is small (0.5 g or less). The fingernail has also been shown to be a convenient position to mount the accelerometers, with wax or double-sided adhesive tape being used to position the accelerometer.

6.4.2 TORSIONAL VIBRATION

It has been suggested that golfers' perceptions of vibration may be more strongly correlated to torsional vibration due to off-centre impacts than the linear vibration reaching their hand

(Roberts et al. 2006). In order to make this connection in player tests, two methods for measuring torsional vibration were considered.

Shaft mounted strain gauges have been used previously to provide information about shaft bending (Butler and Winfield 1994; Lee et al. 2002) and torsional motion of the golf club (Roberts et al. 2006). Roberts et al. mounted two herringbone strain gauges on opposite sides of the shaft directly below the grip* and measured torsional vibrations produced by impact with the golf ball. They noted, however, that the flexible, tapered shaft of a standard driver made precise alignment of the strain gauges hard to attain. Improper alignment of the strain gauges meant that bending loads could potentially contribute to the strain measured. Due to the difficulties found in using this method, another means of measuring torsional vibration was sought.

Piezoelectric accelerometers, capable of measuring linear motion, can also be used to measure torsional movement if they are positioned a known distance from the axis of rotation. In order to measure torsional vibration on a golf shaft, an aluminium adapter was built that locked onto the shaft just below the grip* on which accelerometers could be attached on opposite sides of the shaft (Figure 6.14). With the accelerometers facing opposing directions, the mean motion of the two accelerometers divided by the distance from the centre line of the shaft produces torsional acceleration and the effects of linear motion of the two accelerometers cancel out. Additional benefits of this system include that linear motion at the shaft can also be calculated from the same measurement and the system can be moved from club to club -- meaning an identical set-up will be used for each club.

In order to determine the suitability of the accelerometer measurements for monitoring torsional vibration, a pilot test was conducted, taking measurements with both strain gauges and accelerometers mounted on the shaft of a standard driver (Callaway Big Bertha Steelhead III, 9° loft, graphite shaft). The accelerometer adapter was constructed such that accelerometers could be positioned on either side of the shaft at four different distances from the centreline (at 35, 45, 55 and 65 mm). This was done in order to ensure that the signal-to-noise ratio of the torsional accelerometer measurement was satisfactory and to determine if any errors were introduced into the measurement at larger radii due to bending of the adapter. Two herringbone strain gauges were also attached to the shaft just below the grip* as described by Roberts et al. (2006).

A number of shots were hit with accelerometers located at the various distances from shaft centreline. As the strain gauges measure displacement, angular displacement was computed from the accelerometer data (by double integration). Figure 6.15 shows the power spectrum of angular displacement for each measurement method. Although the units were different, the trends with frequency were the same for both measurements. With the accelerometer

arrangement shown to work for measuring torsional motion, and due to the added benefits mentioned above, this method was chosen for use in player tests.

7.0 GRIP FORCE, VIBRATION TRANSMISSION, AND PLAYER PERCEPTION

A final set of golf grip force tests were conducted in order to investigate a possible link between the difference in vibration seen at the grip* for near-identical shots taken by two golfers and the grip force applied by those golfers near impact. This chapter describes the tests, analysis of the data and the results.

7.1 TEST METHODS

When designing the procedures for this set of player tests, several requirements had to be met. The measurements to be taken included grip force, torsional and linear vibration at or near the grip*, clubhead speed, impact location, and player perceptions of the vibration. Test duration was a concern for the player perception portion of the test, as in order to make a comparison between two clubs a golfer needs to be able to use each in reasonably quick succession. Due to the length of time required to record data from the force sensors, it was decided that the test would have to be broken into two parts – the first being used to acquire the golfer's perception of vibration for the clubs used in the study, the second segment being used to take all necessary objective measurements.

The total length of time and number of shots taken during the test were also considered. In order to avoid problems with fatigue and loss of concentration, it was determined that the entire test should include no more than 50 shots and last less than 1.5 hrs. It was determined that the golfer would receive the clubs in the perception portion of the test in pairs (reasoning for this will be described later in this chapter), and for each paired comparison the golfer would need to take 8 shots. To help guarantee at least one central impact for the objective measurements, it was decided that each player should take 10 shots with each club tested. Because total force does not seem to be influenced by the driver used, a total of 10 shots were necessary for the mean force trace, but these did not need to be from the same club.

With these factors in mind, it was determined that only two clubs could be compared in the study. If three clubs were to be used, the golfer would be required to take 24 shots during the paired comparison portion of the study and another 30 shots during the measurement portion, and the entire test would last longer than 2 hrs. The following sections discuss the various measurements taken and the overall test procedure, keeping in mind these restrictions.

7.1.1 FORCE SENSORS

Of the sensor types used in previous player tests, it was the Flexiforce sensors that provided the most reliable time-varying output while retaining the ability to identify force applied by

specific regions of the hands. Therefore, these sensors were selected for use in this final set of player tests.

Information and experience gained from previous player tests suggested that sensors typically lasted for about 60 golf shots before sensitivity significantly decreased. In addition, the time necessary to incorporate each sensor into the force measuring system and conduct the calibration procedure can be considerable. With this in mind, previous Flexiforce golf grip force data was analysed to determine if any sensors were unnecessary. The maximum force was determined for each sensor for all 20 players, and the mean maximum force was recorded for every sensor. It was noted that 12 of the 31 sensors had mean maximum force outputs of <5 N, and 16 of the 31 sensors had mean maximum force outputs of <7 N. For the final player test, 15 of these 16 sensors were removed and two were added to the left palm to give better coverage in this region. A total of 18 sensors were positioned on two gloves (locations shown in Figure 7.1) in order to gather the most important force data, from regions where the hands make the best contact with the club, using a minimum number of sensors.

As in prior player tests, a sound level meter was used to identify the moment of impact. This data was recorded on one of the 32 channels of the data acquisition system that was used with the force sensors, and data measurements were triggered manually. All channels were sampled at approximately 1000 Hz.

7.1.2 VIBRATION

Based on previous research and the preliminary studies described in Chapter 6.0, four accelerometers were chosen to measure vibration at the grip* and on the shaft. At the grip*, it was determined that a fingernail was the most suitable location at which to place accelerometers because it provides a stable base for accelerometer attachment and avoids the pitfalls of local tissue-accelerometer vibration. The left thumbnail was chosen as the left thumb is placed securely on the golf club regardless of grip configuration and, for most grip-types, the base of the right hand is placed over the thumb ensuring that it remains in constant contact with the club throughout the shot.

Two Endevco piezoelectric accelerometers (model 25B) weighing 0.2 g each were mounted in a small plastic block as shown in Figure 7.2. The weight of the entire set-up, including glue, was under 1 g. The accelerometers were positioned within the block so that measurements would be made in perpendicular directions. When the block was attached to the left thumbnail of the golfers participating in this study, one accelerometer measured vibration approximately in the direction of strike (parallel to the surface of the thumbnail, labelled x_v) and the other measured approximately perpendicular to the direction of strike and the axis of the shaft (perpendicular to the thumbnail, labelled z_v), as shown in Figure 7.3. Linear vibration in the

direction of strike was also recorded on the shaft, using two accelerometers that also provided torsional acceleration data.

On the shaft just below the grip*, the adapter described in §6.4.2 was mounted such that it would hold the two accelerometers for torsional vibration measurement. For the player tests, the length of the torsional vibration adapter was reduced as it was found that the accelerometer positions closest to the shaft produced adequate signal to noise ratios and could be used for testing. Two piezoelectric accelerometers (B&K model 4375) were attached to the first position (35 mm from shaft centreline) of the adapter in opposing directions on either side of the shaft. The adapter was aligned on the shaft such that the accelerometers were recording motion in the direction of strike (denoted x_s).

A multi-channel data acquisition system was used to record output from the four accelerometers for 160 ms at 51.2 kHz with a 1 Hz high pass filter and a 20 kHz low pass filter (~140 dB/octave roll-off rate) to prevent aliasing. The start of the measurement was triggered by one accelerometer channel based on output level, with a 5% pre-trigger. Measurements from the shaft accelerometers were used to compute both linear and angular accelerations by combining the output from the two accelerometers using the following equations, where \ddot{x}_s and α_s are linear and angular acceleration, respectively, \ddot{a}_1 and \ddot{a}_2 are the output from the two shaft accelerometers, and r is the distance between the accelerometer and the shaft centreline:

$$\ddot{x}_s(t) = \frac{\ddot{a}_2(t) - \ddot{a}_1(t)}{2} \quad 7.1$$

$$\alpha_s(t) = \frac{\ddot{a}_1(t) + \ddot{a}_2(t)}{2r} \quad 7.2$$

7.1.3 CLUBHEAD SPEED

Laser light gates were positioned on the artificial turf matt such that the clubhead passed through both beams just prior to impact during the downswing, as shown in Figure 7.4. A counter-timer was used to measure the time it took the club to go from one light beam to the next. To prevent false readings caused by an early trigger due to club movement prior to the shot, the counter-timer was reset during the backswing. The time measured was used to compute the clubhead velocity knowing the distance between the light beams was 100 mm.

7.1.4 IMPACT LOCATION

Impact location was measured for every shot taken during the test using pressure sensitive impact labels from LongShot Golf. The approximate geometric centre of each clubface was marked in advance with lines crossing at this point in the vertical and horizontal directions. The

positions of these datum lines were transferred to each impact label so that the location of the centre of the impact relative to the centre of the clubface could be measured.

7.1.5 PLAYER PERCEPTIONS

Based on previous studies discussed in §6.3.1, it was deemed that the paired comparison method was the best way to present clubs to golfers in order to gain useful information about perceived vibration levels. In order to assess the vibrational characteristics perceived by the golfer for each club, the following questions were asked during the test:

Compared to the first club, how did the second club feel?

- More solid, less solid or no noticeable difference
- Softer, harder or no noticeable difference
- Deader (ball came off slower), livelier (ball came off faster), or no noticeable difference
- More vibration, less vibration, or no noticeable difference
- Which club was preferred? 1st club, 2nd club or no noticeable difference

The first three of these questions have been used successfully by Roberts et al. (2006), the fourth had been found useful in previous works (Roberts 2002), and the final question was added in order to link vibration and user preference.

A golfer's perception of a golf shot does not come entirely from 'feel', but also from hearing impact and viewing the flight of the ball (Hocknell et al. 1996). In order to prevent audio or visual cues from influencing a golfer's perceptions on vibration, pink noise was played to the golfer through headphones to mask the impact sound and all shots were hit into a net.

7.2 TEST SET-UP AND PROCEDURE

Sixteen golfers aged 24.5 ± 4.9 years with handicaps ranging from +2 to 22 were recruited to participate in this study. All tests were conducted with the player using two standard drivers in their original specification with no modifications made. Those used were Club A – Taylor Made 360 and Club B – Ping TiSi. These clubs were chosen as their basic vibration properties have been ascertained and past tests have shown variation in the vibrational characteristics of the two clubs (Roberts et al. 2006). All tests were conducted in an indoor netted enclosure facility, with golf shots being taken from an artificial turf matt with a rubber tee.

Upon arrival, the full test procedure was explained to the golfer, and an informed consent form was signed. The golfer was allowed to warm-up for as long as they liked, using clubs other than the two test drivers. When warm-up was completed, the questions for the player perception portion of the test were presented to the golfer. A copy of the questions was hung in the netted enclosure so that the golfer could refer back to them during the test. The golfer was then asked to put on a pair of headphones playing pink noise and was handed the first club.

The order in which the golfers received clubs A and B was varied randomly. The golfer then took two shots with the first club, two shots with the second club, and then another two shots with each club. They were then asked to answer all five questions. If necessary, additional shots were taken with each club until the golfer felt ready to answer the questions. Upon answering the questions, the headphones were removed for the rest of the test.

For the force and vibration measurement portion of the test, ten shots were taken with each club, with linear and torsional vibration, impact location and clubhead speed being measured for all twenty impacts. Grip force was also measured, but only for the last five shots taken with the first club, and the first five shots taken with the second club. This was done to minimise force sensor degradation as well as time spent putting on and taking off the gloves. Again, the order in which the clubs were presented to the golfer was randomized. Upon completion of each shot, clubhead speed and impact location were recorded, and all accelerometer and force measurements were saved.

7.3 DATA ANALYSIS AND RESULTS

7.3.1 GRIP FORCE

As in previous studies, the moment of impact was noted for each force trace and the total grip force was taken to be the sum over all 18 sensors. The total forces for the left and right hands were also determined individually (Figure 7.5), as were other key locations of the hands (Figures 7.6 and 7.7). It is important to note that the large differences seen in the total left and right hand force traces are due partially to the number of sensors used – 14 on the left hand and only 4 on the right. Similar trends to those presented in Chapter 5.0 were observed within this data, including left hand dominance prior to impact and right hand peaks after impact. The left hand traces also show a higher contribution of force from the palm than the previous test, but again this is due partially to an increase in the number of sensors in that region. It was found that for a majority of the golfers tested, the left palm produced the most force before and during impact.

Ten golfers from this study also participated in the previous Flexiforce grip force test enabling the consistency of the golfers' force profiles to be studied. A cross correlation was conducted between the mean total force of each golfer as produced in the two tests. Figure 7.8 shows the two normalised mean total force traces for each golfer, and includes the cross correlation value. For the ten golfers, the average CC value for the two test comparison was 0.946, three golfers had CC values below 0.95, indicating overall a reasonably high correlation between the two tests. Golfer j had the lowest CC value of 0.874, and this was due mainly to a change in force produced by the left thumb. In the first study, the peak before impact was dominated by force applied by the left thumb, whereas in the second study the contribution of

the left thumb was less noticeable. This could be due to slightly different locations of the left thumb force sensors rather than a large change in how the club was gripped. Another reason for some of the change in the grip force profiles seen between the two tests for all of these golfers might be due to the time span between the tests (4-5 months) and to the fact that the first test was taken during peak golf season (late spring and summer) while the second was toward the end of the season (late autumn).

Once again, grip force signatures were evident for all golfers tested. Example total and left thumb forces for each of the ten shots are shown for three golfers (ee, j and i) in Figures 7.9 and 7.10 to illustrate the consistency of the force profiles. These three golfers were chosen as all of the sensors produced quality data for each shot, although similar levels of consistency were seen in the other golfers as well. A cross correlation of the mean total force trace with the individual traces for each shot produced CC values of 0.980, 0.9733 and 0.9839 for ee, j and i, respectively. In order to identify similarities in grip force signatures between golfers, a cross correlation was conducted between the mean total, left hand and right hand forces of the sixteen golfers and the results are shown in Tables 7.1 to 7.3. It is interesting to note that a large number of golfers have similar total and left hand traces, but there are only two instances in which pairs of golfers have high right hand force correlations. These total, left hand and right hand force traces will also be compared to those of a tour professional golfer later in Chapter 8.0.

A Spearman Rank-Order Correlation was conducted to determine if there was any link between the handicap of each golfer and the maximum and RMS force for each mean total force trace. The results suggested that there was no connection between handicap and either of the two force measurements and instead in this test it was seen that most golfers had similar peak and RMS force levels (as demonstrated in Figure 7.11).

Table 7.1 Cross correlation peak values between mean total force grip force of 16 golfers as measured by Flexiforce sensors in final test

Mean Total Force Trace Used in Cross Correlation	cc. (+2)	1.000															
	a. (0)	0.858	1.000														
	ff. (2)	0.770	0.925	1.000													
	gg. (2)	0.776	0.786	0.867	1.000												
	c. (5)	0.587	0.791	0.758	0.464	1.000											
	e. (5)	0.916	0.859	0.799	0.761	0.543	1.000										
	i. (5)	0.924	0.818	0.808	0.859	0.512	0.879	1.000									
	f. (6)	0.873	0.911	0.931	0.922	0.718	0.824	0.884	1.000								
	h. (6)	0.917	0.837	0.759	0.723	0.662	0.929	0.866	0.850	1.000							
	g. (7)	0.814	0.887	0.960	0.933	0.662	0.818	0.878	0.972	0.802	1.000						
	hh. (7)	0.703	0.796	0.880	0.795	0.657	0.682	0.781	0.853	0.649	0.887	1.000					
	j. (8)	0.893	0.882	0.772	0.639	0.705	0.844	0.868	0.789	0.831	0.738	0.686	1.000				
	l. (8)	0.882	0.914	0.859	0.761	0.777	0.919	0.823	0.899	0.961	0.863	0.721	0.824	1.000			
	dd. (17)	0.914	0.783	0.654	0.604	0.642	0.877	0.809	0.750	0.928	0.661	0.506	0.884	0.882	1.000		
	q. (19)	0.915	0.867	0.731	0.702	0.697	0.851	0.829	0.825	0.899	0.725	0.573	0.900	0.888	0.949	1.000	
	s. (22)	0.828	0.872	0.841	0.790	0.735	0.839	0.762	0.905	0.853	0.873	0.790	0.724	0.928	0.750	0.789	1.000
	cc. (+2)	a. (0)	ff. (2)	gg. (2)	c. (5)	e. (5)	i. (5)	f. (6)	h. (6)	g. (7)	hh. (7)	J (8)	l. (8)	dd. (17)	q. (19)	s. (22)	

Cross Correlation Between Mean Total Force Trace of Golfer Indicated in Top Row and Mean Total Force Trace Indicated on the Left

Table 7.2 Cross correlation peak values between mean left hand grip force of 16 golfers as measured by Flexiforce sensors in final test

Mean Left Hand Force Trace Used in Cross Correlation	ee. (+2)	1.000																
	a. (0)	0.881	1.000															
	ff. (2)	0.768	0.905	1.000														
	gg. (2)	0.716	0.767	0.892	1.000													
	c. (5)	0.815	0.871	0.857	0.692	1.000												
	e. (5)	0.878	0.915	0.861	0.779	0.773	1.000											
	i. (5)	0.937	0.905	0.842	0.785	0.817	0.878	1.000										
	f. (6)	0.836	0.905	0.952	0.889	0.880	0.894	0.819	1.000									
	h. (6)	0.897	0.877	0.799	0.680	0.870	0.918	0.856	0.864	1.000								
	g. (7)	0.826	0.882	0.967	0.939	0.826	0.896	0.888	0.950	0.836	1.000							
	hh. (7)	0.782	0.840	0.916	0.858	0.789	0.803	0.851	0.877	0.731	0.919	1.000						
	j. (8)	0.869	0.908	0.764	0.549	0.889	0.810	0.870	0.769	0.835	0.734	0.735	1.000					
	l. (8)	0.889	0.886	0.831	0.691	0.886	0.925	0.854	0.891	0.983	0.846	0.754	0.852	1.000				
	dd. (17)	0.891	0.806	0.614	0.496	0.796	0.812	0.817	0.700	0.899	0.651	0.558	0.873	0.885	1.000			
	q. (19)	0.891	0.885	0.707	0.605	0.862	0.799	0.849	0.777	0.866	0.705	0.630	0.890	0.871	0.923	1.000		
	s. (22)	0.795	0.808	0.821	0.716	0.816	0.888	0.736	0.913	0.874	0.829	0.774	0.753	0.921	0.721	0.740	1.000	
	ee.	a.	ff.	gg.	c.	e.	i.	f.	h.	g.	hh.	j.	l.	dd.	q.	s.		
	(+2)	(0)	(2)	(2)	(5)	(5)	(5)	(6)	(6)	(7)	(7)	(8)	(8)	(17)	(19)	(22)		

Cross Correlation Between Mean Left Hand Force Trace of Golfer Indicated in Bottom Row and Mean Left Hand Force Trace Indicated on the Left

Table 7.3 Cross correlation peak values between mean right hand grip force of 16 golfers as measured by Flexiforce sensors in final test

Mean Right Hand Force Trace Used in Cross Correlation	ee. (+2)															
	ee. (+2)	a. (0)	ff. (2)	gg. (2)	c. (5)	e. (5)	i. (5)	f. (6)	h. (6)	g. (7)	hh. (7)	j. (8)	l. (8)	dd. (17)	q. (19)	s. (22)
ee. (+2)	1.000															
a. (0)	0.621	1.000														
ff. (2)	0.835	0.822	1.000													
gg. (2)	0.853	0.301	0.640	1.000												
c. (5)	0.377	0.812	0.713	0.112	1.000											
e. (5)	0.713	0.171	0.514	0.804	0.057	1.000										
i. (5)	0.394	0.186	0.311	0.437	-0.065	0.180	1.000									
f. (6)	0.446	0.162	0.288	0.443	-0.131	0.461	0.757	1.000								
h. (6)	0.746	0.298	0.543	0.828	0.083	0.834	0.537	0.733	1.000							
g. (7)	0.652	0.715	0.822	0.529	0.771	0.329	0.197	0.193	0.432	1.000						
hh. (7)	0.394	0.659	0.615	0.117	0.688	0.347	0.022	0.319	0.335	0.506	1.000					
j. (8)	0.755	0.411	0.518	0.608	0.217	0.592	0.496	0.649	0.715	0.479	0.333	1.000				
l. (8)	0.724	0.794	0.838	0.552	0.548	0.326	0.569	0.438	0.524	0.574	0.485	0.445	1.000			
dd. (17)	0.893	0.627	0.829	0.778	0.392	0.642	0.623	0.639	0.785	0.639	0.456	0.759	0.809	1.000		
q. (19)	0.846	0.702	0.794	0.757	0.370	0.485	0.654	0.563	0.691	0.580	0.373	0.600	0.904	0.908	1.000	
s. (22)	0.395	0.438	0.376	0.303	0.033	0.378	0.495	0.752	0.612	0.134	0.514	0.351	0.557	0.561	0.616	1.000

Cross Correlation Between Mean Right Hand Force Trace of Golfer Indicated in Top Row and Mean Right Hand Force Trace Indicated on the Left

7.3.2 VIBRATION

The output from each accelerometer was examined for every shot and traces that were particularly noisy or triggered prematurely (such as occurs when the club struck the ground just prior to impact) were removed. Example vibration measurements from the accelerometers on the left thumb and on the shaft adapter are shown in Figure 7.12. Acceleration levels measured on the shaft adapter were combined to form either linear or angular acceleration traces according to Equations 7.1 and 7.2. Typical torsional vibration measurements for toe (-14 mm, 3 mm), heel (14 mm, -2 mm) and centre (-2 mm, -1 mm) impacts relative to the geometric centre of the clubface are displayed in Figure 7.13.

RMS linear vibration levels at the shaft and on the thumb and RMS torsional vibration at the shaft were calculated for the first 50 ms of these measurements. A combined total linear RMS vibration at the thumb was computed using Equation 7.3, where $\ddot{x}_{i,RMS}$ and $\ddot{z}_{i,RMS}$ are RMS vibrations from the thumb accelerometers.

$$C_{RMS} = \sqrt{(\ddot{x}_{i,RMS}^2 + \ddot{z}_{i,RMS}^2)} \quad 7.3$$

These RMS values and the magnitude of the first peak in the angular acceleration trace are displayed as a function of impact location in Figures 7.14 to 7.17. These plots illustrate, for each impact location (x_i, y_i) on the clubface, the mean vibration levels for all shots within the range $(x_i \pm 3 \text{ mm}, y_i \pm 3 \text{ mm})$, with the mean based on at least three impacts. The four figures show impact position from the viewpoint of looking at a right-handed clubface, with the point (0,0) representing the geometric centre. From measurements taken at both the thumb and shaft, lines of equal total RMS linear vibration were found to run from high toe to low heel for both clubs, although this was more obvious with Club A. As one might expect, vibration at the thumb was considerably lower than that measured at the shaft, but followed the same trends. Roberts et al. (2006) had similar findings in a study of five clubs. For RMS torsional vibration, the mean level increases as impacts move away from the geometric centre of the clubface. Within approximately 10 mm of the centre in any direction, the RMS torsional vibration levels are quite similar. The first peak of the torsional acceleration traces show high positive peaks for high toe impacts, and high negative levels for heel impacts, with bands of equal vibration level running from low toe to high heel. It seems that central impacts tend to have a slightly negative first peak.

The mean combined total linear vibration at the thumb was computed for central impacts (within 10 mm of centre) for each golfer and is shown in Figure 7.18. Three of the golfers did not have at least three central impacts from which to compute mean vibration levels and were therefore not included in the figure. It was found that there were significant differences in the

amounts of vibration experienced at the grip* between several of the golfers. Similar results have been found in previous studies (Roberts et al. 2005; Roberts 2002).

Power spectra for the acceleration measured on the left thumb (\ddot{x}_t and \ddot{z}_t) and linear acceleration of the shaft (\ddot{x}_s) were plotted for shots from each golfer in Figure 7.19. As was found by Roberts (2002), the level of the shaft vibration varies but the shape is remarkably consistent, especially for frequencies over 400 Hz. The different vibration levels recorded are likely due to variations in clubhead speed. The power spectra of vibration on the grip* in the x_t and z_t directions showed greater variation than that for the shaft, but the mean traces for the thumb and shaft accelerometers showed peaks at approximately the same frequencies. Additionally it was noted that there were greater inter-subject variations in the spectra than there were between shots taken by a single golfer, which can be seen in the power spectra for three golfers in Figure 7.20. Of these three, golfer dd has the highest vibration levels for nearly all frequencies at the shaft while golfer ff has the lowest levels. At the grip*, however, the relative vibration levels change such that all three golfers have similar levels, and in some cases, such as vibration in the z_t direction for Club B, ff actually has the highest vibration level. Figure 7.21 shows the total grip force for these three golfers, and it is apparent that golfer ff has a much higher grip force leading up to impact. It is assumed that this higher grip force has led to increased vibration transmission to the golfer's hands, seen as a smaller drop in the vibration levels from the shaft to the grip* than the other two golfers. It is hypothesized that differences in the way golfers grip the club affect vibration transmission to the grip*, producing the variations seen in the power spectra and RMS vibration at the grip*. Comparisons will therefore be made between grip force and change in vibration level between the shaft and grip* for all of the golfers tested to see if any trends can be identified in the following sub-section.

To further examine the change in vibration between the shaft and grip*, cross-spectral density methods were used to compute the shaft to grip* transfer function $H(f)$ using Equation 7.4, where $G_{ii}(f)$ and $G_{oo}(f)$ are the power spectral densities of the input (shaft, denoted with an s) and output (thumb, denoted by an x or z depending on the accelerometer) motion, respectively, and $G_{io}(f)$ is the cross-spectral density. The modulus of this transfer (Equation 7.5) function produces the transmissibility of the vibration from shaft to thumb. The coherence between the input and output motion was computed with Equation 7.6 to determine the influence of noise on the transfer function. The coherence function produces values from 0-1, and an ideal system with no noise will produce the maximum coherence at all frequencies. Lower coherence levels indicate that the output motion is not varying linearly with the input motion (Bendat and Piersol 1986; Griffin 1990; Pelmear and Wasserman 1998; Randall 1987).

Examples of the transmissibility and coherence for several shots taken by three golfers are shown in Figure 7.22a-c. Data for the x-direction thumb and shaft accelerometers are on the left, while z-direction thumb and shaft acceleration data is on the right.

$$H(f) = \frac{G_{io}(f)}{G_{ii}(f)} \quad 7.4$$

$$T_{io}(f) = |H(f)| = \left[(\text{Re}[H(f)])^2 + (\text{Im}[H(f)])^2 \right]^{1/2} \quad 7.5$$

$$\gamma_{io}^2(f) = \frac{|G_{io}(f)|^2}{G_{ii}(f)G_{oo}(f)} \quad 7.6$$

It was noted that the transmissibility measured for each golfer tended to be quite consistent, and there were some common trends between golfers. These include considerably lower vibration at the thumb compared to at the shaft, represented by a transmissibility below 1.0 for most frequencies, and a peak representing a resonance at approximately 70 Hz. It was also observed that there were larger variations in transmissibility between two golfers using the same club than for the transmissibilities of a single golfer using both clubs. The coherence measured was near 1.0 for most frequencies above 25 Hz, indicating that the majority of the motion being measured at the grip* was strongly correlated with the motion that is occurring at the shaft and there is little interference from noise, although some deviation from linearity can also be seen near the resonance frequency.

A final comparison was made between the vibration at the shaft and at the thumb for each shot by computing the ratio between the combined RMS vibration at the thumb and the RMS vibration at the shaft as in Equation 7.7. RMS vibration at the grip* and shaft was calculated in the same manner as mentioned previously, using 50 ms of the recorded data. Ideally, a ratio would be formed between the combined vibration at the grip* and the combined vibration at the shaft, but for this study it was not possible given that the vibration at the shaft was only measured in the direction of strike. However, it has been shown that vibration measured just below the grip* on the shaft in the direction of strike is considerably larger than that measured in the z-direction (Roberts 2002; Roberts et al. 2005). Combining the data by squaring, summing and rooting the vibration in the two directions would only serve to decrease the influence of the z-direction vibration, thereby making the current vibration ratio a sensible alternative. The mean and standard deviation of the vibration ratio for shots with acceleration measurements with little or no noise are plotted in Figure 7.23. The ratio for only 11 golfers is shown in this figure as for five of the golfers there were not at least three shots for which all

four accelerometers produced output with low noise simultaneously. This vibration ratio was quite variable between the golfers, with the mean ratio varying between around 0.23 to 0.47.

$$VR = \frac{C_{RMS}}{S_{RMS}} \quad 7.7$$

7.3.3 FORCE AND VIBRATION

In the hand-arm vibration studies discussed in §6.4.1, it was found that an increase in force produced by the fingers where vibration was being measured led to an increase in the stiffness of the finger (Aldien et al. 2006a; Aldien et al. 2006b). This resulted in an increased magnitude and frequency at resonance for the measured transmissibility (Gurram et al. 1994; Gurram et al. 1995; Mann 1994). Using the three golfers whose power spectra, transmissibility and coherence were shown previously (ee, ff and dd), a comparison was made between the transmissibility magnitude and frequency at resonance and the mean force that each golfer applied to the club just before and during impact. Of these three players golfer ff had the tightest grip on the club just before impact (as shown in Figure 7.21), and therefore it might be hypothesized that this golfer would have the highest resonant frequency and transmissibility magnitude at resonance. This was indeed the case for the resonant frequency of T_{sx} , but golfer ee had a higher transmissibility magnitude at resonance and resonant frequency for T_{sz} . Reasons for this may include that for several shots there was a drop in coherence in the 70 Hz region and the system in question is much more complex than that being described in typical hand-arm vibration studies. Due to the lower levels of coherence near resonance for some shots and the rather coarse frequency resolution, comparing the magnitude of the transmissibility and frequency at resonance to grip force may not produce the most reliable data. Instead, all further comparisons between the drop in vibration between the shaft and thumb and grip force were conducted using the vibration ratio introduced in the previous section.

Table 7.4 Summary of force and vibration characteristics of three golfers; T_{sx} and T_{sz} are the transmissibilities between the accelerometers on the shaft and accelerometers in the x_t and z_t directions, respectively

	ee. (+2)	ff. (2)	dd. (17)
Mean Clubhead Speed (mph)	101	93	96
Mean Total Force, -0.3 s to Impact (N)	68	114	56
Mean Left Thumb Force, -0.3 s to Impact (N)	7	33	7
Mean 1st Resonant Frequency in T_{sx} (Hz)	69	71	55
Mean 1st Resonant Frequency in T_{sz} (Hz)	74	70	67
Mean Magnitude of T_{sx} at Resonance	1.9	1.5	1.3
Mean Magnitude of T_{sz} at Resonance	3.5	1.5	1.3

The vibration ratio was compared to the mean total, left hand, right hand, left thumb and index, left thumb, and top (distal) sensor of the left thumb forces for each golfer, with these forces being computed in the following time intervals: -0.1 to 0 s, -0.1 to 0.1 s, -0.2 to 0 s, -0.3 to 0 s, -0.4 to 0 s, -0.5 to 0 s, and -0.6 to 0 s, where time = 0 s is the moment of impact. Table 7.5 shows the vibration ratio and mean forces for the time intervals -0.1 to 0.1 s and -0.3 to 0 s for 11 golfers, each of whom had several shots for which low noise levels were present in all four accelerometers. Figure 7.24 shows the mean total, left thumb, and top (distal) left thumb sensor forces plotted against the vibration ratio with a linear curve fit. In each case there appears to be a trend towards an increase in vibration ratio with higher grip forces. This trend can also be seen in Figure 7.23 where the mean distal left thumb force is plotted along with mean vibration ratio for eleven golfers. A Spearman rank-order correlation was computed between the force and vibration ratio data in order to determine if there was a significant relationship between the vibration transmission between the shaft and thumb, represented by the vibration ratio, and the grip force applied by the golfer. For $n = 11$ and $\alpha = 0.10$, the critical value of the statistic is $\rho_{crit} = 0.537$. Therefore, for correlations where the value of ρ is higher than this critical value, it is determined that there is a rank order relationship. A statistically significant rank order relationship was found only between the vibration ratio and the force from the top (distal) left thumb sensor. This was found for time intervals -0.3 to 0 s, -0.4 to 0 s, -0.5 to 0 s, and -0.6 to 0 s. For the other three time intervals, the rank-order relationship was approaching significance at the $\alpha = 0.10$ level, with $\rho = 0.536$ in each case. It is unsurprising that force applied in the region closest to the grip* accelerometers has the strongest correlation with vibration transmission to that region.

Table 7.5 Comparison of vibration ratio and mean grip forces for 11 golfers with Spearman rank-order correlation statistic ρ (for $n = 11$ and $\alpha = 0.1$, $\rho_{crit} = 0.537$); TF = total force, LH = left hand, RH = right hand, LT+LI = left thumb and index, LT = left thumb, and LT_{top} = top (distal) left thumb sensor

Golfer (Handicap)		ee. (+2)	a. (0)	ff. (2)	gg. (2)	c. (5)	e. (5)	i. (5)	h. (6)	g. (7)	j. (8)	dd. (17)	ρ ($\alpha = 0.1$)
Vibration Ratio		0.23	0.36	0.47	0.28	0.24	0.30	0.28	0.32	0.38	0.33	0.24	
Mean Force (N) -0.1 to 0.1 s	TF	80	112	106	104	134	163	106	99	107	67	80	0.281
	LH	72	89	93	91	118	133	88	83	99	60	61	0.272
	RH	8	23	13	13	16	30	19	16	8	7	19	-0.072
	LT+LI	17	18	29	29	16	35	20	26	17	10	7	0.264
	LT	16	13	27	28	15	33	19	23	16	8	6	0.227
	LT _{top}	2	7	23	16	8	15	3	8	7	5	3	0.536
Mean Force (N) -0.3 to 0 s	TF	68	112	114	112	113	137	107	71	112	64	56	0.355
	LH	64	94	108	108	106	120	93	62	109	57	42	0.373
	RH	5	18	6	4	6	17	14	10	3	7	14	0.045
	LT+LI	9	15	33	40	14	34	21	20	16	9	8	0.400
	LT	7	13	33	39	14	32	19	18	16	7	7	0.282
	LT _{top}	2	10	32	25	11	20	7	11	13	6	6	0.6

7.3.4 PLAYER PERCEPTION

Responses to the five perception questions were collected for each player after comparing shots taken with Club A – Taylor Made 360 and Club B – Ping TiSi. To help visualise the responses recorded, a value of +1 was given to responses indicating that a club was more solid, harder, livelier, had more vibration or was preferred. Values of -1 represent responses describing a club as less solid, softer, deader, had less vibration and was not preferred. A value of 0 was used for all ‘no noticeable difference’ responses. Figure 7.25 shows the mean and standard deviation of these scores for the five feel characteristics that were addressed during this study. The golfers’ responses were split fairly evenly between the two clubs for solidness, hardness and liveliness of the feel of the club after impact. A majority of golfers felt more vibration with Club A, but preferred Club B.

To determine if there were significant differences in the responses for the two clubs, analysis of data followed the guidelines in BS 5929-2 (1982) for the method of paired comparisons. Answers for each question fell into one of three categories, indicating that when comparing the first club tested to the second, there was more of a specific feel sensation (e.g. solid feeling, vibration, etc), less of that feel sensation, or no noticeable difference. According to the standard, because ‘no noticeable difference’ responses have been allowed, there are two methods of dealing with these responses. First, they can be ignored (i.e. subtract them from the total number of replies), or second, half of the ‘no noticeable difference’ responses can be

allocated to each of the other two categories. The second method was used when determining whether there were significant differences between the responses for the two clubs. Significant differences are found based on a binomial distribution, and in this case, 13 out of the 16 golfers needed to respond in the same manner to a question for the result to be significant at the $\alpha = 0.05$ level. The question about which club produced the most vibration had responses that were significantly different at the $\alpha = 0.10$ level.

7.3.5 VIBRATION AND PERCEPTION

Players' perceptions of vibration level can also be compared to measured vibration. The mean and standard deviation of combined linear RMS vibration at the left thumb for 50 ms intervals of central impacts (within 10 mm of centre) is shown in Figure 7.26. Each of these golfers had at least three central impacts for each of the two clubs. For these seven golfers, all but one (golfer g) had a mean combined vibration in Club A that exceeded that of Club B, but there were few cases for which the difference was significant. Of the fifteen golfers that answered the question on vibration, nine stated the Club A created more vibration at the grip*, one determined that they felt more vibration with Club B, and five could detect no noticeable difference. As vibration was not measured during the actual perception test, it is assumed that similar vibration levels were produced during the second portion of the test.

Torsional vibration may also play a role in golfers' perceptions of vibration. Therefore, the mean torsional RMS vibration was calculated for each golfer for the two clubs as well, and this is shown in Figure 7.27. Vibration levels were considered for impacts at all locations as central impacts generate little torsional vibration for all golfers, but vary more based on impact location. The mean torsional vibration for all impacts gives a more realistic view of what the golfer may have been feeling in terms of torsional vibration during the perception portion of the test. For the majority of golfers, the mean torsional vibration levels were similar with either club.

Although a significant number of the golfers determined that Club A produced more vibration than Club B, this trend was not seen in either torsional vibration on the shaft or linear vibration measured on the left thumb. However, according to the total RMS linear vibration levels produced based on impact location shown in Figure 7.14, it appears that off-centre impacts from Club A produce higher vibration levels than those for Club B, especially for high heel impacts. It could be that it was the linear vibration produced during off-centre impacts that led the golfers to indicate higher vibration levels in Club A. That said though, based on the relatively similar vibration measurements recorded for most golfers for the two clubs, it is unsurprising that the golfers did not produce significantly different responses for solidness, hardness or liveliness of feel from each impact. As found in previous studies, it can be difficult to connect perceptions of vibration to measured quantities (Roberts et al. 2006, Roberts 2002).

This can be due to a number of factors, such as varying interpretations of the perception questions by the golfers and vibration measurements not fully representing the vibration felt by the golfers during the shot.

7.3.6 SUMMARY

Vibration on the shaft and left thumbnail were compared to grip force and players' perceptions of vibration during a golf shot. Power spectra of the linear vibration on the shaft indicated that although level of vibration varies, the shape of the spectra from each golfer is remarkably consistent, especially for frequencies over 400 Hz. The level of measured vibration was considerably lower at the left thumb, and there was much greater variation in the vibration between golfers. It was hypothesized that the way in which the golfers gripped the club affected the vibration transmitted into the hands. A statistically significant relationship between applied grip force under the distal phalanx of the left thumb and the vibration transmitted to the thumb was found, indicating that increased force leads to increased vibration transmission. An evaluation of the players' perceptions of the vibrations produced using two different golf clubs resulted in a significant number of responses indicating that one of the clubs produced less vibration than the other. As found in previous studies it was difficult to link these perceptions of vibration to measured quantities, however, it was interesting to note that the club that the golfers named as producing less vibration was also selected as the preferred club.

8.0 COMPARING GRIP FORCE WITH A PROFESSIONAL GOLFER

Grip force signatures have been found for each golfer tested within the studies presented in this thesis, but thus far data has only been given for golfers who are beginners to high level amateurs. The grip force information for a final golfer, a tour professional that has been ranked in the top 50 in the world and top 30 in Europe for the past three years, and was part of the winning 2004 and 2006 Ryder Cup teams (PGA European Tour 2007), will now be introduced for comparison.

For the testing of the professional golfer, grip force was measured with 18 Flexiforce sensors on two golf gloves using the set-up and procedure described in §7.1.1. A total of twelve tee shots were taken for which grip force and sound pressure were measured, and these were analysed as in previous studies. The individual total grip force traces for the 12 shots are shown in Figure 8.1; the mean total, left hand and right hand traces are displayed in Figure 8.2. As with all other golfers tested, this professional had a clear grip force signature. A cross correlation between the mean total force trace and the total force from each individual shot was conducted, resulting in a value of 0.992. The plots of the individual force traces and this high peak cross correlation value indicate the highly consistent nature of the force this golfer applied at the grip* throughout each shot. A higher cross correlation value was only achieved by 3 of the 20 golfers that participated in the Tekscan 9811 sensor test. Additionally, this golfer exhibited the very common double-peak type total force curve, with the two dominating peaks occurring on either side of impact.

In order to compare the traces of the sixteen golfers that also had grip force measured with this configuration of sensors, a cross correlation was conducted. Again mean force traces from each of the golfers were compared with the professional golfer's mean force traces, with total, left hand and right hand force traces considered. The correlation values for each of the sixteen golfers are listed in Table 8.1.

Table 8.1 Estimated peak cross correlation values obtained from comparisons between a professional golfer and sixteen amateurs for mean total (TF), left hand (LH) and right hand (RH) force traces.

		Golfer (Handicap)							
		cc. (+2)	a. (0)	ff. (2)	gg. (2)	c. (5)	e. (5)	i. (5)	f. (6)
Cross Correlation Value	TF	0.798	0.845	0.848	0.753	0.810	0.779	0.759	0.857
	LH	0.780	0.829	0.814	0.666	0.933	0.772	0.748	0.859
	RH	0.839	0.694	0.794	0.611	0.461	0.517	0.444	0.489
		h. (6)	g. (7)	hh. (7)	j. (8)	l. (8)	dd. (17)	q. (19)	s. (22)
	TF	0.844	0.810	0.676	0.805	0.893	0.851	0.876	0.794
	LH	0.873	0.778	0.678	0.828	0.895	0.839	0.865	0.808
	RH	0.578	0.580	0.414	0.713	0.796	0.913	0.836	0.475

Correlations in bold indicate values greater than 0.9

From the cross correlation it was found that none of the amateur golfers had a total force trace with a high (>0.9) correlation value with respect to the professional, but golfers l and q were close with 0.893 and 0.876, respectively. The total force curves for these three golfers can be seen in Figure 8.3. Golfers c and dd had high correlations with the professional for the left and right hands, respectively, and these traces can be seen in Figure 8.4.

The individual finger forces of the professional golfer were considered as well, and are shown in Figure 8.5. For the left hand, it was found that the highest peak just prior to impact was produced by the little finger. The left thumb and ring finger produced peak forces just before and after impact, and the middle finger had a dominant force peak just after impact. The left palm provided a steady high force throughout impact. The force measured by the index finger was relatively constant and much lower, but this may be due in part to having a smaller region covered by the force sensors. As for the right hand, grip force was dominated by the ring finger, which produced peak forces on either side of impact.

These individual finger forces of the professional golfer can be compared to those produced in the Budney and Bellow studies (1979; 1990). Figure 8.6 shows the summed forces for the right hand, left thumb and left hand for the professional golfer's tee shot measured by the Flexiforce sensors that were in similar regions to where Budney and Bellow were measuring grip force. Peaks in grip force before and after impact were found for the professional golfers, but the timing and relative magnitudes of those peaks differed for each player. By comparison, it was found that the professional golfer from this study had peak forces of lower magnitude for the right hand and left thumb regions, but the left hand forces were much higher than those measured for three professional golfers in the Budney and Bellow studies. This highlights the fact that golfer in this study produced a relatively high level of grip force at the last three fingers of the left hand compared to what was applied in the left thumb and right hand regions. From

the data presented by Budney and Bellow and in the present studies, no substantial differences present themselves between the grip force traces of amateurs and professionals.

High speed video footage of the professional golfer was also recorded at 1000 frames per second. This was used to help explain what was happening during specific portions of the golfer's force trace. Figure 8.7 indicates five key regions of the force trace that were considered, and frames from the high speed video corresponding to each of these points are shown as well. Point 1 is a local minimum that occurs during the backswing when the grip* end of the club has almost reached its highest point. Points 2 and 3 occur during the downswing on either side of wrist release, with the former being a local force maximum that occurs when the left forearm is approximately parallel to the ground, and the latter a local minimum. Point 4 is a local maximum occurring after impact, and point 5 is a local maximum in the right hand force that corresponds with the right wrist cross-over.

Although there is considerable difference in the force traces of the professional and the golfer whose high speed video footage was analysed earlier (§5.3.8), similar moments in their shots were found to create local maximum or minima in their force traces. The biggest similarity comes with the peak in right hand force just after impact (points 6 and 5 on golfer a and the professional's force traces, respectively). In this case both produce the higher right hand force while they are rolling their wrist during follow-through. They also both had a local minimum (point 1 in both cases) toward the end of the backswing when the butt-end of the club had reached its highest point. The key points closest to impact are quite different for these two golfers, as evidenced by their different force profiles. Perhaps the most notable differences between the force profiles of the professional golfer shown and the amateurs tested were the relatively low level of force at the beginning and end of the shot as compared to the peak values and the quick ramping up and down of the force near impact by the professional. It would be interesting to test more golfers of this calibre in the future to see if this is a trend that exists in the force profiles of elite golfers, and if so, what this indicates in terms of shot production.

The method of applying grip force adopted by a high-level professional, when compared to sixteen amateurs of varying ability, was found to be quite different as evidenced by cross correlation values comparing total, left hand and right hand forces. These variations might be indicative of a refined grip technique utilised by the professional, of differences in the physical make-up of the individuals tested or a combination of these and other variables.

9.0 RECOMMENDATIONS & CONCLUSIONS

9.1 RECOMMENDATIONS FOR FURTHER WORK

Prior to this study, only limited information was available about how golfers grip the club during a typical tee shot. A means of measuring grip force without altering club characteristics has been established and the force profiles for golfers of varying ability studied. The logical next steps with this research would be to relate grip force to actual shot production with aims of developing potential training aids, to make use of the measurement system in alternative scenarios, and to advance the system by making it wireless, all of which are described below.

9.1.1 RELATING GRIP FORCE TO MOTION

Grip force gives an idea of how a golfer grasps the club throughout the shot, but to fully understand how the grip contributes to performance, more needs to be known about the connection between the motion of the club and golfer relative to the grip force. Such information could better explain what portion of the measured grip force is voluntary and how changes in grip affect clubhead motion.

One possible way of relating the motion of the club to grip force is through the use of shaft strain measurements. Butler and Winfield (1994) measured deflection of the shaft during the downswing using strain gauges attached near the grip* end of the club. Measurements were taken in the toe up/down and lead/lag directions for hundreds of test trials, and they found that most swing profiles fit into three categories. It is possible that the variations in these three common shaft deflection profiles are linked to variations seen in grip force traces between golfers. One example of such a comparison is displayed in Figure 9.1, where total grip force measured by 31 Flexiforce sensors is compared to shaft deflection for a single golfer.

The motion of the golfer relative to grip force would be another useful comparison. High speed video and motion analysis systems that allow the user to measure limb motion and joint angles would give more insight into the role that grip force plays in moving the clubhead during a shot. Such information could be useful in the development of training aids and biomechanical models of the golfer and club and would give a better idea of how grip influences shot production.

9.1.2 GRIP FORCE MEASUREMENT

One issue the literature review in Chapter 2.0 highlighted was the lack of spatial resolution in previous sports grip force studies. The studies presented for tennis, cricket and baseball typically measured force in 2-4 locations. These measurements, although acceptable for total or local force measurements, are incapable of giving the level of detail produced using the sensor

systems described in this thesis. One result of conducting an in-depth study with the system described was the discovery of the grip force 'signature' in golf. It would be interesting to see if such repeatable force traces exist in other sports. In the same way that this study has provided information on how a club is gripped during a golf shot, similar testing methods could give potentially useful insight in other sports.

In transferring these measurement systems to other sports and fields, an important advancement for the system would be to make it less intrusive and easier to set-up. One way of making the system less intrusive would be to reduce or eliminate the wiring that extends from the hand-grip* interface. Wireless Tekscan systems are already available, as are systems designed for use with the Flexiforce sensors. At the moment it appears that number the of sensing elements and sampling rate are limited with these commercial systems, indicating that the use of a self-designed system with the Flexiforce sensors might be a better option for optimisation based on application requirements.

9.2 CONCLUSIONS

The aim of this study was to develop techniques and evaluate sensors for the purpose of making time-resolved measurements of grip force, the principal application of which was a golf shot. For this purpose, force sensors were carefully selected, evaluated and applied in such a way to fit within the hand-grip* interface without significantly altering the characteristics of the club. The established measuring techniques were then utilized in player tests in order to gain information about how golfers of varying ability grip the club, with the aim of providing information that could lead to improved training techniques and grip* design in the future.

Thin, flexible force sensors were found to be a viable option for grip force measurement. These sensors fit easily over curved surfaces, are extremely light-weight and are available in a wide variety of formats, allowing for measurements over irregularly shaped surfaces such as a golf grip* or the hands. However, sensor characteristics for this type of sensor were not well established and therefore a novel set of tests were developed to examine and compare thin-film force sensor performance under controlled laboratory conditions to give an indication of each sensor's quasi-static accuracy, hysteresis, repeatability and drift errors, dynamic accuracy and drift errors, and the effects of shear loads and surface curvature. Five varieties of thin-film force sensor utilizing four different technologies were evaluated, with three varieties being chosen for further use in player tests.

Three of the sensors performed well under static and quasi-static loading conditions, with accuracy errors of 10% or less, hysteresis errors near 6%, repeatability near 6% or below, and drift at 60 s after load application under 15%. Two of these sensors were further tested and demonstrated little change in sensor output to loads applied over curved surfaces, although

shear sensitivity and dynamic accuracy errors were more substantial. It was also found that some of the sensors lost sensitivity with repeated loading. Even with these drawbacks, the potential of these sensors to provide useful grip force information was evident.

A series of three studies were conducted using three different force sensors positioned either on the golf club or gloves. A means of determining the moment of impact on the force traces by synchronizing measurements with a sound level meter was introduced. Upon analysing the force traces measured during these tests it was discovered that each golfer, regardless of ability, produced a unique and very repeatable grip force 'signature'. Trends were seen in the force traces between golfers, and a cross correlation was used to determine the level of consistency for the force profiles of a single golfer and to examine the similarities between golfers. It was found that nearly all golfers tested had swings that were dominated by the left hand, especially before impact, and most notable contributions by the right hand occurred after impact. For the majority of the tests, no correlation was found between peak or RMS grip force and player ability; although in one case a weak correlation was found indicating higher peak grip forces were produced by golfers with lower handicaps. These three studies also gave a good indication of the usability of this type of sensor for measurements of this nature, and this was corroborated by the high cross correlation values of force traces measured with the three different sensor types for a given golfer.

A final test was conducted with the goal of examining the effects of grip force on vibration transmission into the hands and arms and players' perceptions of vibration. It was found that the level of the linear acceleration power spectra for vibration on the shaft varies between golfers but the shape is remarkably consistent, especially for frequencies over 400 Hz. The power spectra on the grip* displayed much greater variation, and it was hypothesized that this was due to variations in the way the golfers gripped the club. A vibration ratio was computed as the RMS vibration at the grip* divided by the RMS vibration at the shaft. This ratio was compared to grip force prior to impact for various regions of the hand. A correlation was found between the force measured at the distal force sensor under the left thumb (directly below where the vibration was being measured) and the vibration ratio, indicating that increased force in this region correlated with increased vibration transmission. This result matches trends seen in related ergonomic studies, and could very likely explain differences seen in the power spectra of the grip* vibration.

Players' perceptions of vibration were also recorded for two different golf clubs. The golfers tested gave responses that were significant in two categories – level of vibration and preferred club. Interestingly, the club that was deemed to vibrate less at impact was the club that was preferred. There were no obvious links between linear or torsional vibration measurements taken on the shaft or grip* and the golfers' perceptions; however it was noted

that the club that was perceived to vibrate more by the golfers produced higher linear vibration levels for off-centre impacts.

REFERENCES

- Aldien, Y., Marcotte, P., Rakheja, S., and Boileau, P.-E. (2006a). "Influence of hand forces and handle size on power absorption of the human hand-arm exposed to zh-axis vibration." *Journal of Sound and Vibration*, 290, 1015-1039.
- Aldien, Y., Marcotte, P., Rakheja, S., and Boileau, P.-E. (2006b). "Influence of hand-arm posture on biodynamic response of the human hand-arm exposed to zh-axis vibration." *International Journal of Industrial Ergonomics*, 36, 45-59.
- Aldridge, J. (1994). "Grip technology." *Golf the Scientific Way*, A. Cochran, ed., Ashton Publishing Group, Hemel Hempstead, Hertfordshire, 81-82.
- Alliss, P. (1926). *Better Golf*, A & C Black, London.
- Alliss, P., and Trevillion, P. (1969). *Easier Golf*, Stanley Paul, London.
- Amis, A. A. (1987). "Variation of finger forces in maximal isometric grasp tests on a range of cylinder diameters." *Journal of Biomedical Engineering*, 9, 313-320.
- An, K. N., Chao, E. Y. S., and Askew, L. J. (1980). "Hand strength measurement instruments." *Archives of Physical Medicine & Rehabilitation*, 61, 366-368.
- Ashruf, C. M. A. (2002). "Thin flexible pressure sensors." *Sensor Review*, 22(4), 322-327.
- Bachus, K. N., DeMarco, A. L., Judd, K. T., Horwitz, D. S., and Brodke, D. S. (2006). "Measuring contact area, force, and pressure for bioengineering applications: Using Fuji Film and TekScan systems." *Medical Engineering & Physics*, 28(5), 483-488.
- Bao, S. (2000). "Grip strength and hand force estimation." *65-1-2000*, Department of Labor and Industries, Olympia, WA.
- Barnett, S., Cunningham, J. L., and West, S. (2001). "A comparison of vertical force and temporal parameters produced by an in-shoe pressure measuring system and a force platform." *Clinical Biomechanics*, 16, 353-357.
- Bendat, J. S., and Piersol, A. G. (1986). *Random Data: Analysis and Measurement Procedures*, John Wiley & Sons, New York.
- Blackwell, J. R., Kornatz, K. W., and Heath, E. M. (1999). "Effect of grip span on maximal grip force and fatigue of flexor digitorum superficialis." *Applied Ergonomics*, 30, 401-405.
- Bray, A., Barbato, G., and Levi, R. (1990). *Theory and Practice of Force Measurement*, Academic Press, London.
- Brisben, A. J., Hsiao, S. S., and Johnson, K. O. (1999). "Detection of Vibration Transmitted Through an Object Grasped in the Hand." *Journal of Neurophysiology*, 81(4), 1548-1558.
- Brody, H. (1986). "The sweet spot of a baseball bat." *American Journal of Physics*, 54(7), 640-643.
- Brody, H. (1989a). "Models of baseball bats." *American Journal of Physics*, 58(8).
- Brody, H. (1989b). "Vibration Damping of Tennis Racquets." *International Journal of Sport Biomechanics*, 5, 451-456.
- Brüel & Kjær. (2007). "Selecting the right accelerometer." <http://www.bksv.com/3859.asp>, last accessed 19 January 2007.
- BS 5929-2. (1982). "Methods for sensory analysis of food: paired comparison test."
- Budney, D. R. (1979). "Measuring grip pressure during the golf swing." *Research Quarterly*, 50.
- Budney, D. R., and Bellow, D. G. (1990). "Evaluation of golf club control by grip pressure measurement." *Science of Golf I*.
- Buis, A. W. P., and Convery, P. (1997). "Calibration problems encountered while monitoring stumps/socket interface pressures with force sensing resistors: techniques adopted to minimise inaccuracies." *Prosthetics and Orthotics International*, 21, 179-182.
- Burström, L., and Sörensson, A. (1999). "The Influence of Shock-Type Vibrations on the Absorption of Mechanical Energy in the Hand and Arm." *International Journal of Industrial Ergonomics*, 23, 585-594.
- Butler, J. H., and Winfield, D. C. (1994). "The dynamic performance of the golf shaft during the downswing." *Science and Golf II: Proceedings of the World Scientific Congress of Golf*, A. J. Cochran and M. R. Farrally, eds., E & FN Spon, London, 259-264.

- Carlsöö, S. (1972). *How Man Moves: Kinesiological Studies and Methods*, W. P. Michael, translator, William Heinemann Ltd, London.
- Chadwick, E. K. J., and Nicol, A. C. (2001). "A novel force transducer for the measurement of grip force." *Journal of Biomechanics*, 34(1), 125-128.
- Christine M. Kleinert Institute for Hand and Microsurgery. (2005). "The Wonders of the Hand and Upper Limb." Christine M. Kleinert Institute for Hand and Microsurgery, <http://www.cmki.org/about/HWAchapter.cfm>.
- Cochran, A., and Stobbs, J. (1968). *Search for the Perfect Swing*, Triumph Books, Chicago, IL.
- Cormier, J. M., Stitzel, J. D., Hurst, W. J., and Duma, S. M. (2002). "High-speed and continuous pressure measurements: a comparison of active pressure sensors and pressure film." Virginia Tech, Impact Biomechanics Laboratory.
- Cotton, H. (1948). *This Game of Golf*, Country Life Limited, London.
- Couples, F. (1994). *Total Shotmaking: The Golfers Guide to Low Scoring*, HarperCollins Publishers.
- Cross, R. (1998). "The sweet spot of a baseball bat." *American Journal of Physics*, 66(9), 772-778.
- Dempsey, P. G., and Ayoub, M. M. (1996). "The influence of gender, grasp type, pinch width and wrist position on sustained pinch strength." *International Journal of Industrial Ergonomics*, 17, 259-273.
- Eggemen, G. W., and Noble, M. L. (1985). "Design and testing of a baseball bat transducer." *Experimental Techniques*, 20-23, 20-23.
- Eksioglu, M. (2004). "Relative optimum grip span as a function of hand anthropometry." *International Journal of Industrial Ergonomics*, 34, 1-12.
- Elliott, B. C. (1982). "Tennis: The Influence of Grip Tightness on Reaction Impulse and Rebound Velocity." *Medicine and Science in Sports and Exercise*, 14(5), 348-352.
- Engel, J. (1995). "Tennis: dynamics of racket-grip interaction." *Journal of Hand Surgery*, 20A(3), 77-81.
- Faldo, N., and Saunders, V. (1989). *Golf - The Winning Formula*, Lyons & Burford, New York.
- Farrally, M. R., Cochran, A. J., Crews, D. J., Hurdzan, M. J., Price, R. J., Snow, J. T., and Thomas, P. R. (2003). "Golf science research at the beginning of the twenty-first century." *Journal of Sports Sciences*, 21, 753-765.
- Ferguson-Pell, M., Hagnosisawa, S., and Bain, D. (2000). "Evaluation of a sensor for low interface pressure applications." *Medical Engineering & Physics*, 22, 657-663.
- Freund, J., Toivonen, R., and Takala, E. P. (2002). "Grip forces of the fingertips." *Clinical Biomechanics*, 17(7), 515-520.
- Girdhar, P. (2004). *Practical Machinery Vibration Analysis and Predictive Maintenance*, Newnes, Oxford.
- Griffin, M. J. (1990). *Handbook of Human Vibration*, Academic Press Limited, London.
- Griffin, M. J., Macfarlane, C. R., and Norman, C. D. (1982). "The transmission of vibration to the hand and the influence of gloves." *Vibration Effects on the Hand and Arm in Industry*, A. J. Brammer and W. Taylor, eds., John Wiley & Sons, Inc., New York, 103-116.
- Gurram, R., Rakheja, R., and Gouw, G. J. (1994). "Vibration transmission characteristics of the human hand-arm and gloves." *International Journal of Ergonomics*, 13, 217-234.
- Gurram, R., Rakheja, R., and Gouw, G. J. (1995). "Mechanical impedance of the human hand-arm system subject to sinusoidal and stochastic excitations." *International Journal of Industrial Ergonomics*, 16, 135-145.
- Hallbeck, M. S., and McMullin, D. L. (1993). "Maximal power grasp and three-jaw chuck pinch force as a function of wrist position, age and glove type." *International Journal of Industrial Ergonomics*, 11, 195-206.
- Hamill, J., and Knutzen, K. (2003). *Biomechanical Basis of Human Movement*, Lippincott Williams & Wilkins, Baltimore, MD.
- Harris, M. L., Morberg, P., Bruce, W. J. M., and Walsh, W. R. (1999). "An improved method for measuring tibiofemoral contact areas in total knee arthroplasty: a comparison of K-scan sensor and Fuji film." *Journal of Biomechanics*, 32, 951-958.

- Hatze, H. (1976). "Forces and duration of impact, and grip tightness during the tennis stroke." *Medicine and Science in Sports*, 8(2), 88-95.
- Hatze, H. (1992). "The effectiveness of grip bands in reducing racquet vibration transfer and slipping." *Medicine and Science in Sports and Exercise*, 24(2), 226-230.
- Hay, A. (1980). *The Golf Manual*, Faber & Faber, London.
- Hay, J. (1993). *The Biomechanics of Sports Techniques*, Prentice-Hall, Englewood Cliffs, NJ.
- Hedrick, M., and Twigg, M. (1994). "The feel of a golf shot: how can we measure it?" *Golf the Scientific Way*, A. Cochran, ed., Ashton Publishing Group, Hemel Hempstead, Hertfordshire, 131-133.
- Henning, E. M., Rosenbaum, D., and Milani, T. L. (1992). "Transfer of Tennis Racket Vibrations onto the Human Forearm." *Medicine and Science in Sport and Exercise*, 24(10), 1134-1140.
- Hocknell, A., Jones, R., and Rothberg, S. J. (1996). "Engineering 'feel' in the design of golf clubs." *The Engineering of Sport: Proceedings of the 1st International Conference on the Engineering of Sport*, S. J. Haake, ed., A.A.Balkema, Rotterdam, NL.
- Hsiao, H., Guan, J., and Weatherly, M. (2002). "Accuracy and precision of two in-shoe pressure measurement systems." *Ergonomics*, 45(8), 537-555.
- Hurkmans, H. L. P., Bussmann, J. B. J., Selles, R. W., Horemans, H. L. D., Benda, E., Stam, H. J., and Verhaar, J. A. N. (2006). "Validity of the Pedar Mobile system for vertical force measurement during a seven-hour period." *Journal of Biomechanics*, 39, 110-118.
- Irwin, H. (1980). *Play Better Golf with Hale Irwin*, Octopus, London.
- Jackson, J. (1993). *Total Clubfitting: A Step-By-Step Guide for Fitting Golf Equipment*, Dynacraft Golf Products, Inc., USA.
- Jacobs, J. (1963). *Golf By John Jacobs*, Stanley Paul, London.
- Jung, M. C., and Hallbeck, M. S. (2002). "The effect of wrist position, angular velocity, and exertion direction on simultaneous maximal grip force and wrist torque under the isokinetic conditions." *International Journal of Industrial Ergonomics*, 29(3), 133-143.
- Kihlberg, S. (1995). "Biodynamic response of the hand-arm system to vibration from an impact hammer and a grinder." *International Journal of Industrial Ergonomics*, 16, 1-8.
- Kitazaki, S., and Griffin, M. J. (1995). "A data correction method for surface measurement of vibration on the human body." *Journal of Biomechanics*, 28(7), 885-890.
- Knudson, D. (1991). "Forces on the Hand in the Tennis One-Handed Backhand." *International Journal of Sport Biomechanics*, 7, 282-292.
- Knudson, D. V., and White, S. C. (1989). "Forces on the hand in the tennis forehand drive: application of force sensing resistors." *International Journal of Sport Biomechanics*, 5, 324-331.
- Kong, Y.-K., and Lowe, B. D. (2005). "Optimal cylindrical handle diameter for grip force tasks." *International Journal of Industrial Ergonomics*, 35, 495-507.
- Kotze, J., Mitchell, S. R., and Rothberg, S. J. (2000). "The role of the racket in high-speed tennis serves." *Sports Engineering*, 3(2).
- Lancaster, J. (1994). "Grip selection." *Golf the Scientific Way*, A. Cochran, ed., Ashton Publishing Group, Hemel Hempstead, Hertfordshire, 85-87.
- Leadbetter, D. (1993). *Faults and Fixes*, HarperCollins Publishers Inc., New York.
- Leadbetter, D. (2000). *The Fundamentals of Hogan*, Co-Published by Sleeping Bear Press and Doubleday.
- Lee, J. W., and Rim, K. (1990). "Measurement of finger joint angles and maximum finger forces during cylinder grip activity." *Journal of Biomedical Engineering*, 13, 152-161.
- Lee, N., Erickson, M., and Cherveney, P. (2002). "Measurement of the behavior of a golf club during the golf swing." *Science and Golf IV*, E. Thain, ed., 374-386.
- Lewis, B. (1990). *Play Better Golf - Golf Clinic*, Quadrillion Publishing, New York.
- Li, Z.-M. (2002). "The influence of wrist position on individual finger forces during forceful grip." *The Journal of Hand Surgery*, 27(5), 886-896.
- Locke, B. (1954). *Bobby Locke on Golf*, Simon & Schuster, New York.
- Lopez, N., and Wade, D. (1987). *Lopez on Golf*, Stanley Paul, London.

- Loskutovaa, N. V., Novikova, A. V., and Smirnova, G. V. (1998). "Normal characteristics of cylindrical grip." *Journal of Biomechanics*, 31(1), 99.
- Luxton, T. (1985). *The Real Truth About the Golf Swing*, The Kingswood Press, Surrey.
- Macht, D. (2000). "Development of a mathematical model during a golf swing." Rocky Mountain Musculoskeletal Research Laboratory.
- Mann, N. A. J. "Factors affecting the transmission of vibration to the fingernail." *U.K. Informal Group Meeting on Human Response to Vibration*, Institute of Naval Medicine, Alverstoke, Gosport, Hampshire.
- Mather, J. S. B. "The role of club response in the design of current golf clubs." *Proceedings of the 14th International Modal Analysis Conference*, Michigan, USA, 397-403.
- Mather, S. (1994). "Golf club dynamics." *Golf the Scientific Way*, A. Cochran, ed, Ashton Publishing Group, Hemel Hempstead, Hertfordshire, 61-65.
- Mathiowetz, V., Kashman, N., Volland, G., Weber, K., Dowe, M., and Rogers, S. (1985). "Grip and pinch strength: normative data for adults." *Archives of Physical Medicine & Rehabilitation*, 66(2), 69-74.
- Matsuda, S., Williams, V. G., Whiteside, L. A., and White, S. E. "A comparison of pressure sensitive film and digital electronic sensors to measure contact area and contact stress." *41st Annual Meeting, Orthopaedic Research Society*, Orlando, Florida.
- McGorry, R. W. (2001). "A system for the measurement of grip forces and applied moments during hand tool use." *Applied Ergonomics*, 32(3), 271-279.
- Miller, J. (1976). *Pure Golf*, DoubleDay, New York.
- Miwa, T. (1967). "Measurements of threshold and equal sensation contours on hand for vertical and horizontal sinusoidal vibrations." *Industrial Health*, 5, 213-220.
- Mogk, J., and Keir, P. (2003). "The effects of posture on forearm muscle loading during gripping." *Ergonomics*, 46(9).
- Nelson, B. (1947). *Byron Nelson's Winning Golf*, A. S. Barnes And Company, New York.
- Nicklaus, J., and Bowden, K. (1974). *Golf My Way*.
- Nicolay, C. W., and Walker, A. L. (2005). "Grip strength and endurance: Influences of anthropometric variation, hand dominance, and gender." *International Journal of Industrial Ergonomics*, 35(7), 605-618.
- Nikonovas, A., Harrison, A. J. L., Hoult, S., and Sammut, D. (2004). "The application of force-sensing resistor sensors for measuring forces developed by the human hand." *Proceedings of the IMechE Part H Journal of Engineering in Medicine*, 218, 121-125.
- Noble, D. T. (1963a). "An analysis of hand grip as a factor influencing the power of the golf swing." *Golf Society of Great Britain; Scientific Working Party*.
- Noble, D. T. (1963b). "Comments on some of the factors influencing the type of grip used by the golfer." *Golf Society of Great Britain; Scientific Working Party*.
- Noble, L., and Walker, H. (1994). "Baseball bat inertial and vibrational characteristics and discomfort following ball-bat impacts." *Journal of Applied Biomechanics*, 10, 132-144.
- Nordin, M., and Frankel, V. H. (2001). *Basic Biomechanics of the Musculoskeletal System*, Lippincott Williams & Wilkins, Baltimore.
- Novel. (2007). "Novel GmbH." www.novel.de, last accessed 10 April 2007.
- Oatis, C. A. (2004). *Kinesiology: The Mechanics & Pathomechanics of Human Movement*, Lippincott Williams & Wilkins, Philadelphia, PA.
- Otto, J. K., Brown, T. D., Heiner, A. D., Pedersen, D. R., and Callaghan, J. J. "Characterization of the dynamic response of a piezoresistive contact stress sensor." *44th Annual Meeting, Orthopaedic Research Society*, New Orleans, Louisiana, 808.
- Paddan, G. S. "Effect of pull force on the transmission of vibration through the finger to the fingernail." *U.K. Group Meeting on Human Response to Vibration*, ISVR, University of Southampton, Southampton, England, 459-470.
- Palmer, A. (1965). *My Game and Yours*, Simon & Schuster, New York.
- Pavlovic, J. L., Takahashi, Y., Bechtold, J. E., Gustilo, R. B., and Kyle, R. F. "Can the Tekscan sensor accurately measure dynamic pressures in the knee joint." *17th Annual Meeting, American Society of Biomechanics*, Iowa City, Iowa.

- PD 6461-3. (1995). "General Metrology: Guide to the Expression of Uncertainty in Measurement."
- Pelmeur, P. L., and Wasserman, D. E. (1998). *Hand-Arm Vibration: A Comprehensive Guide for Occupational Health Professionals*, OEM Press, Beverly Farms, Massachusetts.
- Peratech. (2007). "Peratech Ltd." www.peratech.com, last accessed 10 April 2007.
- PGA European Tour. (2007). "europeantour.com - Official Website of the PGA European Tour." The PGA European Tour.
- Polliack, A. A., Sieh, R. C., Craig, D. D., Landsberger, S., McNeil, D. R., and Ayyappa, E. (2000). "Scientific validation of two commercial pressure sensor systems for prosthetic socket fit." *Prosthetics and Orthotics International*, 24, 63-73.
- Putti, A. B., Arnold, G. P., Cochrane, L., and Abboud, R. J. (2006). "The pedar in-shoe system: repeatability and normal pressure values." *Gait and Posture*, In-Print.
- Randall, R. B. (1987). *Frequency Analysis*, Brüel & Kjær.
- Reynolds, D. D., and Angevine, E. N. (1977). "Hand-Arm Vibration, Part 2: Vibration Transmission Characteristics of the Hand and Arm." *Journal of Sound and Vibration*, 51(2), 255-265.
- Reynolds, D. D., and Keith, R. H. (1977). "Hand-Arm Vibration, Part 1: Analytical Model of the Vibration Response Characteristics of the Hand." *Journal of Sound and Vibration*, 51(2), 237-253.
- Reynolds, D. D., Standlee, K. G., and Angevine, E. N. (1977). "Hand-Arm Vibration, Part 3: Subjective Response Characteristics of Individuals to Hand-Induced Vibration." *Journal of Sound and Vibration*, 51(2), 267-282.
- Roberts, J. R. (2002). "Mechanical and Psychological Influences on the Feel of a Golf Shot," Loughborough University, Loughborough, UK.
- Roberts, J. R., Jones, R., Mansfield, N. J., and Rothberg, S. J. (2005). "Evaluation of vibrotactile sensations in the 'feel' of a golf shot." *Journal of Sound and Vibration*, 285, 303-319.
- Roberts, J. R., Jones, R., Rothberg, S. J., Mansfield, N. J., and Meyer, C. (2006). "Influence of sound and vibration from sports impacts on players' perceptions of equipment quality." *IMechE part L*, 220, 215-227.
- Rosse, C., and Gaddum-Rosse, P. (1997). *Hollinshead's Textbook of Anatomy*, Lippincott-Raven Publishers, Philadelphia.
- Schmidt, R. T., and Toews, J. V. (1970). "Grip strength as measured by the Jamar Dynamometer." *Archives of Physical Medicine & Rehabilitation*, 321-327.
- Shih, Y.-C., and Ou, Y.-C. (2005). "Influences of span and wrist posture on peak chuck pinch strength and time needed to reach peak strength." *International Journal of Industrial Ergonomics*, 35, 527-536.
- Snead, S. (1961). *Sam Snead on Golf*, Prentice Hal, Englewood Cliffs.
- Sörensson, A., and Burström, L. (1996). "Energy absorption of vibration in the hand for higher frequencies."
- Sörensson, A., and Burström, L. (1997). "Transmission of vibration energy to different parts of the human hand-arm system." *International Archives of Occupational Environmental Health*, 70, 199-204.
- Sörensson, A., and Lundström, R. (1992). "Transmission of vibration to the hand."
- Sporting Goods Manufacturers Association. (2004a). "Recreation Market Report." Sporting Goods Manufacturers Association.
- Sporting Goods Manufacturers Association. (2004b). "Sports Participation Topline Report." Sporting Goods Manufacturers Association.
- Tekscan. (2004). "Tekscan User Manual: Sensing Solutions for the 21st Century."
- Tekscan. (2007). "Tekscan, Inc." www.tekscan.com, last accessed 10 April 2007.
- The Institute of Measurement and Control. (1998). "Guide to the Measurement of Force." The Institute of Measurement and Control.
- Torrance, B. (1989). *Room at the Top - Golf the Torrance Way*, Mainstream Publ., Edinburgh.
- Tortora, G. J. (1995). *Principles of Human Anatomy*, HarperCollins College Publishers, New York.
- Trevino, L. (1976). *Swing My Way*, Scribner, New York.

- Tsaousidis, N., and Freivalds, A. "Effects of gloves on maximum force and the rate of force development in wrist flexion and grip." *Twenty-First Annual Meeting of the American Society of Biomechanics*, Clemson University, South Carolina.
- Tsaousidis, N., and Freivalds, A. (1998). "Effects of gloves on maximum force and the rate of force development in pinch, wrist flexion and grip." *International Journal of Industrial Ergonomics*, 21(5), 353-360.
- Turrell, Y. N., Li, F.-X., and Wing, A. M. (1999). "Grip force dynamics in the approach to a collision." *Experimental Brain Research*, 128, 86-91.
- Van der Kamp, M., Conway, B. A., and Nicol, A. C. (2001). "A novel instrumented ring for the measurement of grip force adjustments during precision grip tasks." *Proceedings of the Institution of Mechanical Engineers*, 215(2), 421-427.
- Vander, A., Sherman, J., and Luciano, D. (2001). *Human Physiology: The Mechanisms of Body Function*, McGraw-Hill, New York.
- Verrillo, R. T. (1963). "Effect of Contactor Area on the Vibrotactile Threshold." *Journal of the Acoustical Society of America*, 35(12), 1962-1966.
- Verrillo, R. T., and Smith, R. L. (1976). "Effect of Stimulus Duration on Vibrotactile Sensation Magnitude." *Bulletin of the Psychonomic Society*, 8(2), 112-114.
- Wakeling, J. M., and Nigg, B. M. (2001). "Soft-tissue vibrations in the quadriceps measured with skin mounted transducers." *Journal of Biomechanics*, 34, 539-543.
- Watanabe, T. I. Y., and Miyashita, M. (1979). "Tennis: The Effects of Grip Firmness on Ball Velocity after Impact." *Medicine and Science in Sports and Exercise*, 11(4), 359-361.
- Welcome, D., Rakheja, R., Dong, R., Wu, J. Z., and Schopper, A. W. (2004). "An investigation on the relationship between grip, push and contact forces applied to a tool handle." *International Journal of Industrial Ergonomics*, 34, 507-518.
- Werner, F. W., Green, J. K., Fortino, M. D., Mann, K. A., and Short, W. H. "Evaluation of a dynamic intra-articular contact pressure sensing system." *41st Annual Meeting, Orthopaedic Research Society*, Orlando, Florida, 705.
- Wicks, A. L., Knight, C. E., Braunwart, P., and Neighbors, J. "The dynamics of a golf club." *17th International Modal Analysis Conference*.
- Wicks, A. L., Knight, C. E., and Neighbors, J. "Identification of the 'sweet spot' for golf clubs." *16th International Modal Analysis Conference*, Santa Barbara, CA, USA.
- Wilson, D. C., Niosi, C. A., Zhu, Q. A., Oxland, T. R., and Wilson, D. R. (2006). "Accuracy and repeatability of a new method for measuring facet loads in the lumbar spine." *Journal of Biomechanics*, 39(2), 348-353.
- Wilson, D. R., Apreleva, M. V., Eichler, M. J., and Harrold, F. R. (2003). "Accuracy and repeatability of a pressure measurement system in the patellofemoral joint." *Journal of Biomechanics*, 36, 1909-1915.
- Wiren, G. (1990). *PGA Teaching Manual - The Art and Science of Golf Instruction*.
- Wishon, T. (1996). *The Golfsmith Practical Clubfitting Program*, Golfsmith International, Inc., Austin, TX.
- Woodburn, J., and Helliwell, P. S. (1996). "Observations on the F-Scan in-shoe pressure measuring system." *Clinical Biomechanics*, 11(5), 301-304.
- Wowk, V. (1991). *Machinery Vibration: Measurement and Analysis*, McGraw-Hill.
- Yun, M. H., Kotani, K., and Ellis, D. "Using force sensitive resistors to evaluate hand tool grip design." *Proceedings of the Human Factors Society 36th Annual Meeting*.

CHAPTER 1 FIGURES

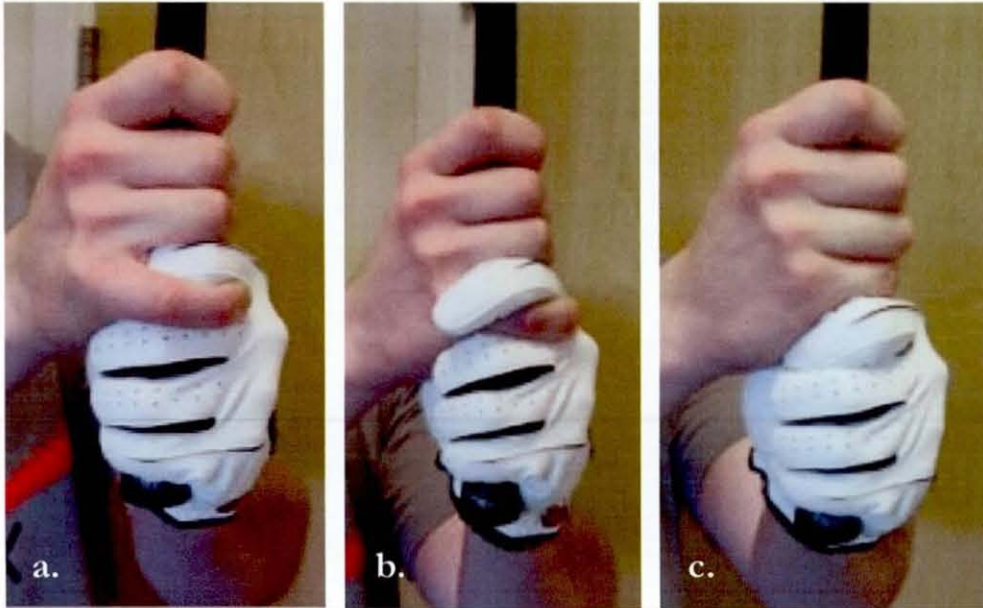


Figure 1.1 Three primary golf grips; (a.) overlapping, (b.) interlocking, and (c.) 10-finger

CHAPTER 2 FIGURES

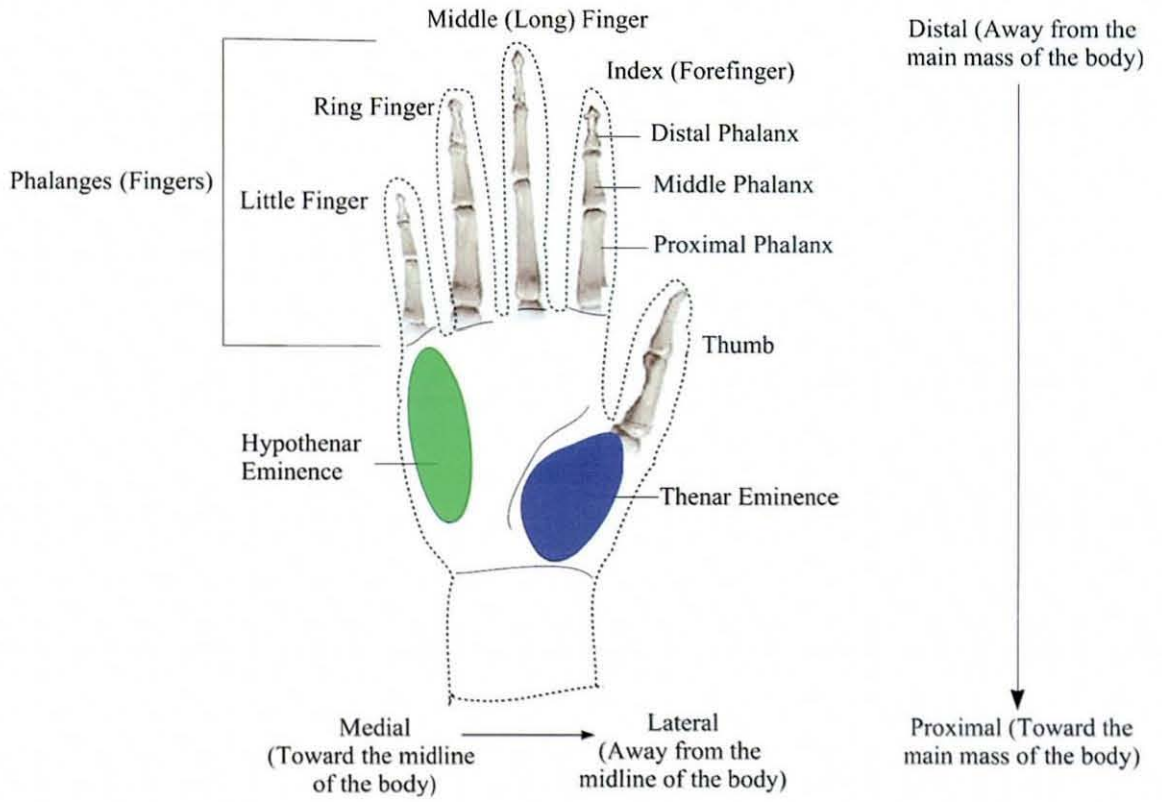


Figure 2.1 Anatomical features of the right hand (anterior view)

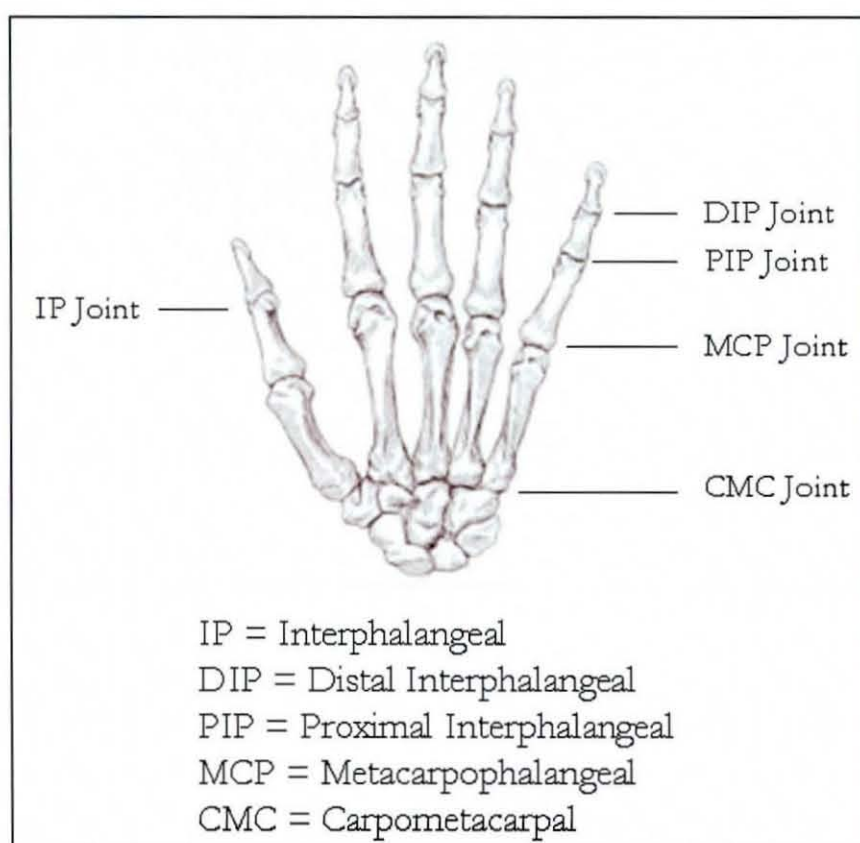


Figure 2.2 Joints of the hand

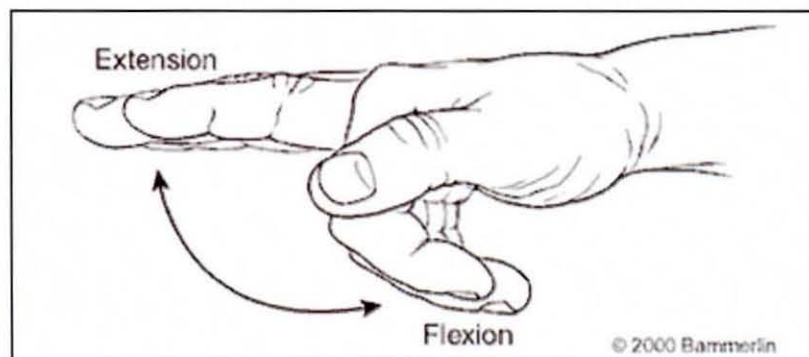


Figure 2.3 Directions of finger motion
 (Christine M. Kleinert Institute for Hand and Microsurgery 2005)

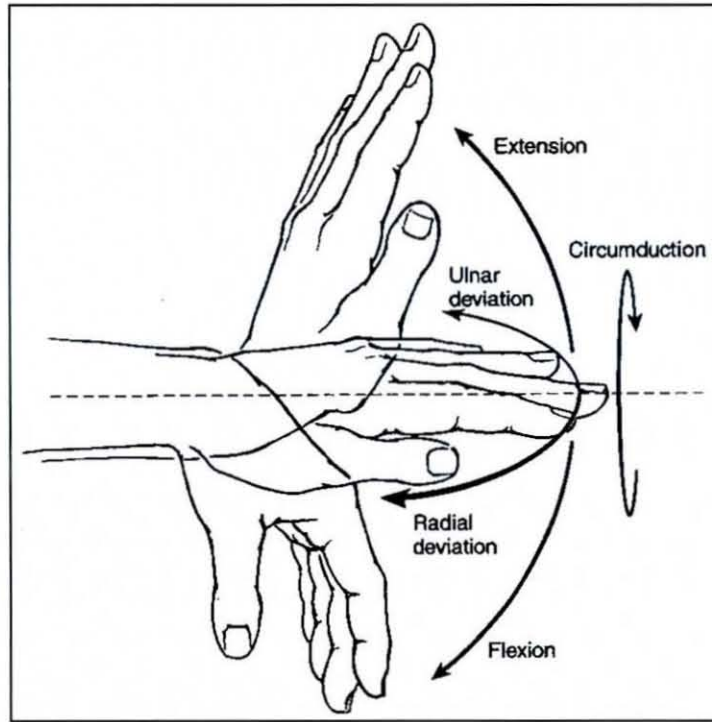


Figure 2.4 Total or global motions of the wrist

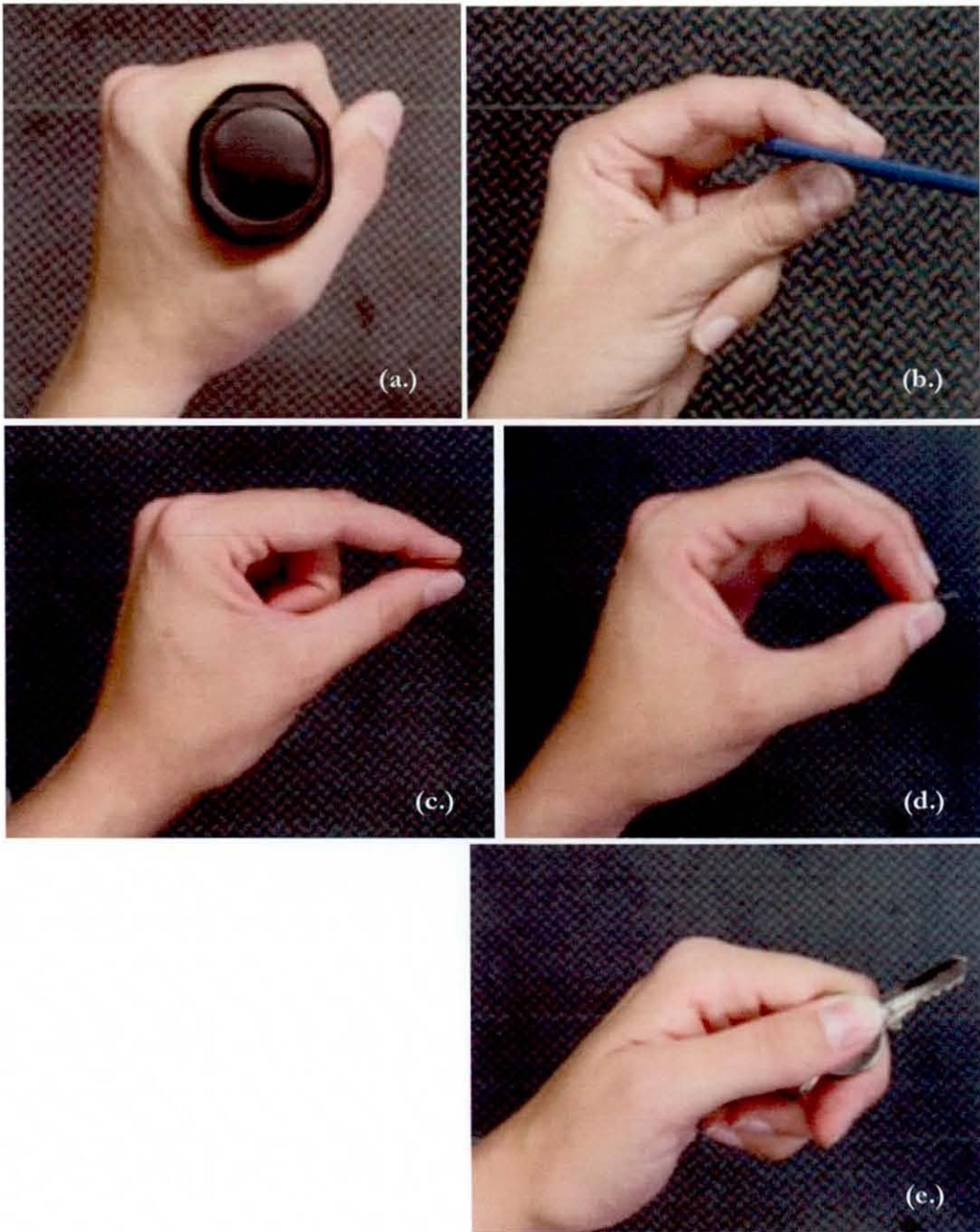


Figure 2.5 Typical grip and pinch patterns; (a.) power grip, (b.) chuck pinch, (c.) pulp pinch, (d.) tip pinch, (e.) lateral (key) pinch

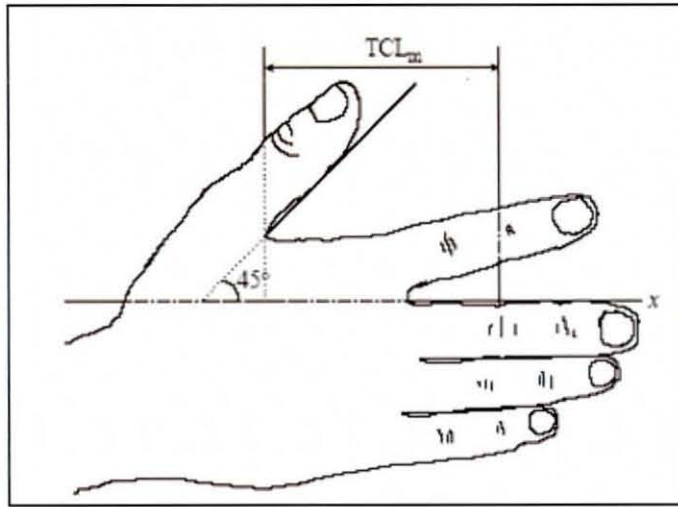


Figure 2.6 Modified thumb crotch length as defined by Eksioglu (2004)

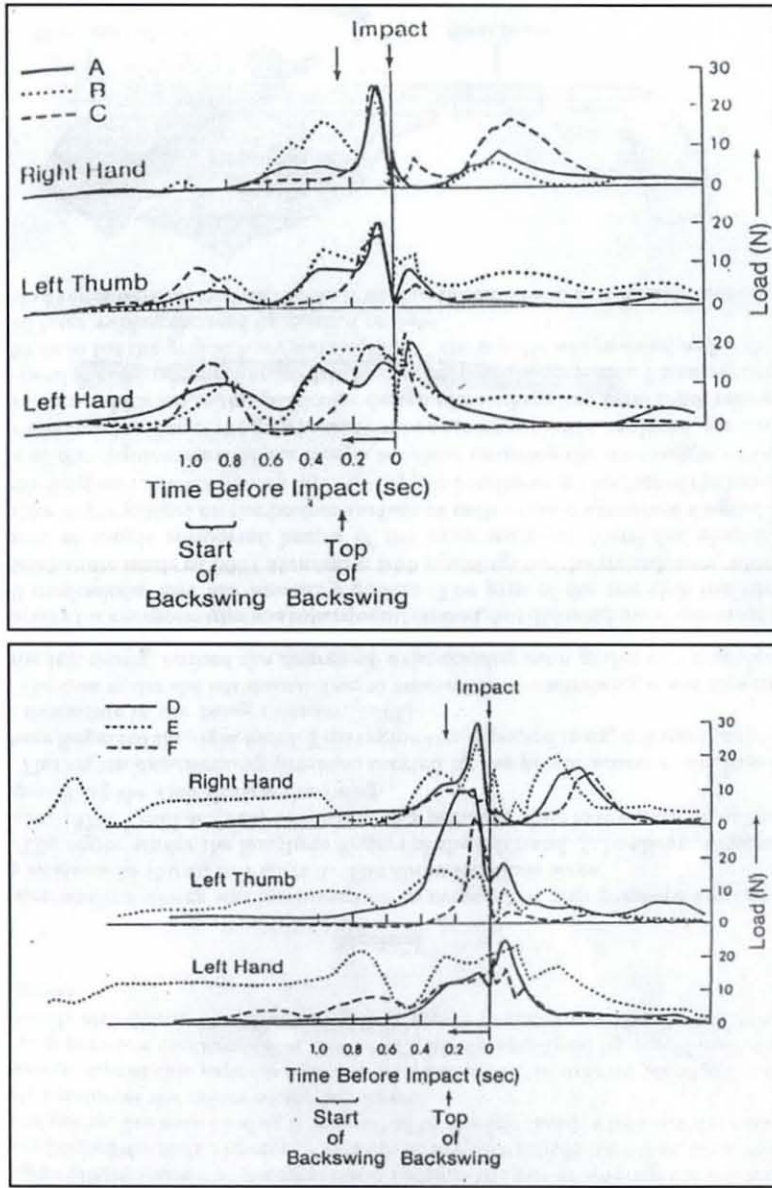


Figure 2.7 Grip pressure for three professional (top) and three amateur golfers (bottom) (Budney 1979)

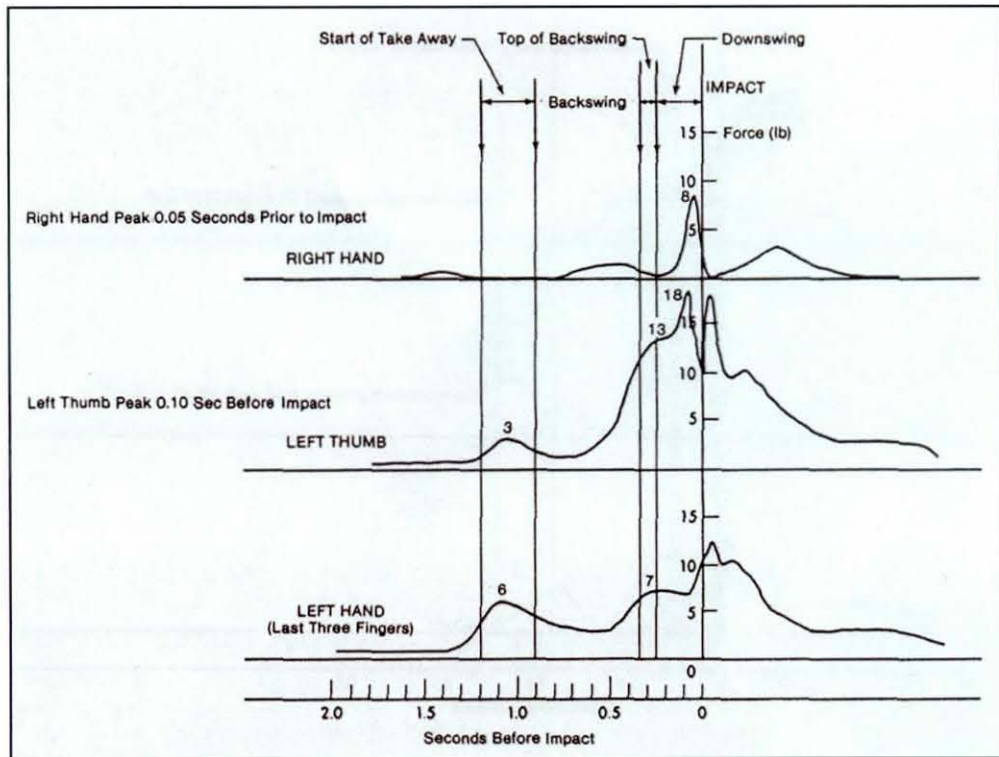


Figure 2.8 Grip pressure for a professional golfer (Budney and Bellow 1990)

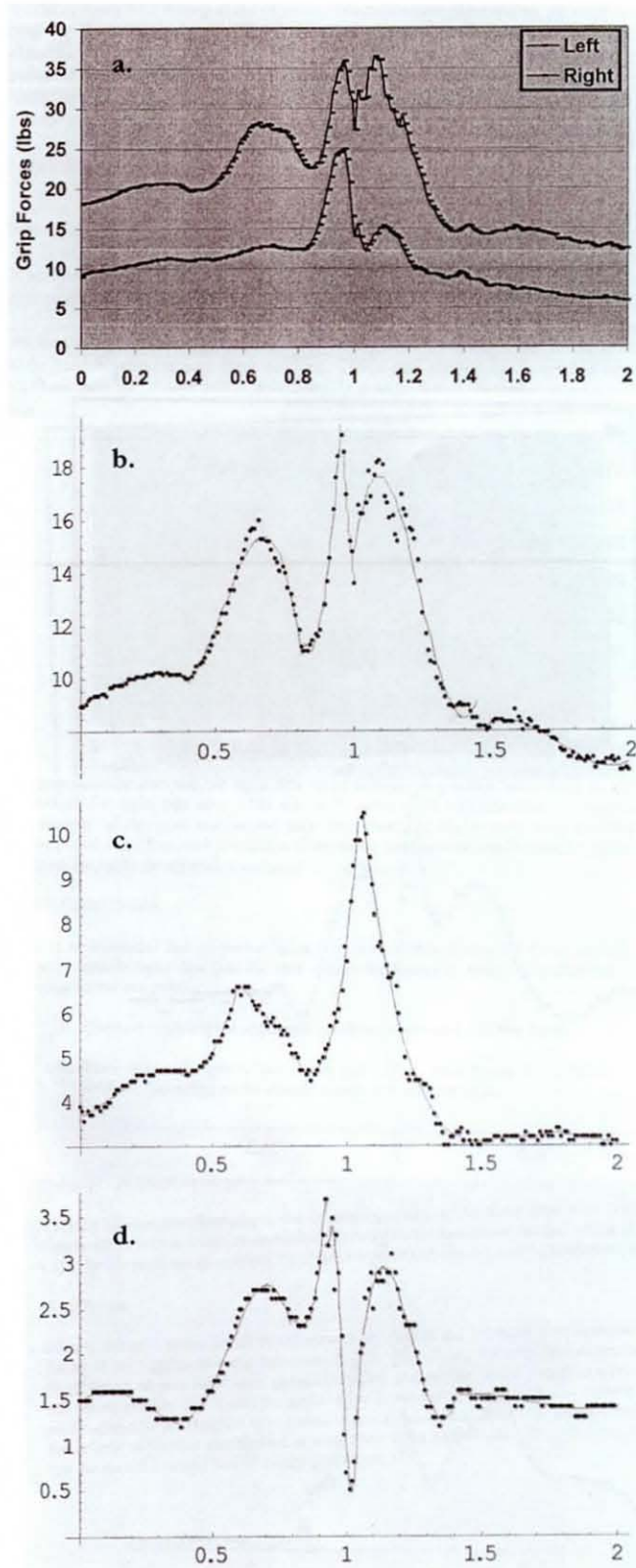


Figure 2.9 Golf grip force; each plot showing time (sec) vs. force (lbf), with (a.) total left and right hand force, (b.) left palm force, (c.) left finger forces, (d.) left thumb force (Macht 2000)

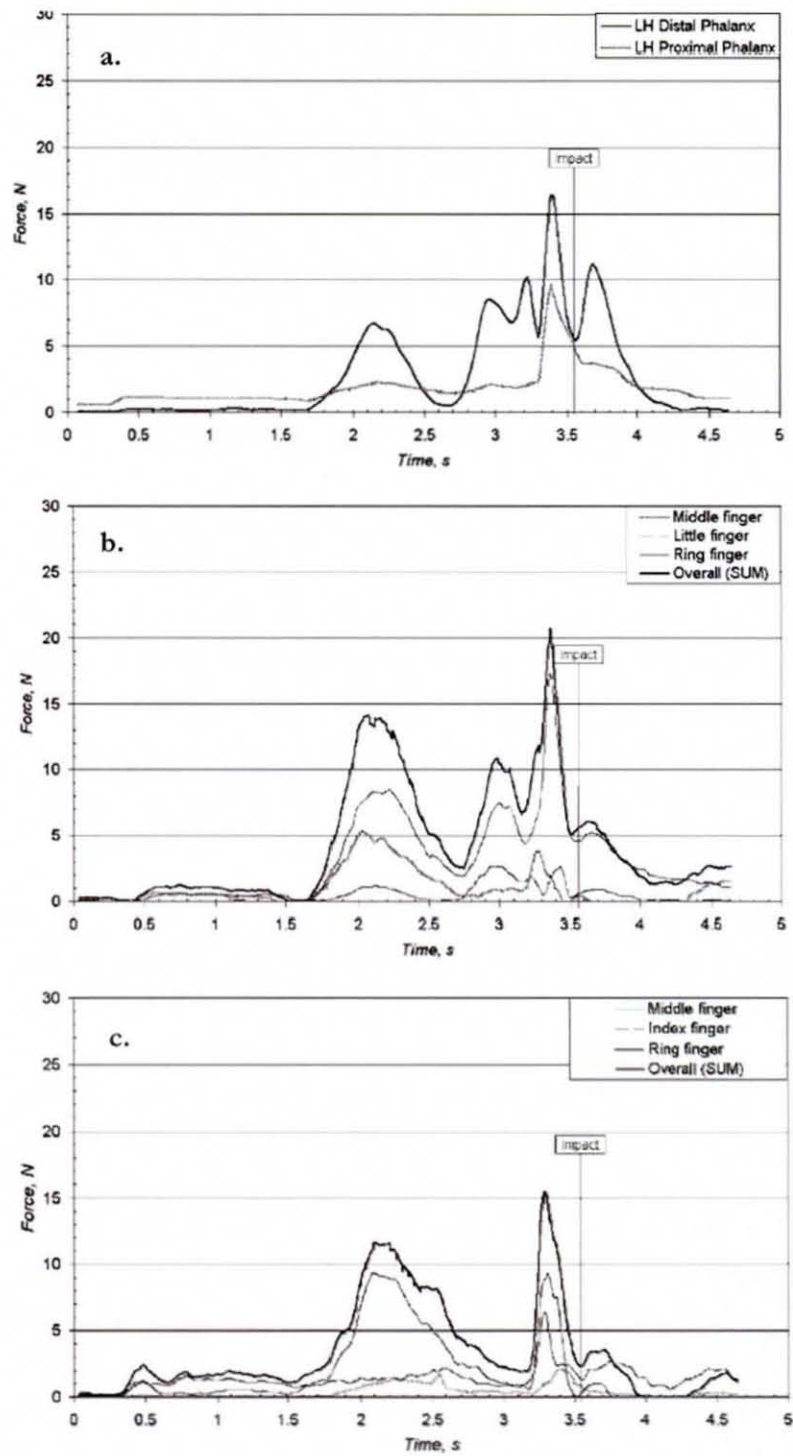
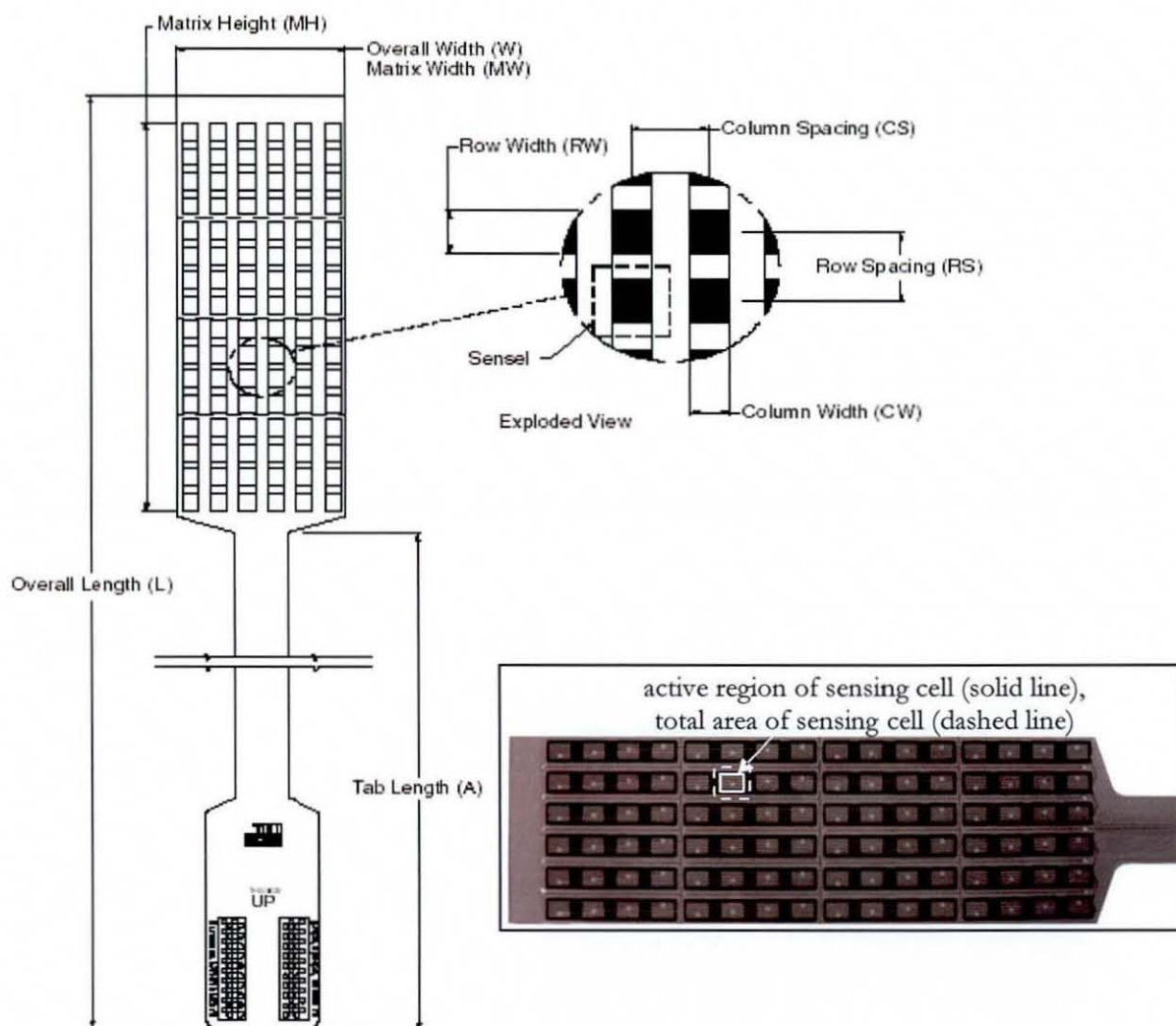



Figure 2.10 Forces exerted on hands during golf swing; (a.) left thumb, (b.) proximal phalanges of the left-hand middle, ring and little fingers, (c.) proximal phalanges of right-hand index, middle and ring fingers (Nikonovas et al. 2004)

CHAPTER 3 FIGURES



General Dimensions			Sensing Region Dimensions								Summary	
Overall Length L	Overall Width W	Tab Length A	Matrix Width MW	Matrix Height MH	Columns			Rows		No. of Sensels	Sensel Density	
					CW	CS	Qty	RW	RS			Qty
622 mm	76 mm	394 mm	76 mm	203 mm	6.35 mm	12.7 mm	6	6.35 mm	12.7 mm	16	96	0.62/cm ²
24.5 inch	3 inch	15.5 inch	3 inch	8 inch	0.25 inch	0.5 inch	6	0.25 inch	0.5 inch	16	96	4/in ²

Figure 3.1 Tekscan 9811 sensor and details from manufacturer, with active and total sensing regions labelled in image on bottom right (Tekscan 2007)



Physical Properties	Standard Force Ranges	Typical Performance
Thickness 0.008" (0.127mm) Length 8" (203mm) Width 0.55" (14mm) Active Sensing Area 0.375" (9.53mm) Diameter	0-1 lb. (4.4 N) 0-25 lb. (111 N) 0-100 lb. (444 N)	Linearity (Error) $< \pm 5\%$ Repeatability $< \pm 2.5\%$ of Full Scale Hysteresis $< 4.5\%$ of Full Scale Drift $< 3\%$ logarithmic time Rise Time $< 5\mu\text{sec}$ Operating Temperature 15°F-140°F (-9°C-60°C)

Figure 3.2 Tekscan Flexiforce single load cell type sensor and details from manufacturer (Tekscan 2007)

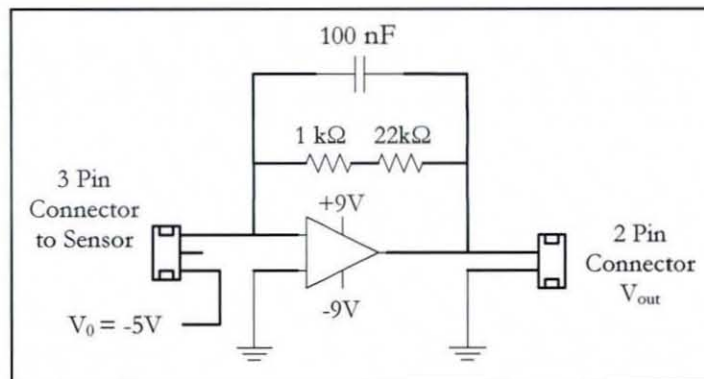


Figure 3.3 Simple circuit used with Flexiforce sensors

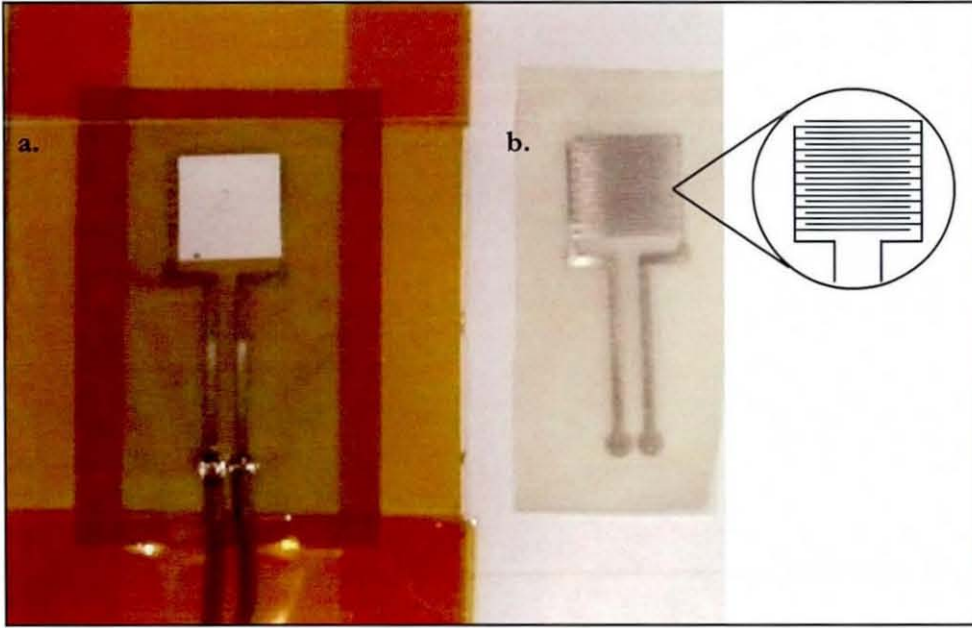


Figure 3.4 (a.) QTC sensor with square piece of sensing material on electrode, (b.) QTC electrode

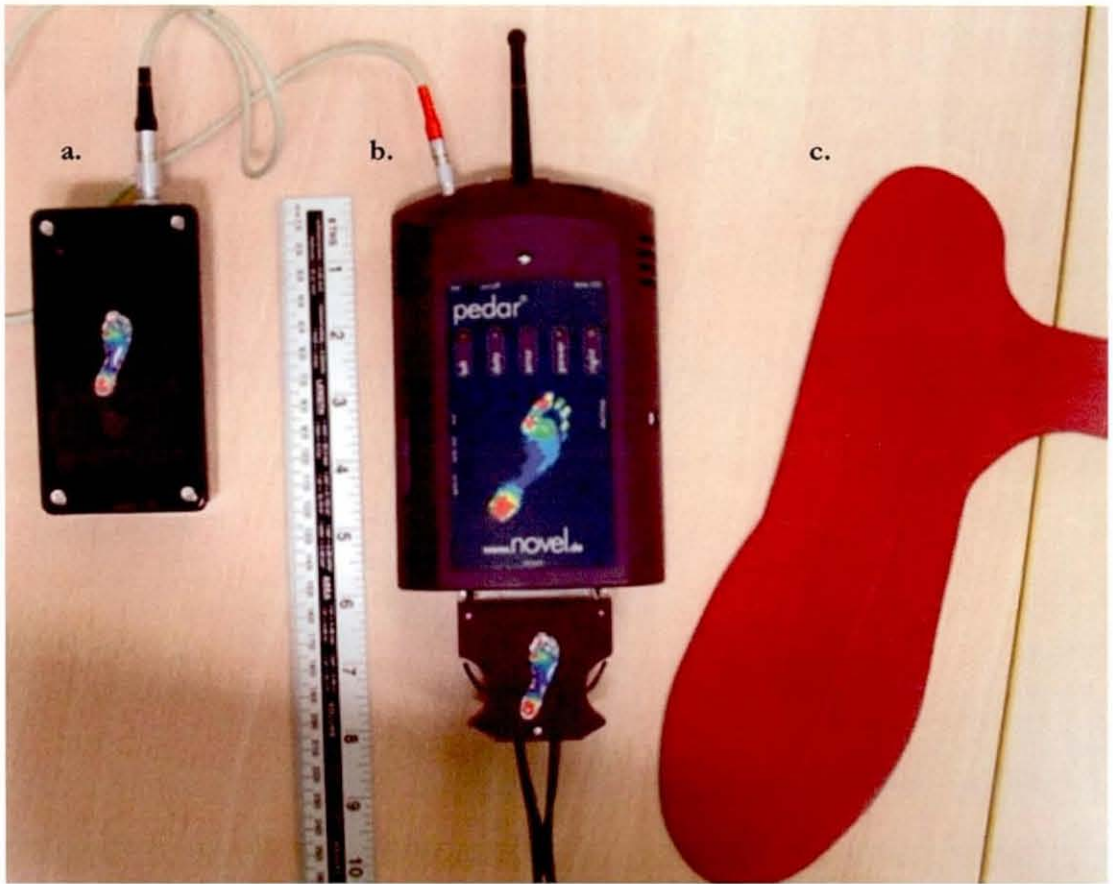


Figure 3.5 Novel Pedar wireless pressure measurement system; (a.) battery, (b.) wireless output box, (c.) size Y insole sensor

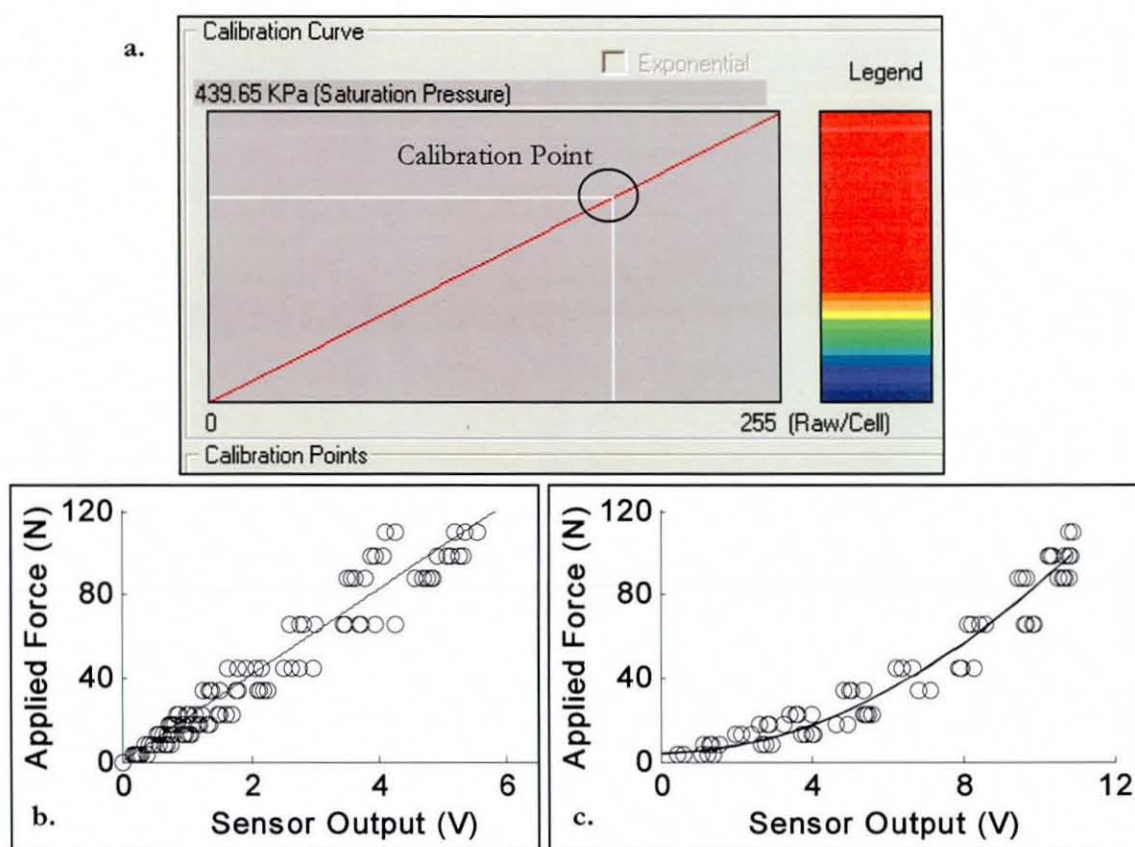


Figure 3.6 Calibration curves for (a.) Tekscan 9811, (b.) Flexiforce and (c.) QTC sensors

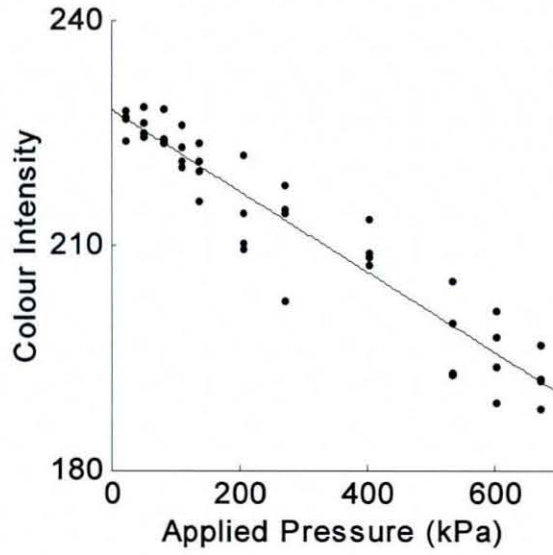


Figure 3.7 Pressurex calibration curve, with colour intensity values from 0 (black) to 255 (white)

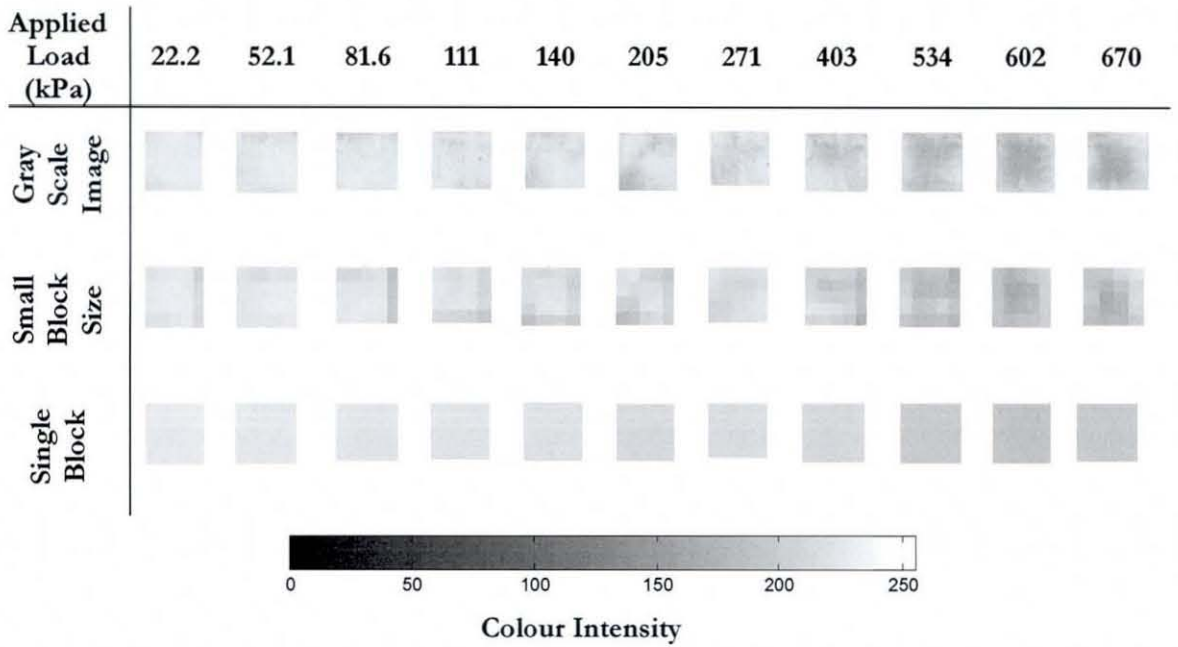


Figure 3.8 Results from one set of Pressurex film calibration, showing film in grey scale and blocked with mean colour intensity displayed in each region

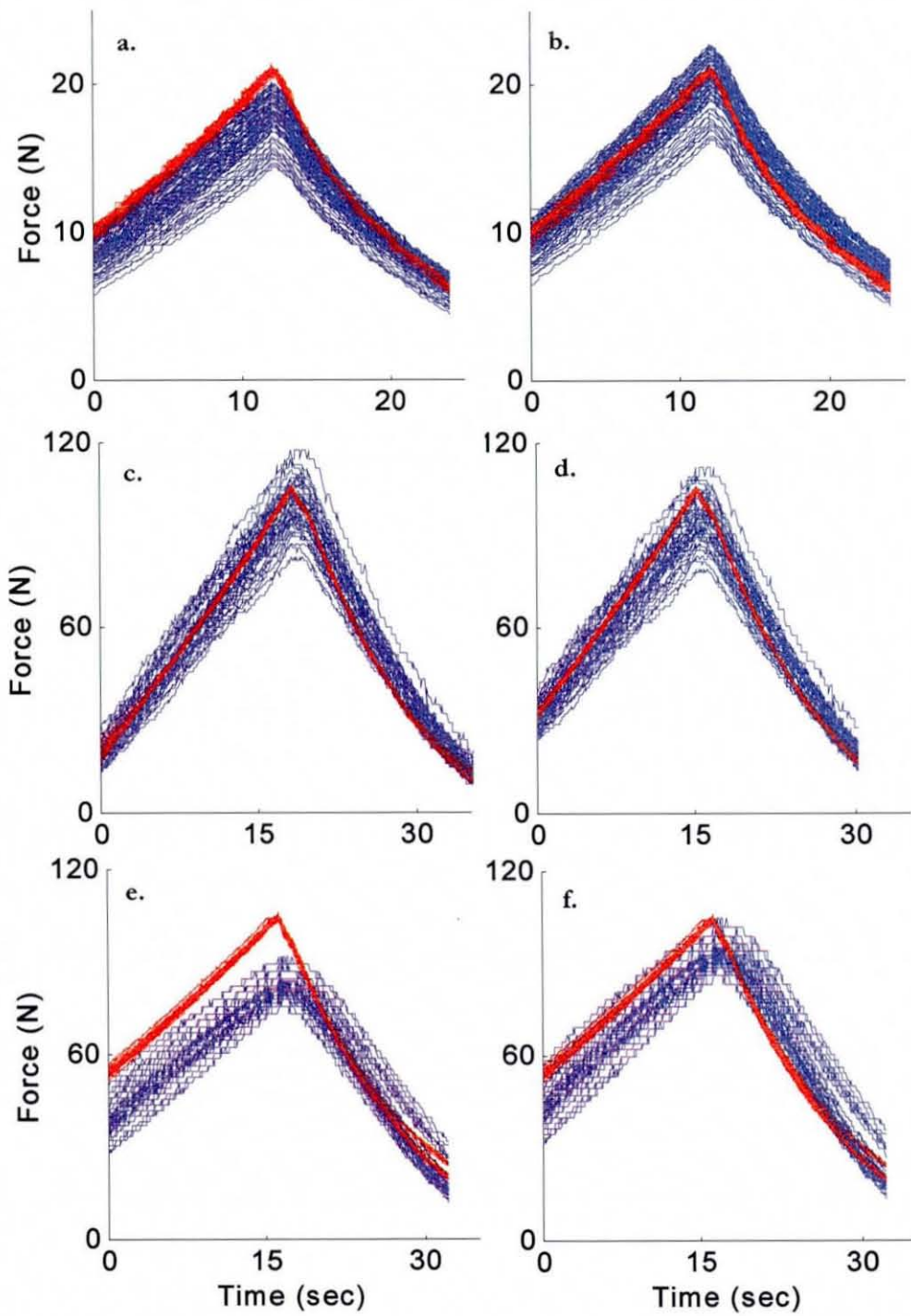


Figure 3.9 Results from quasi-static accuracy test, (a.) Tekscan 9811 (uncorrected), (b.) Tekscan 9811 with calibration drift correction, (c.) Flexiforce (uncorrected), (d.) Flexiforce (corrected), (e.) QTC (uncorrected), and (f.) QTC (corrected); — applied load, — measured load

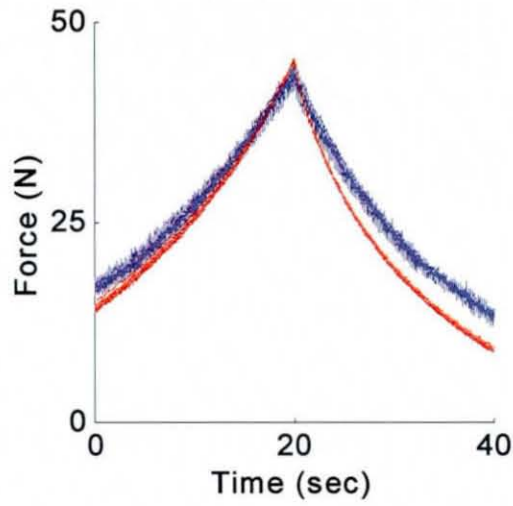


Figure 3.10 Novel results from quasi-static accuracy test; — applied load, — measured load

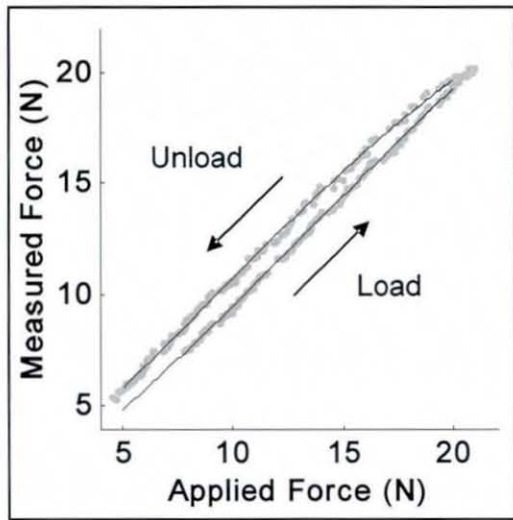


Figure 3.11 Example Tekscan 9811 test applied versus measured force for hysteresis calculation, * measured points, — curve fit

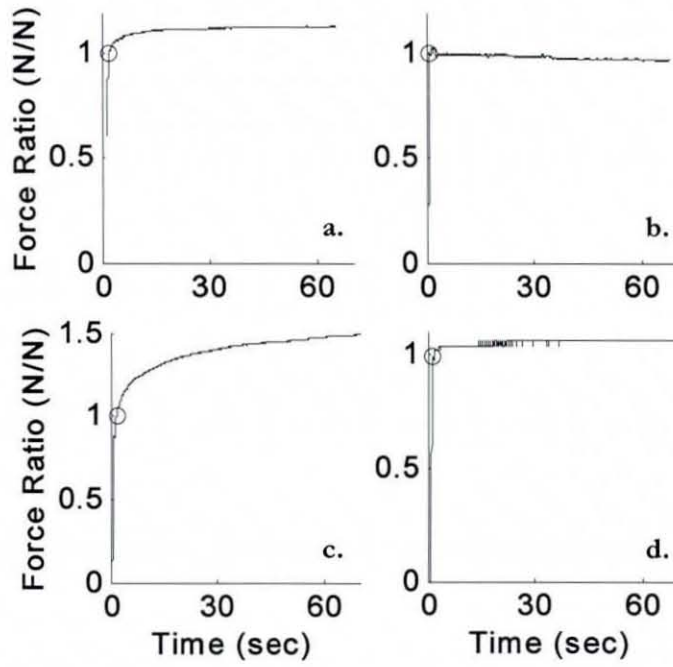


Figure 3.12 Static drift test example results with (a.) Tekscan 9811, (b.) Flexiforce, (c.) QTC, and (d.) Novel sensors; \circ indicates the 'Starting Point' from where drift is calculated

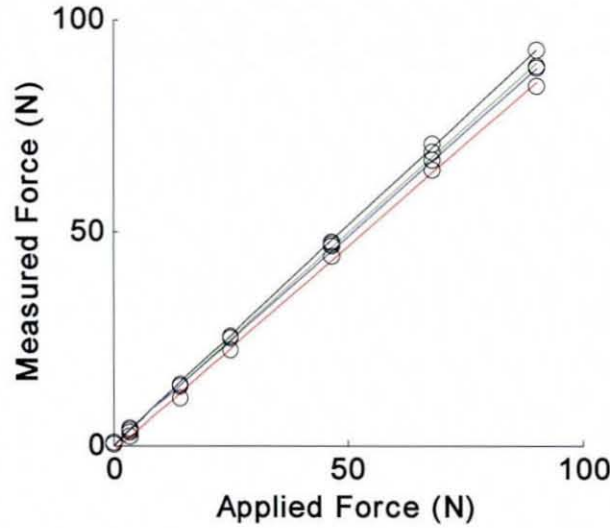


Figure 3.13 Flexiforce output of one sensor during a single curved surface test; — flat surface, — 30 mm, — 25 mm, — 20 mm

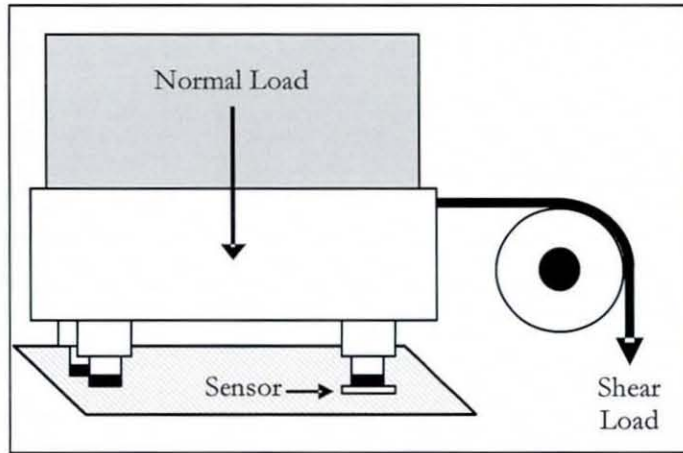


Figure 3.14 Shear force test set-up

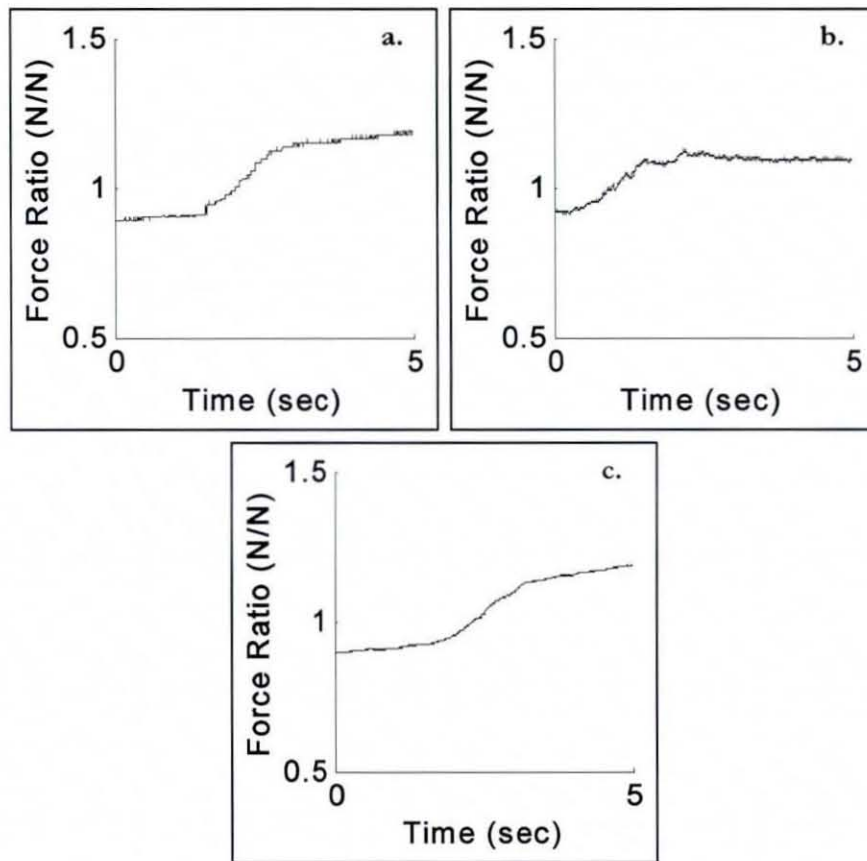


Figure 3.15 Shear force test example results with (a.) Tekscan 9811, (b.) Flexiforce, and (c.) QTC sensors; force ratio is the measured sensor output divided by the applied normal load

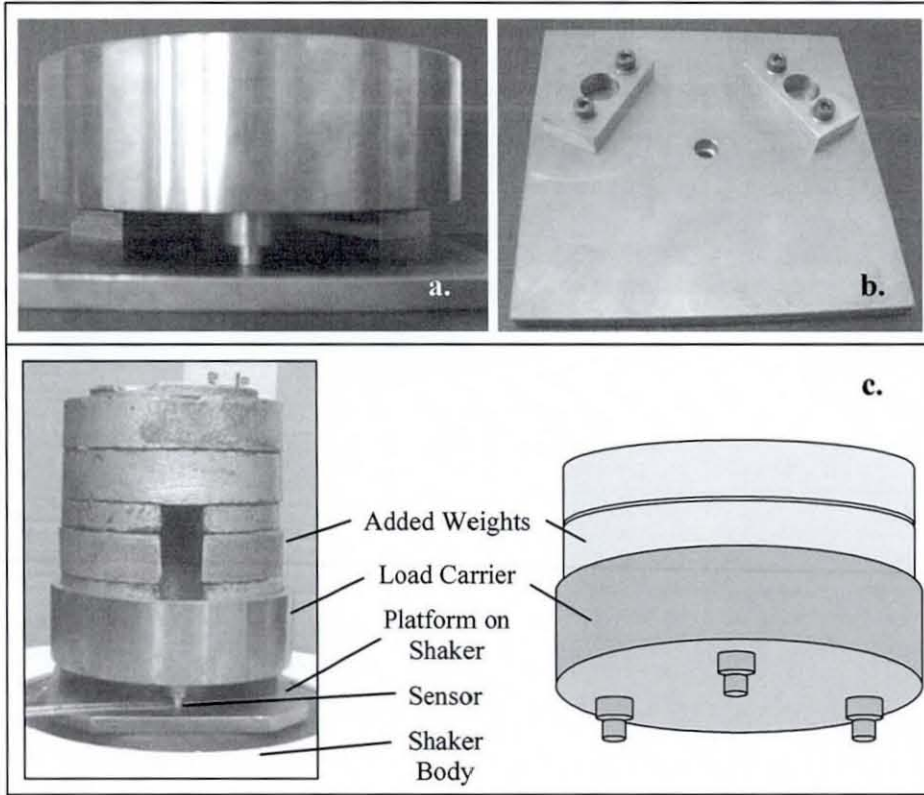


Figure 3.16 Dynamic test set-up; (a.) load carrier, (b.) platform, and (c.) weights, load carrier and platform resting on the shaker

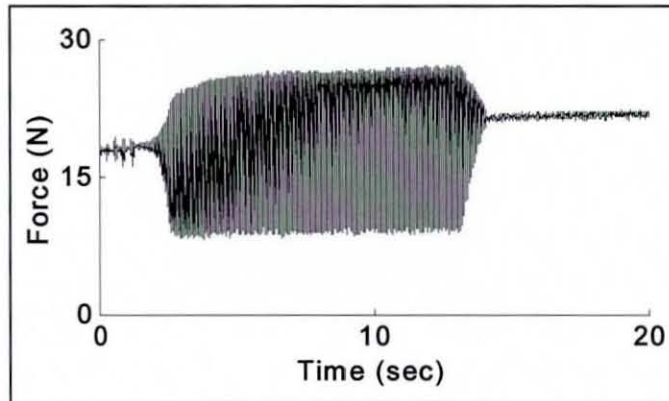


Figure 3.17 Tekscan 9811 sensor output in response to an applied dynamic load of 15 N at 60 Hz

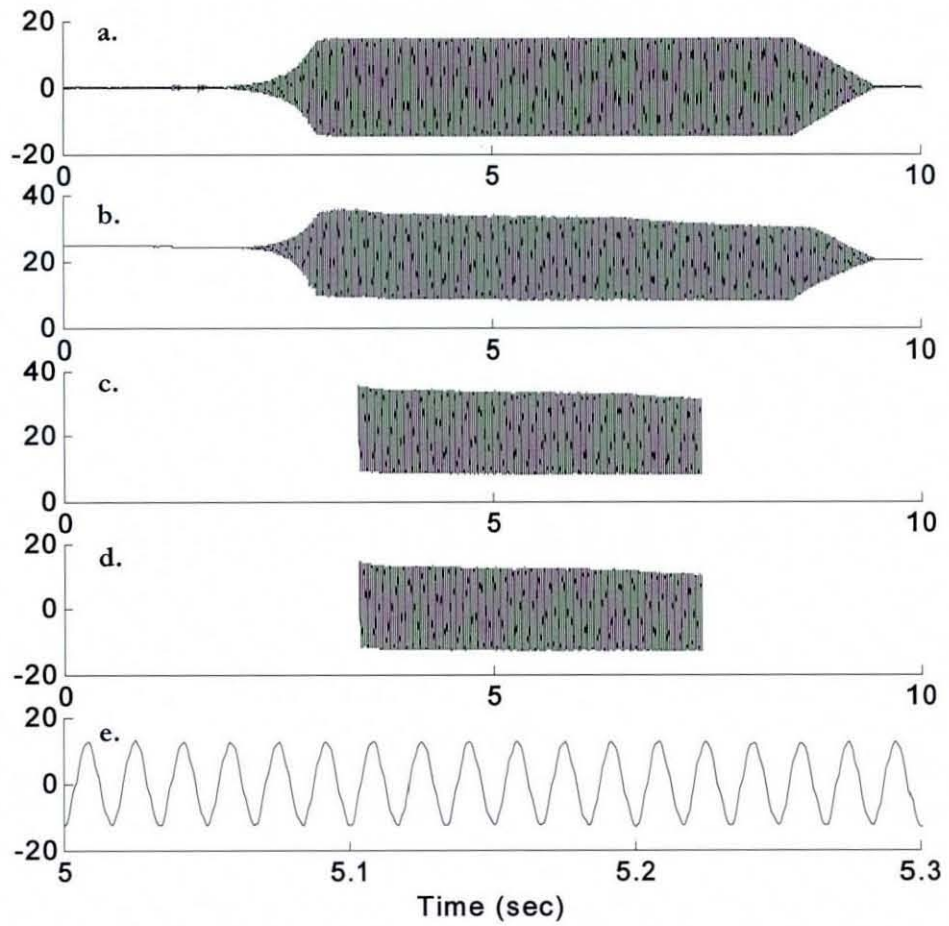


Figure 3.18 Flexiforce dynamic test results, all values in Newtons; (a.) applied force as measured with accelerometer, (b.) Flexiforce measured force, (c.) data segment analysed for accuracy calculation, (d.) data segment after preload and low frequency drift were removed, (e.) close-up of segment

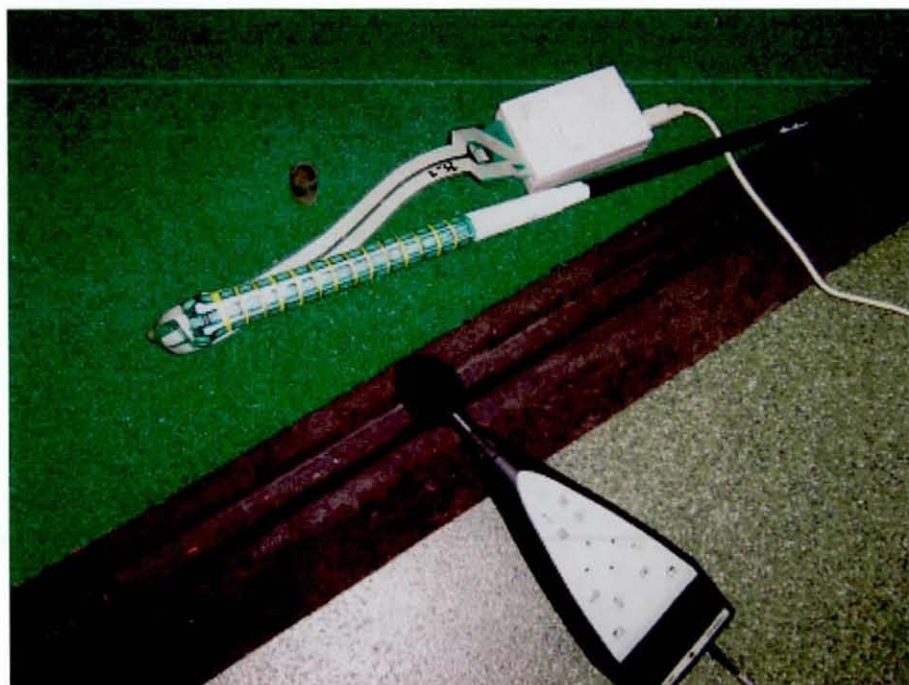


Figure 4.1 Sound level meter and golf club with 6-sided grip* and 9811 sensor near tee on artificial turf matt

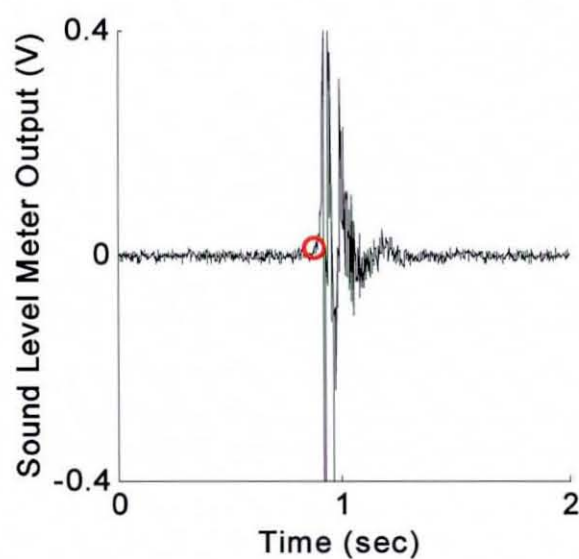


Figure 4.2 Typical sound level meter output at impact; \circ indicates the calculated moment of impact

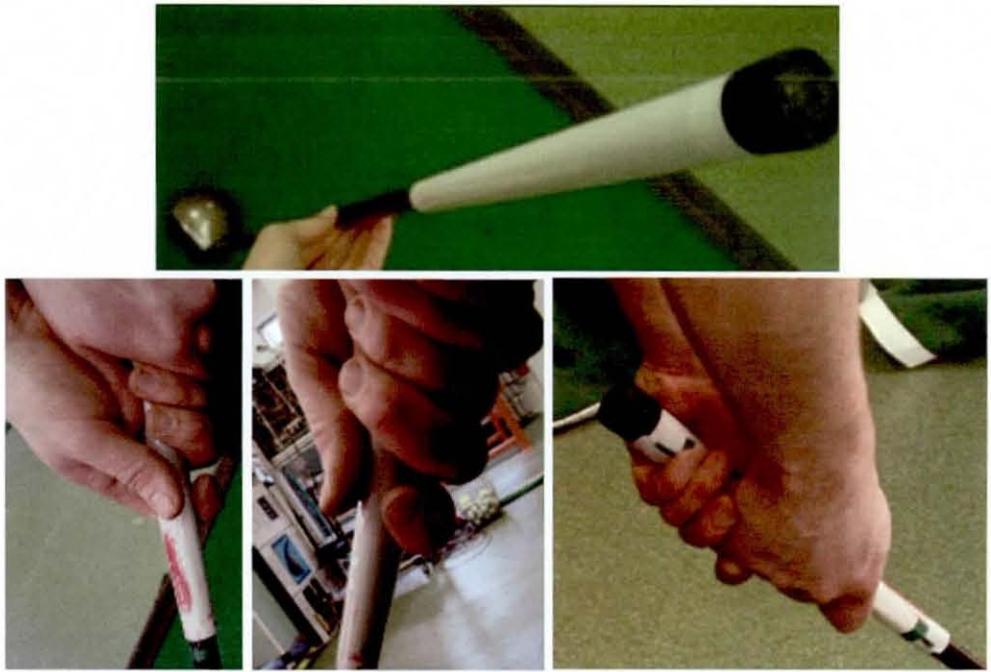


Figure 4.3 Pressurex film on grip* prior to player test

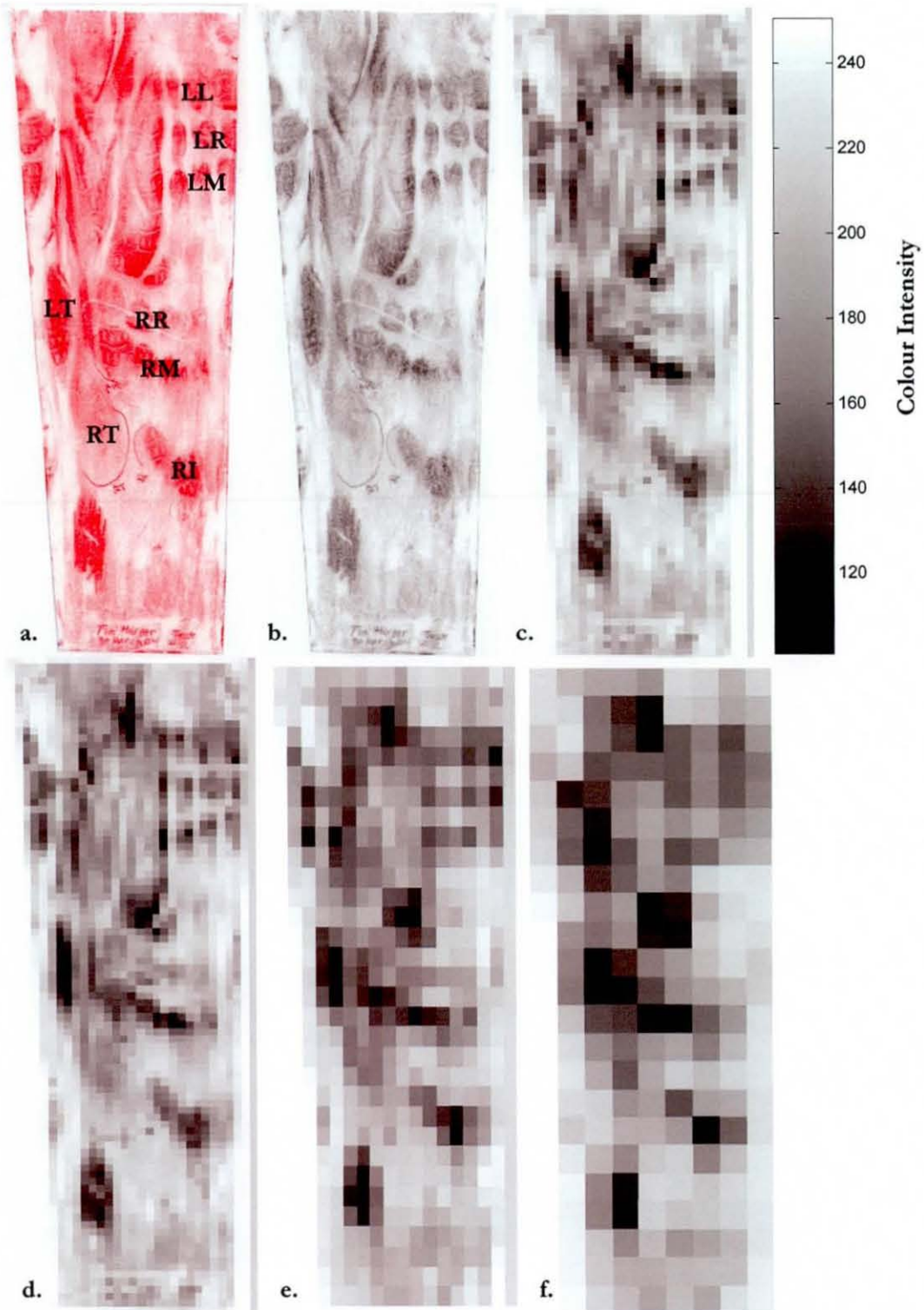


Figure 4.4 Pressurex on grip* test, (a.) film after test with finger position noted (LL = left little, LR = left ring, LM = left middle, LT = left thumb, RR = right ring, RM = right middle, RI = right index, RT = right thumb), (b.) film in greyscale, (c.)-(f.) film with block lengths of 20, 40, 60, and 80 pixels, respectively



Figure 4.5 32 pieces of Pressurex film on hands

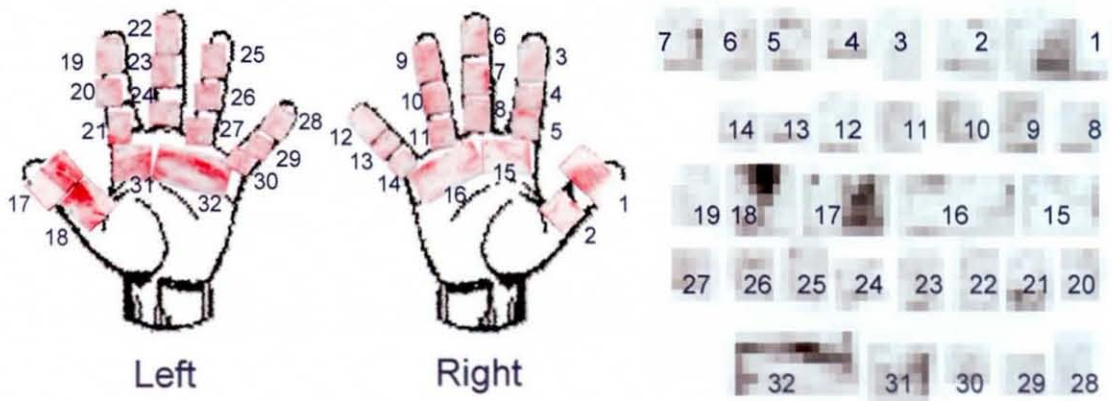


Figure 4.6 Pressurex film after player test; 32 pieces shown where they were positioned on the hands and how they looked during analysis

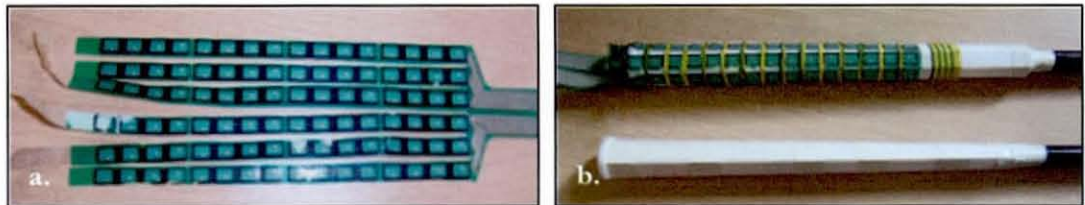


Figure 4.7 (a.) Tekscan 9811 sensor cut along columns, (b.) 6-sided grips* on standard drivers

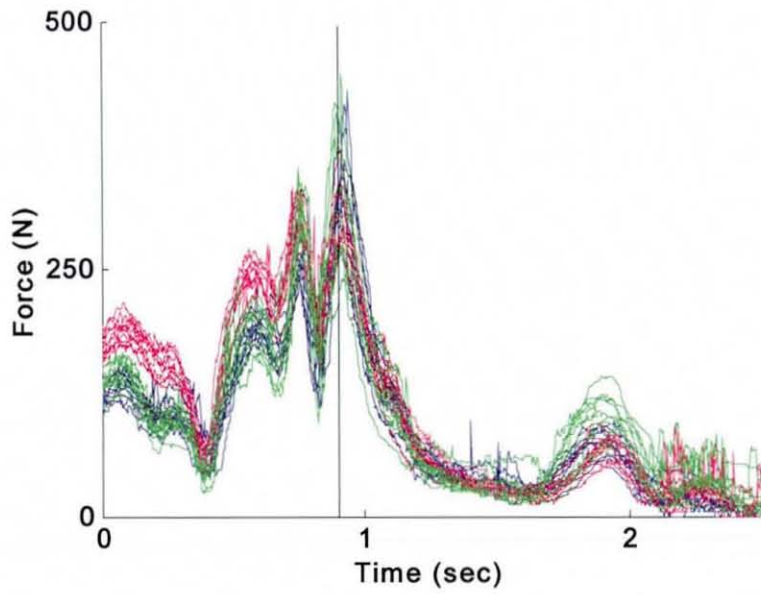


Figure 4.8 Total grip force from one player test with 30 shots taken with 9811 sensors on 6-sided grips*; — small, — medium, — large grip* sizes, and — impact

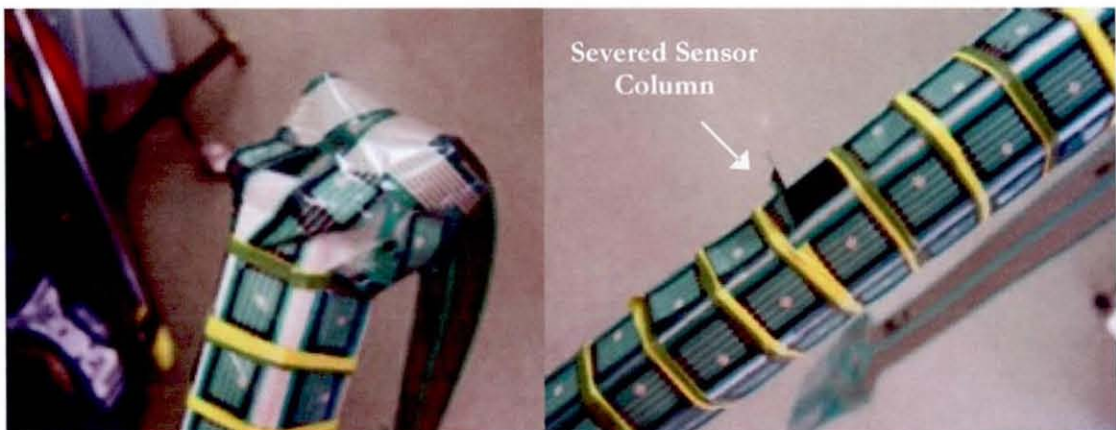


Figure 4.9 Sensor damage caused during player tests

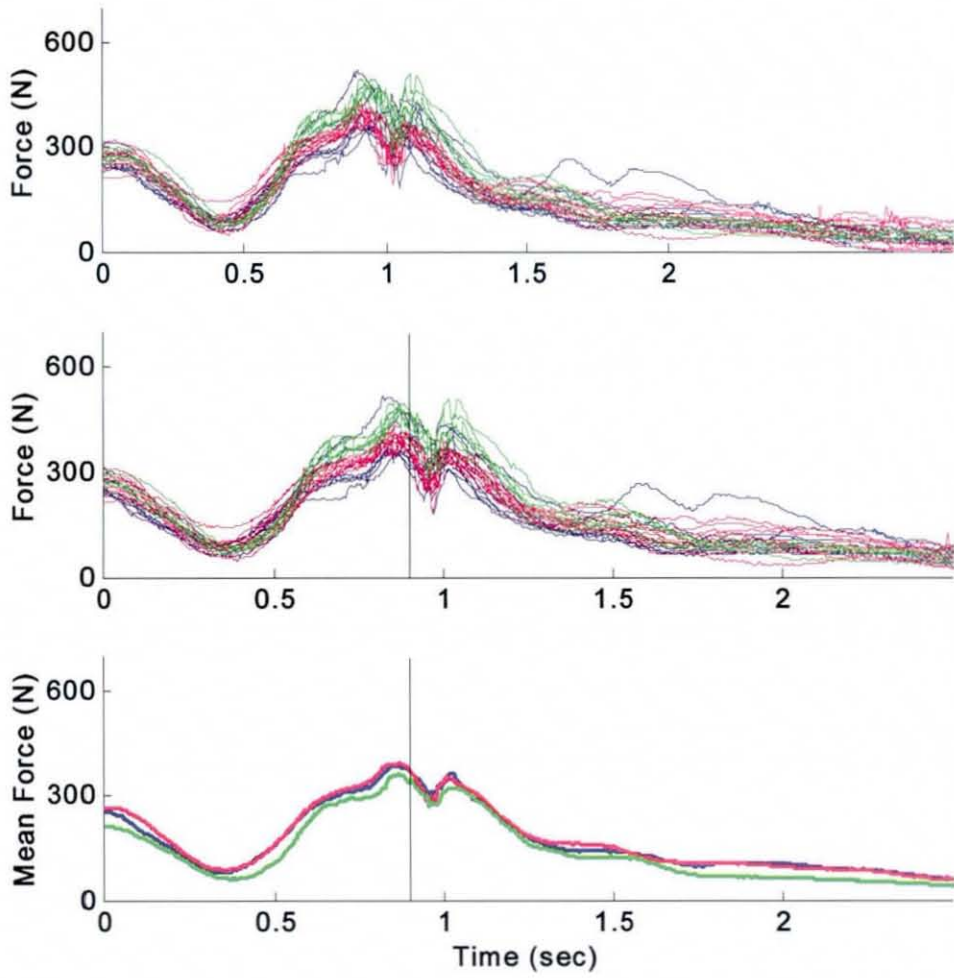


Figure 4.10a Player A total grip force results using 6-sided grip*; (a.) 30 original force curves, (b.) data aligned based on impact time, (c.) mean force trace for each club; — small, — medium, — large grip* sizes, and — impact

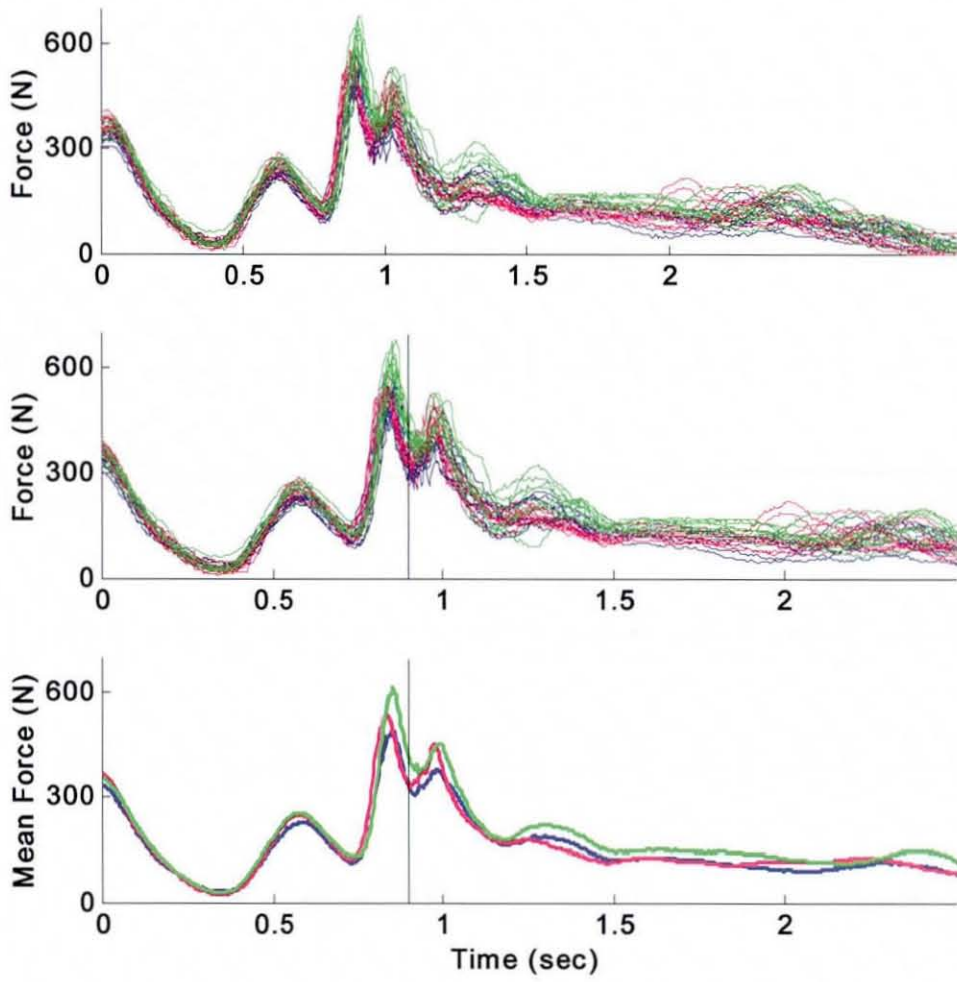


Figure 4.10b Player B total grip force results using 6-sided grip*; (a.) 30 original force curves, (b.) data aligned based on impact time, (c.) mean force trace for each club; — small, — medium, — large grip* sizes, and — impact

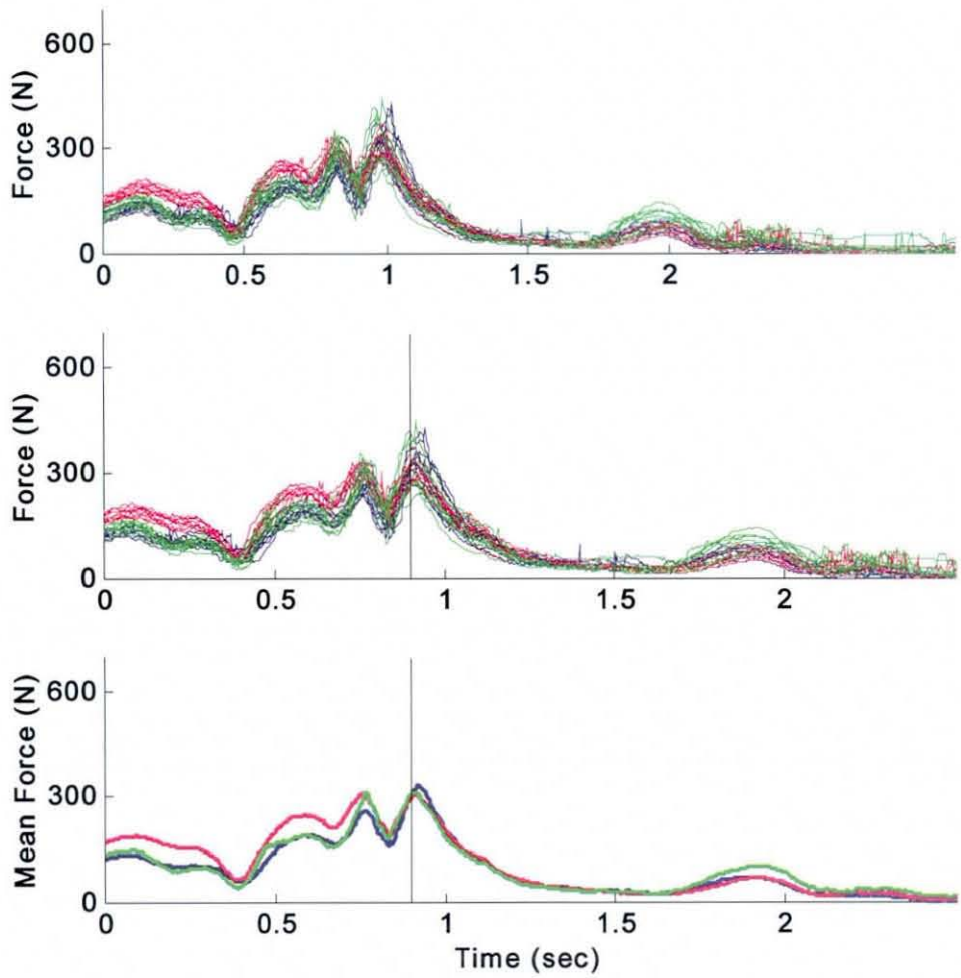


Figure 4.10c Player C total grip force results using 6-sided grip*; (a.) 30 original force curves, (b.) data aligned based on impact time, (c.) mean force trace for each club; — small, — medium, — large grip* sizes, and — impact

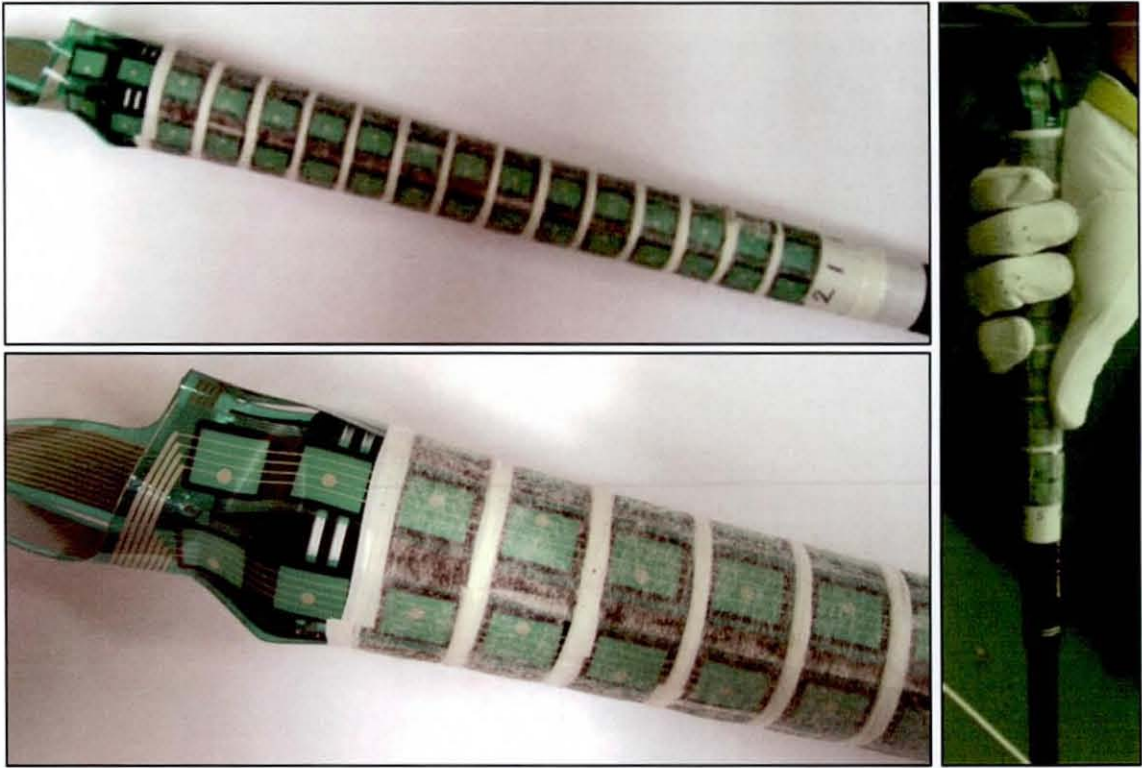


Figure 5.1 Tekscan 9811 sensor on standard golf grip* as used during player tests

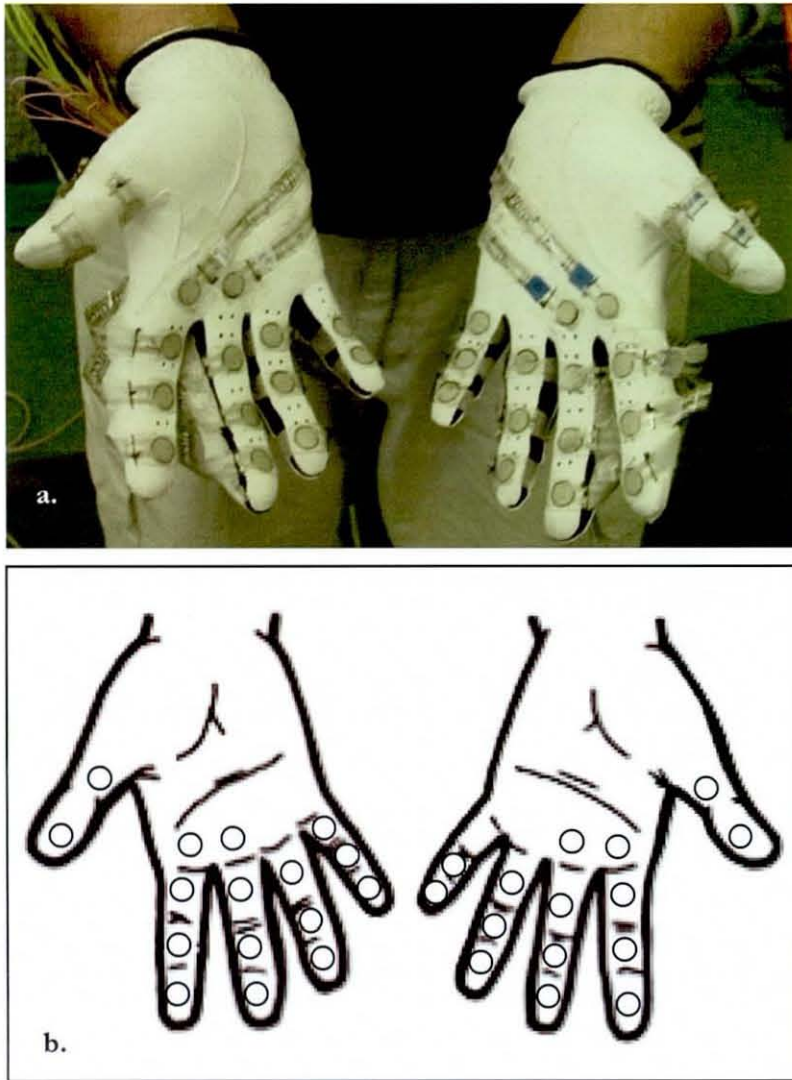


Figure 5.2 31 Flexiforce sensors on two golf gloves; (a.) example gloves used during player tests, (b.) sensor locations on the hands

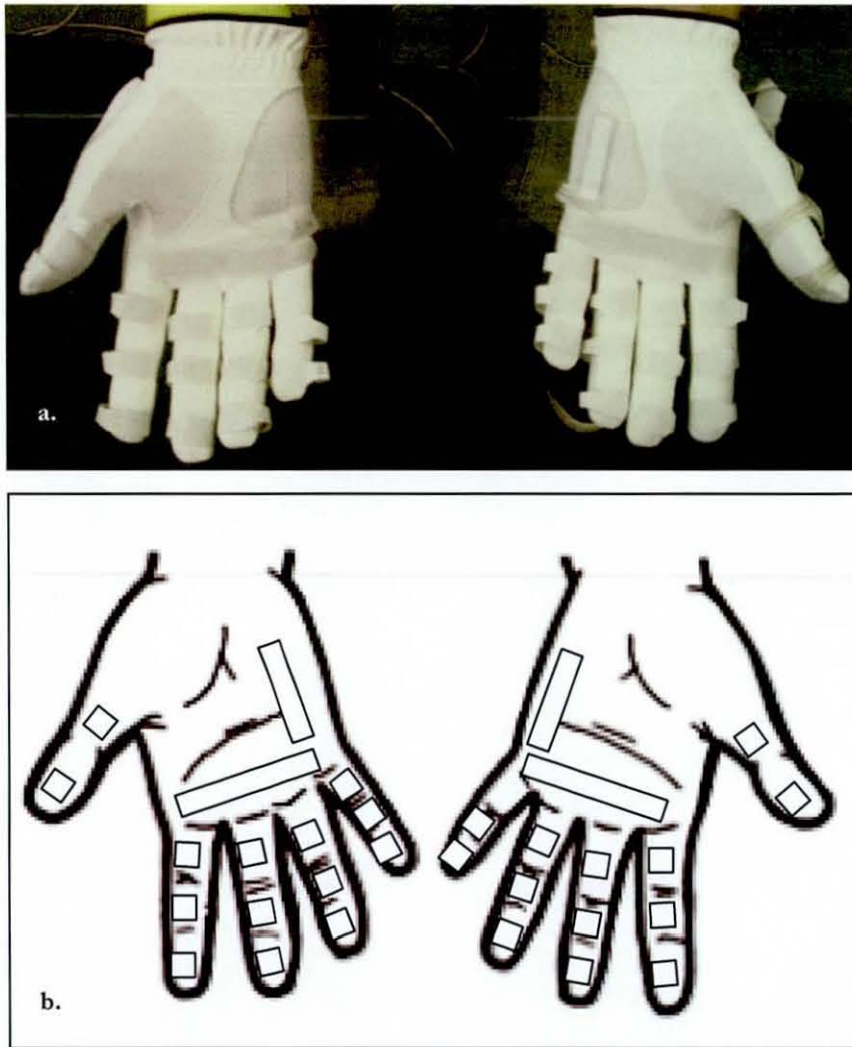


Figure 5.3 31 QTC sensors on two golf gloves; (a.) example gloves used during player tests, (b.) sensor locations on the hands

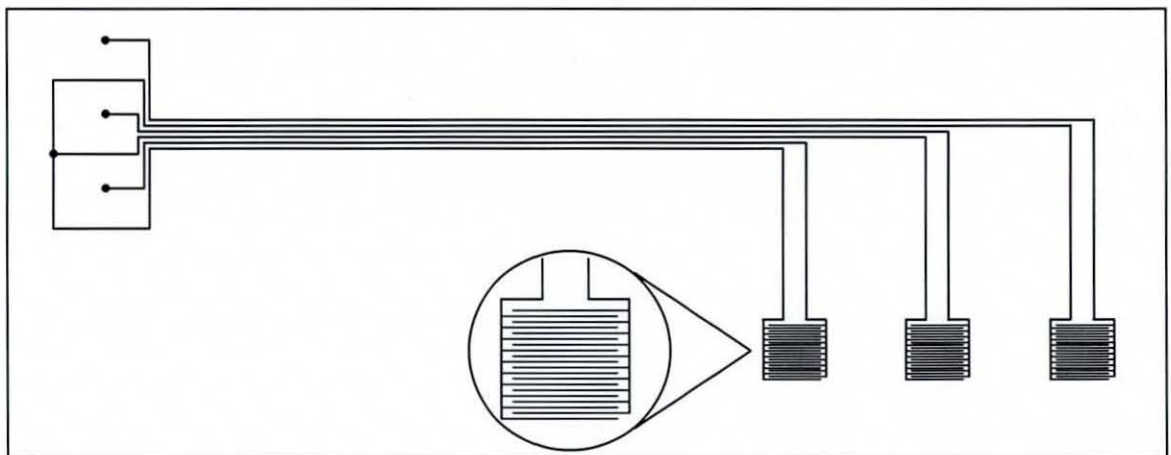


Figure 5.4 Schematic of QTC electrode for measuring at three locations per finger

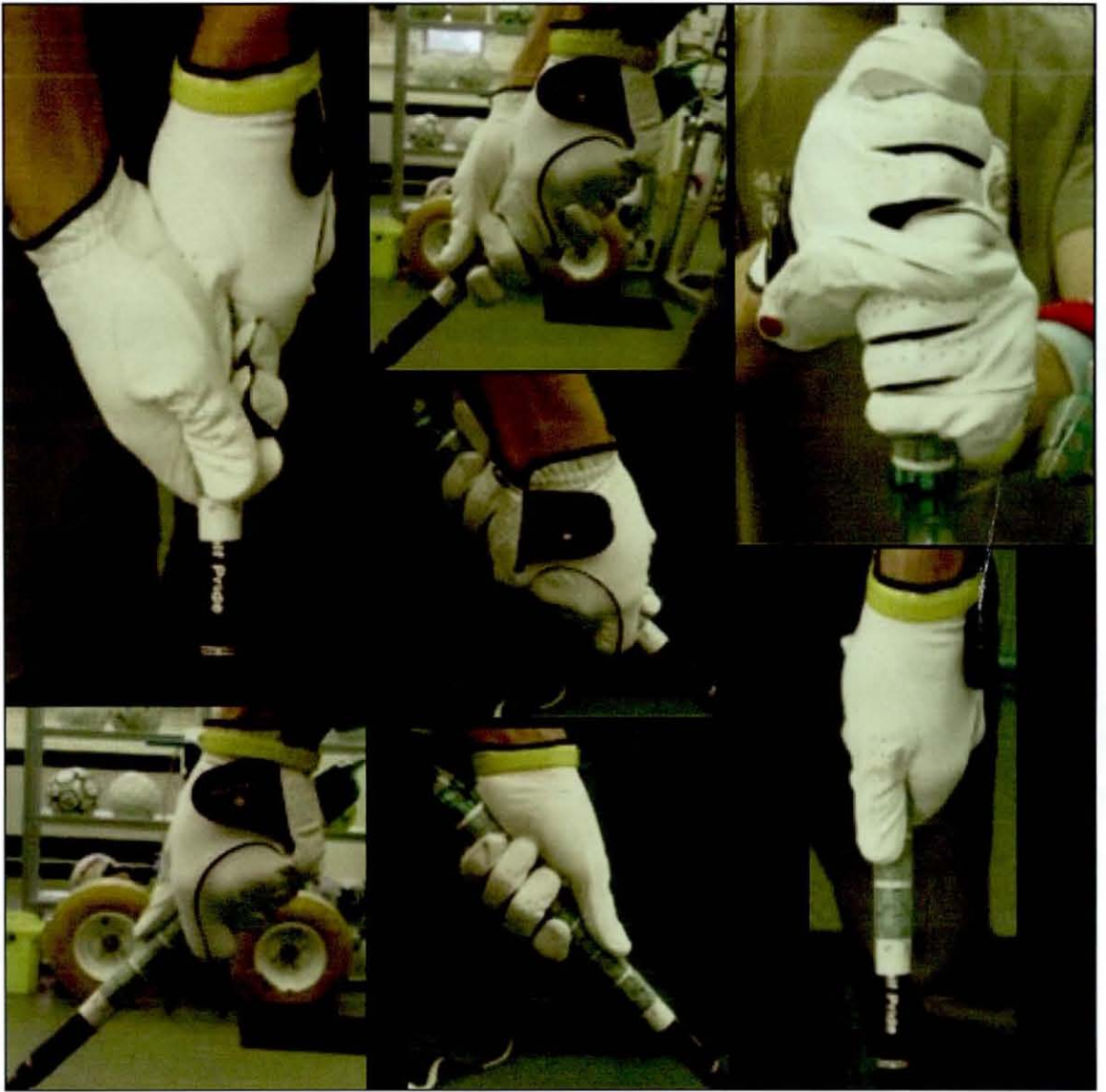


Figure 5.5 Example of the seven photographs taken after the completion of each 9811 grip force test

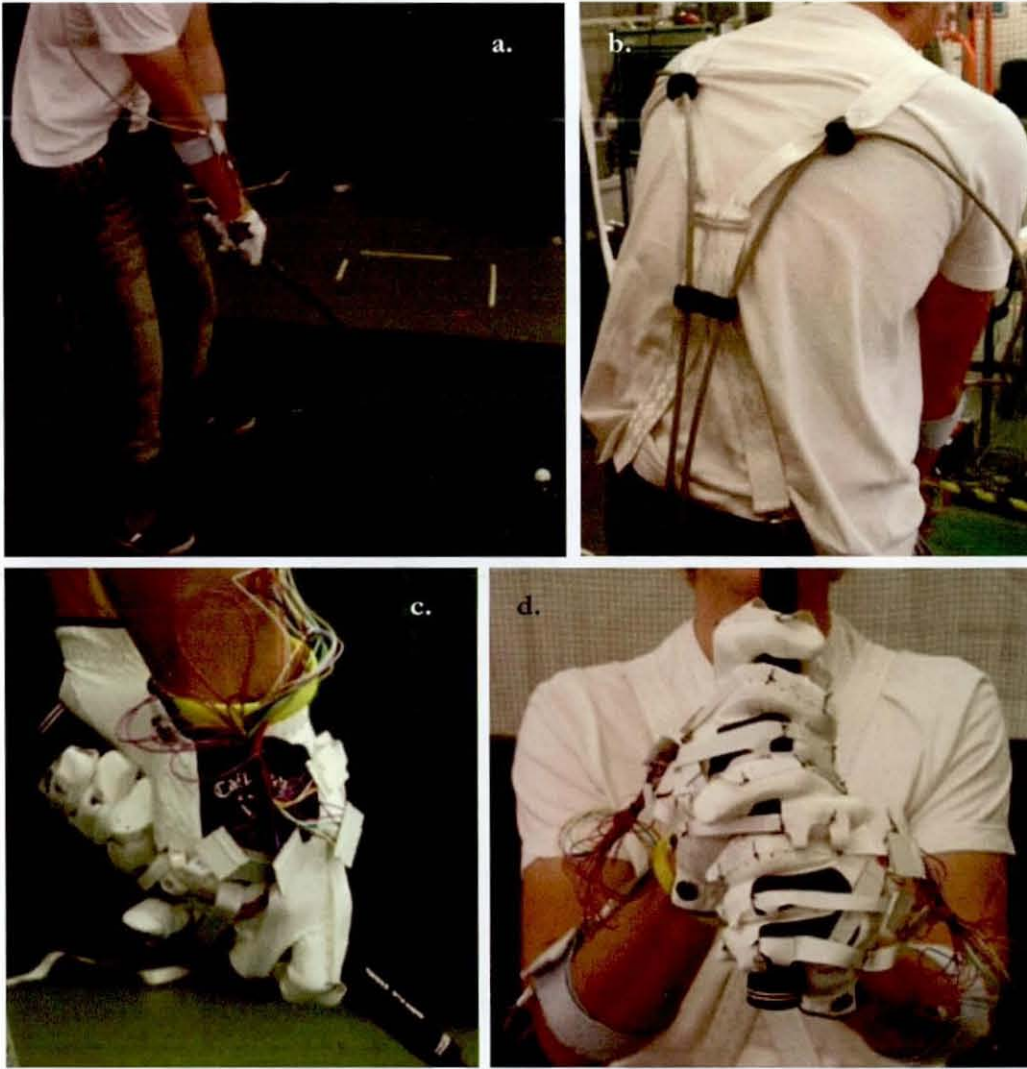


Figure 5.6 Player test set-up; (a.) and (b.) show the cables required for Flexiforce and QTC tests with the method of attachment on the forearms with elastic Velcro straps and over the shoulders with the cables attached to braces, respectively, while (c.) and (d.) show the gloves with QTC sensors

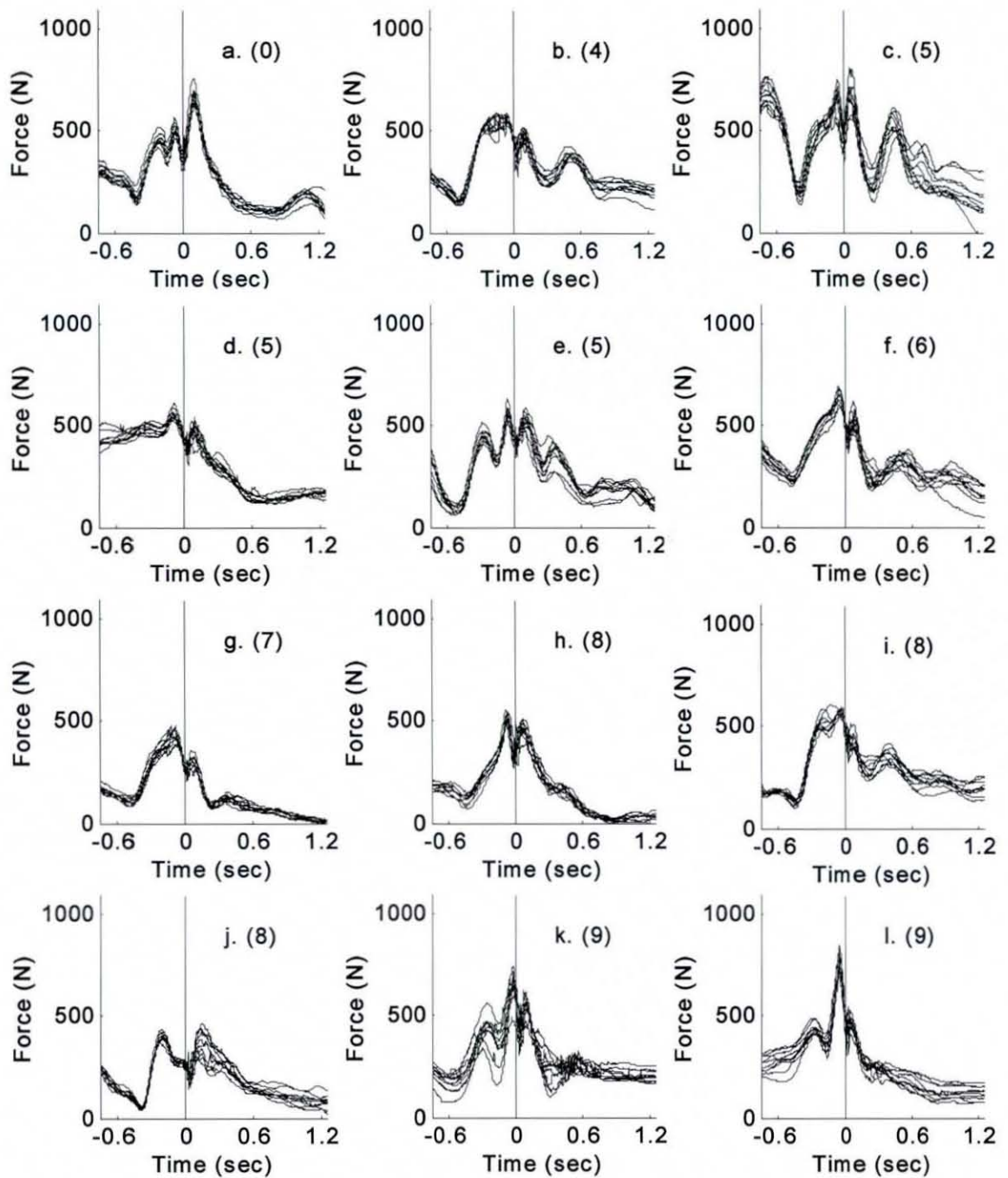


Figure 5.7a Total force from 10 shots taken by golfers and with 9811 sensor on grip*, all shots aligned at impact (time = 0 s) and handicap is shown in parentheses

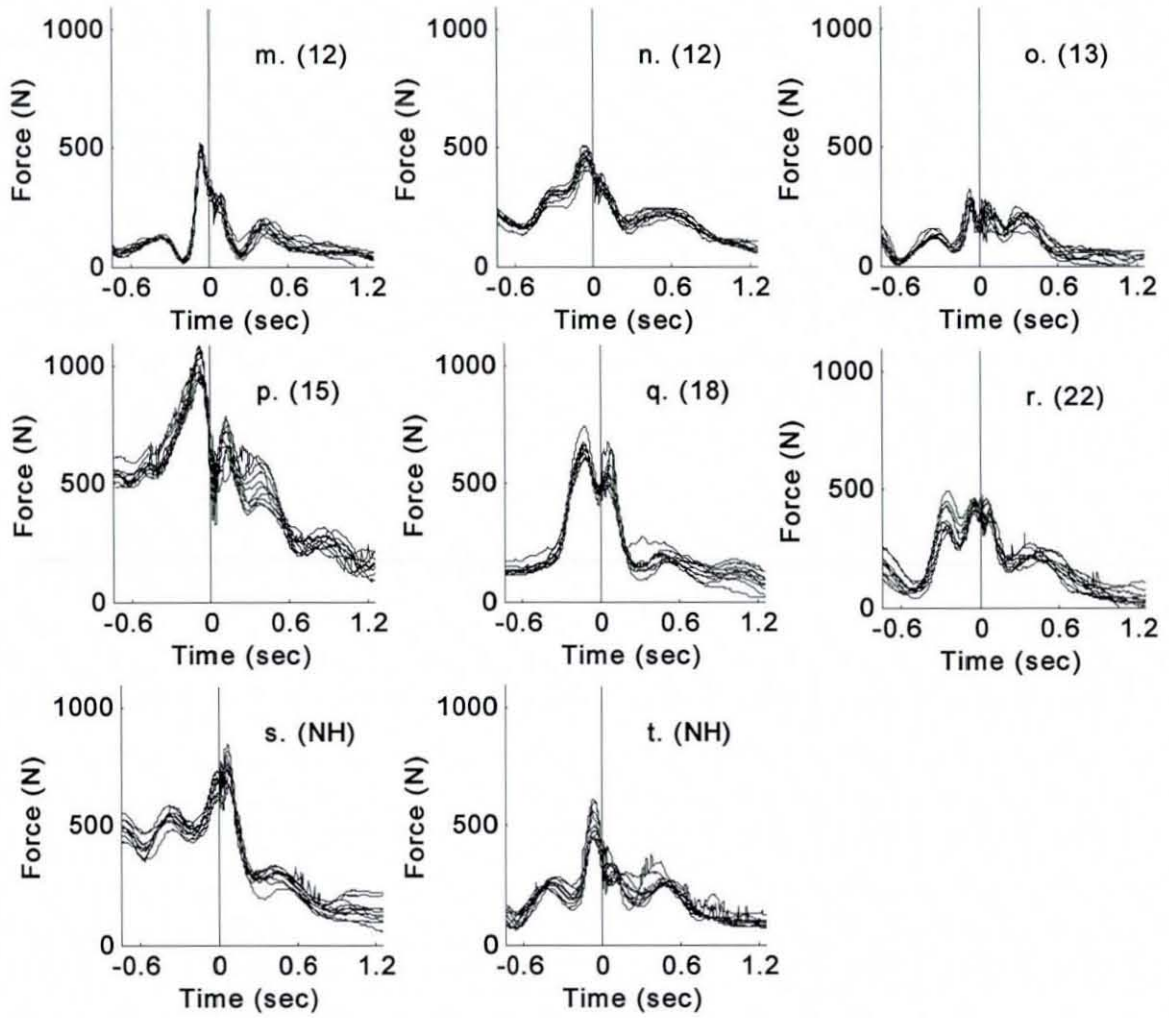


Figure 5.7b Total force from 10 shots taken by golfers and with 9811 sensor on grip*, all shots aligned at impact (time = 0 s) and handicap is shown in parentheses

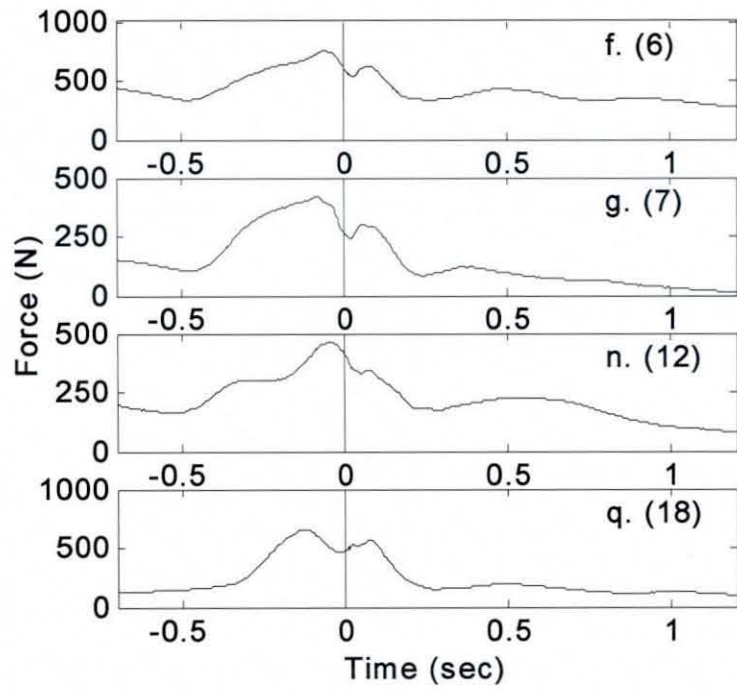


Figure 5.8 Mean total grip force from 9811 test for four golfers with high cross correlation values; handicap shown in parentheses

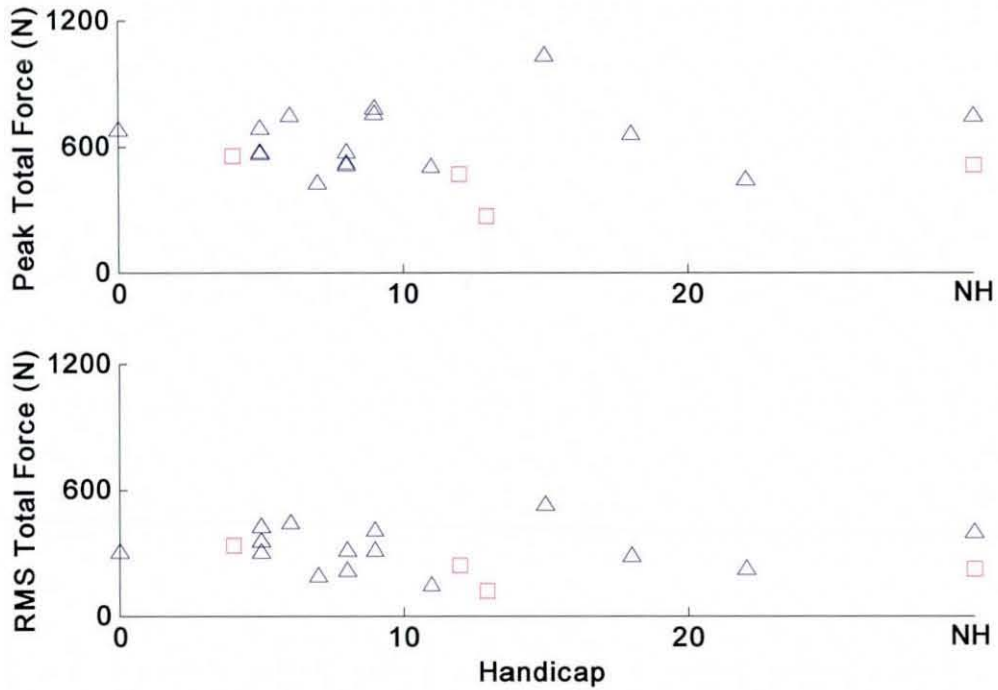


Figure 5.9 Peak and RMS total mean grip force versus handicap for Tekscan 9811 sensor on grip* tests; Δ men, \square women

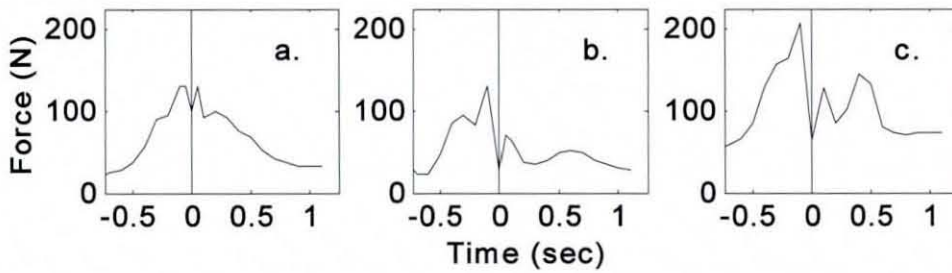


Figure 5.10 Total grip force traces produced in study by Budney and Bellow (1990); each trace is the summation of forces from three transducers, with shots being taken by two professional golfers (a. and b.) and one amateur (c)

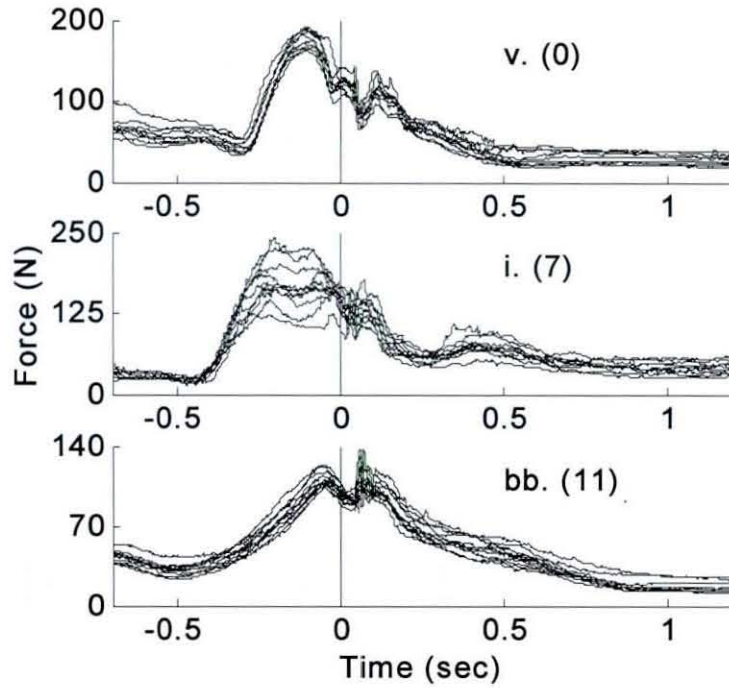


Figure 5.11 Twelve total force traces for three golfers as measured by Flexiforce sensors; golfer handicap in parentheses

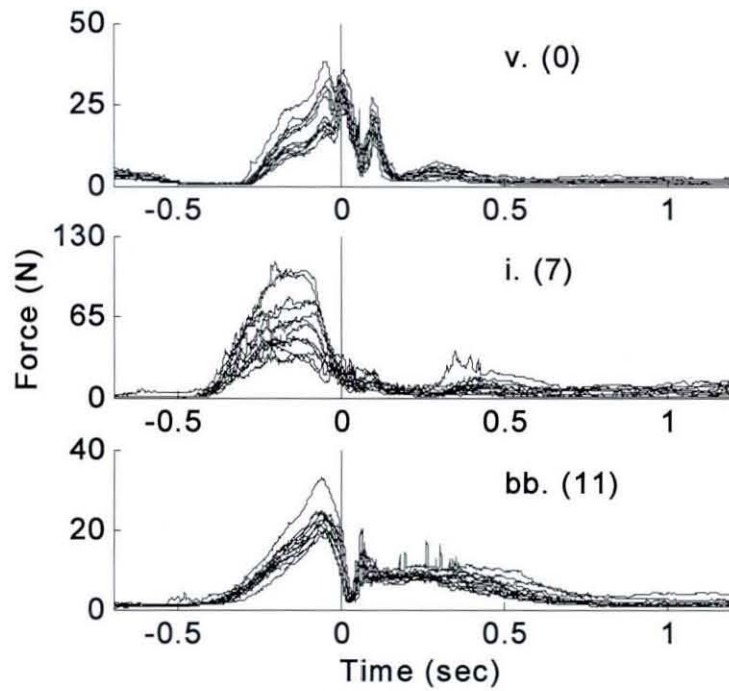


Figure 5.12 Twelve left thumb force traces for three golfers as measured by Flexiforce sensors; handicap in parentheses

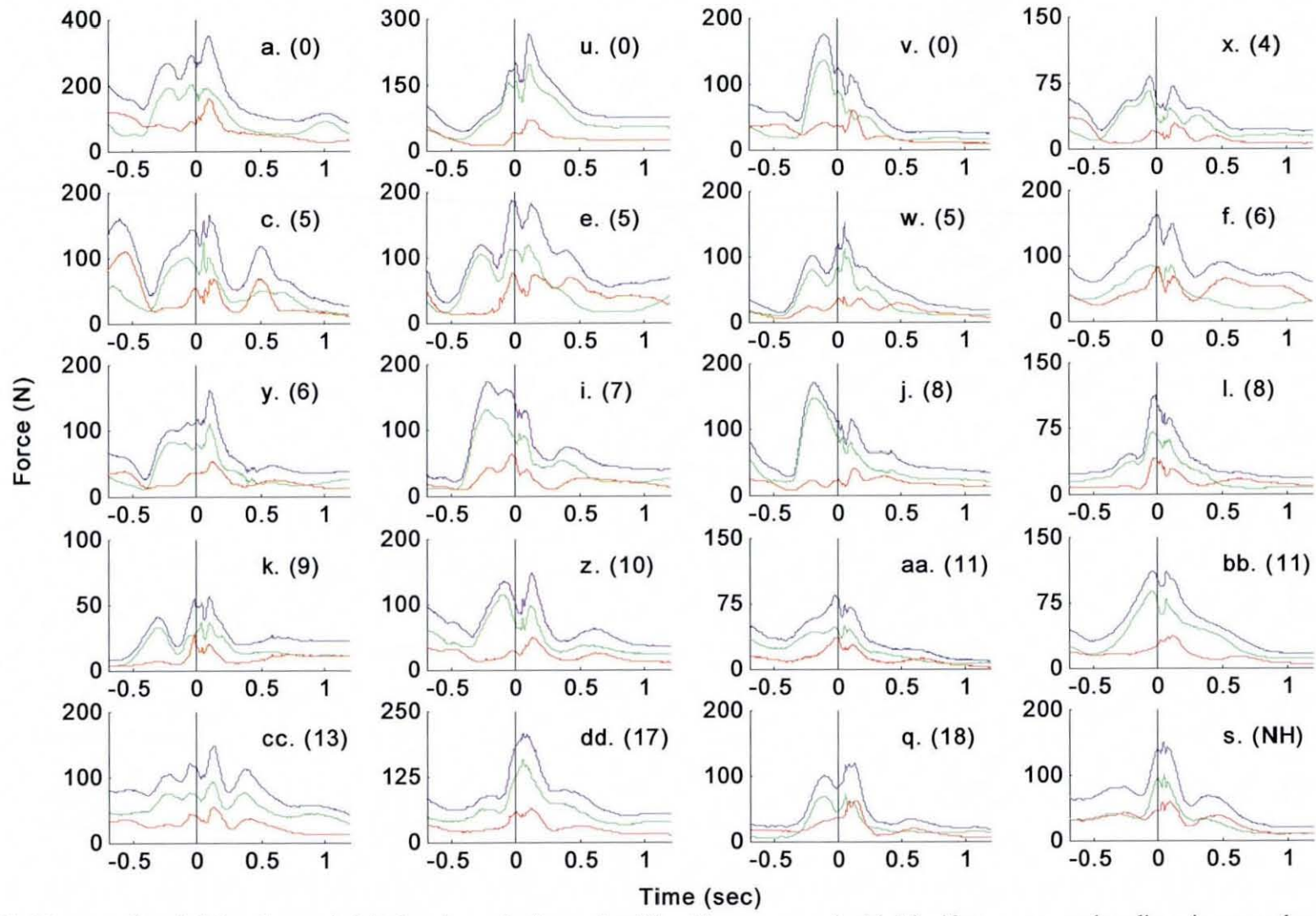


Figure 5.13 Mean total —, left hand — and right hand — grip forces for 20 golfers measured with Flexiforce sensors; handicap in parentheses

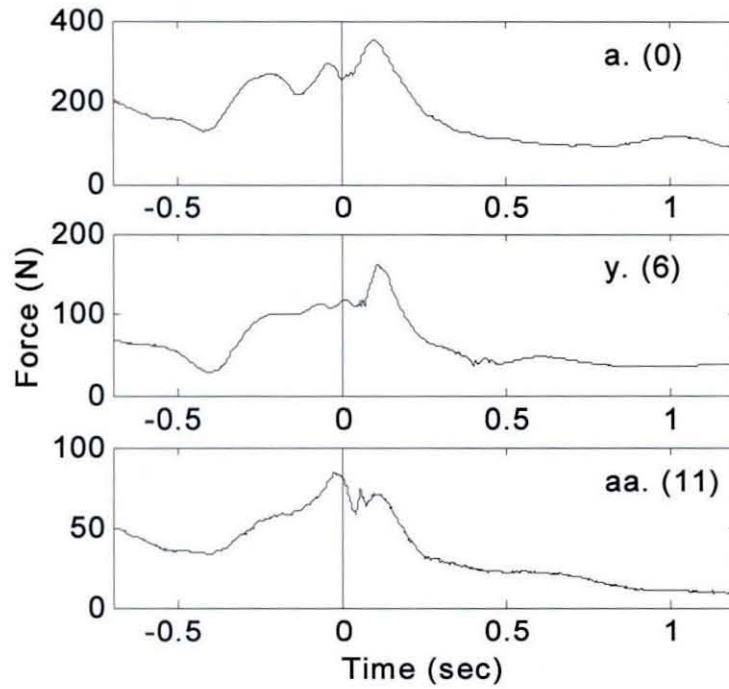


Figure 5.14 Mean total grip force for three golfers with high cross correlation values; handicap shown in parentheses

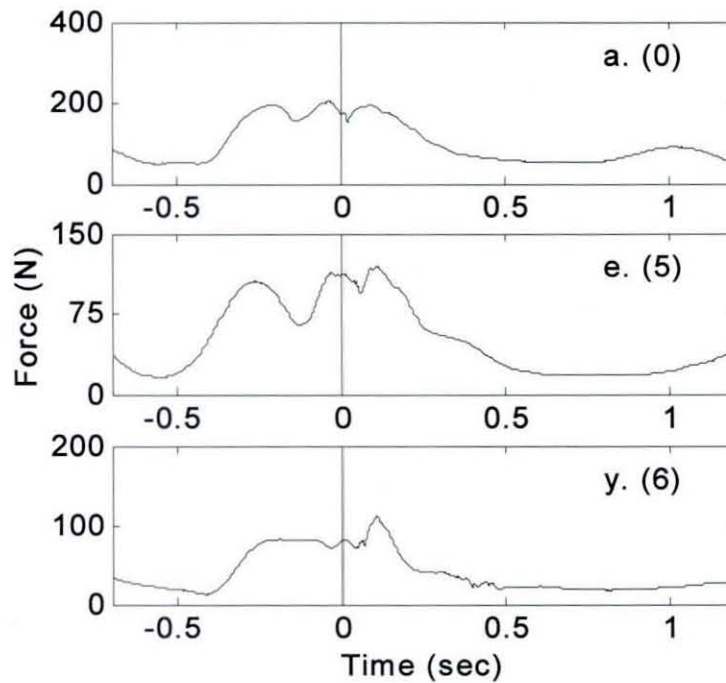


Figure 5.15 Mean left hand grip force for three golfers with high cross correlation values; handicap shown in parentheses

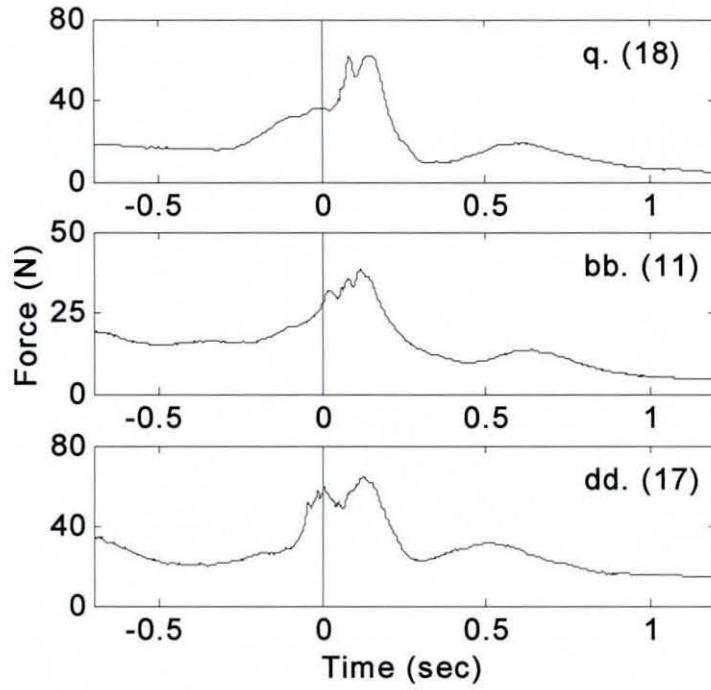


Figure 5.16 Mean right hand grip force for three golfers with high cross correlation values; handicap shown in parentheses

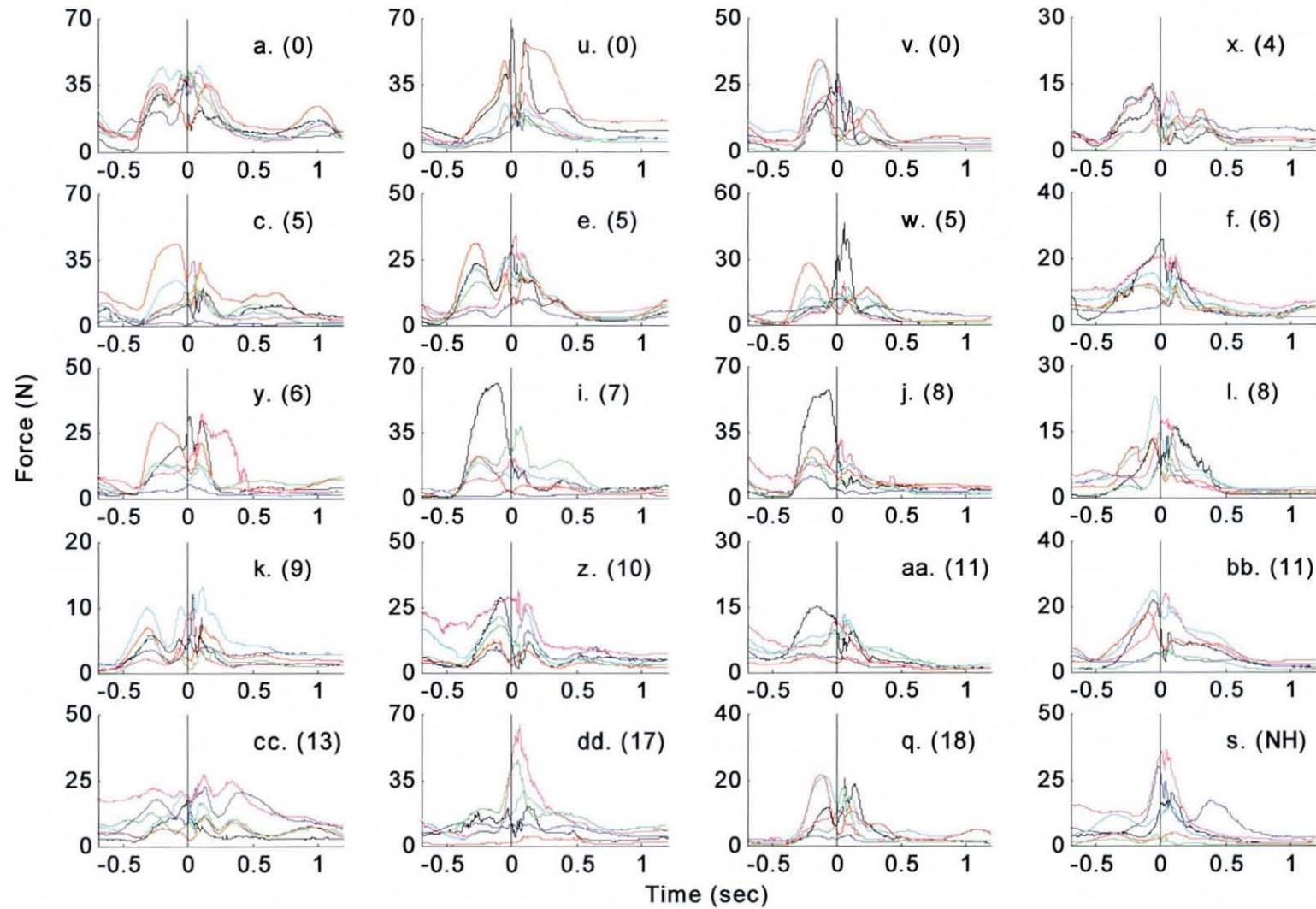


Figure 5.17 Left hand forces from Flexiforce tests; — thumb, — index, — middle, — ring, — little, — palm

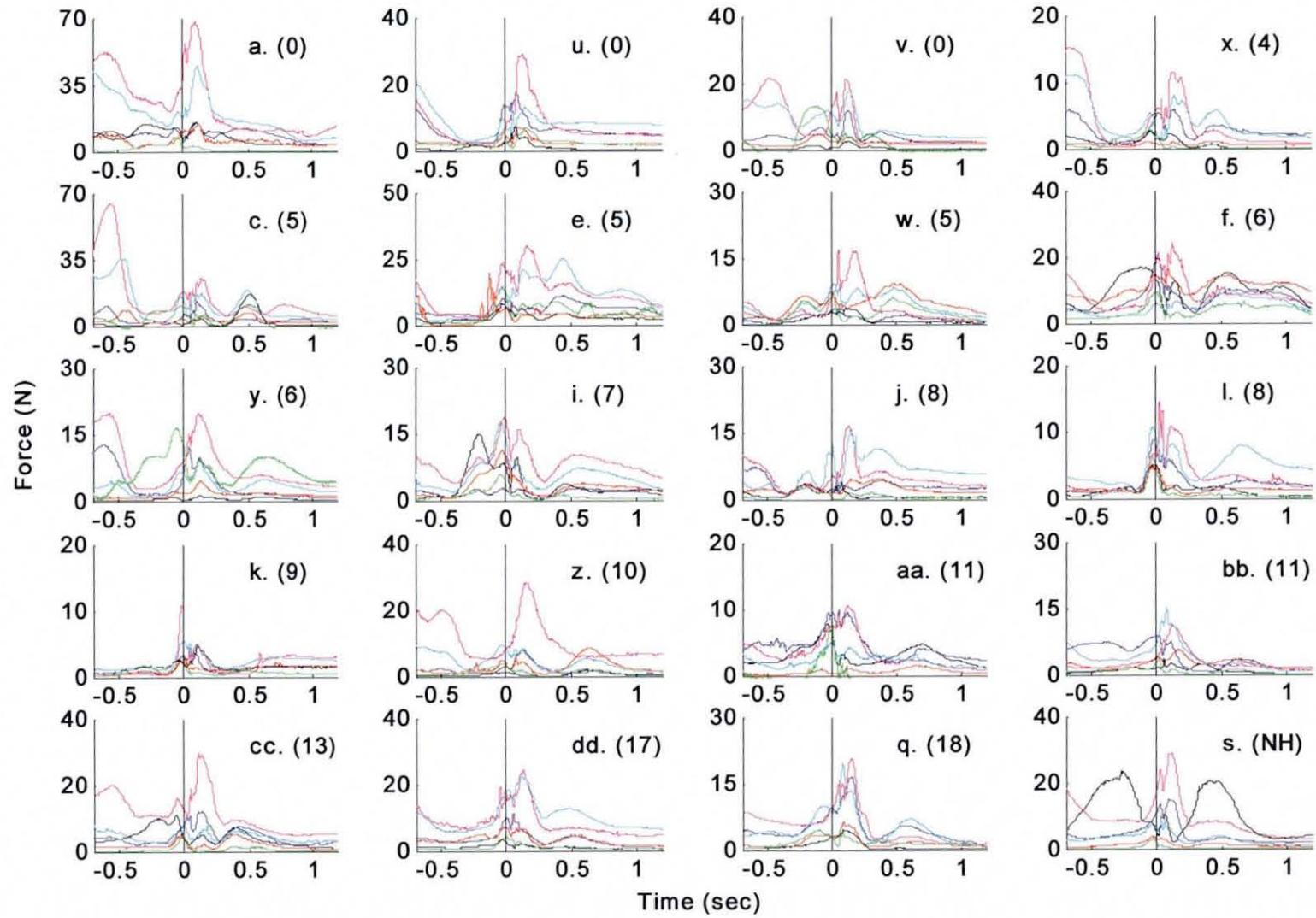


Figure 5.18 Right hand forces from Flexiforce tests; — thumb, — index, — middle, — ring, — little, — palm

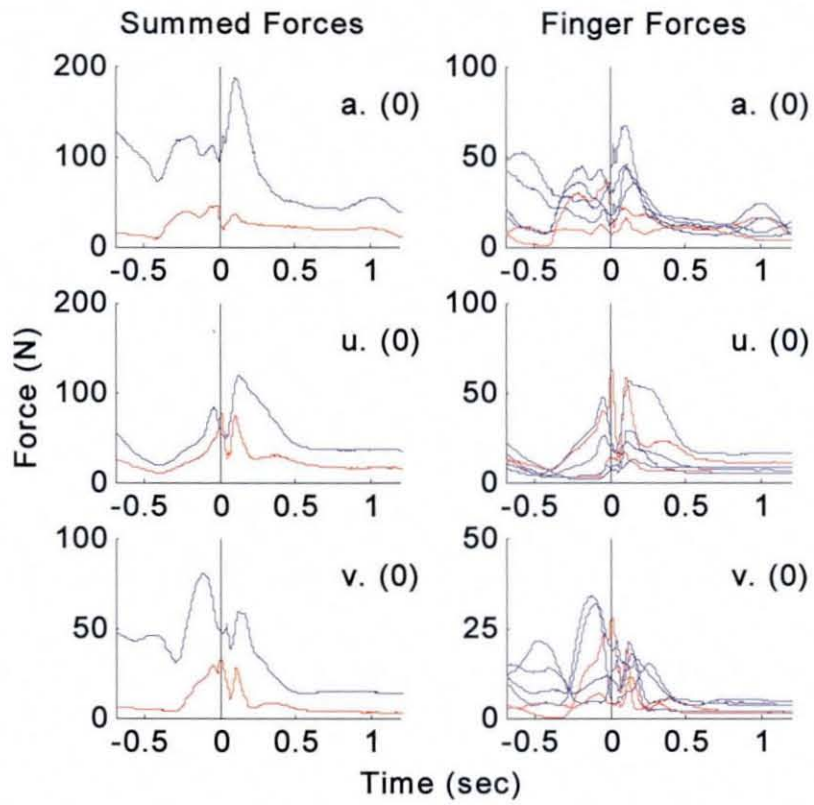


Figure 5.19 Grip force at specific locations indicated as key by golf instructors; — left thumb and right index finger, — left ring, left little, right middle and right ring fingers

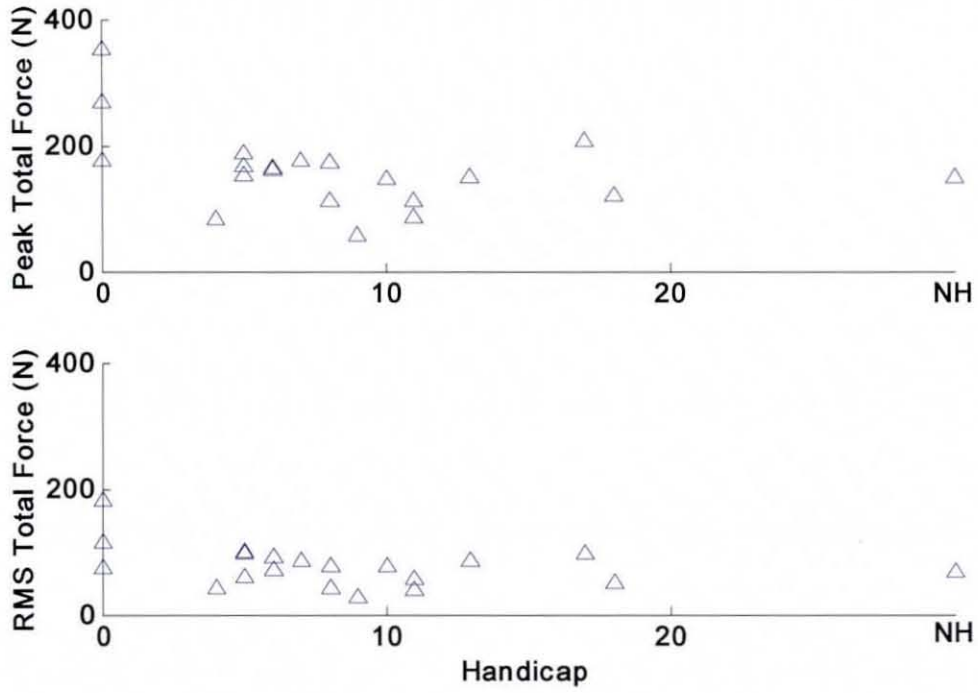


Figure 5.20 Peak and RMS total mean grip force versus handicap for Flexiforce sensor on grip* tests

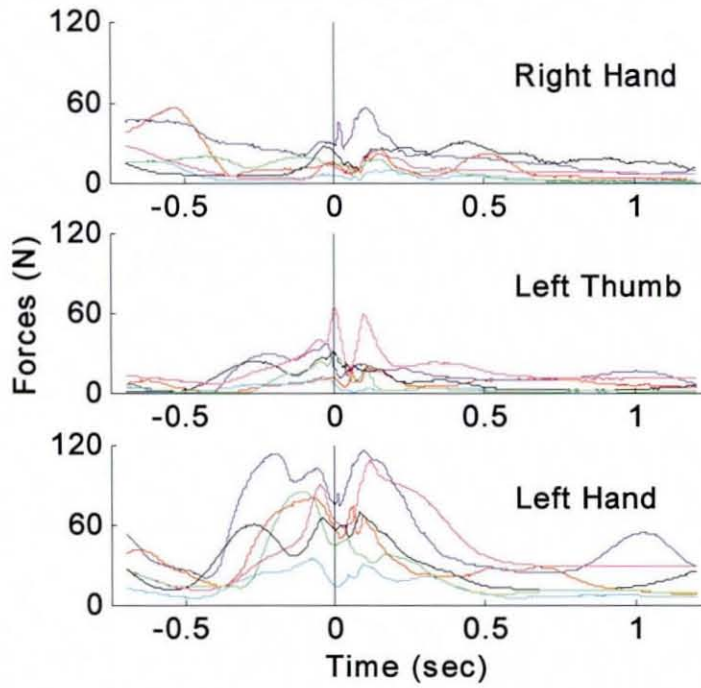


Figure 5.21 Grip force from Flexiforce on gloves test in regions considered by Budney and Bellow, six category 1 golfers shown

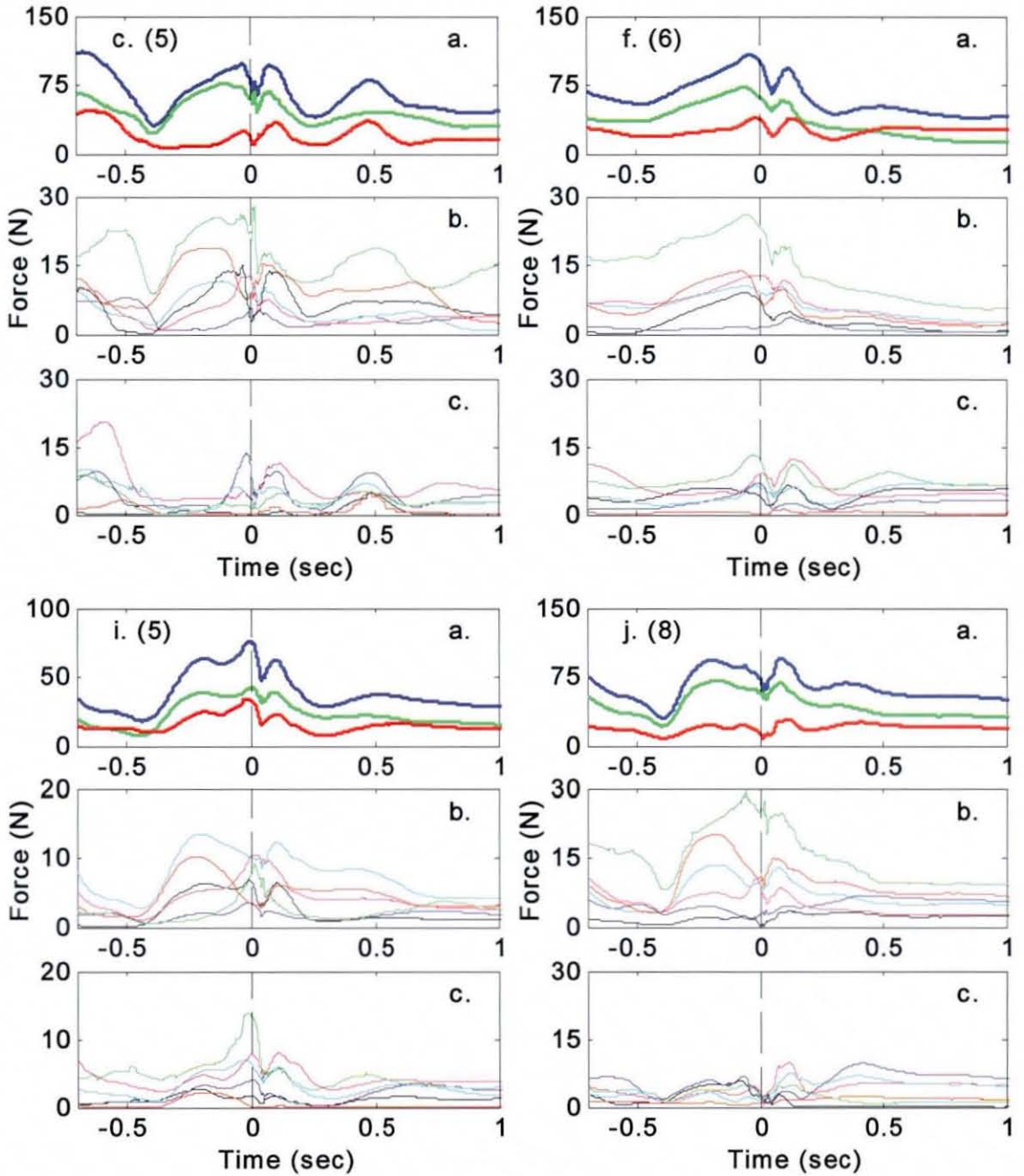


Figure 5.22a QTC grip force results from 4 golfers, (a.) player handicap shown in parentheses and — total force, — left hand force, and — right hand force, (b.) and (c.) individual finger and palm forces for the left and right hands, respectively, showing — thumb, — index finger, — middle finger, — ring finger, — little finger, — palm, and --- impact time; note: force magnitude on axes varies by golfer

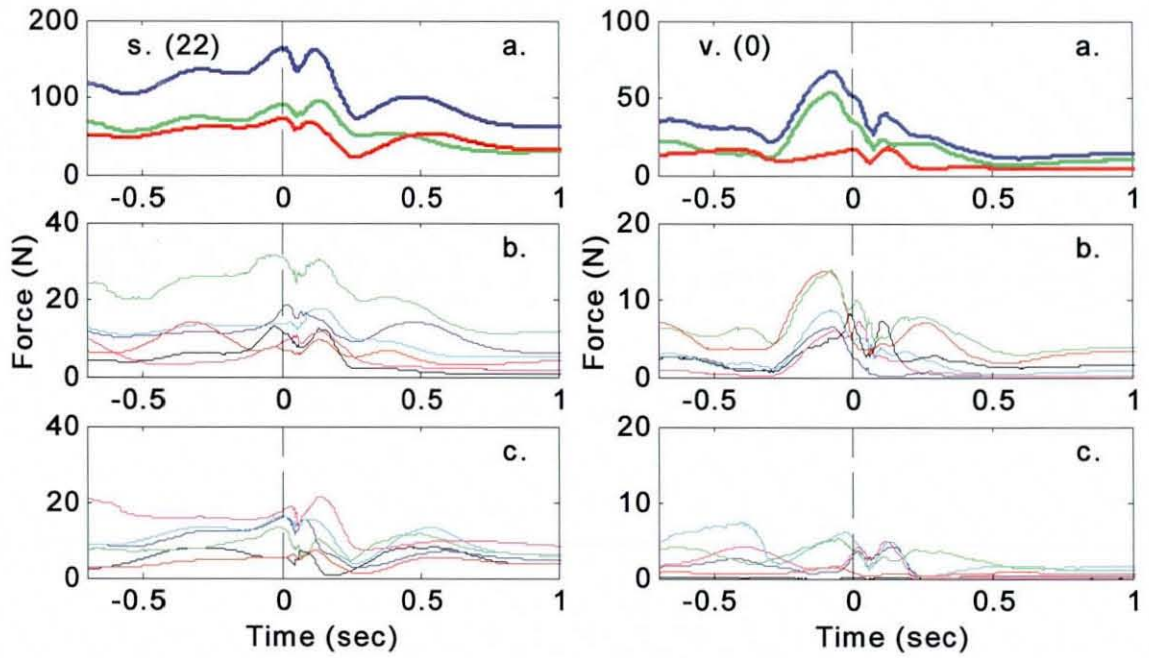


Figure 5.22b QTC grip force results from 2 golfers, (a.) player handicap shown in parentheses and — total force, — left hand force, and — right hand force, (b.) and (c.) individual finger and palm forces for the left and right hands, respectively, showing — thumb, — index finger, — middle finger, — ring finger, — little finger, — palm, and --- impact time; note: force magnitude on axes varies by golfer

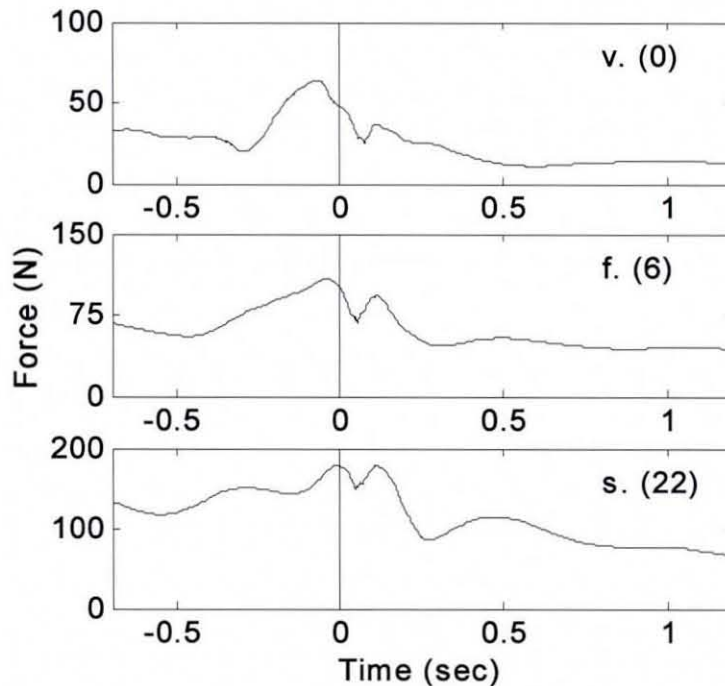


Figure 5.23 Mean total grip force curves for three golfers with highest cross correlation values from QTC grip force test

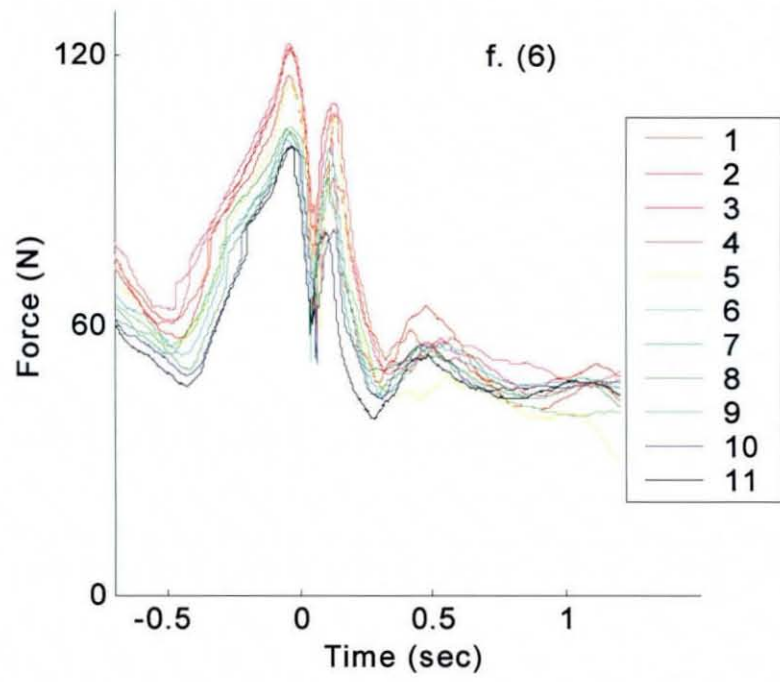


Figure 5.24 Total grip force traces from eleven consecutive shots taken by player f measured by QTC sensors on gloves; note decrease in force as the test proceeds

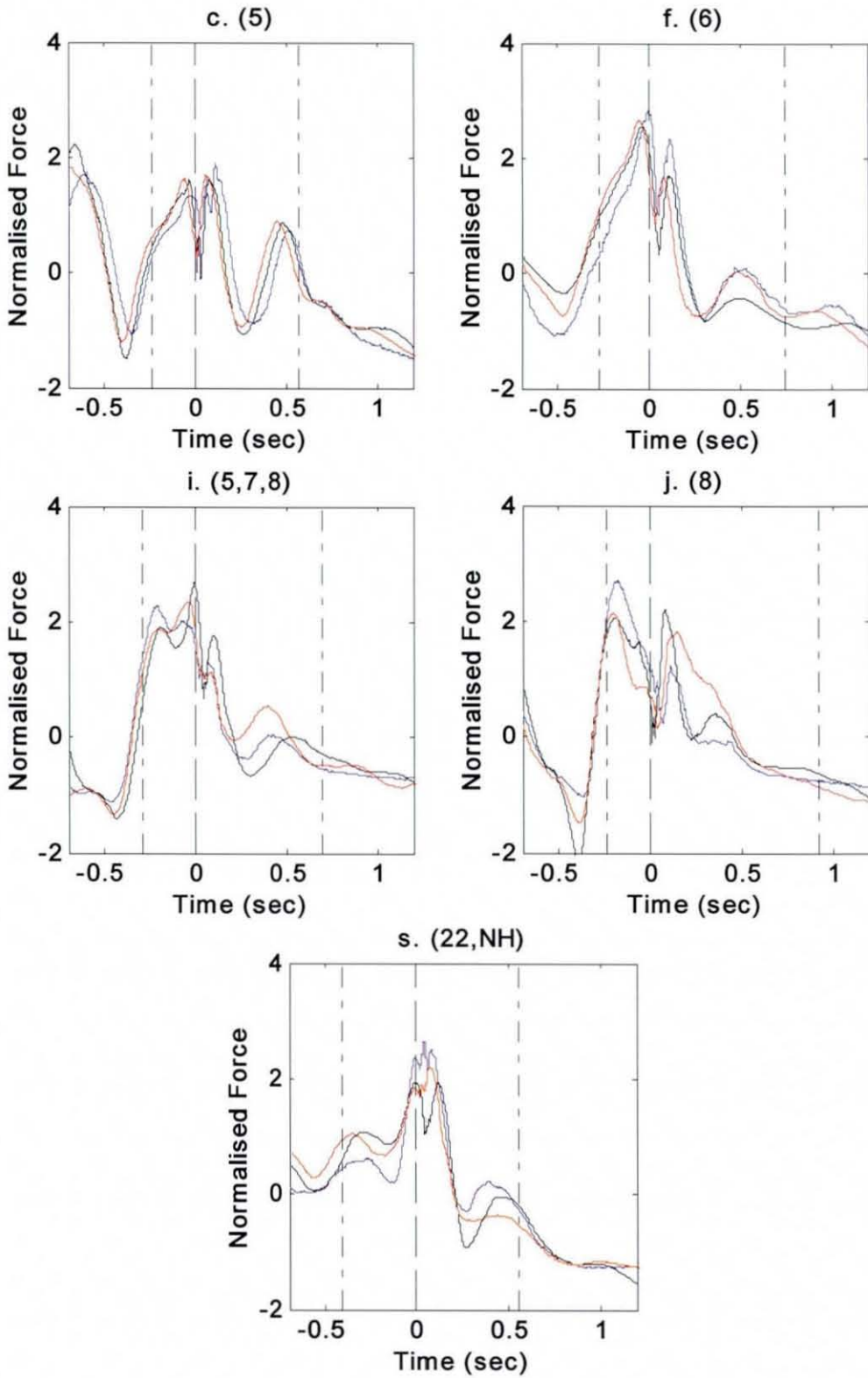


Figure 5.25 Normalised mean total force traces from — 9811, — Flexiforce and — QTC player tests; -- start of downswing and end of follow-through, respectively, - - impact, and handicap is labelled in parentheses

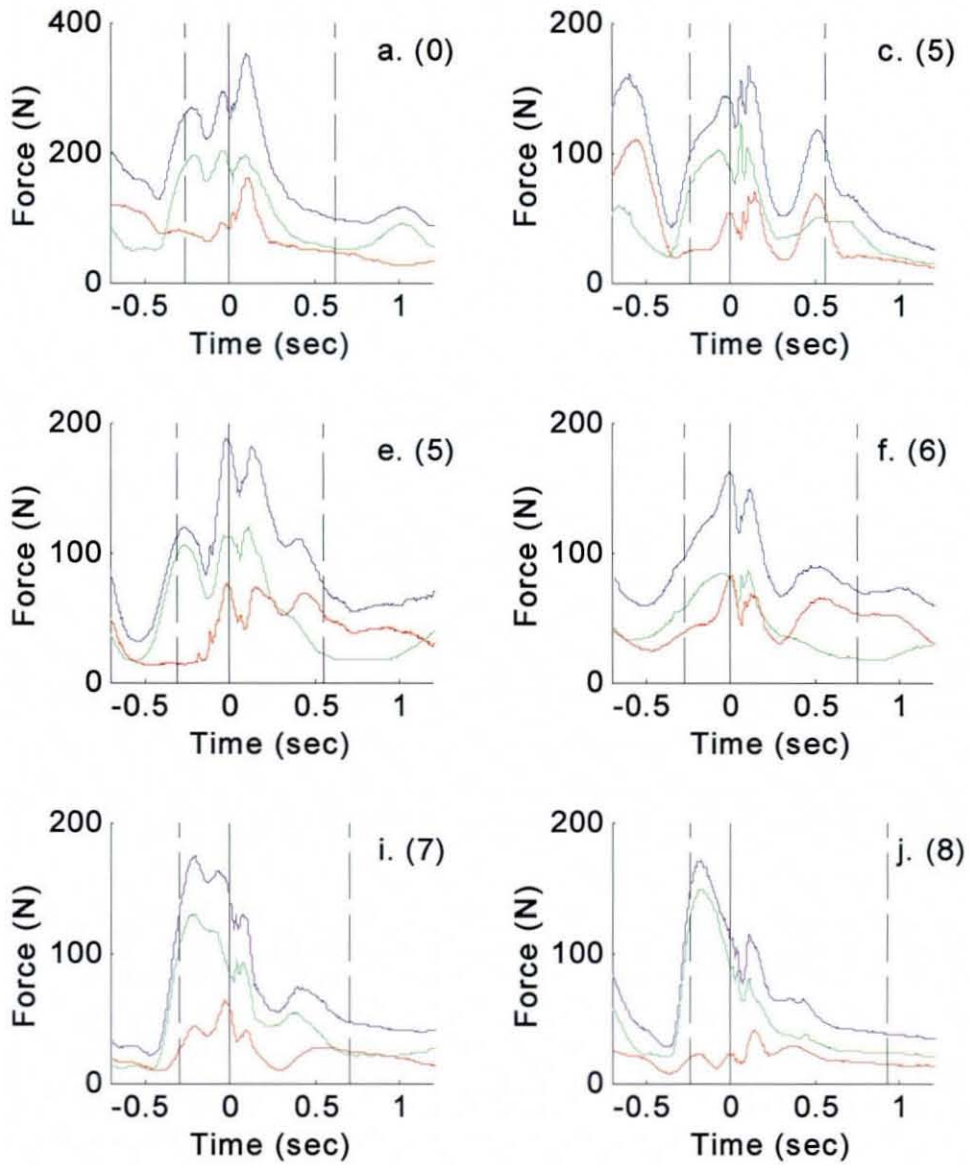


Figure 5.26a Each individual plot shows output from 31 Flexiforce sensors on gloves from one golfer (handicap in parentheses); — total force, — left hand force, — right hand force, — impact, --- start of downswing (before impact) and end of follow-through (after impact)

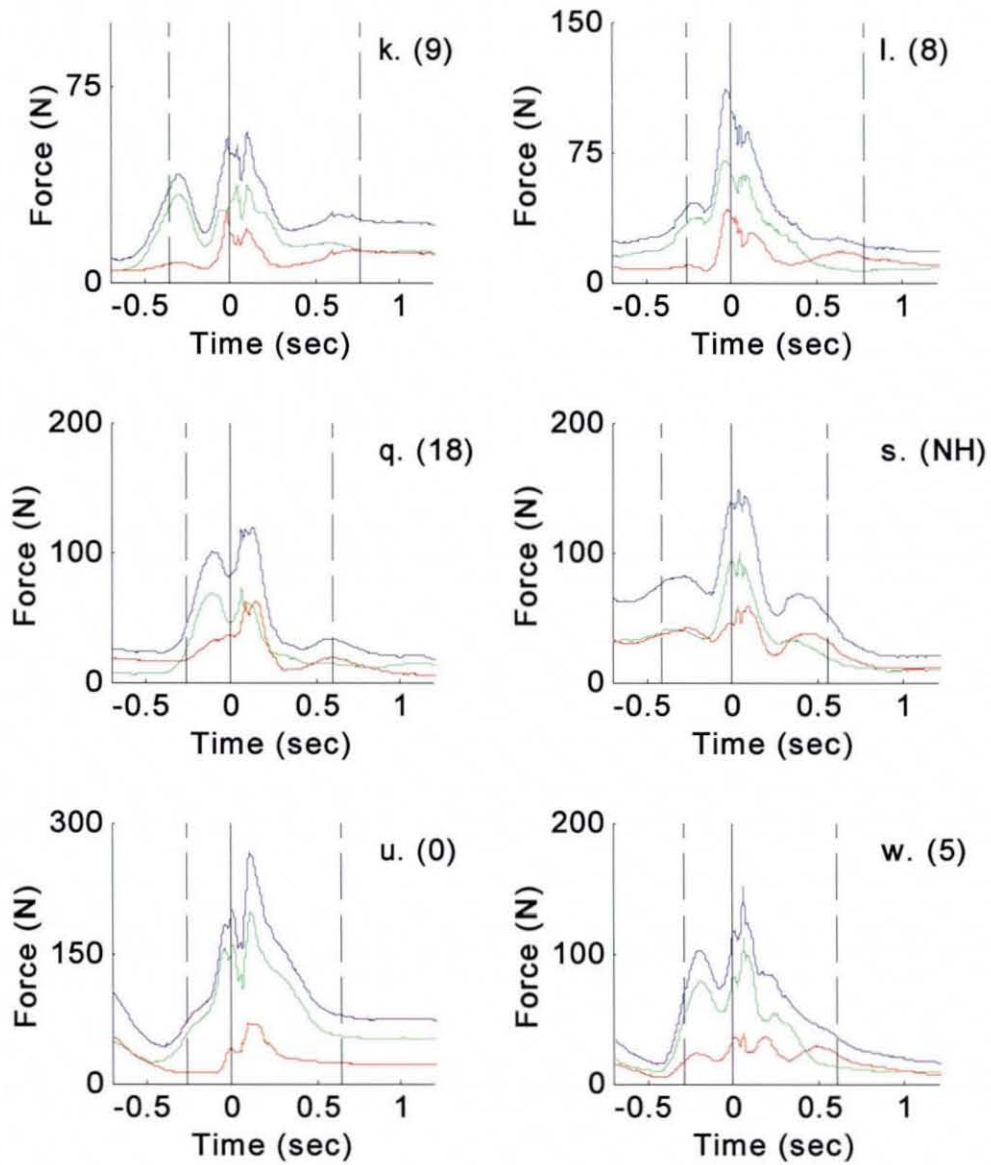


Figure 5.26b Each individual plot shows output from 31 Flexiforce sensors on gloves from one golfer (handicap in parentheses); — total force, — left hand force, — right hand force, — impact, --- start of downswing (before impact) and end of follow-through (after impact)

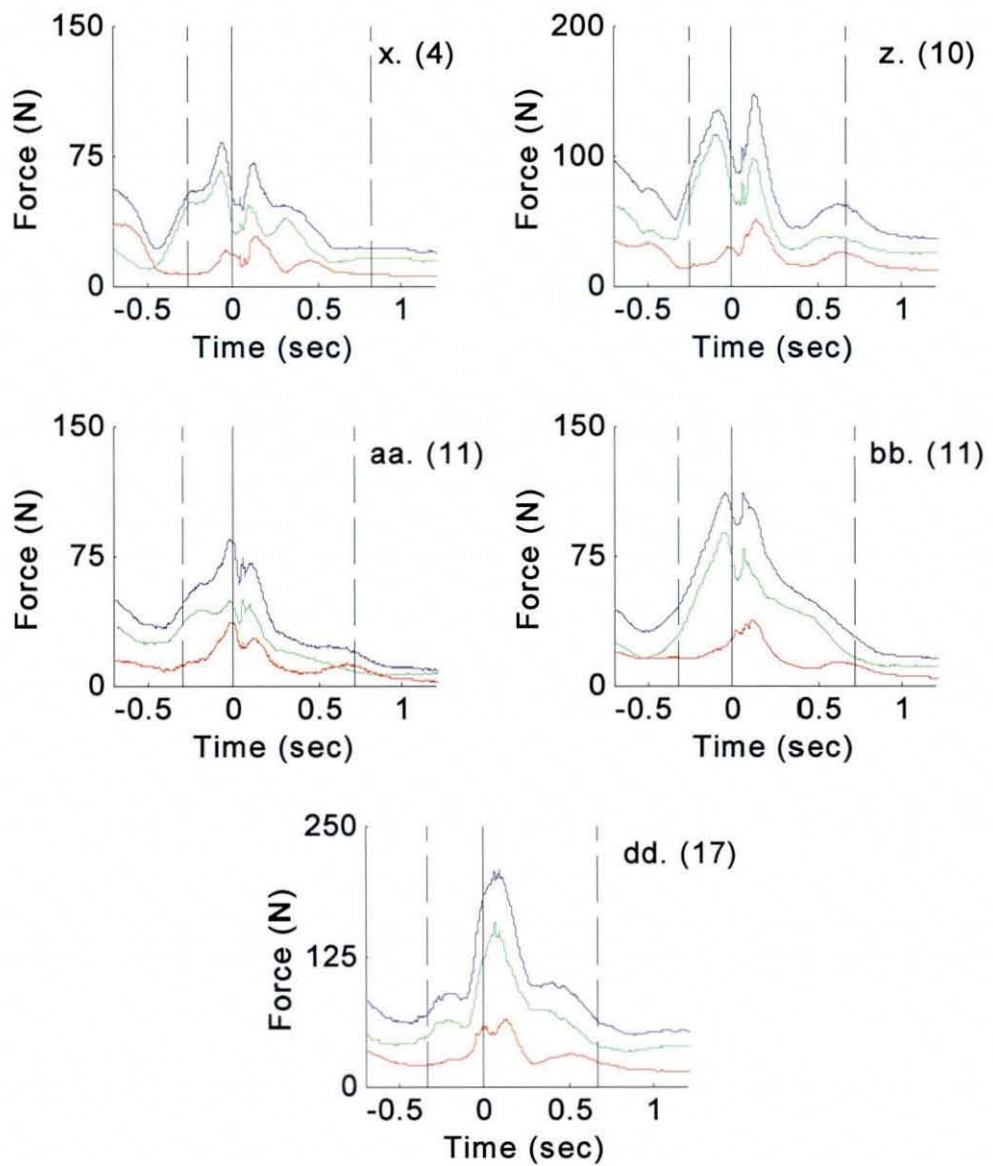


Figure 5.26c Each individual plot shows output from 31 Flexiforce sensors on gloves from one golfer (handicap in parentheses); — total force, — left hand force, — right hand force, — impact, --- start of downswing (before impact) and end of follow-through (after impact)

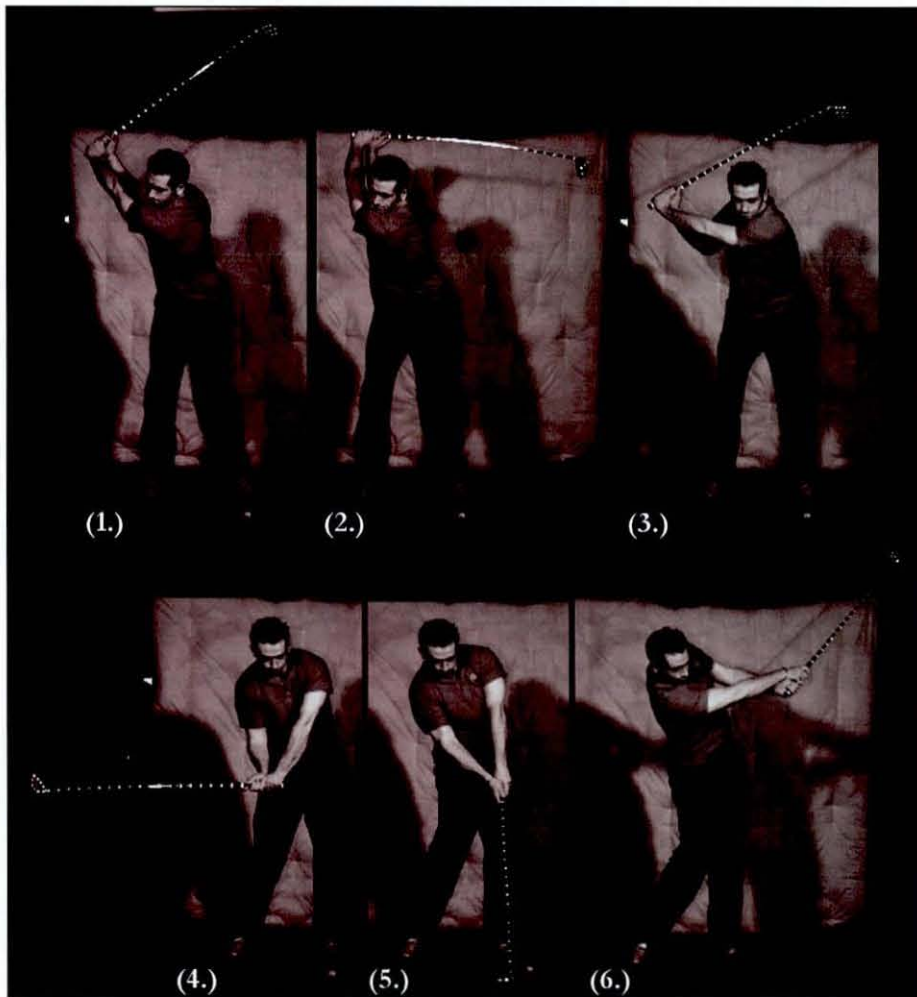
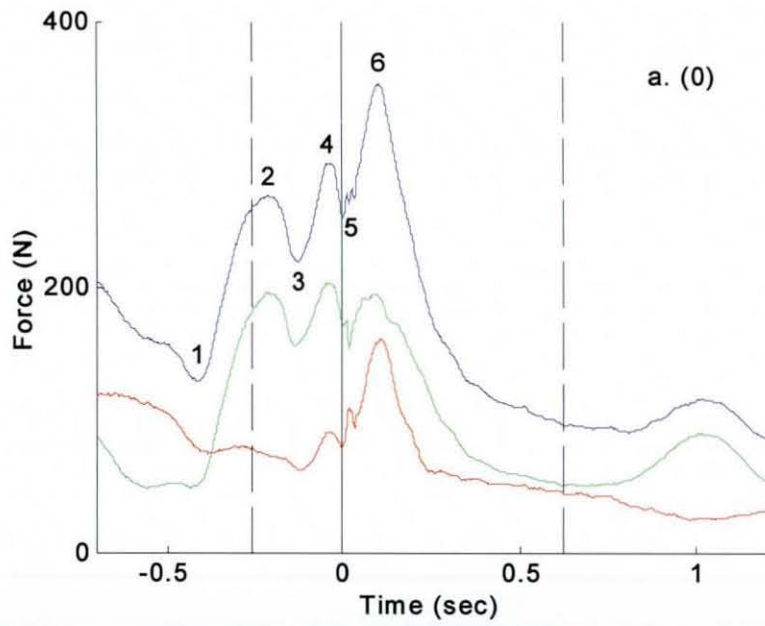
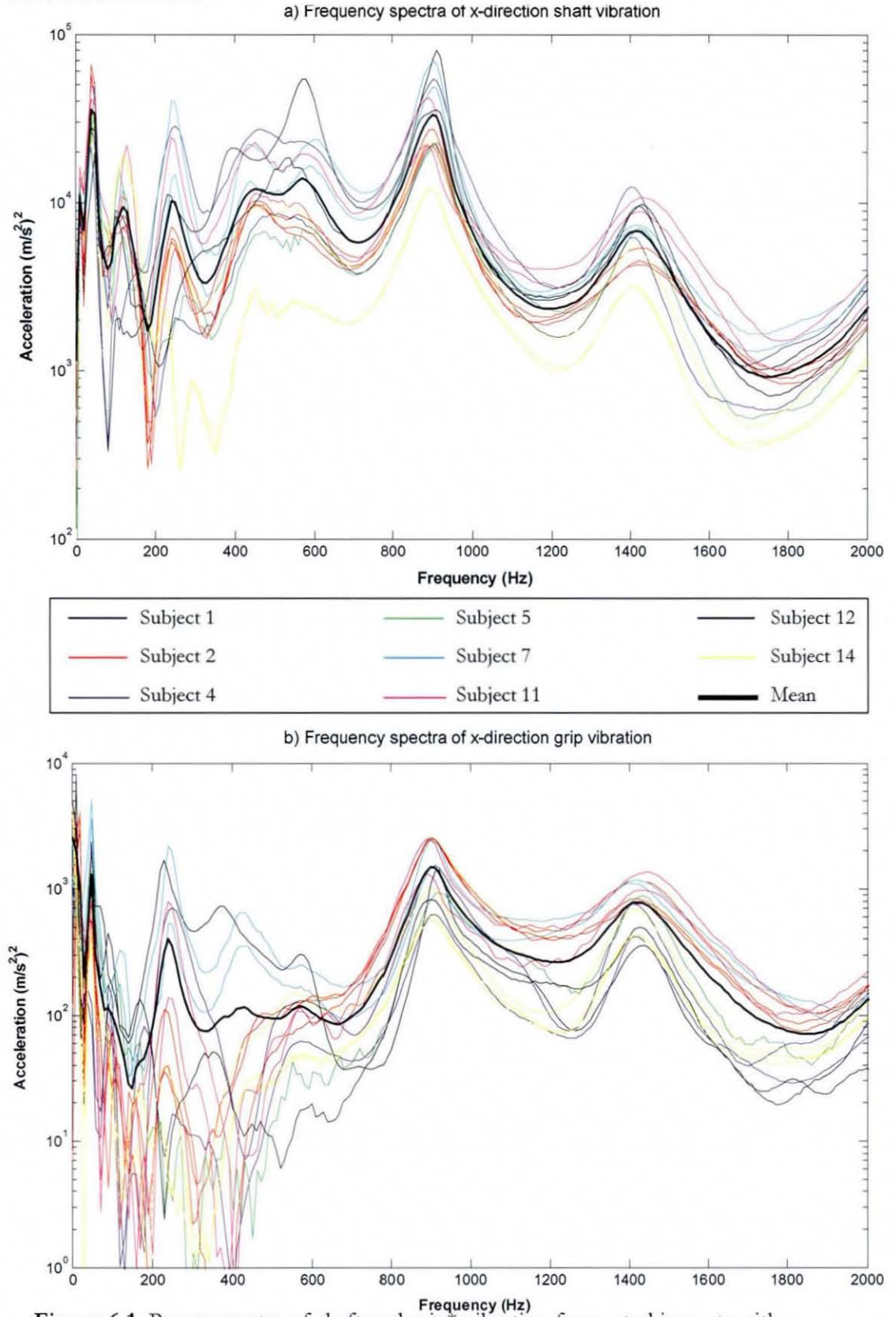


Figure 5.27 Six key points on the total grip force curve for golfer a with corresponding still images; — total force, — left hand force, — right hand force, — impact, --- start of downswing and end of follow-through, respectively



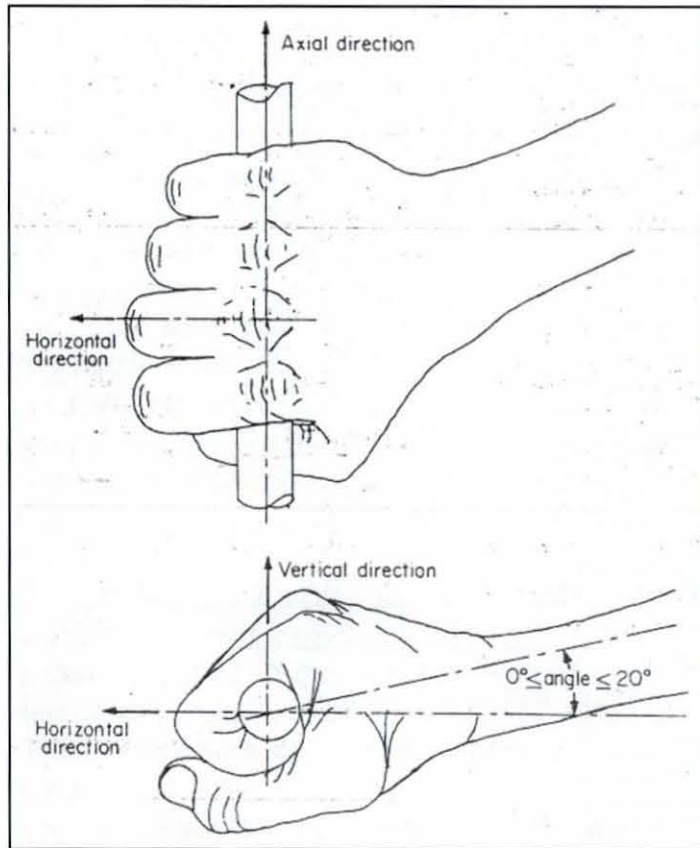


Figure 6.2 Directions of vibration (Reynolds and Keith 1977)

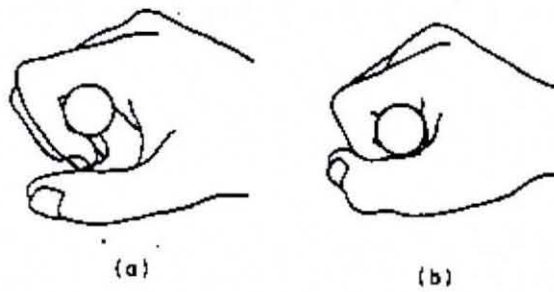


Figure 6.3 Grip types; (a.) finger grip and (b.) palm grip (Reynolds and Keith 1977)

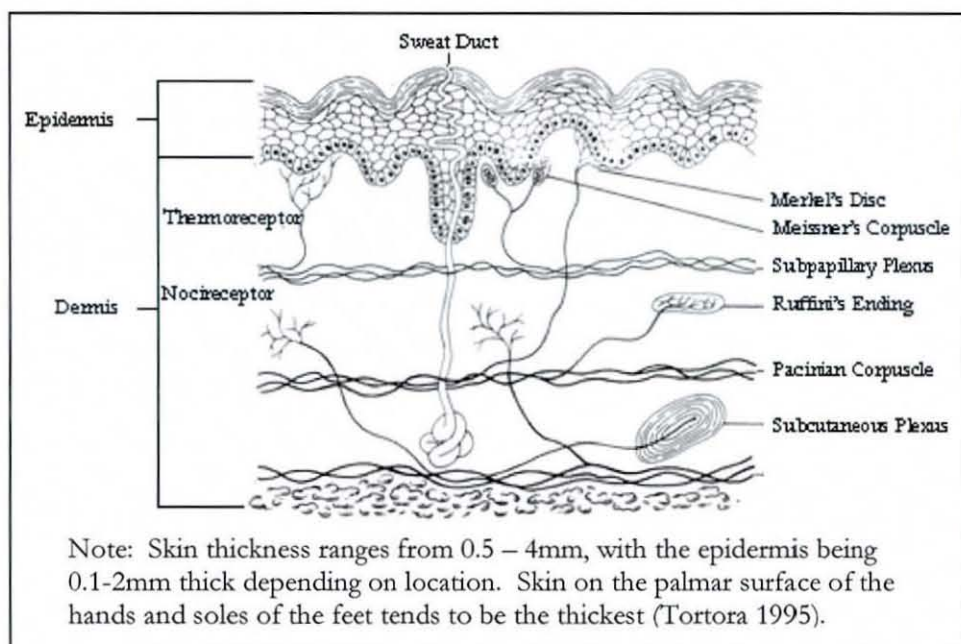


Figure 6.4 Cross-section of the skin (Griffin 1990)

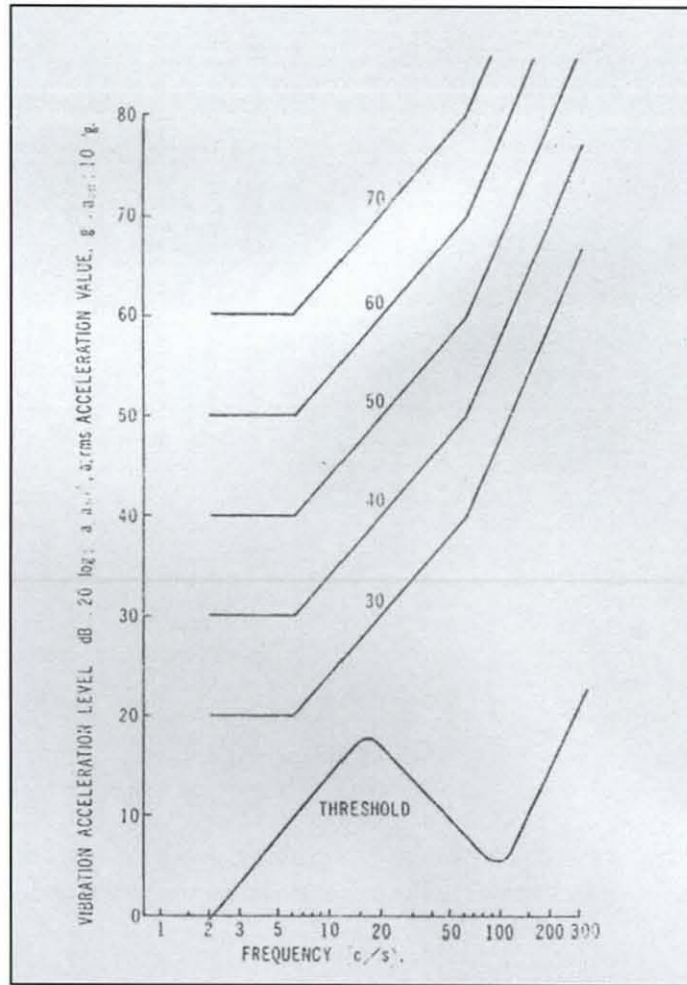


Figure 6.5 Equal sensation and vibration perception threshold contours; ordinate indicated vibration acceleration levels (dB) and abscissa frequencies (c/s) (Miwa 1967)

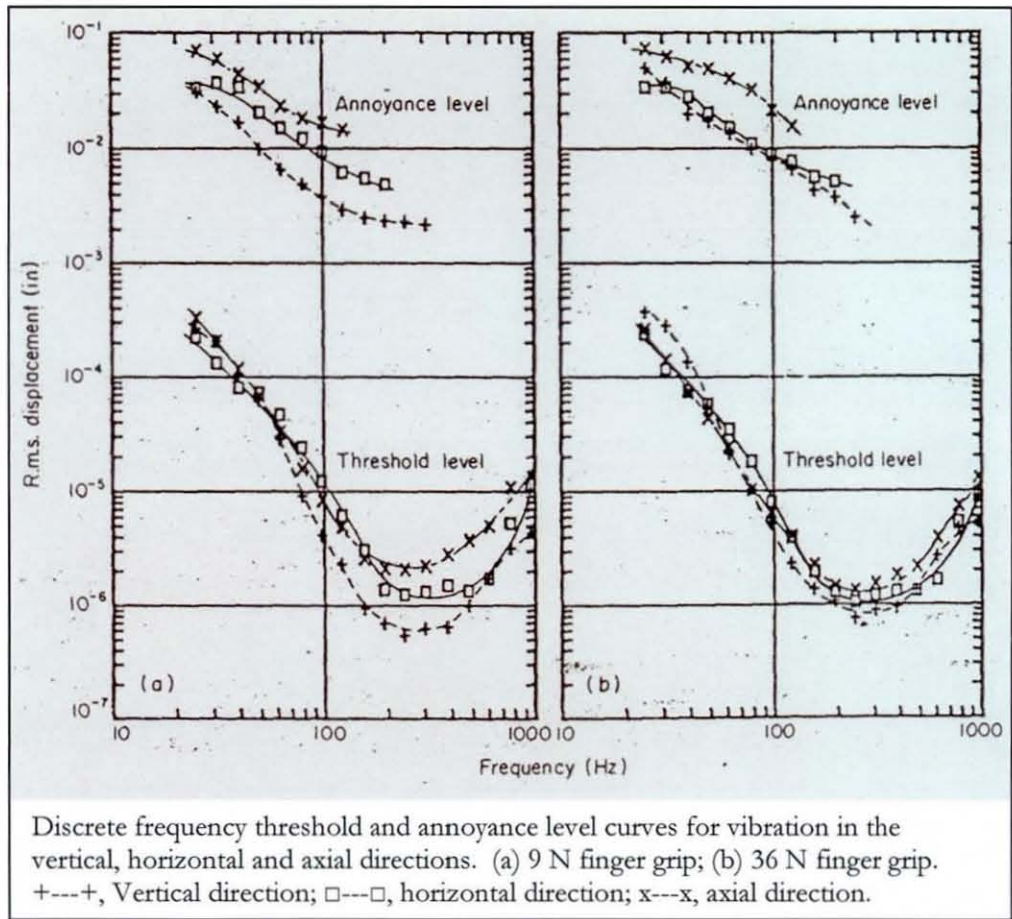


Figure 6.6 Vibration threshold and annoyance curves; finger grip (Reynolds et al. 1977)

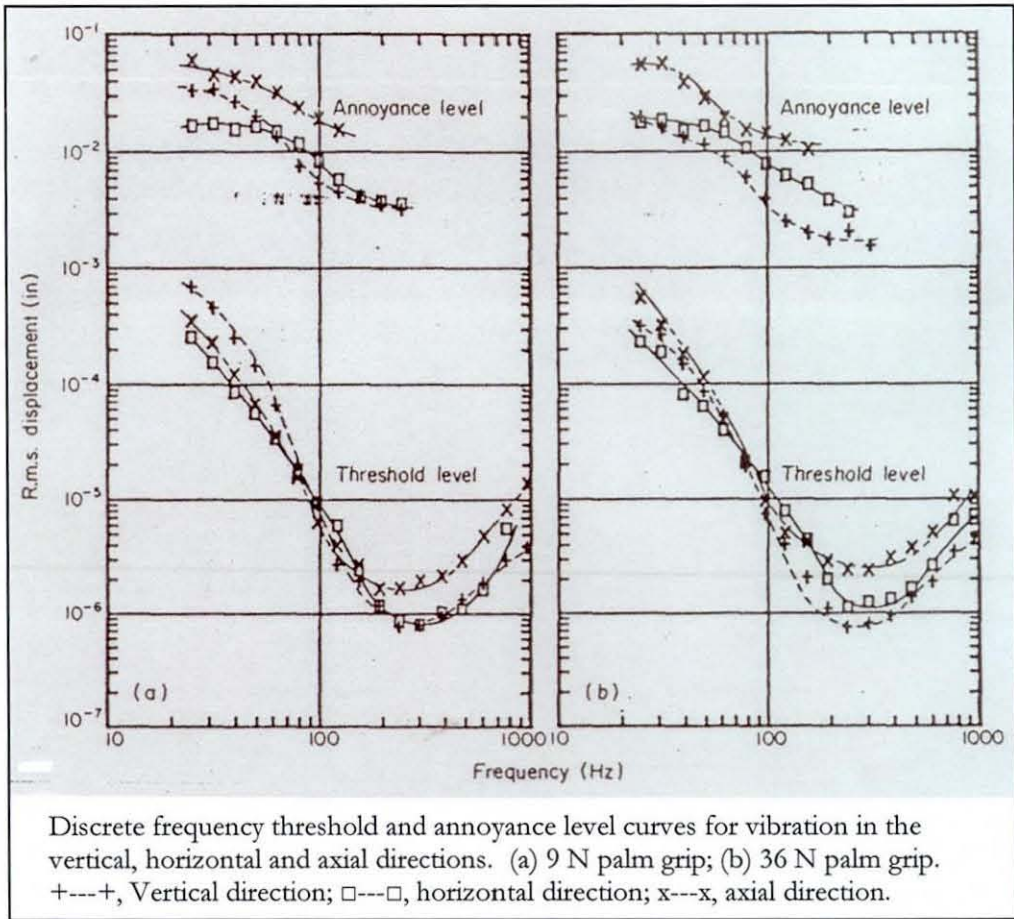


Figure 6.7 Vibration threshold and annoyance curves, palm grip (Reynolds et al. 1977)

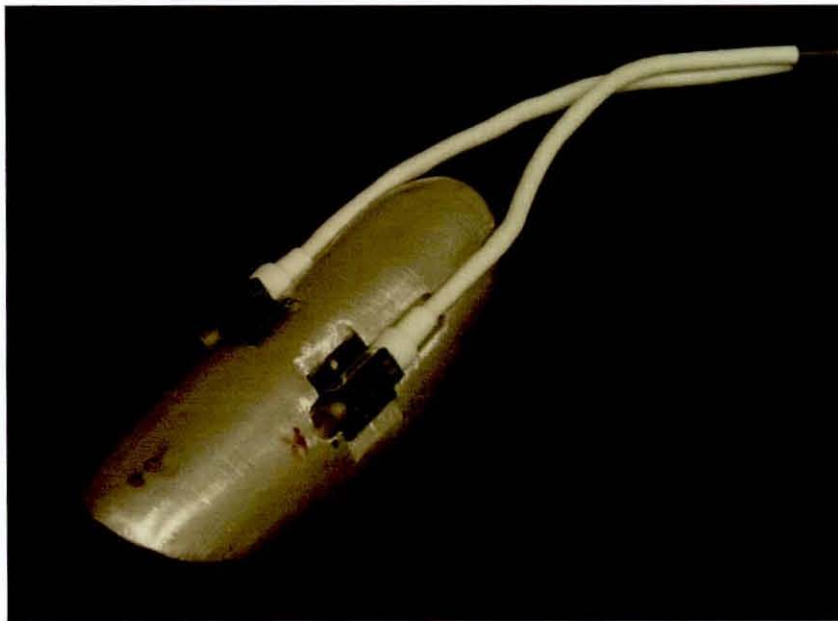


Figure 6.8 Grip* adapter used by Roberts et al. (2002; 2005; 2006) to measure acceleration in two directions

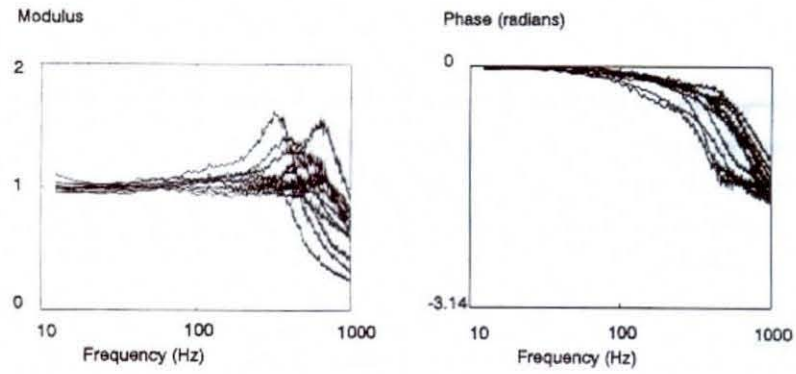


Figure 6.9 Transfer functions for 12 subjects; 10 mm diameter contactor under centre of fingernail, 2 N force, 0.5 g accelerometer, finger straight (Mann 1994)

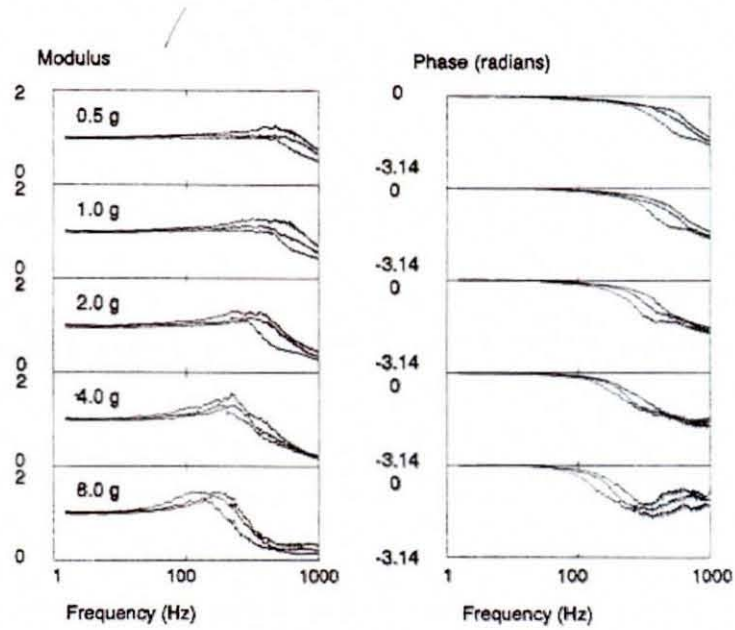


Figure 6.10 Effect on transfer functions of mass added to the fingernail; median and interquartile range (Mann 1994)

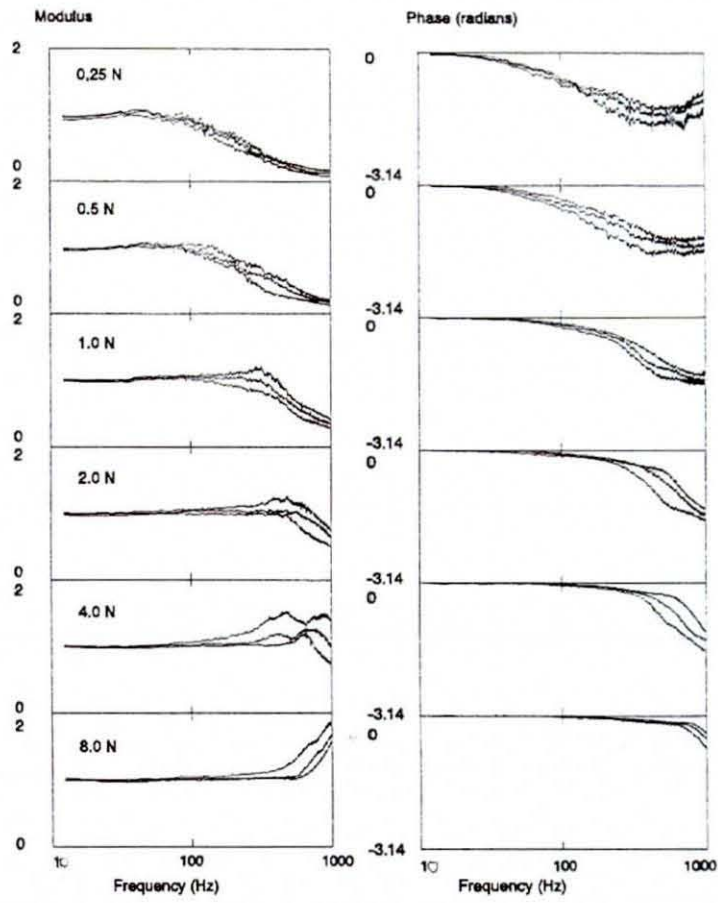


Figure 6.11 Effect of variation of feed force on transfer functions; median and interquartile range (Mann 1994)

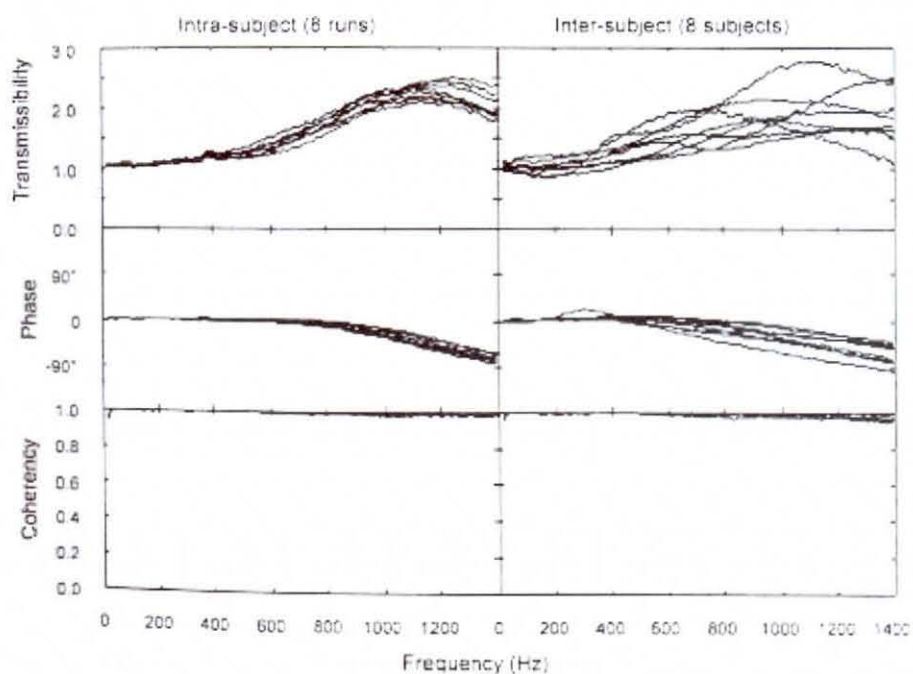


Figure 6.12 Transmissibilities between the handle and the fingernail for subjects pulling at the handle with a force of 30 N (Paddan 1997)

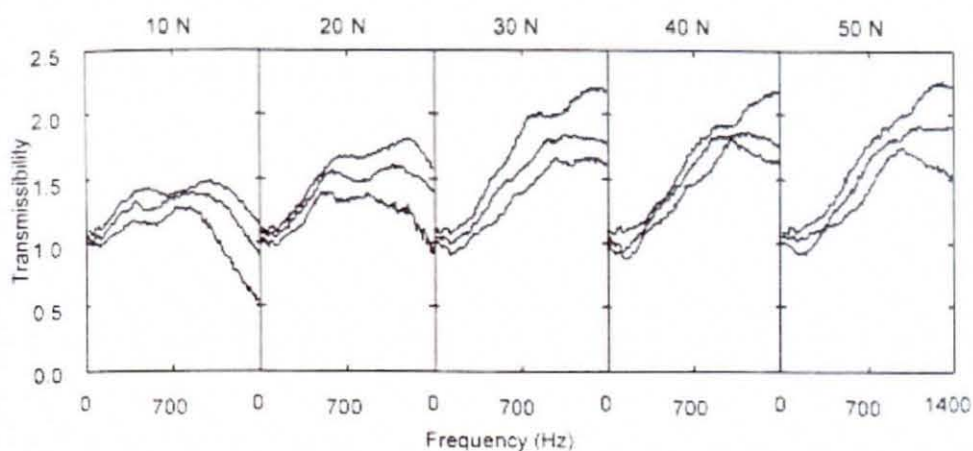


Figure 6.13 Median and interquartile range of transmissibilities between the handle and the fingernail for the subjects pulling at the handle with five different pull forces (Paddan 1997)

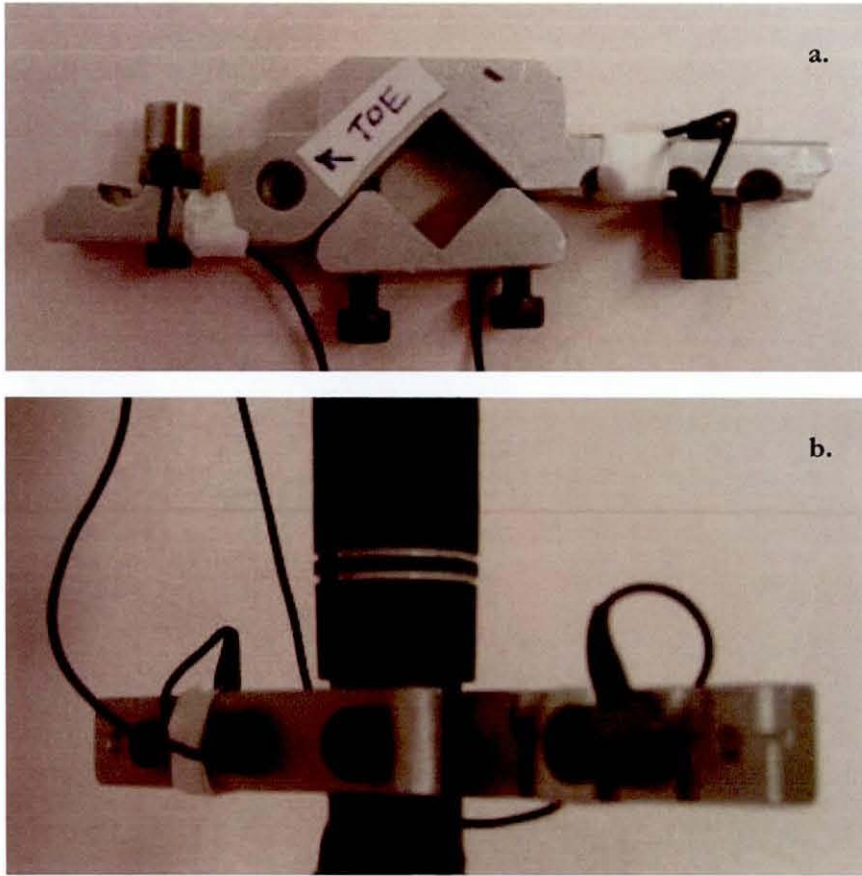


Figure 6.14 (a.) Shaft vibration adapter and (b.) adapter on club just below grip*

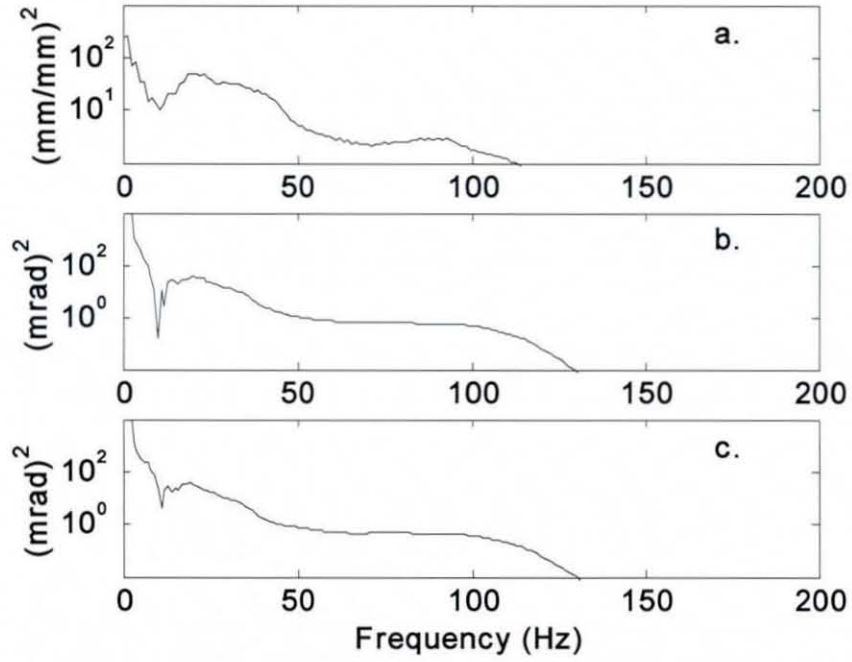


Figure 6.15 Power spectra of angular displacement as measured on the shaft below the grip* by (a.) strain gauges and accelerometers at (b.) position 2 and (c.) position 4 on the adapter

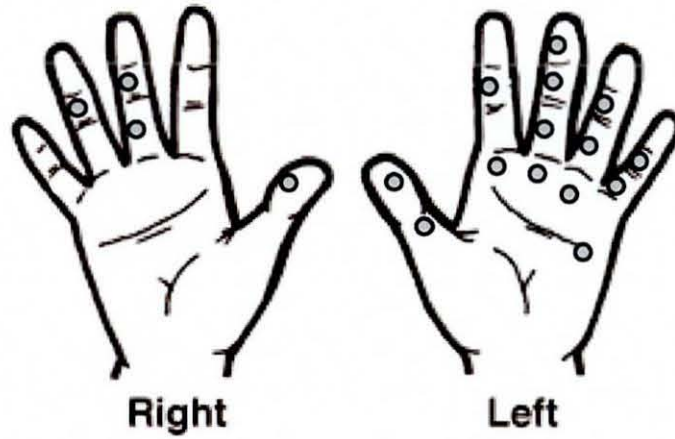


Figure 7.1 Location for 18 Flexiforce sensors used in final set of player tests

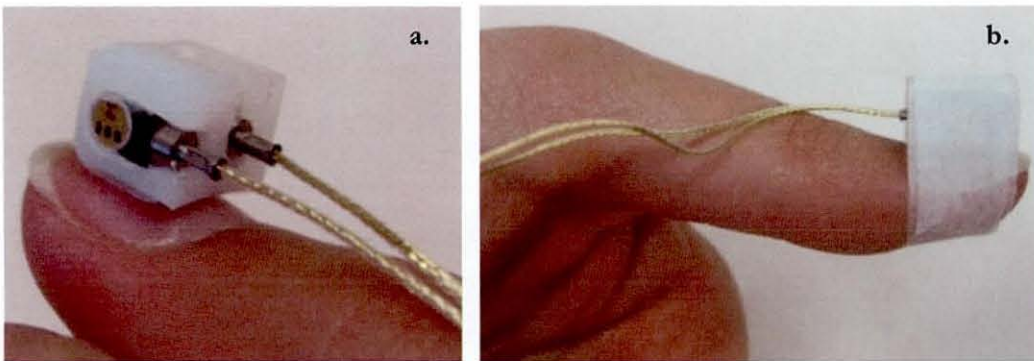


Figure 7.2 Thumbnail block adapter, (a.) on thumbnail and (b.) with Micropore tape

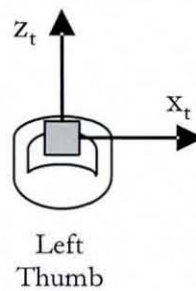


Figure 7.3 Diagram of thumbnail block adapter, showing the two directions of vibration measurement, x_t and z_t

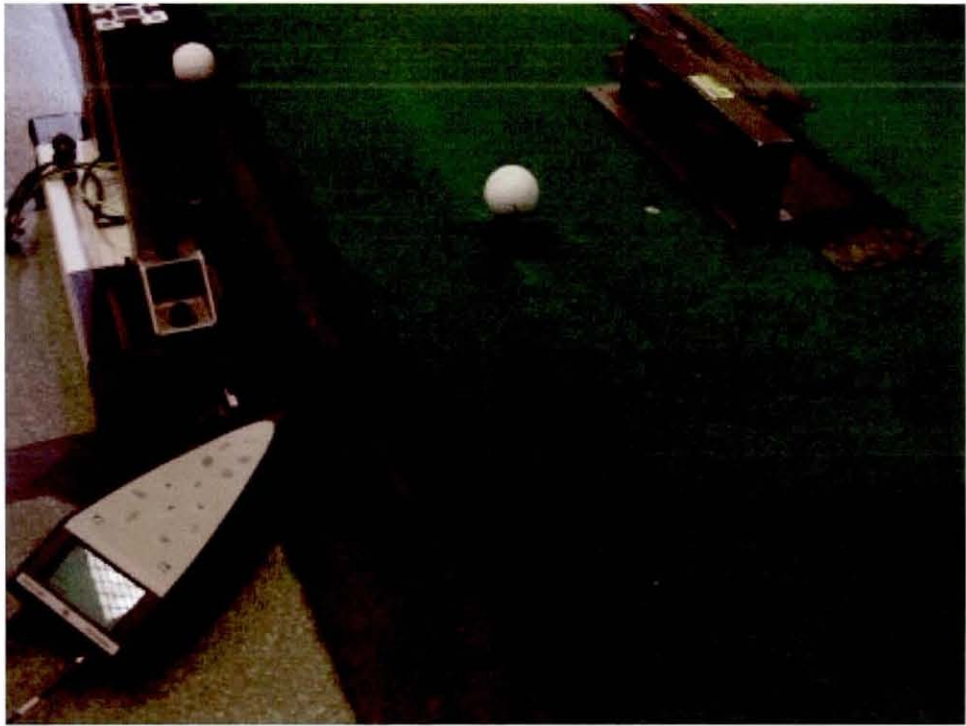


Figure 7.4 Laser light gates positioned just behind tee to capture clubhead speed at impact

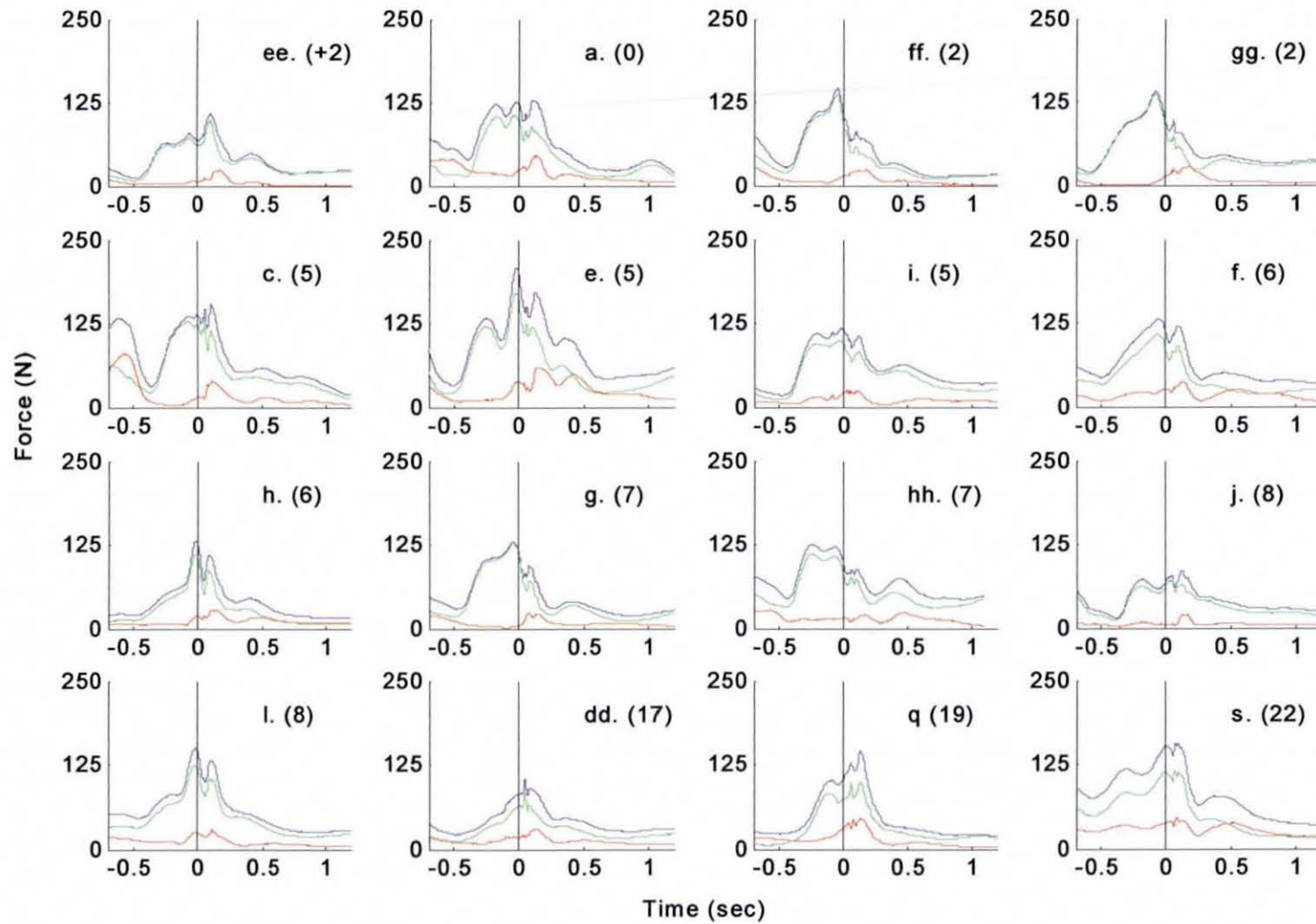


Figure 7.5 Mean total —, left hand — and right hand — grip forces for 16 golfers measured with 18 Flexiforce sensors; handicap in parentheses

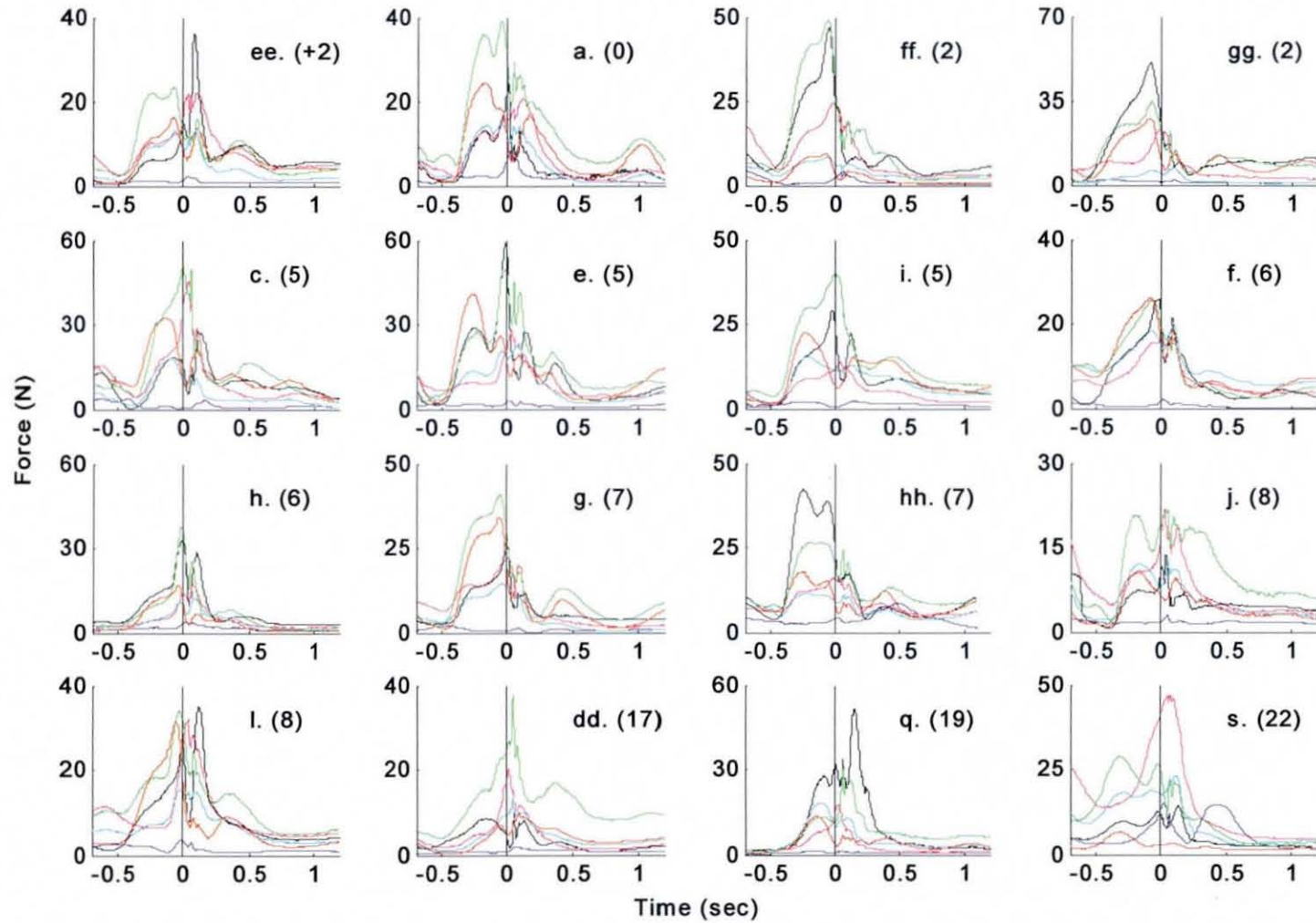


Figure 7.6 Left hand forces from final Flexiforce tests; — thumb, — index, — middle, — ring, — little, — palm

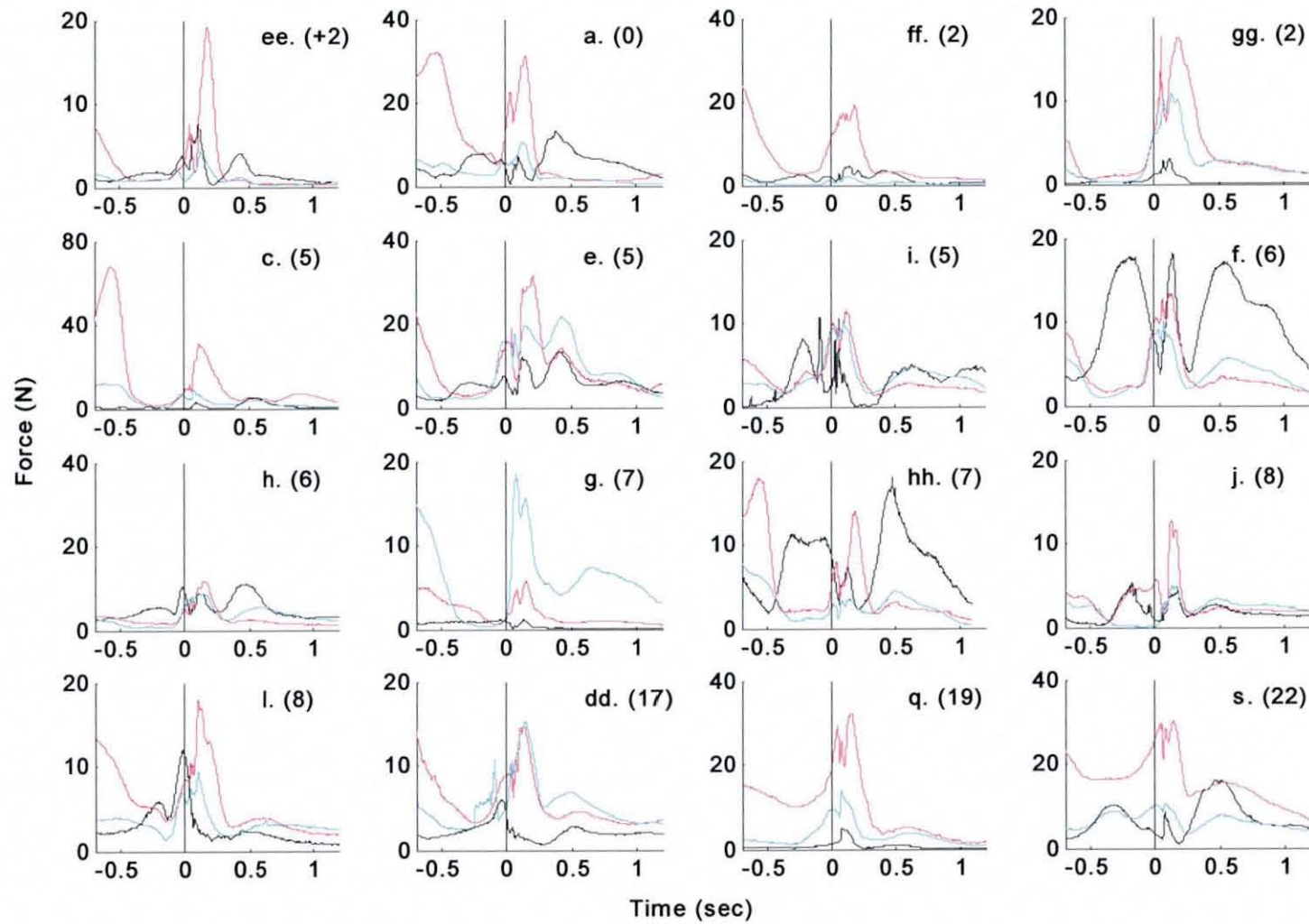


Figure 7.7 Right hand forces from final Flexiforce tests; — thumb, — middle, — ring

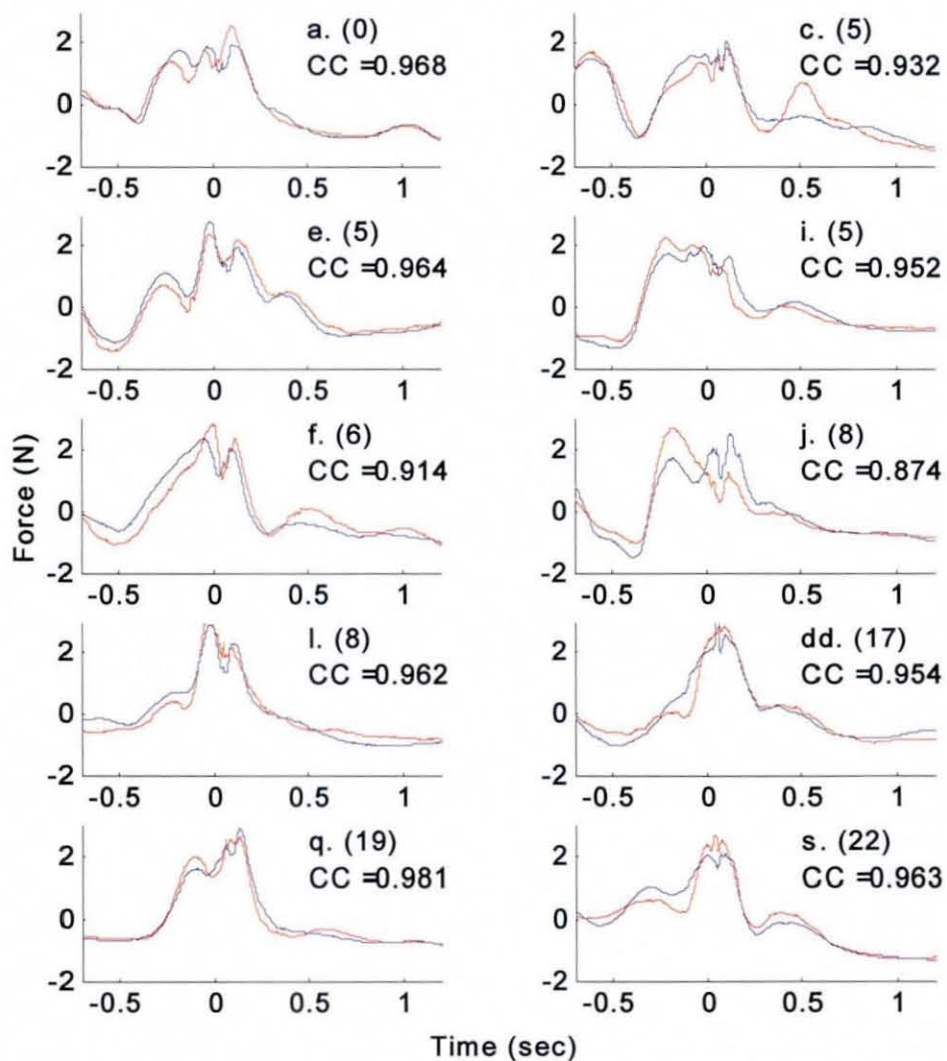


Figure 7.8 Normalised mean total grip force for golfers participating in both Flexiforce tests, (a.) — 31 sensors, (b.) — 18 sensors; handicap in parentheses and cross correlation value for the two curves is indicated

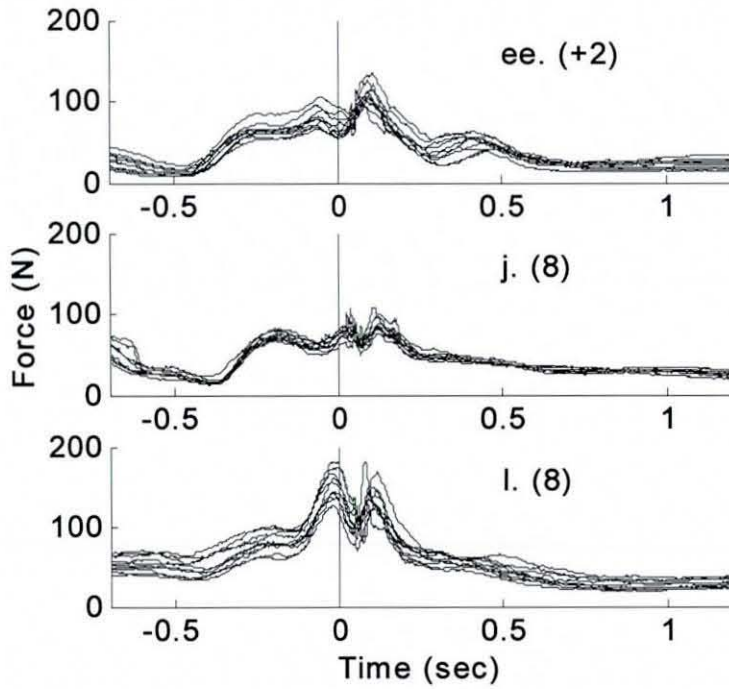


Figure 7.9 Ten total force traces for three golfers as measured by Flexiforce sensors in final test; golfer handicap in parentheses

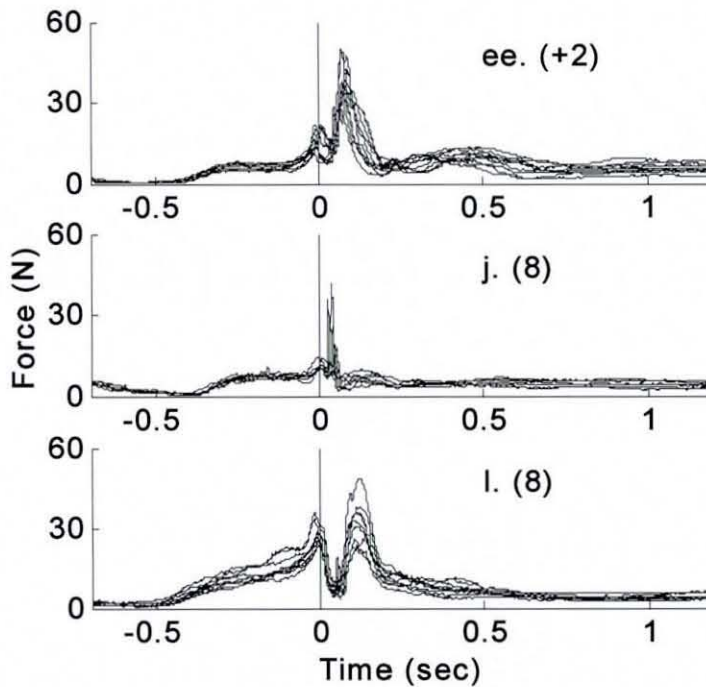


Figure 7.10 Ten left thumb force traces for three golfers as measured by Flexiforce sensors in final test; golfer handicap in parentheses

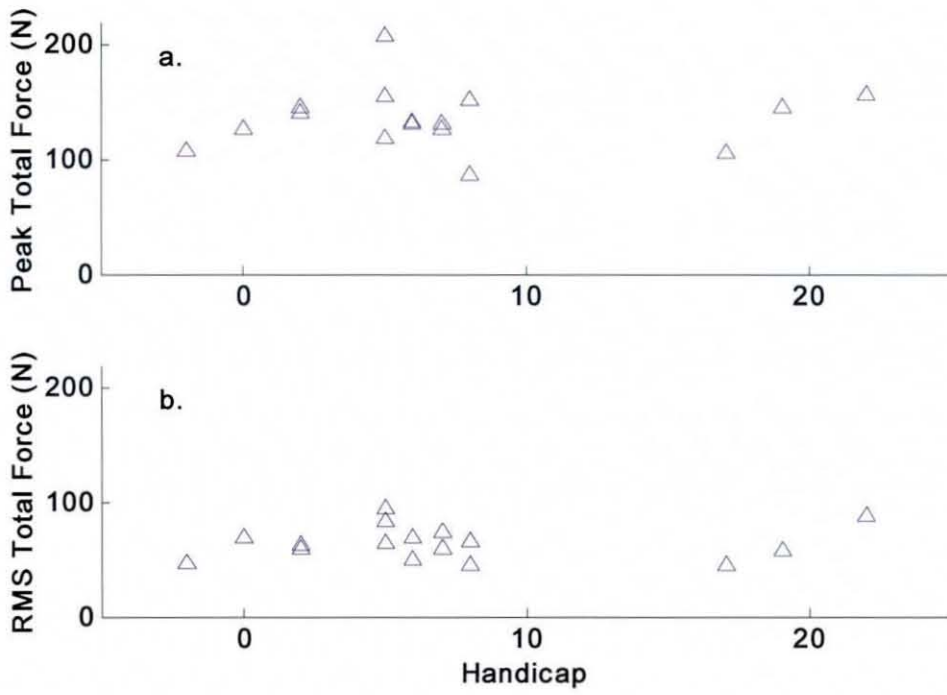


Figure 7.11 (a.) peak and (b.) RMS total mean grip force versus handicap for final Flexiforce sensor on glove tests

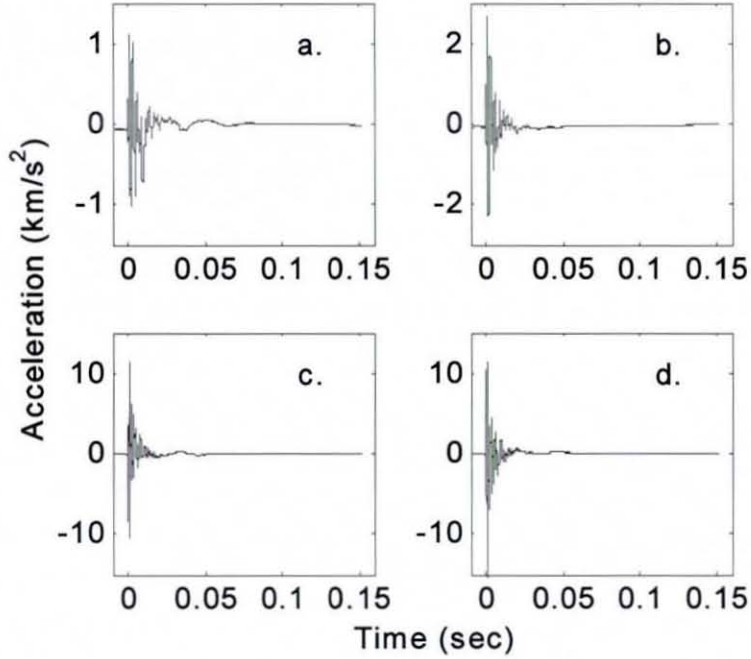


Figure 7.12 Example vibration measurements at both left thumb and shaft; (a.) thumb \ddot{x}_t , (b.) thumb \ddot{z}_t , (c.) shaft \ddot{a}_1 and (d.) shaft \ddot{a}_2

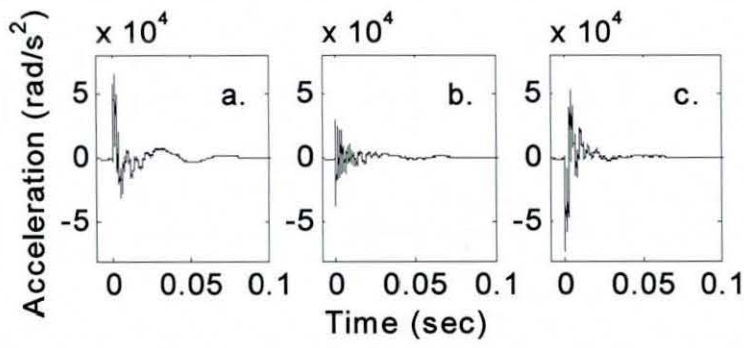


Figure 7.13 Typical torsional vibration measurements for (a.) toe, (b.) central and (c.) heel impacts

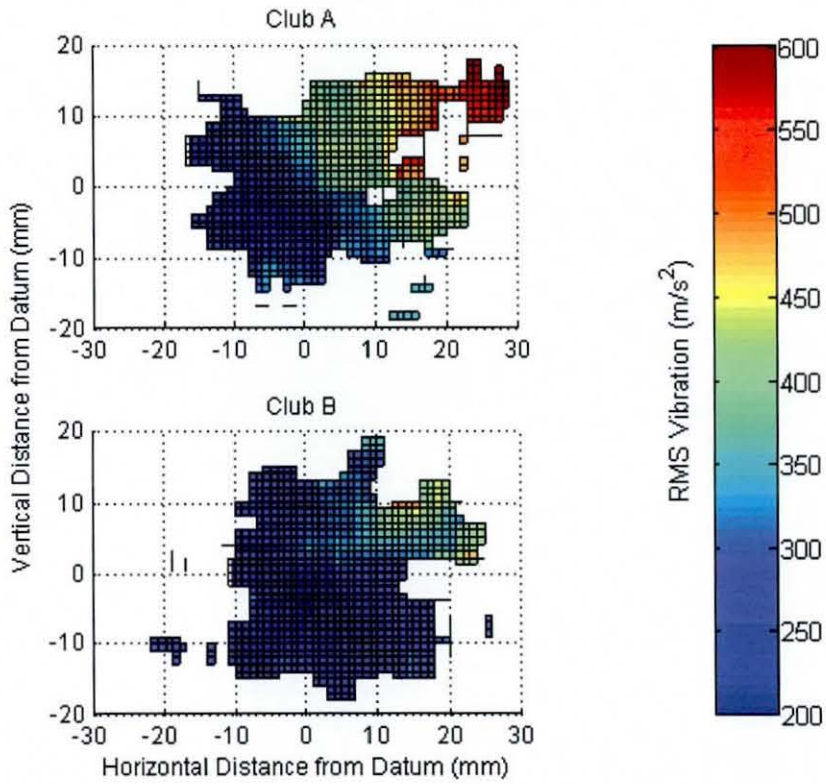


Figure 7.14 Total RMS linear vibration at the thumb as a function of impact location

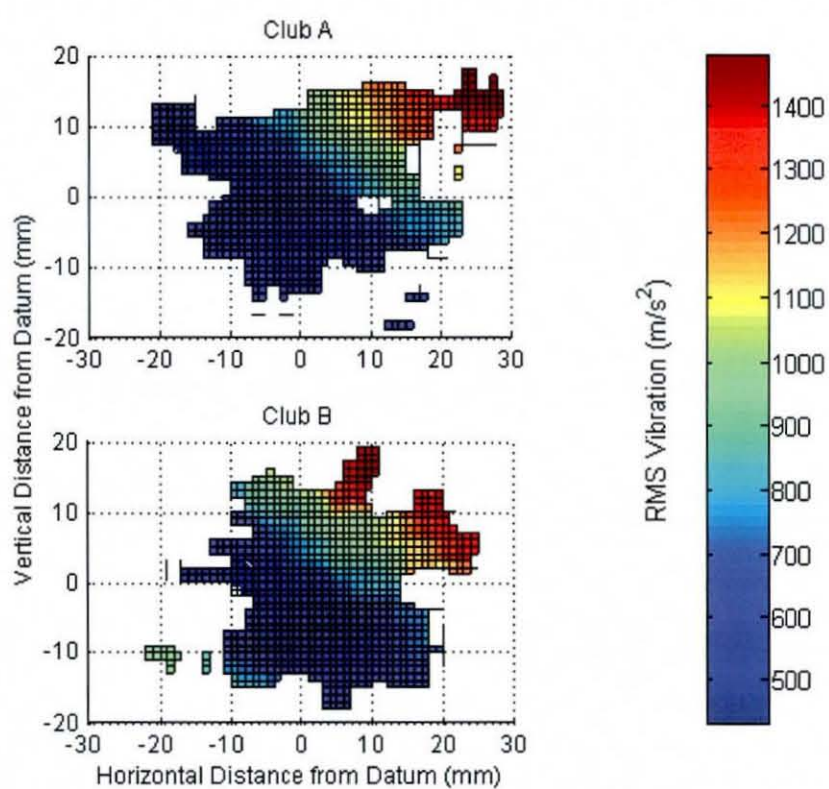


Figure 7.15 Total RMS linear vibration at the shaft as a function of impact location

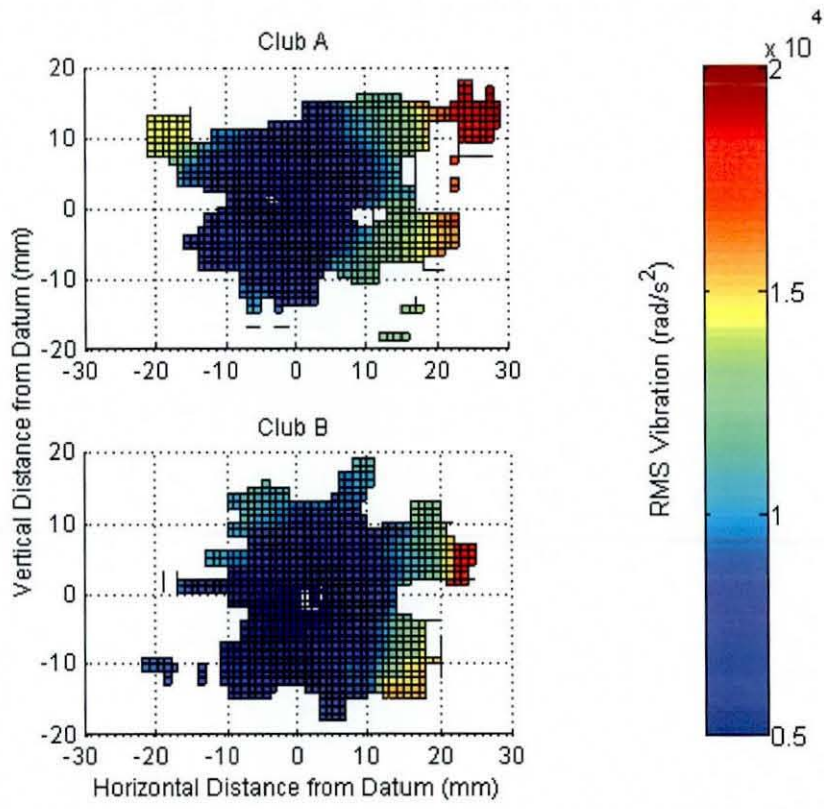


Figure 7.16 RMS torsional vibration as a function of impact location

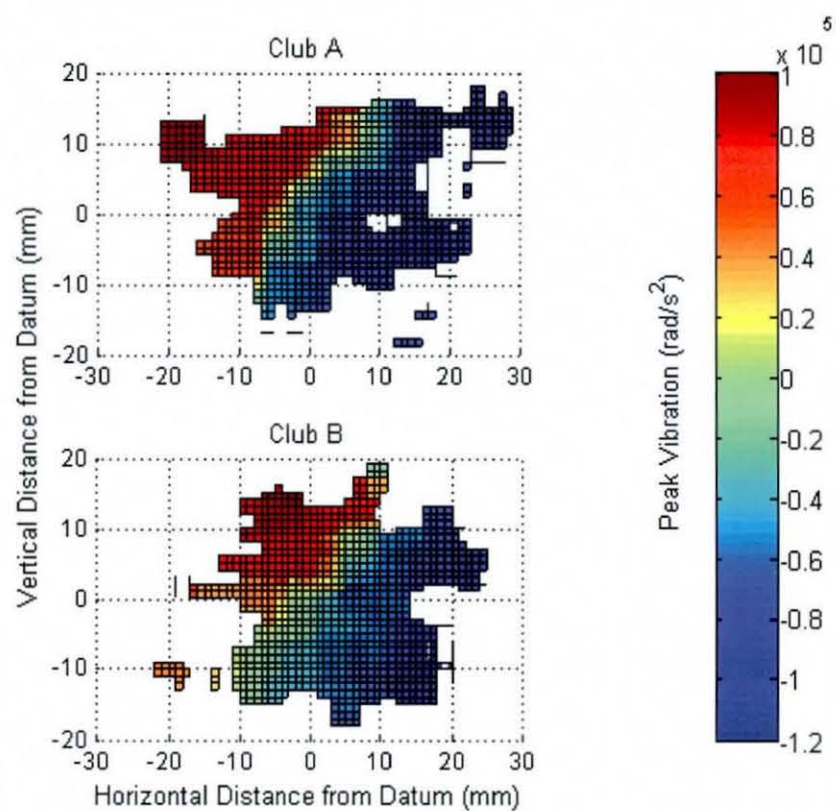


Figure 7.17 Magnitude of first peak in angular acceleration trace as a function of impact location

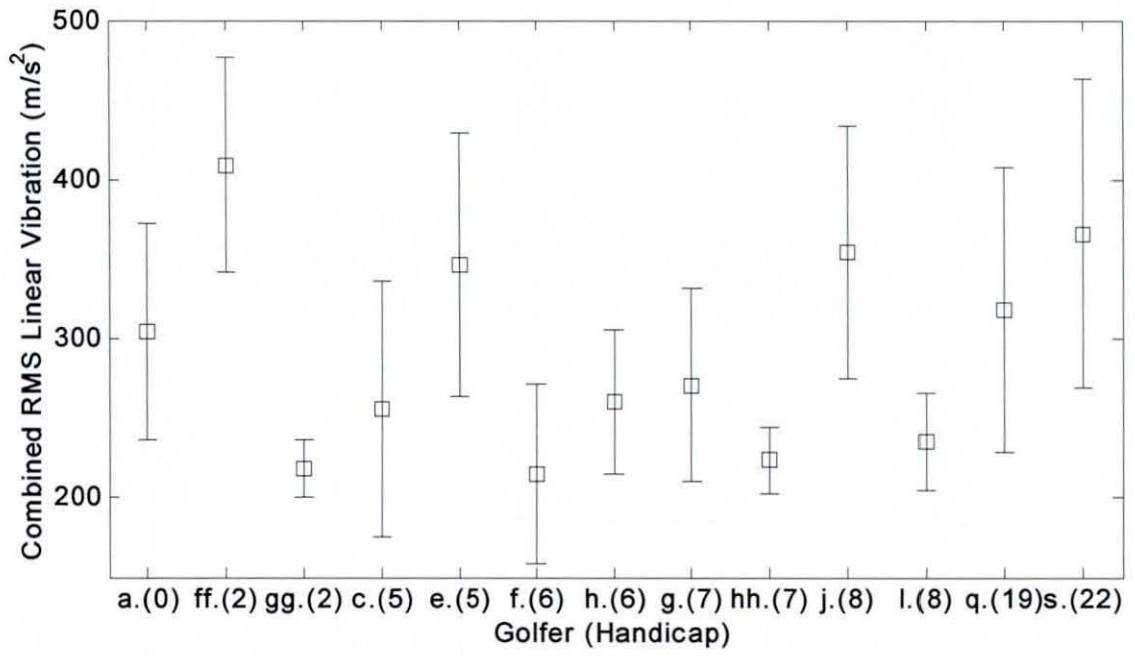


Figure 7.18 Mean combined RMS linear vibration measured on the left thumb \pm one standard deviation for central impacts

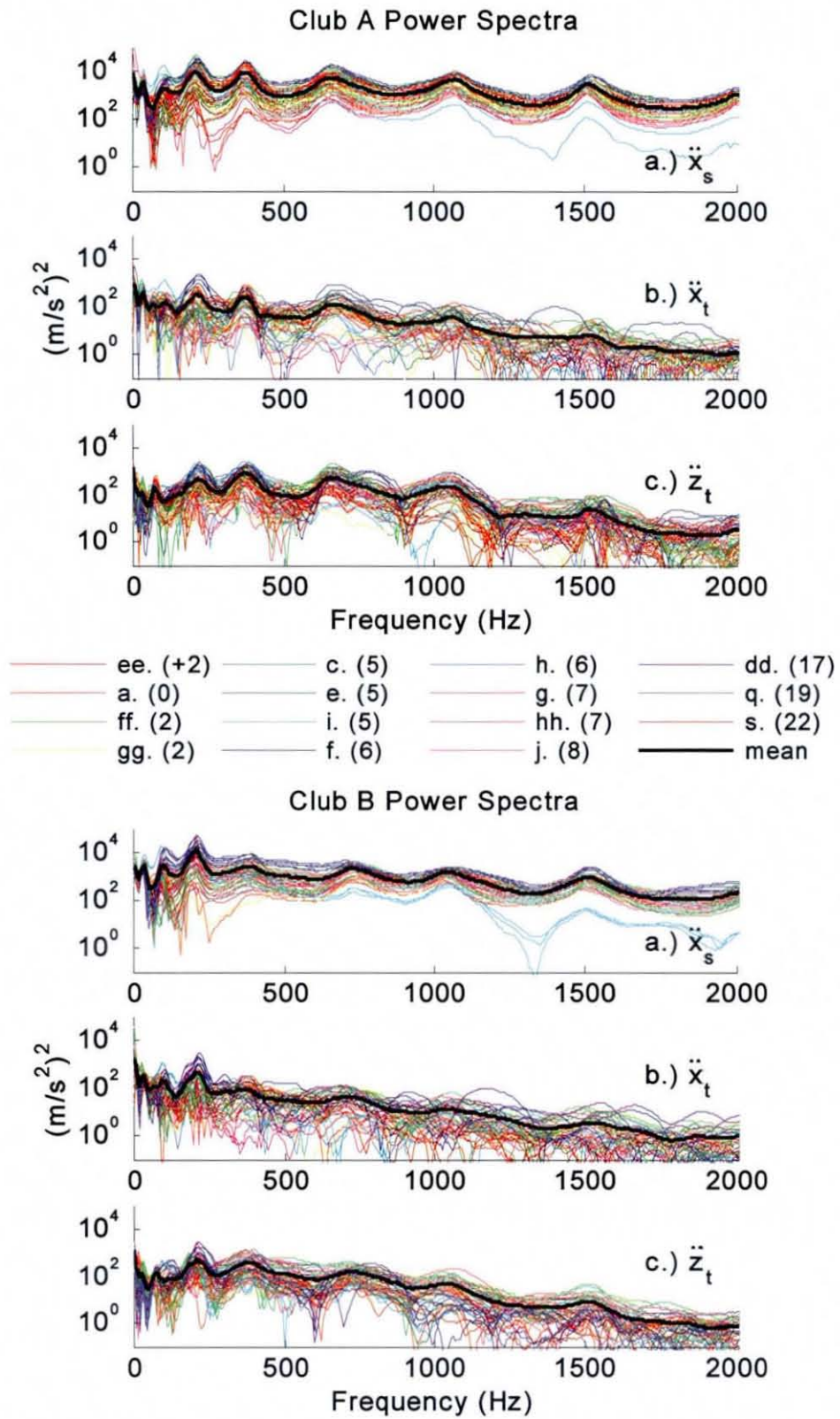


Figure 7.19 Power spectra for clubs A and B, accelerometers on the (a.) shaft and (b. & c.) left thumb

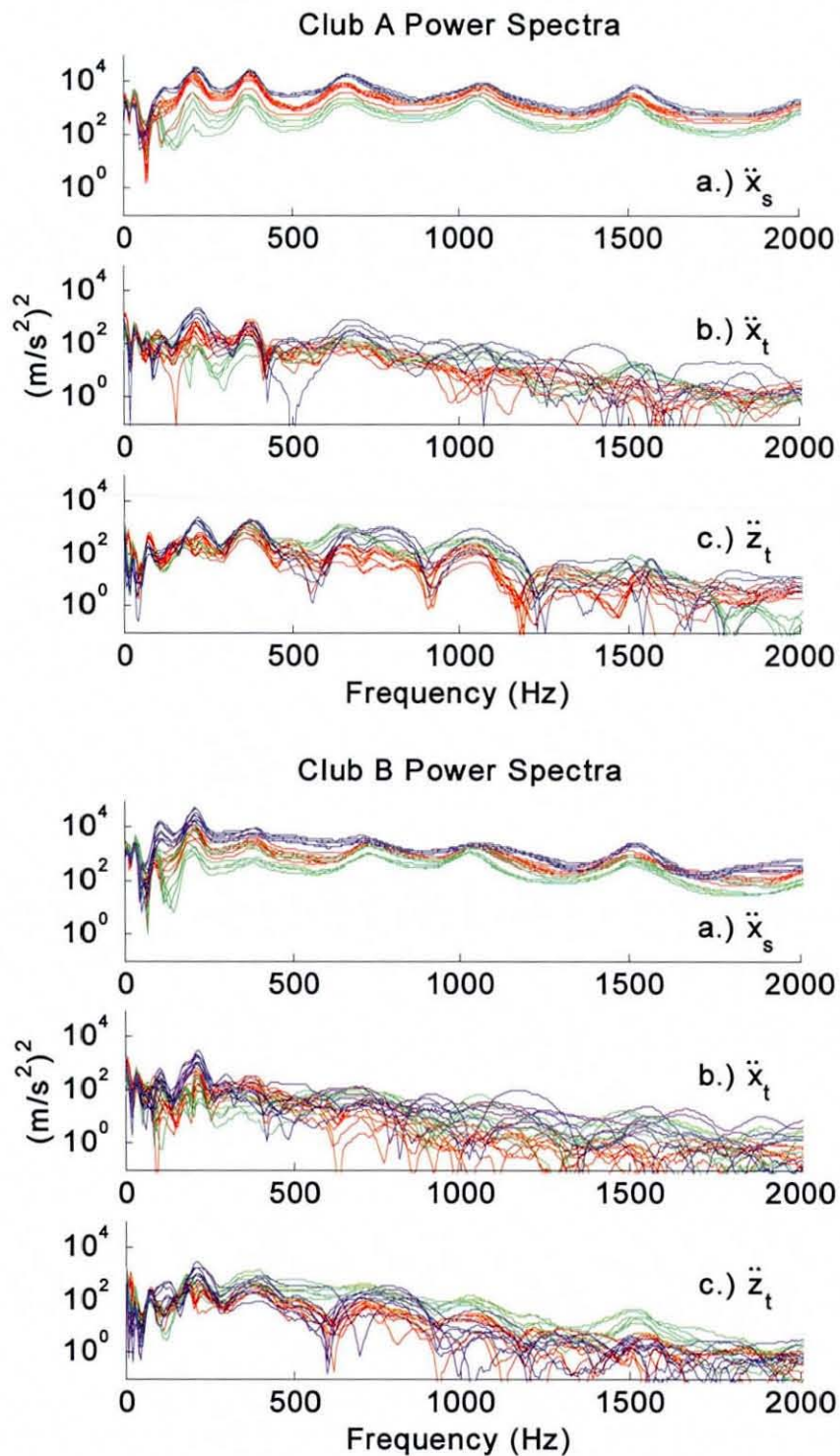


Figure 7.20 Power spectra of three golfers for clubs A and B, accelerometers on the (a.) shaft and (b. & c.) left thumb; — golfer ee, — golfer ff, and — golfer dd (grip forces for these golfers displayed in Figure 7.21 for comparison)

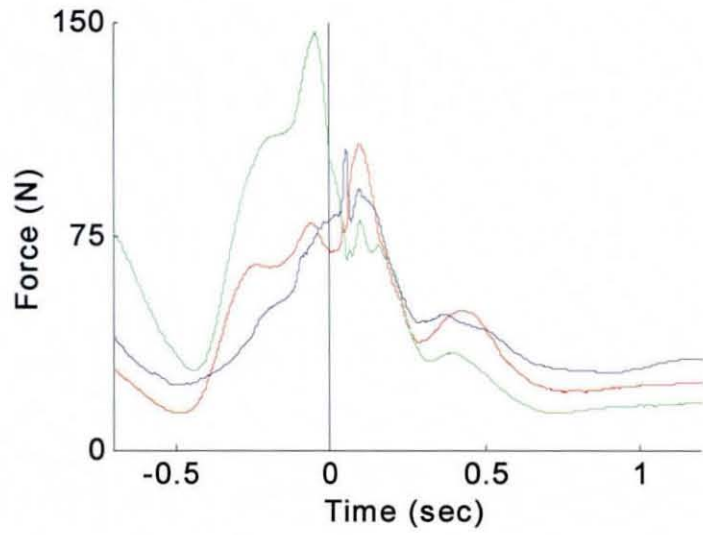


Figure 7.21 Total force trace from 18 Flexiforce sensors for 3 golfers; — golfer ee, — golfer ff, and — golfer dd

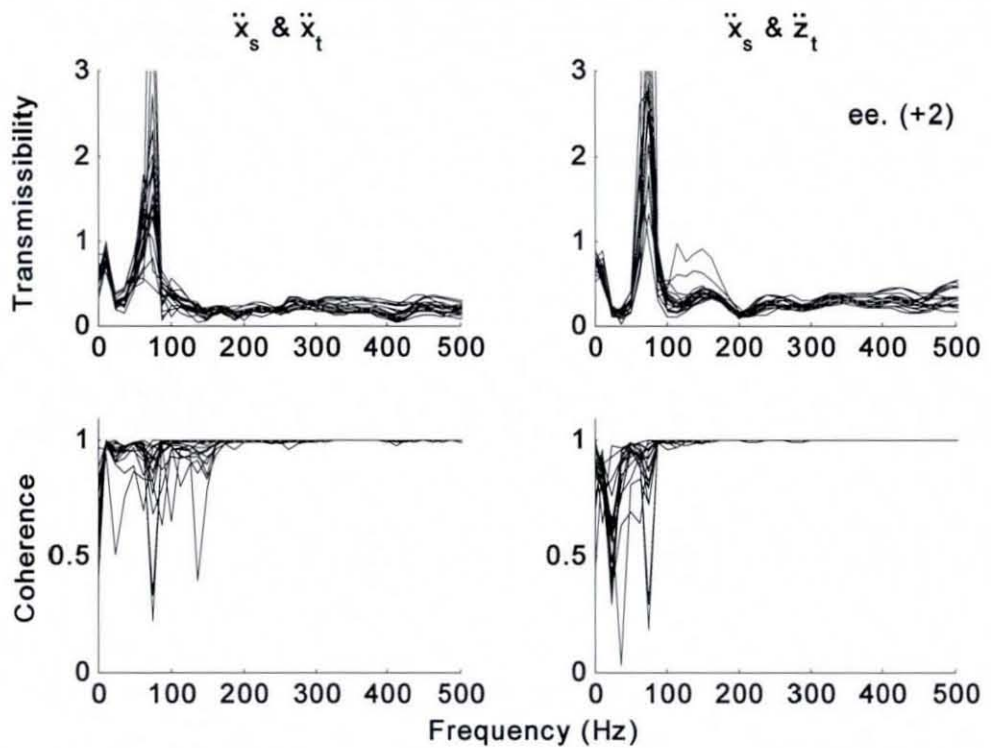


Figure 7.22a Transmissibility and coherence for several shots taken by golfer ee; plots in left and right columns are for comparisons between the shaft and x- and z-direction thumb accelerometers, respectively

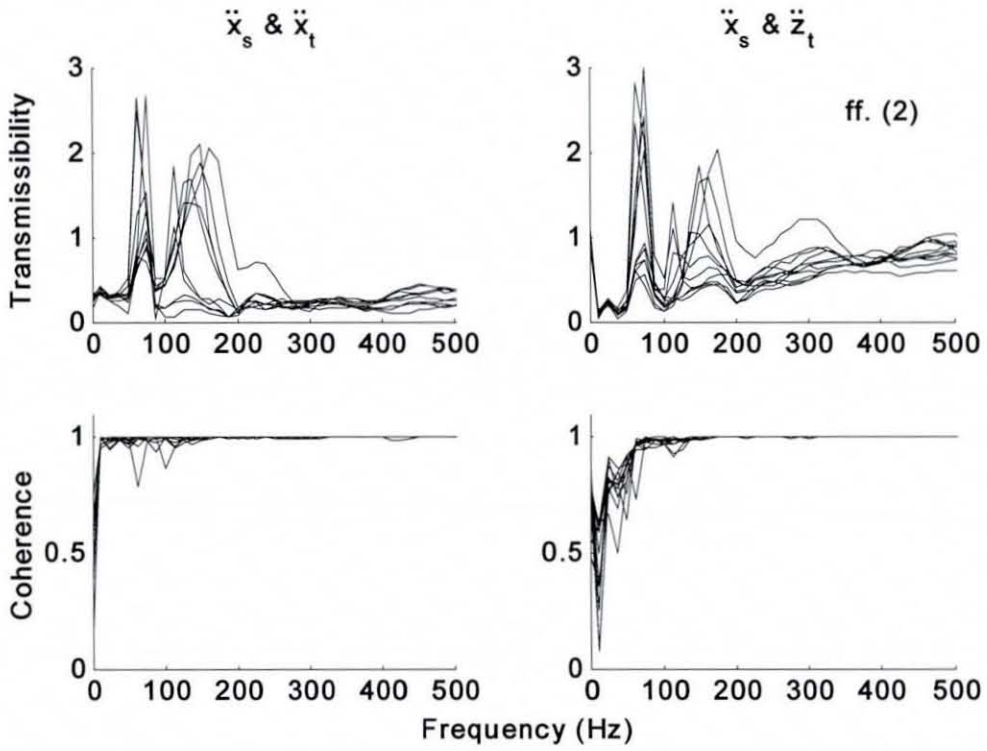


Figure 7.22b Transmissibility and coherence for several shots taken by golfer ff; plots in left and right columns are for comparisons between the shaft and x- and z-direction thumb accelerometers, respectively

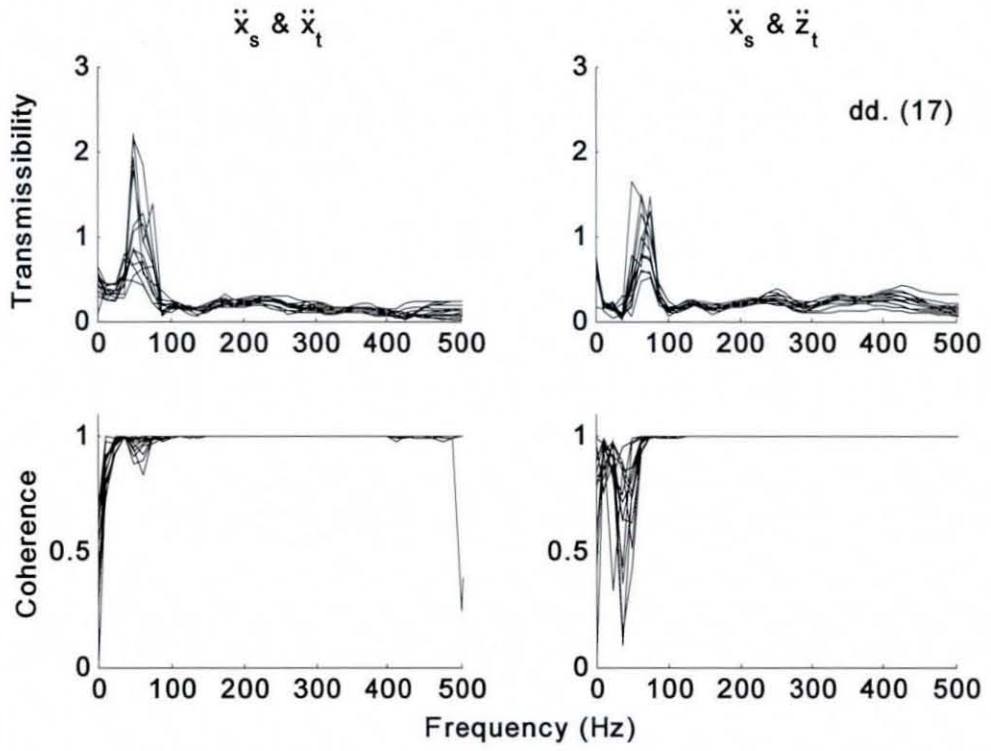


Figure 7.22c Transmissibility and coherence for several shots taken by golfer dd; plots in left and right columns are for comparisons between the shaft and x- and z-direction thumb accelerometers, respectively

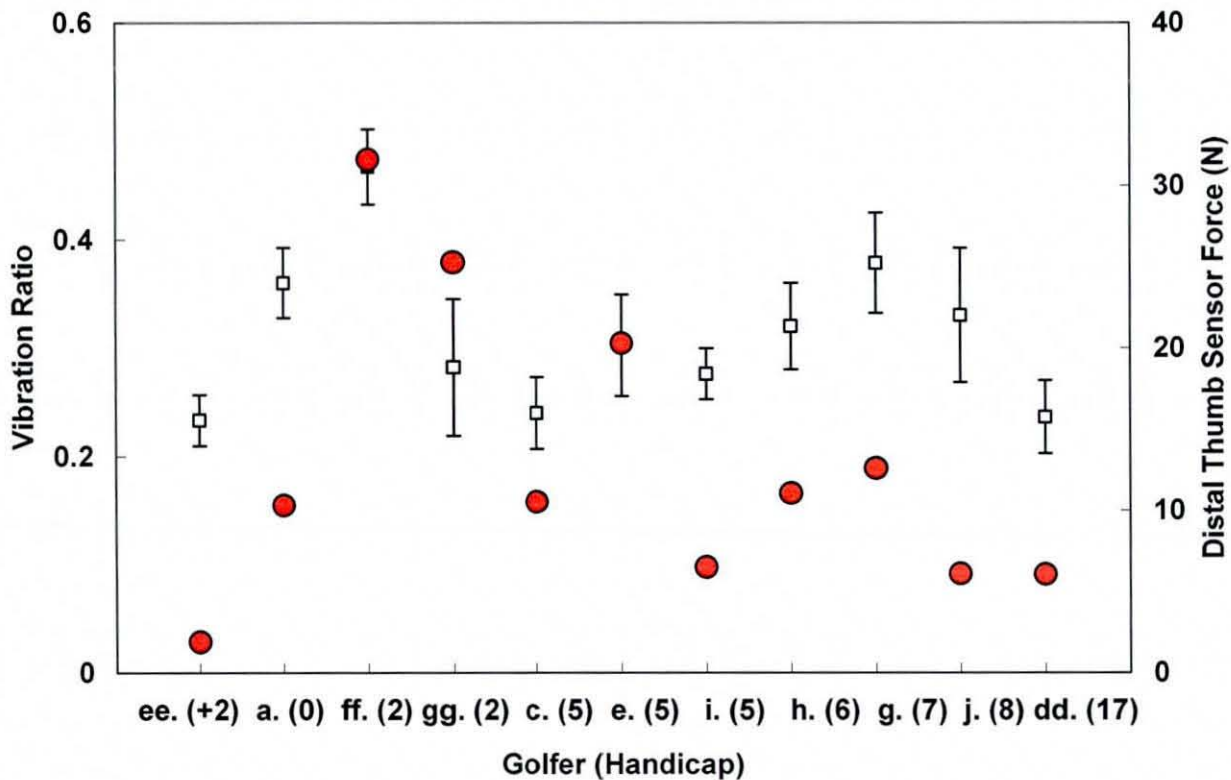


Figure 7.23 Mean vibration ratio (\pm standard deviation) for several shots by each golfer and mean force from distal thumb sensor during -0.3 to 0 s; □ vibration ratio, ● force

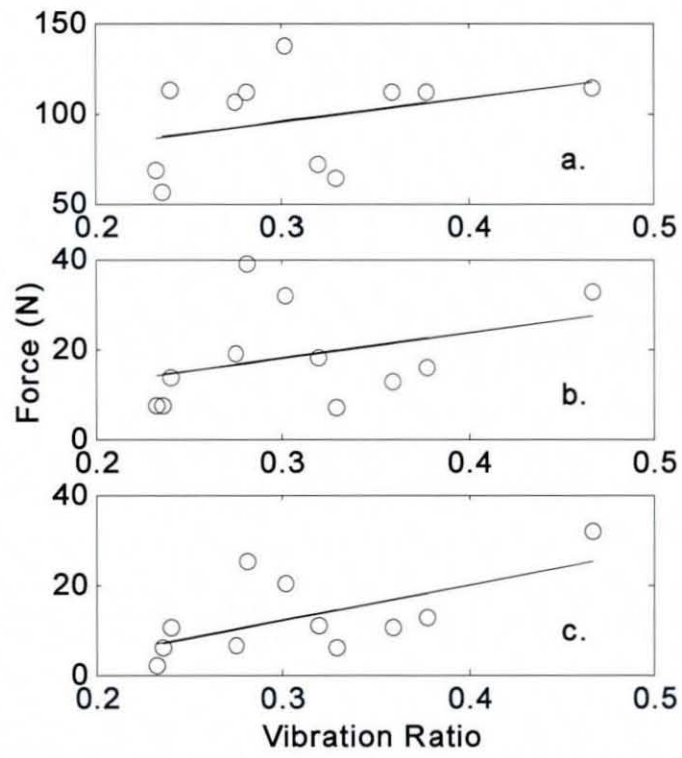


Figure 7.24 Mean vibration ratio versus mean grip force for time interval -0.3 s to impact for 11 golfers with linear curve-fit; (a.) total force, (b.) total left thumb force, (c.) force output from top (distal) left thumb sensor

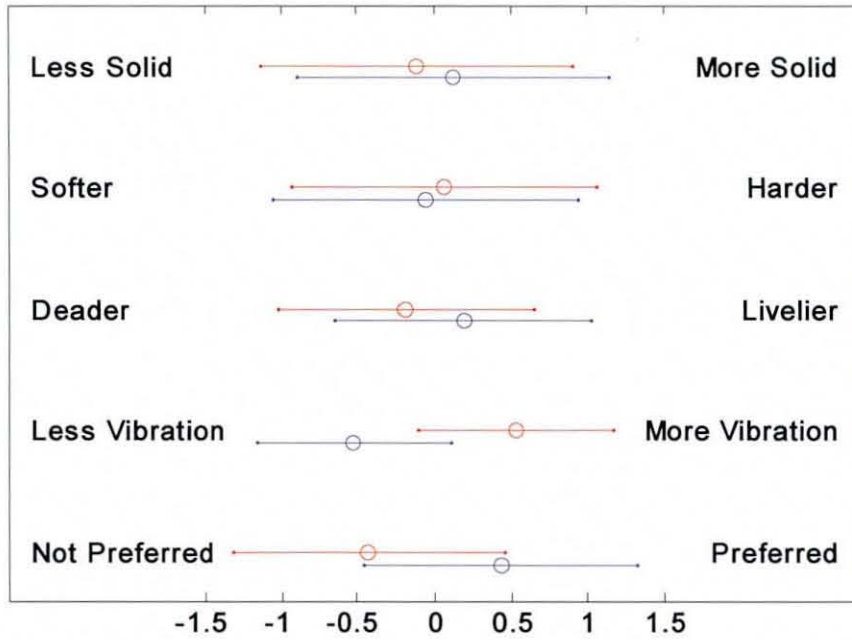


Figure 7.25 Mean values \pm one standard deviation for five 'feel' characteristics from golf impacts; — Club A (Taylor Made 360), — Club B (Ping TiSi)

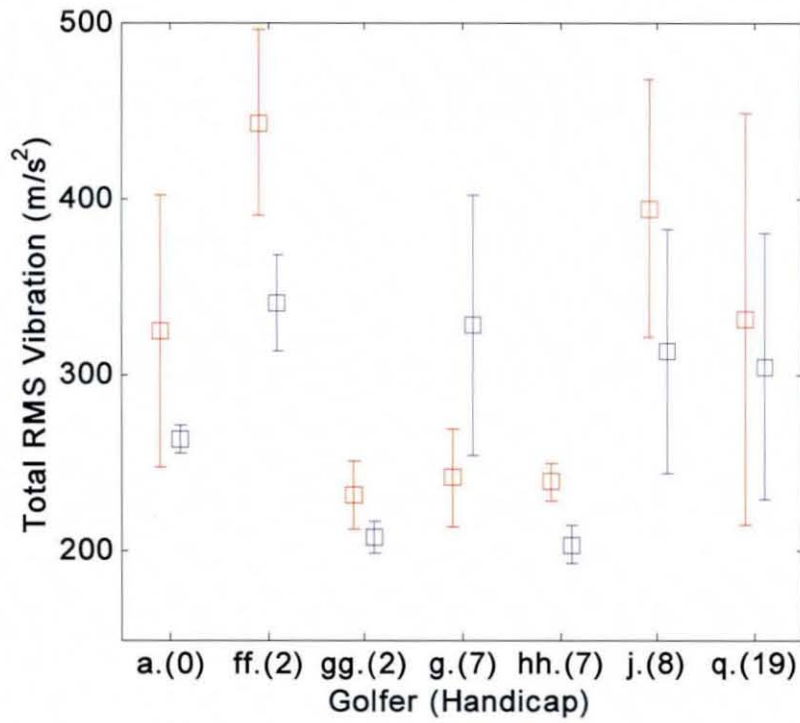


Figure 7.26 Mean combined RMS vibration measured on the left thumb \pm one standard deviation for central impacts; — Club A (Taylor Made 360), — Club B (Ping TiSi)

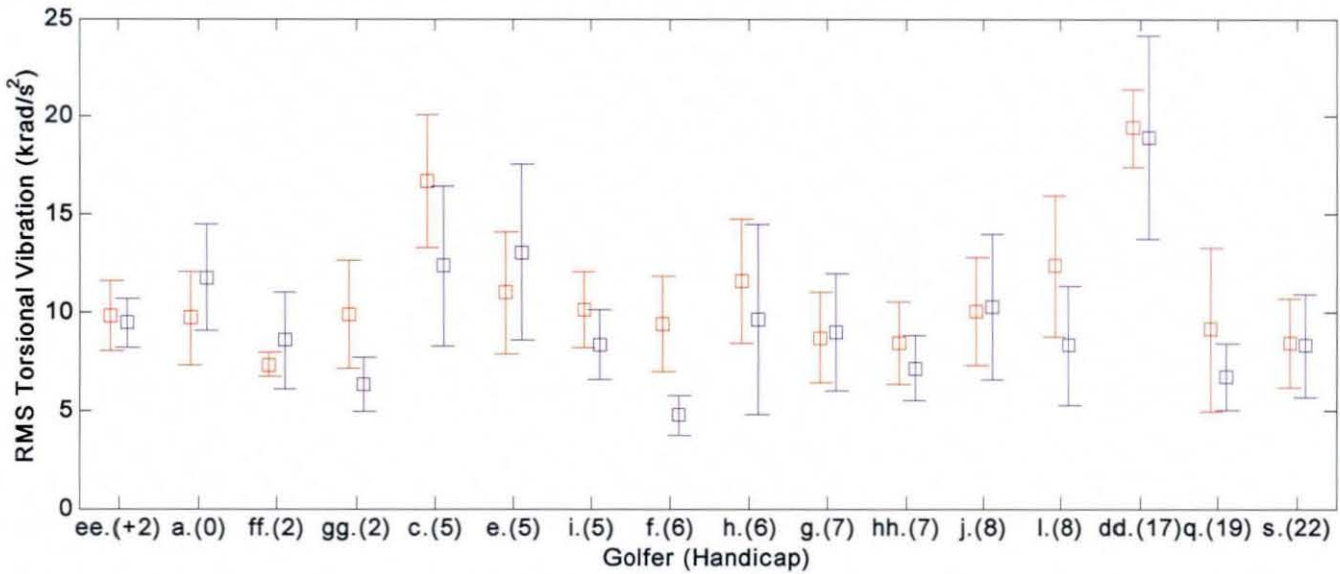


Figure 7.27 Mean torsional vibration level \pm one standard deviation for several impacts for each golfer; — Club A (Taylor Made 360), — Club B (Ping TiSi)

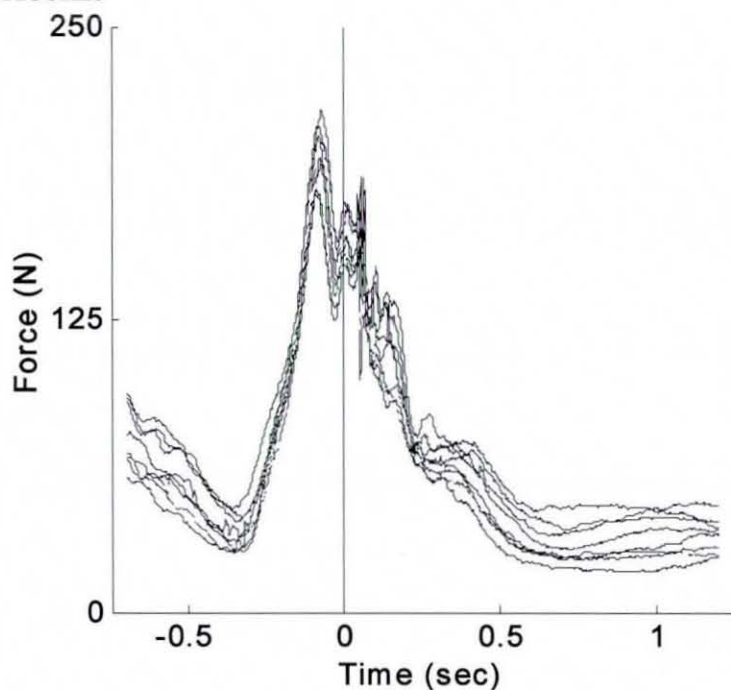


Figure 8.1 Twelve total force traces produced with 18 Flexiforce sensors on gloves by a professional golfer

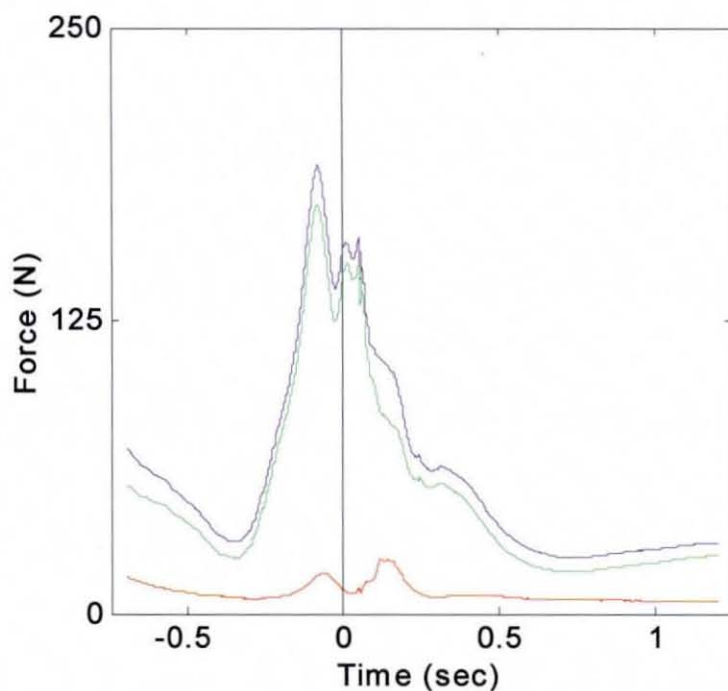


Figure 8.2 Mean force traces produced by a professional golfer with 18 Flexiforce sensors on gloves; — total force, — left hand force and — right hand force

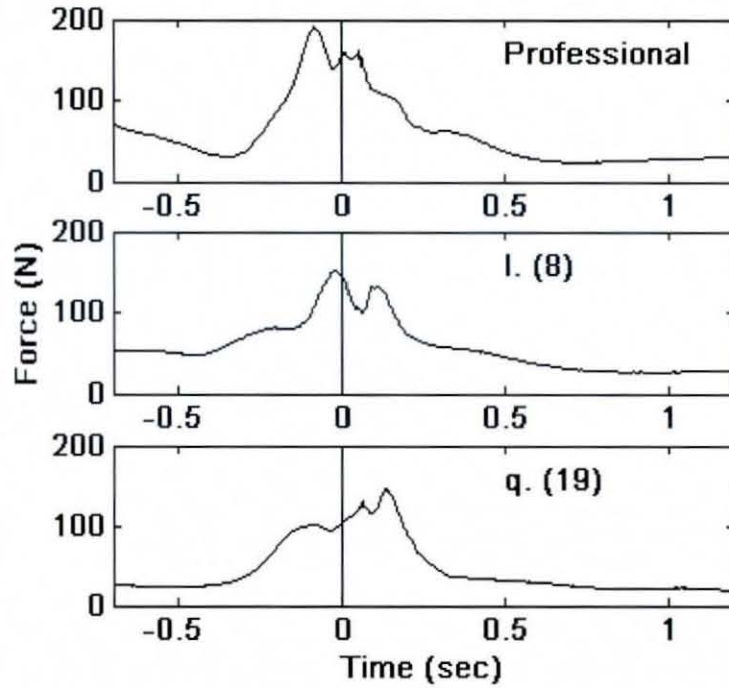


Figure 8.3 Mean total grip force curves for two golfers with highest cross correlation values when compared to a professional; forces measured with 18 Flexiforce sensors on gloves

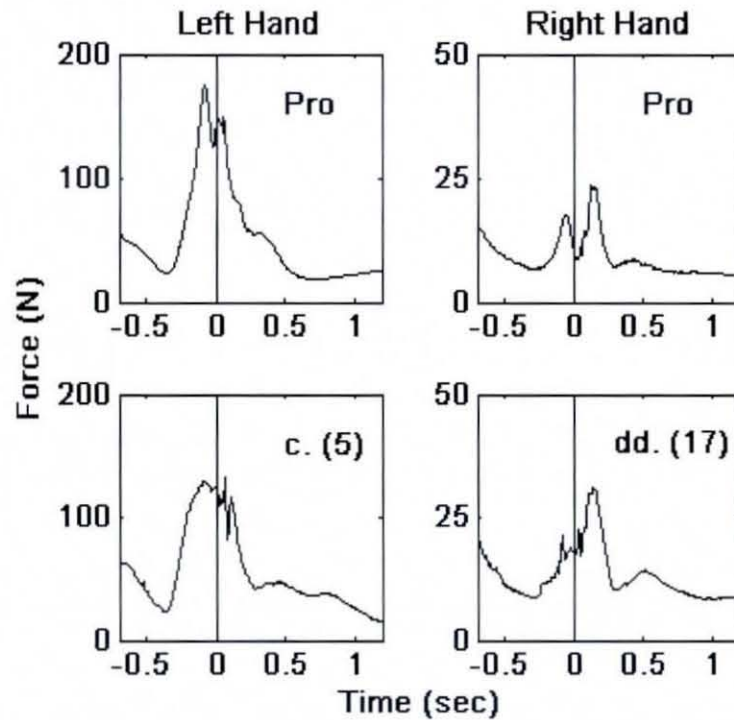


Figure 8.4 Mean left and right hand grip force curves for two golfers with highest cross correlation values when compared to a professional; forces measured with 18 Flexiforce sensors on gloves

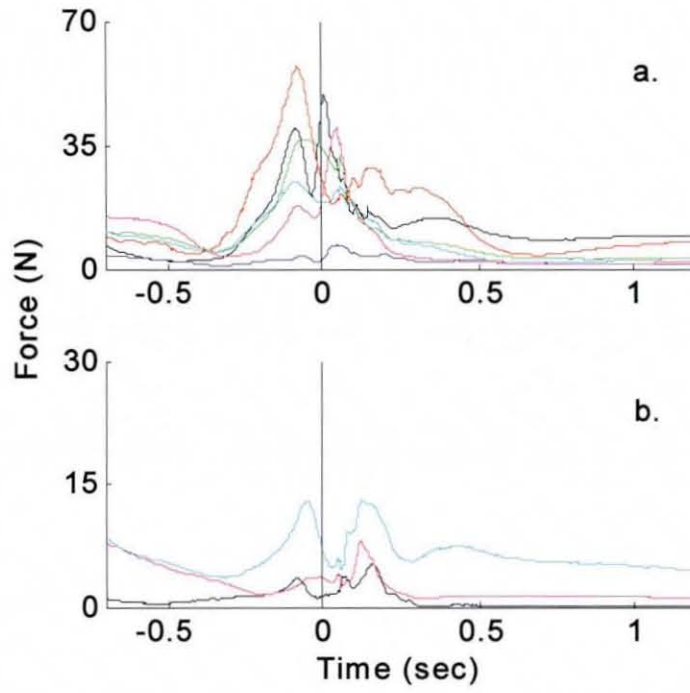


Figure 8.5 Individual finger forces for a professional golfer measured by 18 Flexiforce sensors; (a.) left hand: — thumb, — index, — middle, — ring, — little, — palm, (b.) right hand: — thumb, — middle, — ring

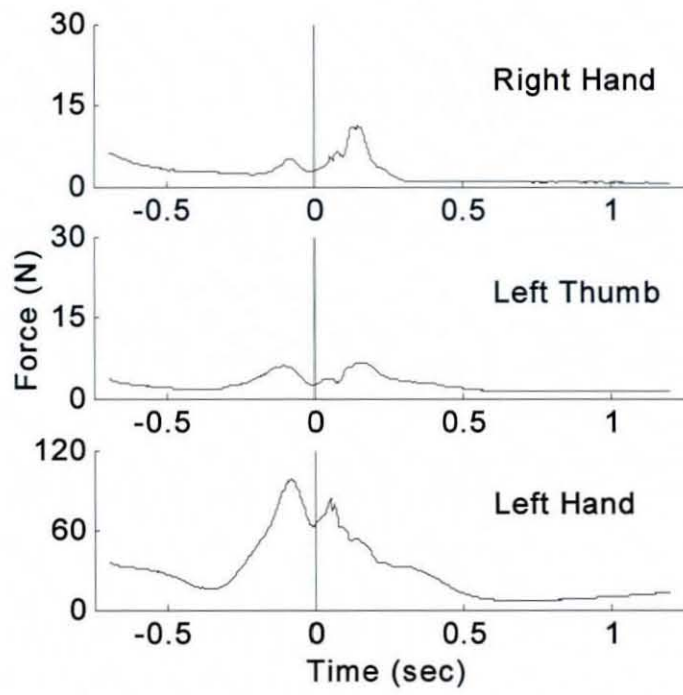


Figure 8.6 Grip force of professional golfer measured by Flexiforce sensors on gloves in regions considered by Budney and Bellow

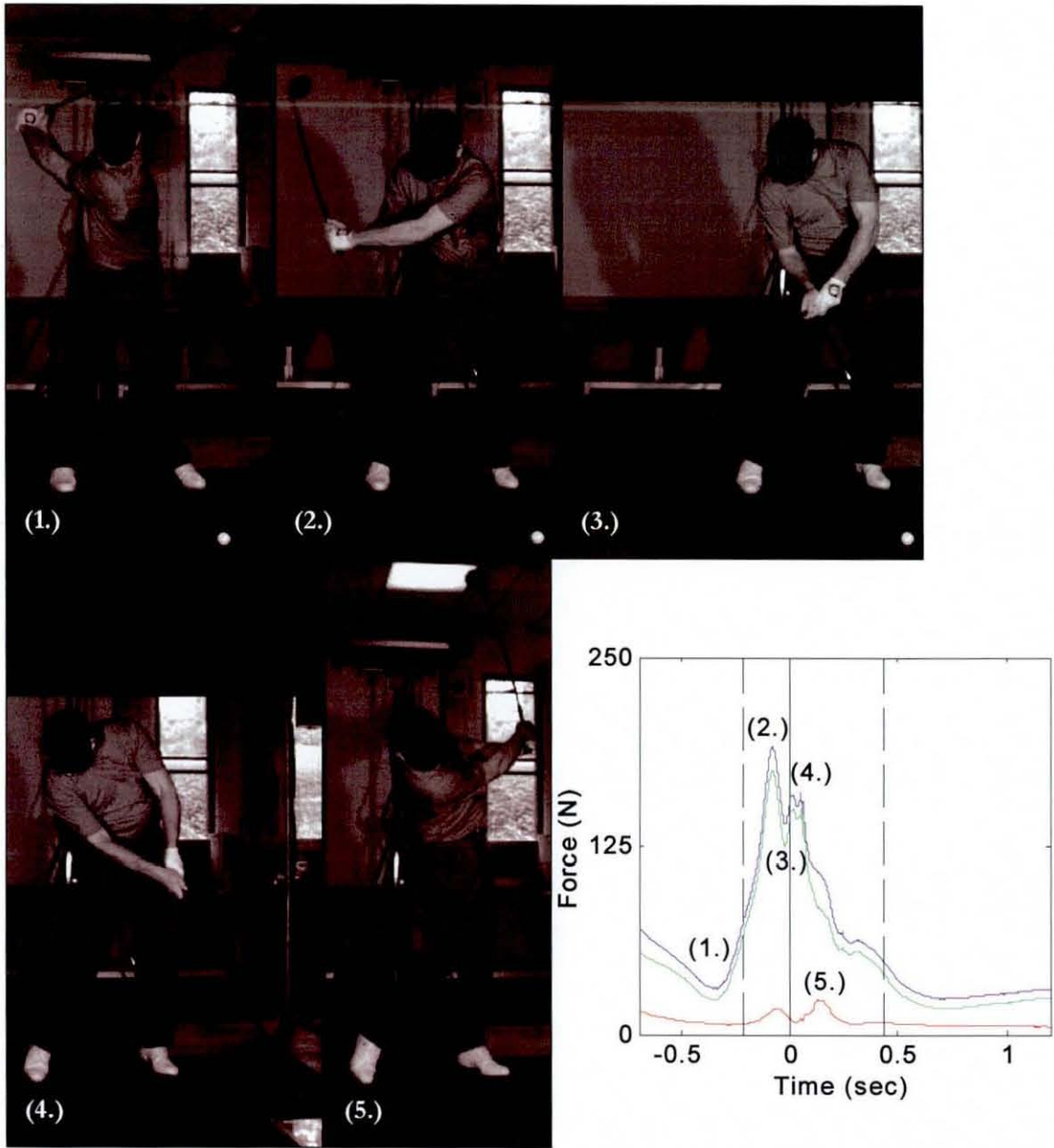


Figure 8.7 Images of professional golfer at five points during the swing as noted in the total grip force traces (bottom right); — total force, — left hand force, — right hand force, — impact, --- start of downswing (before impact) and end of follow-through (after impact)

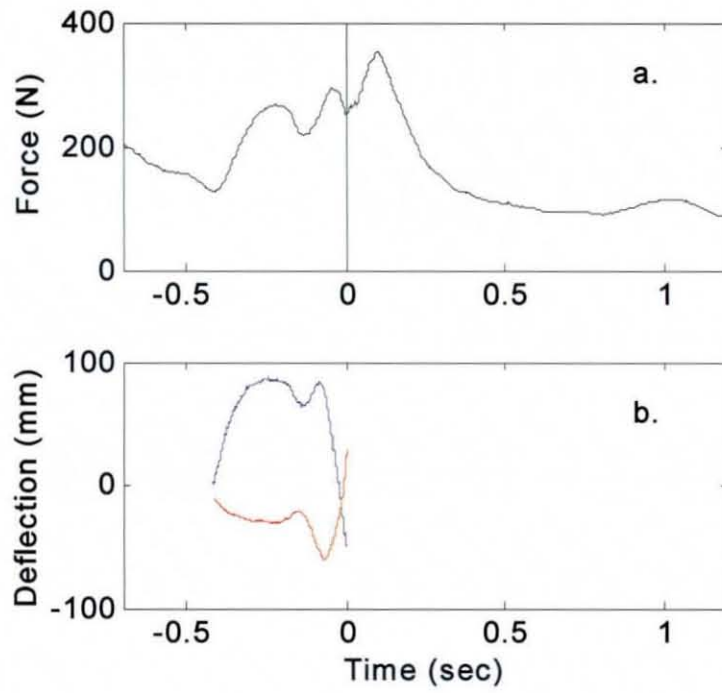


Figure 9.1 Comparison of (a.) total grip force and (b.) shaft deflection for a single golfer; — toe up/down and — lead/lag directions

APPENDIX 1 – MAXIMUM GRIP AND PINCH FORCE SUMMARY

Paper	Measurement Method	Values Obtained																				
Schmidt, 1970	Jamar Dynamometer used with 3.8 cm diameter; 1,128 males and 80 females tested	Mean Grip Strength: Male major hand = 503±73 N, minor hand = 488±73 N Female major hand = 310 N, minor hand = 284 N																				
An, 1980	Pinch meter, grasp meter, lateral deviation strength meter, and universal meter used	Grip force distribution among the phalanges, expressed in N: <table border="1" style="margin-left: 20px;"> <thead> <tr> <th></th> <th>Distal</th> <th>Middle</th> <th>Proximal</th> </tr> </thead> <tbody> <tr> <td>Index</td> <td>57</td> <td>29</td> <td>43</td> </tr> <tr> <td>Middle</td> <td>67</td> <td>37</td> <td>32</td> </tr> <tr> <td>Ring</td> <td>41</td> <td>29</td> <td>18</td> </tr> <tr> <td>Little</td> <td>30</td> <td>17</td> <td>11</td> </tr> </tbody> </table>		Distal	Middle	Proximal	Index	57	29	43	Middle	67	37	32	Ring	41	29	18	Little	30	17	11
	Distal	Middle	Proximal																			
Index	57	29	43																			
Middle	67	37	32																			
Ring	41	29	18																			
Little	30	17	11																			
Mathiowetz, 1985	Jamar dynamometer (2 nd handle position); B&L pinch gauge	Grip Strength Mean Men Right: 464 N, high=783 N, Left: 414 N, high=712 N Women Right: 279 N, high=609 N, Left: 240 N, high=512 N Mean key pinch: Men Right: 109 N, high=182 N, Left: 105 N, high=187 N Women Right: 72 N, high=111 N, Left: 68 N, high=116 N Highest palmar pinch: Men Right: 104 N, high=200 N, Left: 102 N, high=187 N Women Right: 73 N, high=151 N, Left: 70 N, high=142 N																				
Amis, 1987	Three finger pads on cantilever beams with foil strain gauges to measure the three segments of the finger being tested	Mean contribution of each finger: Index 30%, Middle 30%, Ring 22%, Little 18% Approximate forces on each phalanx for diameter of 31 mm, expressed in Newtons: <table border="1" style="margin-left: 20px;"> <thead> <tr> <th></th> <th>Distal</th> <th>Middle</th> <th>Proximal</th> </tr> </thead> <tbody> <tr> <td>Index</td> <td>78</td> <td>30</td> <td>45</td> </tr> <tr> <td>Middle</td> <td>72</td> <td>36</td> <td>48</td> </tr> <tr> <td>Ring</td> <td>54</td> <td>32</td> <td>36</td> </tr> <tr> <td>Little</td> <td>48</td> <td>24</td> <td>32</td> </tr> </tbody> </table>		Distal	Middle	Proximal	Index	78	30	45	Middle	72	36	48	Ring	54	32	36	Little	48	24	32
	Distal	Middle	Proximal																			
Index	78	30	45																			
Middle	72	36	48																			
Ring	54	32	36																			
Little	48	24	32																			
Lee, 1990	Five cylinders with diameters 25.4 – 50.8 mm with Fuji pressure sensitive film on them	Mean Contribution of each finger: Middle 32.5%, Index 29.5%, Ring 22.6%, Little 15.4% Finger forces for 25.4 mm cylinder: Middle=180 N Index=170 N Ring=125 N Little=80 N																				
Hallbeck, 1993	Vital Signs hand dynamometer and B&L pinch gauge	Mean maximum chuck pinch (kg): Males = 8.8, Females = 6.9 (78% of male max) Mean maximum grip strength (kg): Males = 25.6, Females = 19 (74% of male max)																				

Dempsey, 1996	Pinch gauge constructed of aluminium and steel with 4 strain gauges in full Wheatstone bridge	Mean maximum pinch for chuck, lateral, pulp 2 and pulp 3 types, respectively (kg): Males = 6.7 ± 2.2 , 8.1 ± 2 , 5 ± 1.6 , 5 ± 1.6 ; Females = 4.4 ± 1.5 , 4.7 ± 1.3 , 3.4 ± 1.1 , 3.1 ± 1 (63% of male max on average)				
Tsaousidis, 1997	Used 4.5 cm cylindrical handle with pressure transducer	Maximum grip force dropped 15% with glove and rate of force development decreased 24-38%.				
Loskutovaa, 1998	Used Tekscan F-Scan system and looked at four parts of the hand; measured both left and right	Pressure distribution (% maximum):				
			1 Finger	Thenar	Palm	2-5 Fingers
		Woman Left	29.0%	18.7%	27.1%	43.7%
		Woman Right	29.3%	17.7%	27.5%	43.2%
Men Left	21.8%	23.5%	29.0%	49.2%		
Men Right	23.3%	21.6%	28.0%	48.7%		
Tsaousidis, 1998	Used 4.5 cm cylindrical handle with pressure transducer	Average maximum grip: No glove: 470.9 N, Glove: 405.8 N				
Blackwell, 1999	Jamar Dynamometer with four grip sizes 100-180 mm and surface EMG; subjects all right-handed males	Maximal voluntary contraction grip force: 100 mm: 350 N, 130 mm: 530 N, 160 mm: 550 N, 180 mm: 490 N				
Bao, 2000	Digital dynamometer, EMG	Mean power grip: Men: 472 N, Women: 294 N Mean pinch grip: Men: 125 N, Women: 89 N				
Chadwick, 2001	Strain gauge transducer on cylinder with diameter of 30 mm measures radial forces in six locations	Total applied force for several grip types: Chuck Grip (thumb and 3 fingers): 113 N, Vertical Power: 464 N, Horizontal Power: 331N, Hook Grip: 334 N				
Freund, 2002	Load cell and nylon buttons on three handles (4-6cm diameter)	Mean value of force distribution between fingers: Little = 12%, Ring = 22%, Middle = 31%, Index = 35%				
Mogk, 2003	Grip dynamometer from MIE Medical Research Ltd.	Mean maximum grip force: Males = 393 ± 97 , Females = 249 ± 30 (63% of male max)				
Eksioglu, 2004	Modified Lafayette hand grip dynamometer (grip diameter adjustable from 30-105 mm)	Mean maximum voluntary grip force of the subjects tested 450 ± 51 N				
Kong, 2005	Attached 16 Tekscan Flexiforce sensors to each of two golf gloves on the phalanges of digits 2-5, and on the palm just proximal of the MCP joint for these same fingers	Mean total finger force, males = 562 N, females = 324 N (58% of male max) Average contribution of the fingers to total grip force: index = 25%, middle = 35%, ring = 27%, little = 14% Average contribution of the phalanges to total grip force: distal = 42%, middle = 24%, proximal = 19%, metacarpal 16%				
Shih, 2005	Fabricated pinch gauge with embedded load cell	Mean MVC for chuck pinch, males = 90 N and females = 54 N (60% of the male max)				
Nicolay, 2005	Hand dynamometer from Qubit Systems, Inc.	Mean MVC for dominant and non-dominant hand, respectively (kg): Males = 40 ± 7 , 40 ± 10 ; Females = 20 ± 5 , 17 ± 6 (52% of male max)				

APPENDIX 2 – GRIP FORCE IN SPORT SUMMARY

	Paper	Measurement Method	Values Obtained
Golf	Budney, 1979	Steel-shafted driver fitted with three force transducers consisting of aluminium simply supported beams and metal foil strain gauges	Peak forces for three professionals: 25 N right hand, 20 N left thumb, 20 N left hand Peak forces for three amateurs: 30 N right hand, 30 N left thumb, 20 N left hand
	Budney, 1990	Steel-shafted driver fitted with three force transducers consisting of aluminium simply supported beams and metal foil strain gauges; another strain gauge was located on shaft near clubhead to detect impact	At top of backswing left hand at 31 N and left thumb at 58 N to brake backswing and initiate downswing 0.10 sec before impact peak force of 80 N applied to left thumb 0.05 sec before impact right hand impulse reaches peak of 36 N
	Macht, 2000	Fitted gloves with 13 Tekscan sensors on each hand, five on the fingers and eight on the palm	Peak forces: 165 N left hand total, 111 N right hand total, 49 N left-hand fingers, 89 N left-hand palm, 18 N left thumb
	Nikonovas, 2004	Applied 20 Tekscan Flexiforce sensors directly to each hand; 14 on each of the phalanges and 6 on the palm	Peak forces of 17 and 9 N from distal and proximal phalanges of left thumb, respectively; left hand proximal phalanges had a peak combined force of 21 N; right hand proximal phalanges had a peak combined force of 16 N
Tennis	Knudson, 1989	Used two force sensing resistors; top one placed at base of index finger, bottom placed to record force on last three fingers of the hand	Forces at hypothenar eminence were consistent, ranging from 5-71 N Post-impact peak forces at base of the index finger were highly variable, ranging from 4-309 N
	Knudson, 1991	Tennis racket instrumented with two miniature load cells - one placed at the base of the thenar eminence and one at the lower portion of the hypothenar eminence	Mean post-impact force on thenar and hypothenar eminences were in a similar range of about 50 N, which corresponds to a pressure of 380 kPa Peak forces on the thenar eminence ranged from 6-124 N
Cricket	Stretch, 1994	Two force sensors applied to a cricket bat to record forces from the top and bottom hands	Average peak force, medium-paced bowler on turf pitch: top hand = 129 ± 42 N, bottom hand = 74 ± 38 N
	Stretch, 1995	Two piezoresistive pressure sensors placed at two locations to record grip forces from both hands; also used dynamometer to determine grip strength of subjects	Mean range of grip forces between subjects (0.75s pre- to 0.10s post-impact): Top hand = 88-138 N, Bottom hand = 33-103 N Mean peak forces: Top hand = 199 N, Bottom hand = 92 N
	Stretch, 1998	Cricket bat instrumented with two pressure sensors to measure forces applied by top and bottom hands separately	Peak grip forces: Top hand: forward defensive stroke = 129 ± 42 N, front foot drive = 199 ± 40.9 N Bottom hand: forward defensive stroke = 52.2 ± 16.9 N, front foot drive = 91.8 ± 41.1 N
	Glazier, 2002	Collected numbers from research of others	Grip peak force on drive, Top hand = 195 N, Bottom hand = 102 N Grip peak force on forward defensive, Bottom hand = 58 N Drive against spin bowler on artificial surface peak forces, Top hand = 74 N Forward defensive bottom hand = 34 N

Baseball	Eggeman, 1985	Two simply supported beam with double-element strain gauges were placed at opposite sides of the handle so that readings on one side of the bat could be taken for each hand per swing	Top hand peak forces for a right-handed batter: Thenar eminence = 340 N, Fingers = 260 N Bottom hand peak forces for right-handed player: Thenar eminence = 270 N, Fingers = 180 N
----------	---------------	--	---

